BRITISH ANTARCTIC SURVEY
SCIENTIFIC REPORTS
No. 107

THE GEOLOGY OF SOUTH GEORGIA:
V. DRYGALSKI FJORD COMPLEX

By

BRYAN C. STOREY, B.A., Ph.D.
Earth Sciences Division, British Antarctic Survey

CAMBRIDGE: PUBLISHED BY THE BRITISH ANTARCTIC SURVEY: 1983
NATURAL ENVIRONMENT RESEARCH COUNCIL

BRITISH ANTARCTIC SURVEY SCIENTIFIC REPORTS: No. 107

THE GEOLOGY OF SOUTH GEORGIA:
V. DRYGALSKI FJORD COMPLEX

By

BRYAN C. STOREY, B.A., Ph.D.

Earth Sciences Division, British Antarctic Survey

(Manuscript received 9 May 1980; accepted in revised form 4 September 1981)

ABSTRACT

THE Drygalski Fjord Complex represents a fragment of pre-Jurassic continental crust that was intruded by a wide variety of basic and acidic plutonic rocks during the early stages of the formation of the Upper Mesozoic island-arc–back-arc basin system of South Georgia.

Sedimentary and metasedimentary country rocks are divided into three spatially distinct formations: the Salomon Glacier, Cooper Island and Novosilski Glacier Formations. The Salomon Glacier Formation comprises siliceous *para*gneisses and layered migmatites regionally metamorphosed up to amphibolite facies. The Cooper Island and Novosilski Glacier Formations are deformed low-grade quartz-rich clastic sediments. Porphyritic felsites are tentatively assigned to the Novosilski Glacier Formation. Subsequent to deformation and metamorphism, magmatic activity commenced in the early Jurassic with emplacement of a sub-alkaline tholeiitic magma. Differentiation of this magma produced a wide variety of layered gabbros, intermediate and granitoid rocks. Some granitoid rocks, however, show calc-alkaline trends. Continued emplacement of basic magma formed basic dyke suites with chilled margins cutting the cumulate gabbro and acidic rocks.

As a result of the magmatic activity, a heterogeneous migmatite aureole surrounds the plutonic rocks. The basic, granitoid and metasedimentary country rocks are broken up, injected and net-veined by anatectic granitoid veins, and by emplacement of acid–basic intrusive breccias. The migmatite complex is cut by aplites, pegmatites and occasional basic dykes. Subsequent retrogression has resulted in widespread secondary and disequilibrium mineral assemblages.

A zone of intensely mylonitized rocks up to 1 km wide (the Cooper Bay dislocation zone), formed by both pure and simple shear, separates the complex on the north-eastern side from deformed volcaniclastic sediments of the Cooper Bay Formation.

It is concluded that the sediments and metasediments were probably deformed during the Gondwanian orogeny and that the magmatic activity of the Drygalski Fjord Complex may be the precursor of the basic magma which formed the floor of the Upper Jurassic–Lower Cretaceous island-arc–back-arc basin of South Georgia.

CONTENTS

I. INTRODUCTION

1. *Location and scope of study*

South Georgia (lat. 54°–55°S, long. 36°–38°W) is a sub-Antarctic island, 160 km long and 5–40 km wide, situated approximately 2 000 km east of Cape Horn in the South Atlantic Ocean (Fig. 1). Detailed mapping of the southern part of South Georgia was undertaken by C. M. Bell, B. F. Mair and B. C. Storey during the austral field season of 1974–75 and by B. C. Storey in 1975–76. The author was responsible for re-mapping the south-eastern igneous complex (Fig. 2) (Trendall, 1959), which has long been known to exist in this area (Heim, 1912). The present mapping has indicated that intrusive igneous rocks, metasedimentary and anatectic rocks crop out over a well-defined area which stretches as far north as Spenceley Glacier (Fig. 3). As the rocks of the south-eastern igneous complex crop out over a more extensive area than that envisaged by Trendall (1959) and include a large proportion of sedimentary, metasedimentary and metamorphic rocks, it is proposed that the terms "south-eastern" and "igneous" are unsuitable and that the area is subsequently referred to as the Drygalski Fjord Complex (Fig. 2) (Storey and others, 1977). Although summaries of the geological history of this area have been published which relate it to an island-arc and marginal basin tectonic setting (Bell and others, 1977; Storey and others, 1977; Tanner, 1982*b*), this report presents for the first time the details of this geologically complex area (Table I). Some of the rocks within the area have been radiometrically dated using both K-Ar and Rb-Sr methods (Tanner and Rex, 1979) and these data are also given (Table II) and discussed.

Due to the high mountainous terrain (Fig. 4) and the deeply crevassed glaciers, detailed mapping was restricted to accessible areas within walking distance of coastal camp sites. However, a number of manhauling trips were made to inland areas to map the limits of the complex. The use of an inflatable Gemini craft was provided by RRS *John Biscoe* for a number of days during which it was possible to visit coastal exposures inaccessible from the camp site, and a few days' valuable helicopter support was provided by HMS *Endurance*.

An enlarged section of the D.O.S. 1: 200 000 map compiled by the South Georgia Survey Expeditions, 1951–59, is used here as a base map (Fig. 3). A detailed geological outcrop map of the southern part of the complex (Fig. 5) was compiled from plane-table maps (surveyed by D. J. Orchard and B. F. Mair), air photographs and the enlarged base map. Air photographs taken by HMS *Endurance* were useful for field mapping but they are inadequate for accurate map-making, because of helicopter tilt and the high terrain. The high mountains also make mapping by plane-tabling techniques difficult.

A magnetic variation of 7° was allowed for during field work

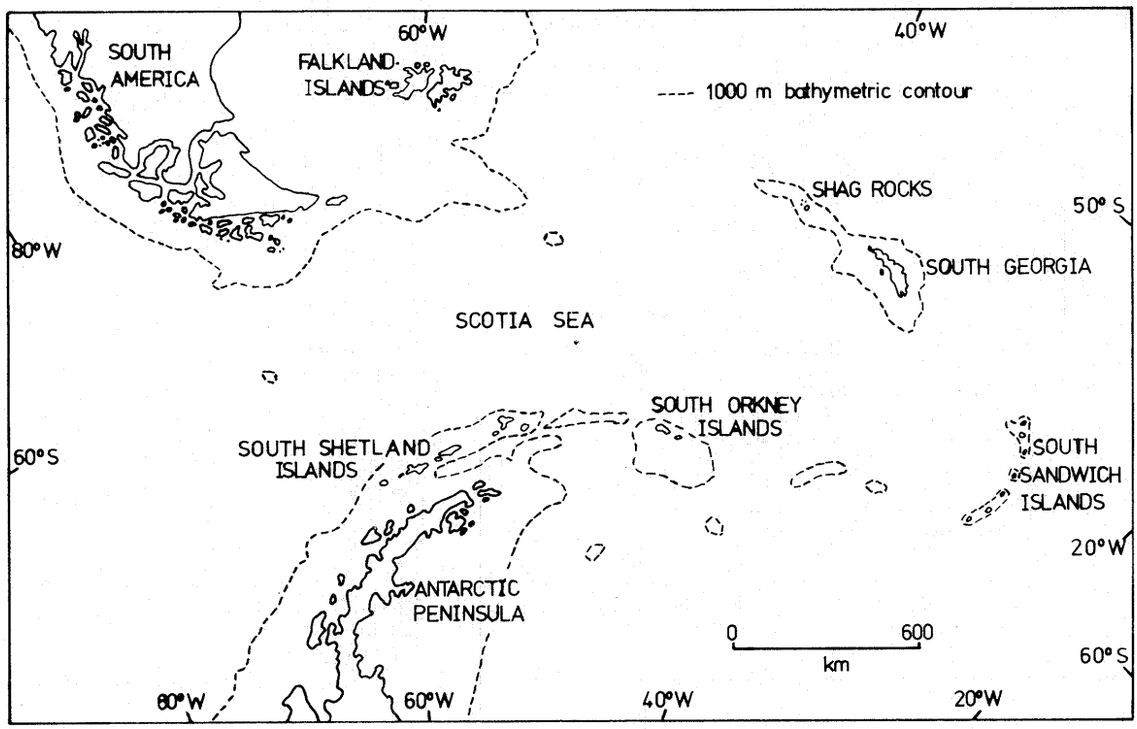

FIGURE 1
Location map of South Georgia.

TABLE I

SUMMARY OF THE GEOLOGICAL HISTORY OF THE DRYGALSKI FJORD COMPLEX AND COOPER BAY FORMATION

		Salomon Glacier Formation	*Cooper Island Formation*	*Novosilski Glacier Formation*	*Cooper Bay Formation*
Upper Mesozoic	Andean orogeny	Faulting		Faulting	Faulting
		Folding		Folding (F1, F2)	Folding (F1*, F2*, F3*, F4*)
		Mylonitization and shearing		Mylonitization	Mylonitization
		Basic dyke intrusion	Basic dyke intrusion		Basic sill intrusion
		Quartz and feldspar veining			
		Aplite and pegmatite formation	Aplite and pegmatite formation	Aplite and pegmatite formation	
		Deformation and ductile shearing			
120	–	Migmatization II; acid–basic breccia and granitoid dyke intrusion	Acid–basic breccia intrusion	Migmatization II; net-veining and formation of feldspar porphyroblasts	Sedimentation (volcaniclastic)
140	–	Basic, diorite, granitoid dyke intrusion	Basic dyke intrusion	Basic dyke intrusion	Marginal-basin formation
181	–	Trendall Crag granodiorite intrusion, hybrid diorite formation and amphibolitization	Cooper Island granophyre and porphyritic felsite intrusion	Microgranitoid and porphyritic felsite intrusion	
186	–	Layered gabbro intrusion	Gabbro–diorite intrusions	Gabbro intrusion	
Lower Mesozoic	Gondwanian orogeny	COOLING AND UPLIFT			
		Folding (F3)			
		Folding	Folding (F2) and boudinage	Open folding	Folding
		Migmatization	Migmatization I		
		Metamorphism (MS1 amphibolite facies)	Metamorphism (MS1 amphibolite facies)	Metamorphism (low grade)	Metamorphism (greenschist facies)
		Folding	Folding (F1)	Folding (F1)	Folding
		Structural area A	Structural area B		
		Sedimentation		Sedimentation	? Porphyritic felsite extrusion Sedimentation

TABLE II

SUMMARY OF K–Ar AND Rb–Sr AGES FROM THE DRYGALSKI FJORD COMPLEX (TANNER AND REX, 1979)

Station number	*Rock type*	*Method*	*Material analysed*	*Age*
M.1320	Cumulate gabbro	K–Ar	Intercumulus hornblende	201±7
M.1410	Cumulate gabbro	K–Ar	Intercumulus hornblende	186±9
M.4173.2	Gabbro-pegmatite	K–Ar	Biotite	149±6
M.2038.7	Trendall Crag granodiorite	K–Ar	Biotite	144±6
M.1695.3	Quartz-diorite dyke	K–Ar	Biotite	141±6
M.1252	Trendall Crag granodiorite	K–Ar	Biotite	139±5
M.1688.3	Quartz-diorite dyke	K–Ar	Biotite	137±5
M.1695.1	Migmatitic tonalite	K–Ar	Biotite	135±5
M.1683.10	Migmatitic granite	K–Ar	Biotite	120±5
M.1804.1 M.2050.A M.4137.1 M.4137.2 M.4145.6	Trendall Crag granodiorite	Rb–Sr	Whole rock	181±30

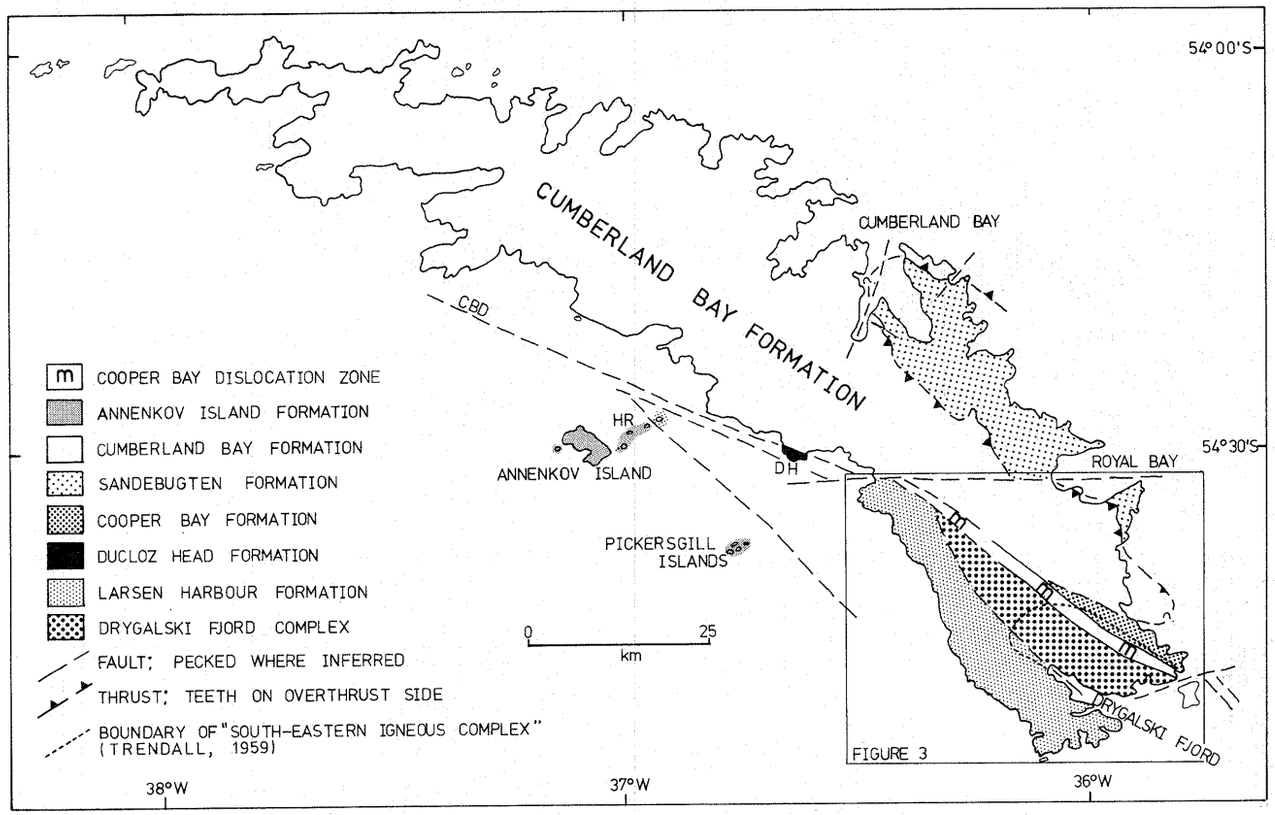

FIGURE 2

Simplified geological map of South Georgia. CBD, Cooper Bay dislocation zone; HR, Hauge Reef; DH, Ducloz Head.

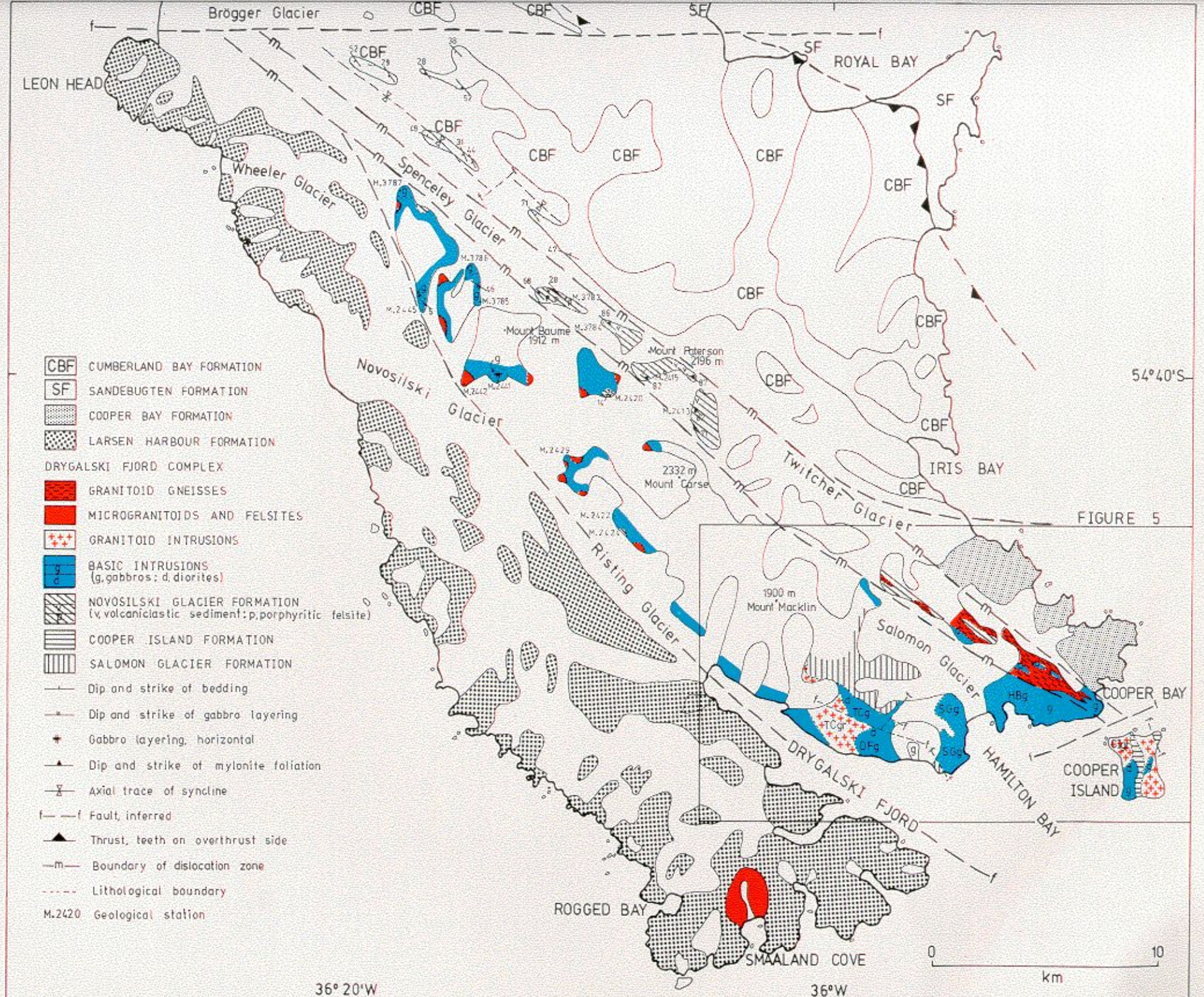
Brögger Glacier
LEON HEAD
Wheeler Glacier
Spenceley Glacier
Novosilski Glacier
Risting Glacier
Twitcher Glacier
Salomon Glacier
ROYAL BAY
IRIS BAY
COOPER BAY
COOPER ISLAND
HAMILTON BAY
DRYGALSKI FJORD
ROGGED BAY
SMAALAND COVE
Mount Baume 1912 m
Mount Paterson 2196 m
2332 m Mount Carse
1900 m Mount Macklin
54°40'S
36° 20'W
36°W
0
10
km
FIGURE 5
CBF CUMBERLAND BAY FORMATION
SF SANDEBUGTEN FORMATION
COOPER BAY FORMATION
LARSEN HARBOUR FORMATION
DRYGALSKI FJORD COMPLEX
GRANITOID GNEISSES
MICROGRANITOIDS AND FELSITES
GRANITOID INTRUSIONS
BASIC INTRUSIONS (g, gabbros; d, diorites)
NOVOSILSKI GLACIER FORMATION (v, volcaniclastic sediment; p, porphyritic felsite)
COOPER ISLAND FORMATION
SALOMON GLACIER FORMATION
Dip and strike of bedding
Dip and strike of gabbro layering
Gabbro layering, horizontal
Dip and strike of mylonite foliation
Axial trace of syncline
Fault, inferred
Thrust, teeth on overthrust side
Boundary of dislocation zone
Lithological boundary
M.2420 Geological station

FIGURE 4
South coast of South Georgia with part of Cooper Island in the foreground.

and therefore all bearings given in the text are true. Structural data are plotted on the lower hemisphere of an equal-area projection and plutonic rocks are named in accordance with the nomenclature recommended by the International Union of Geological Sciences (Streckeisen, 1973).

2. *Physiography*

The Drygalski Fjord Complex forms part of the central mountain range of southern South Georgia with jagged peaks rising to over 2 000 m a.s.l. The high peaks are deeply dissected by three large glaciers, Novosilski, Spenceley and Salomon Glaciers (Fig. 3), and numerous small active valley glaciers.

3. *History of geological exploration*

After the discovery of South Georgia by Captain James Cook in 1775, members of many expeditions visited the island, collected rocks and studied the geology; this work has been summarized in detail by Trendall (1953). Since Filchner's German South Polar Expedition, igneous and metamorphic rocks, which were initially described by Heim (1912), were known to exist in the southern part of South Georgia. Holtedahl (1929), Douglas (1930), Tyrrell (1930), Barth and Holmsen (1939) and Trendall (1959) subsequently described igneous and metamorphic rocks from this area.

Trendall, geologist to the South Georgia Survey Expeditions

TABLE III
SUMMARY OF THE MAJOR GEOLOGICAL DIVISIONS, STRATO-TECTONIC UNITS AND FORMATIONS OF SOUTH GEORGIA

Divisions		*Strato-tectonic units*	*Formations*
Upper Mesozoic Island-arc assemblage		Island-arc facies	Annenkov Island Formation Ducloz Head Formation (inland member)
		Island-arc plutonic suite	
Upper Mesozoic Marginal-basin assemblage	Infill	Andesitic turbidite facies	Cumberland Bay Formation
		Silicic turbidite facies	Sandebugten Formation Cooper Bay Formation Ducloz Head Formation (coastal member)
	Floor	Mafic crust Drygalski Fjord Complex	Larsen Harbour Formation
Lower Mesozoic Continental-crust assemblage		Drygalski Fjord Complex	Novosilski Glacier Formation Cooper Island Formation Salomon Glacier Formation

(1951–52 and 1953–54) led by V. D. Carse, carried out some detailed mapping of these igneous rocks and referred to the area as the "south-eastern igneous complex". He described an intrusive complex of granite, granite-gneiss, migmatite, quartz-diorite and layered gabbro bodies with xenoliths of quartz-granulite "floating" in the granites (Trendall, 1959); two intersecting sets of basic dykes were noted cutting both the igneous complex and the local sediments. According to Trendall (1959), the emplacement of the acid intrusive rocks was probably contemporaneous with orogenic movements which resulted in folding and local metamorphism of the sediments, the basic rocks probably being intruded later.

4. *Summary of the geological history of South Georgia*

South Georgia is a fragment of an extensive island-arc–marginal-basin system (Dalziel and others, 1974, 1975; Suárez and Pettigrew, 1976), which was separated after the early Cretaceous and possibly during the early Tertiary from its original position adjacent to the southern Andes (Barker and Griffiths, 1972). The geology of South Georgia can be divided into three major divisions containing six stratotectonic units (Table III) which are related to specific continental margin, island-arc and back-arc basin features. As tectonic breaks are the only exposed contacts between the above units, their true relationship is not certain.

During the late Jurassic (Tanner and Rex, 1979), a marginal basin formed by emplacement of mafic rocks and by sea-floor spreading within an active magmatic arc (Dalziel and others, 1974). The Larsen Harbour Formation (Mair, in press, *a, b*) (Fig. 3) is the upper part of an ophiolite sequence and may represent part of this basic magma which formed the floor of the basin (Bell and others, 1977). The Drygalski Fjord Complex, which may also be part of the floor of the basin, is a fragment of Lower Mesozoic continental crust and magmatic arc that was rifted off during formation of the basin (Storey and others, 1977).

The marginal basin was infilled during the late Jurassic and early Cretaceous by thick sequences of andesitic and silicic volcaniclastic turbidites (Dalziel and others, 1975), which now form the greater part of South Georgia (Fig. 2). The andesitic turbidite facies (Cumberland Bay Formation) was derived from an active island arc (Trendall, 1959; Dalziel and others, 1975; Suárez and Pettigrew, 1976; Stone, 1980), which was situated on the Pacific side of the basin on the south-west side of South Georgia. The Sandebugten Formation (Trendall, 1959; Stone, 1980), part of the silicic volcaniclastic turbidite facies, was derived from a continental margin source of silicic volcanic rocks, quartzites, granites and gneisses that was probably situated to the north of the basin (Dalziel and others, 1975; Winn, 1978). The Cooper Bay Formation (Stone, 1982) and the coastal member of the Ducloz Head Formation (Storey, in press) are similar to the Sandebugten Formation and were derived from a continental margin and from silicic volcanic rocks.

The island-arc assemblage, situated on the south-west side of South Georgia (Fig. 2), is composed of thick undeformed sequences of Lower Cretaceous andesitic tuffs, mudstones and volcaniclastic breccias (Annenkov Island Formation) intruded by andesitic sills and associated intrusive rocks of an island-arc plutonic suite. These rocks were initially described from Annenkov Island (Pettigrew, 1981) but similar tuffs, mudstones and intrusive rocks crop out within Hauge Reef and the Pickersgill Islands (Tanner and others, 1981), and on Ducloz Head (Storey, in press).

Polyphase deformation and metamorphism up to prehnite–pumpellyite and lower greenschist facies, which have affected the Upper Mesozoic sediments of the marginal basin, may be related to the closing of the basin and migration of the island arc towards the continental landmass (Dalziel and others, 1974, 1975; Bruhn and Dalziel, 1977). At a late stage in the orogenesis, the andesitic greywackes were thrust north-eastward over the quartzose greywackes so that the two formations are now separated by a major thrust plane (Dalziel and others, 1975; Stone, 1980; Tanner, 1982*b*).

A number of basic sheets (Stone, 1980; Mair, 1981), which were probably derived from the same basic magma as that forming the floor of the back-arc basin, intruded the greywackes prior to their deformation.

II. SEDIMENTARY AND METASEDIMENTARY ROCKS

SEDIMENTARY and metasedimentary rocks, which are the country rock of the intrusive rocks, form about 30% of the total outcrop and vary from sediments with identifiable angular clastic grains to intensely deformed *para*gneisses. The sedimentary facies, the degree of metamorphism and deformation, and spatial distribution are used to define the following formations:

i. The *Salomon Glacier Formation,* which crops out in the southern part of the complex, is composed of silicious *para*gneisses and layered migmatites (type locality: M.1697). These were regionally metamorphosed up to amphibolite facies, migmatized and polyphase-deformed prior to and during intrusion of the igneous rocks.

ii. The *Cooper Island Formation* is an inverted sequence of low-grade, quartz-rich clastic sediments and banded hornfelses which crop out on Cooper Island (type locality: M.4131).

iii. The *Novosilski Glacier Formation,* which crops out in the northern part of the complex (type locality: M.2420) and within the dislocation zone, is a sequence of deformed low-grade, quartz-rich clastic sediments, silicious volcaniclastic sediments and porphyritic felsites.

Although the relationship between these formations is not exposed, they are thought to have been deposited along an active continental margin during the early Mesozoic.

A. SALOMON GLACIER FORMATION

The metasediments of the Salomon Glacier Formation were previously described by Trendall (1959) as a flat-lying block of

quartz-granulite which resembled in field appearance a sedimentary quartzite. They range from fine-grained *para*gneisses showing relict sedimentary structures to intensely deformed banded gneisses and layered migmatites. They generally occur as enclaves in the margins of the migmatitic granites and as remnant lenses between the numerous basic dykes, but large blocks up to 10 m long, dissected by basic and acidic dykes, are found within the complex.

1. *Field description*

The banding of the *para*gneisses is defined by biotite-rich and biotite-poor zones. The biotite-rich zones vary in thickness from thin laminated horizons (0.04 cm wide) to bands up to 10 cm wide. The paler biotite-poor zones are quartz-rich and appear in the hand specimen as a pale massive quartzite with occasional biotite-rich horizons. Large-scale bedded units (Fig. 6) crop out to the east of Bogen Glacier (Fig. 5). The "beds", which vary in thickness from 5 cm to 1.5 m, consist of massive quartzo-feldspathic rock separated by thin-bedded and laminated biotite-rich horizons. Gradations from a biotite-poor base to a biotite-rich top, which may represent former graded beds, exist within some thin-bedded horizons. It was not possible to detect grading in the massive fine-grained units.

FIGURE 6
Banded gneisses of the Salomon Glacier Formation.

A sedimentary origin for these rocks is indicated by the preservation of occasional fine cross laminations which exist within laminated beds 1 cm in thickness. Disturbed bedding and laminations, defined by irregular inclined biotite partings, are more widespread. Small slump folds, compressed by later tectonic deformation, also occur within the thin 1 cm beds. Isolated load and flame structures occur on the junction between some biotite-rich zones and quartzo-feldspathic zones.

The banding of the intensely deformed gneisses, although similar to that described above, is tectonic in origin and the rock is devoid of sedimentary structures.

Layered migmatites (*lit-par-lit* injection gneisses), formed during the first migmatization event, are found throughout the *para*gneisses (Fig. 7). Pale-coloured, quartzo-feldspathic pegmatitic layers (neosome) of variable thickness (0.3–5.0 cm) occur repetitively, at 2–3 cm intervals, in the banded gneisses. There is a markedly even distribution of the pegmatitic layers which generally occur parallel to, but occasionally cross-cut, the banding of the gneisses. In the least-deformed gneisses the layering tends to be more irregular in form.

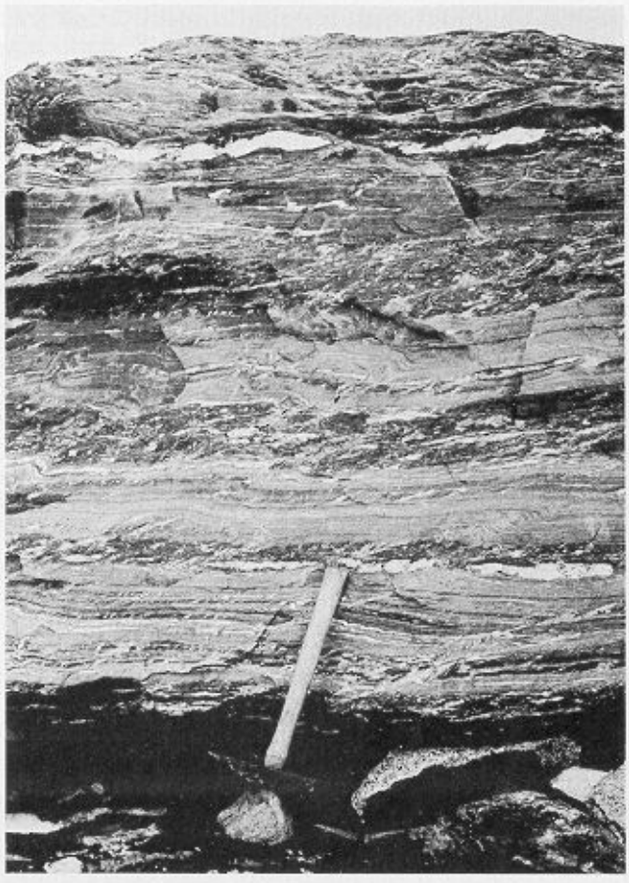

FIGURE 7
Layered migmatites and minor F3 kink folds. The hammer shaft is 35 cm long.

2. *Petrography*

Scattered biotite and subsidiary chlorite flakes exist in a groundmass of fine-grained (0.1–0.2 mm) granoblastic quartz and plagioclase (banded quartz-plagioclase-microcline-perthite-biotite-*para*gneiss). Quartz and plagioclase form equant grains with regular triple junctions. The plagioclase, which may form up to 20% of the rock, is variable in composition (An_{10-35}) with both multiple-twinned and non-twinned feldspars. Potash feldspar, although usually absent, is present within some felsic bands. It occurs as fine crystals, interstitial between the granoblastic quartz and plagioclase, and has a characteristic tricuspate shape moulded around the equant quartz and plagioclase.

The gneissic fabric is defined by a variation in the biotite content. Biotite forms up to 80% of the biotite-rich bands. It is mainly aligned parallel to the banding but metasediments with some disorientated biotite (hornfels texture) and colourless to

pale green poikilitic muscovite plates also occur. Small grains of euhedral to subhedral apatite and zircon (0.05 mm), anhedral and acicular opaque minerals and minute crystals of brown, high-birefringent rutile are common as accessory minerals. The apatite and zircon are often enclosed within biotite.

There is some evidence of retrograde alteration in the *para*gneisses. Pale green pleochroic penninite, epidote, muscovite and prehnite occur as ragged disorientated crystals and as secondary minerals replacing biotite. Prehnite is usually contained within deformed biotite lamellae. Biotite is also present with radiating sheaves of pale green actinolite and chlorite (M.2025.3); sericitization and saussuritization of the plagioclase are common in the more altered rocks. Epidote, chlorite and quartz–prehnite veins cut the metasediments.

The layered migmatites are characterized by fine-grained quartz-oligoclase-microcline-biotite bands (paleosome), similar to the above with coarser-grained lenses of quartz, plagioclase and potash feldspar (neosome). The crystals of the neosome tend to be elongated, xenoblastic in shape (1.0–1.5 mm), with irregular interpenetrating margins giving a ribbon texture to the rock. The neosome is variable in composition, mainly quartz, with about 30% oligoclase and andesine and up to 40% potash feldspar with occasional plates of biotite and poikiloblastic muscovite and chlorite. The potash feldspar varies from rounded xenomorphic crystals intergrown with the plagioclase and quartz to scattered tricuspate interstitial blebs and intruding veinlets; microcline twins and flame-perthitic intergrowths of plagioclase occur. The contact between the neosome and the paleosome is not abrupt but transgressed by irregular veinlets of quartz and feldspar. Rounded corroded quartz and twinned oligoclase may occur at the margins of some of the quartz and feldspar crystals of the neosome, indicating a blastic growth, overgrowing the groundmass of the paleosome. The paleosome is similar to the fine-grained *para*gneisses described above. A concentration of biotite flakes may occur along the margins of the neosome. Poikiloblastic quartz and feldspar crystals occur randomly in the paleosome; interstitial potash feldspar may form up to 15% of the rock. Primary assemblages are as follows:

quartz–plagioclase(An_{35})–biotite±K-feldspar–apatite–zircon.

Secondary assemblages are:

chlorite–epidote±muscovite,
chlorite–epidote–muscovite–prehnite,
chlorite–epidote–prehnite–actinolite.

The above assemblages indicate metamorphism up to amphibolite facies. With the exception of the disorientated poikilitic muscovite and secondary crystals, which may be related to a contact effect of the later intrusions, muscovite is absent. As these rocks were originally of arkosic plagioclase–K-feldspar–biotite–quartz–muscovite composition (see p. 21), they have been metamorphosed up to a high-temperature amphibolite facies where primary muscovite breaks down at the expense of K-feldspar (Turner, 1968). The absence of cordierite, sillimanite and garnet, characteristic minerals of a high-temperature amphibolite facies, may in part be due to temperature or pressure conditions during metamorphism but also due to the bulk composition of the rocks and in particular the Fe, Mn, Mg and Al values. The euhedral apatite and zircon probably crystallized during the metamorphic event; anhedral crystals enclosed in biotite indicate a pre-biotite and perhaps a detrital origin for some of the accessory minerals.

3. *Structural history*

The gneisses and layered migmatites of the Salomon Glacier Formation are subdivided into two structural areas:

A. The weakly deformed *para*gneisses preserved as enclaves in the Trendall Crag granodiorite and as remnant lenses between the basic dykes on the north side of Trendall Crag and on the nunatak north of Storey Glacier (Fig. 8).
B. The intensely deformed gneisses and layered migmatites cropping out in the margins of Salomon Glacier and Bogen Glacier (Fig. 8).

Area A. These *para*gneisses still retain their sedimentary character and have not suffered the intense deformation which has affected the metasediments of area B. The gneissic banding is flat-lying in one part of the area and steeply dipping, almost vertical, elsewhere (Fig. 8, inset A). In the steeply dipping strata, minor isolated close folds (wave-length up to 1 m), with angular and rounded hinge zones and sub-vertical axial surfaces, are found. Open folds, which die out along their length, are also present. The relationship of these folds to possible large-scale structural features was not apparent due to the predominance of igneous rocks in the area.

The segregated quartzo-feldspathic veins are not aligned along a planar surface as in the layered migmatites but are more irregular in form. A complex series of ptygmatic and folded quartz veins, which may be associated with the intrusion of the Trendall Crag granodiorite, cut the banded gneisses and neosome. Basic dykes cut the ptygmatic veins and are in turn intruded and brecciated by granitic veins produced during a second migmatization event.

Area B. Three main periods of deformation have affected the remaining gneisses and layered migmatites, which were studied in detail in one area of good exposure (M.1697; Fig. 8). The rocks are characterized by a well-developed gneissic banding and lack the sedimentary structures of the former section.

Isolated isoclinal folds (Fl) exist within the gneissic banding. These folds, which represent the earliest evidence of deformation in the area (D1), are associated with syn-tectonic metamorphism to amphibolite facies and separation of the migmatitic segregations (migmatization I). The migmatitic segregations and biotite are aligned axial planar to the folds.

During subsequent intense deformation (D2) the migmatitic segregations and MS1 biotite were folded about tight and isoclinal F2 folds. With intense compression, the limbs of the F2 folds were attenuated, folds became completely disrupted and boudinaging of the more competent migmatitic segregations occurred. The form of the boudins (chocolate-block type) indicates that extension took place in two directions, parallel to the *X* and *Y* directions of the disrupted isoclinal folds. During the deformation, the F2 folds became tight or isoclinal; many were destroyed by shearing parallel to the axial plane of the folds. The original fabric (SS and S1) became re-aligned parallel to the axial plane of the folds (transposed fabric of Sander *from* Turner and Weiss (1963)) and formed the present banding of the layered migmatites (S2). A strong lineation, defined by rodding and disruption of the pre-existing quartzo-feldspathic segregations and F2 fold hinges, occurs on the S2 planes. The quartz-rodding lineation is parallel to the fold hinges of the isoclinal

folds. A mineral lineation, defined by alignment of the biotite flakes, also occurs parallel to the quartz-rodding lineation. In the absence of re-folded folds and a set of minor structures associated with each fold phase, it is possible that the F1 and F2 fold phases described above were formed by progressive deformation during a single event. However, as the D2 deformation was so intense and only isolated occurrences of F1 fold hinges were identified, it is not surprising that the re-folded folds and minor structures were not observed.

The (S2) gneissic banding and disrupted migmatitic segregations were subjected to a further deformation event (D3) of varied intensity which resulted in the development of a series of F3 folds, a crenulation cleavage and great variation in the orientation of the banding of the layered migmatites (Fig. 8). At station M.1697, on the western margin of Salomon Glacier, the banding is flat-lying (Fig. 8, inset H), whereas throughout the remainder of the area the banding forms a vague girdle (Fig. 8, inset D) about the F3 fold axis. The folds vary from fine crenulations to "similar" folds with a wave-length up to 2 m. At the base of station M.1697, the folds are represented by widely spaced kink bands (Fig. 7). In the upper parts of the outcrop, close similar folds with well-defined hinge zones (Fig. 9) plunge

FIGURE 9
F3 folding of the layered migmatites. The hammer shaft is 35 cm long.

gently (0–10°) to the north-east and south-west. Gently inclined hinge surfaces dip at 15–20° to the north-west (Fig. 8, inset J). Throughout the remainder of the area there is great variation in the trend of the fold hinges (Fig. 8, inset E). This may be a primary or a secondary feature due to more than one phase of folding. A crenulation lineation, parallel to the hinges of the F3 folds, occurs on the S2 planes at an angle to the quartz-rodding lineation of the D2 event (Fig. 8, inset J).

Although the majority of the basic and acidic dykes, and brecciating veinlets, cut the F3 folds, there is some inter-relationship between igneous activity and deformation. The inclined layering of the gabbros, to the west of Bogen Glacier (Fig. 8, inset C), has a similar orientation to the banding of the gneisses. Bell and others (1977) previously suggested that D3 (D4 *op. cit.*) deformation occurred after formation of the migmatites. Although in most instances the migmatitic granites cut and destroyed F3 folds, irregular ductile folding (Fig. 10) and zones of intense disharmonic (? F3) folding (Fig. 11) indicate some relationship between migmatization and deformation; the ductile folds may represent the final stages of the D3 event. A foliated gneissic fabric in the migmatitic granites also indicates deformation during the second migmatization event.

Closely spaced, 20–50 cm sub-horizontal joints and kink planes occur in the Salomon Glacier gneisses and migmatites. They are seen as pale green bands cutting the darker biotite-rich gneisses and represent zones of hydrothermal alteration with formation of chlorite, prehnite and epidote.

Although the relationship between the structural areas A and B is uncertain, it is most likely that the deformation, metamorphism and slight segregation of the quartz veins of area A is equivalent to the F1 deformation and metamorphism of area B. With the exception of open folding, area A was not deformed during the subsequent intense F2 and F3 deformation of area B.

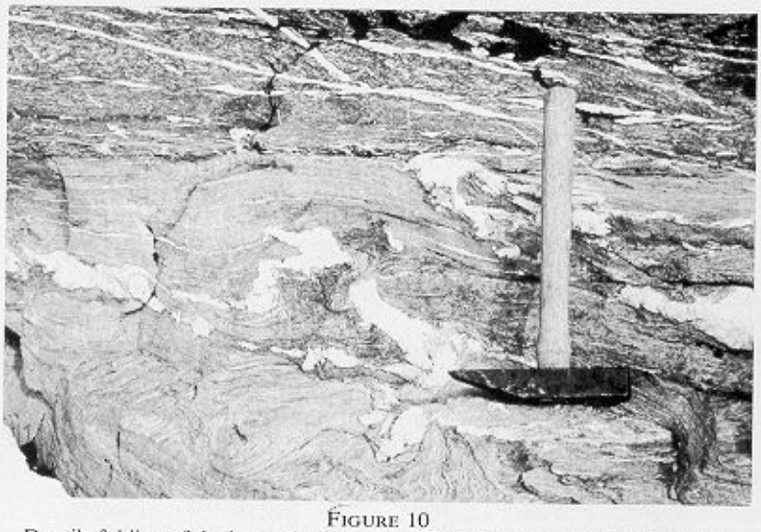

FIGURE 10
Ductile folding of the layered migmatites. The hammer shaft is 35 cm long.

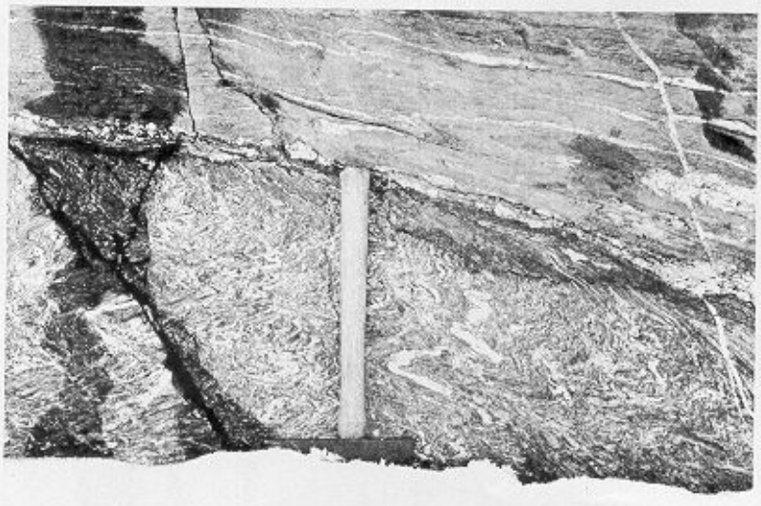

FIGURE 11
Zone of intense F3 folding of the layered migmatites. The hammer shaft is 35 cm long.

B. Cooper Island Formation

Clastic sediments intruded by basic and acidic rocks are best preserved on the north-east promontory of Cooper Island (M.4131; Fig. 5). They form a 50 m thick, inverted flat-lying sequence of laminated mudstones, siltstones and massive sandstones. Throughout the remainder of Cooper Island, scattered lenses of sediment, recrystallized to hornblende-hornfels facies (banded hornfelses), are found between the numerous basic and acidic intrusions.

1. *Field description*

Thin-bedded, pale green fine-grained sandstones, dark brown to black siltstones and black mudstones form isolated laminated units up to 10 m thick (Fig. 12) within a sequence of pale grey to green massive sandstone units. Convolute laminations, micro- and ripple cross laminations and graded beds are well preserved within the laminated units. The massive sandstone units (Fig. 13), which are up to 5 m thick, are mainly fine- to medium-grained (0.05–0.8 mm) with a marked lack of coarse-grained material. Isolated flakes of re-worked black siltstone, up to 3 cm long, occur at the base of some units. Bottom structures are well developed and include load and flame structures (Fig. 14), rill and groove casts, and prod marks. Narrow (up to 3 cm) sedimentary dykes of varied orientation and small-scale syn-sedimentary slumps (orientation unknown) and faults also occur. Rare plant-stem impressions, vermicular trace fossils and irregular burrows are preserved in the mudstone horizons.

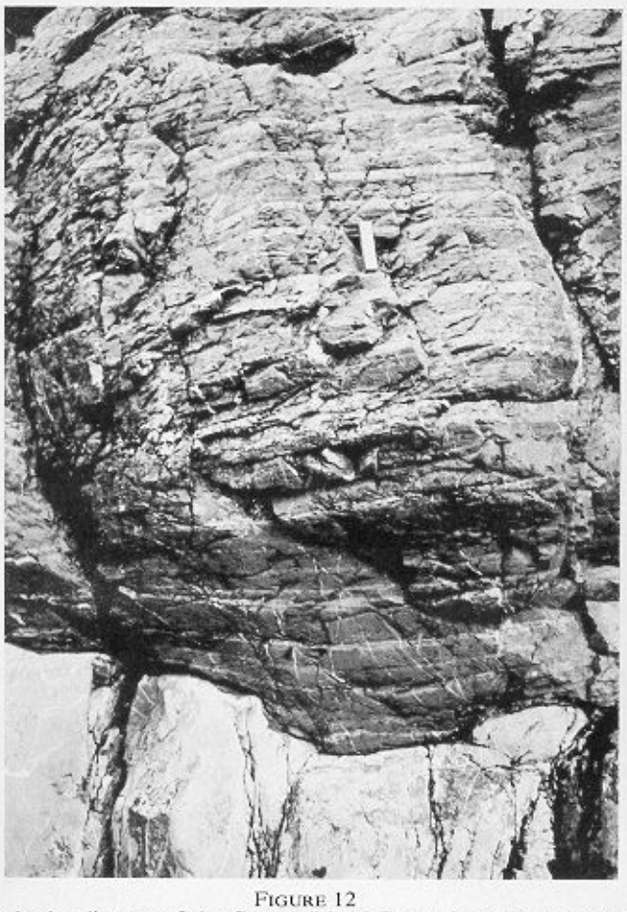

Figure 12
Fine-grained sediments of the Cooper Island Formation. The scale is 10 cm long.

Figure 13
Massive sandstone unit of the Cooper Island Formation. The bird in the foreground is 18 cm high.

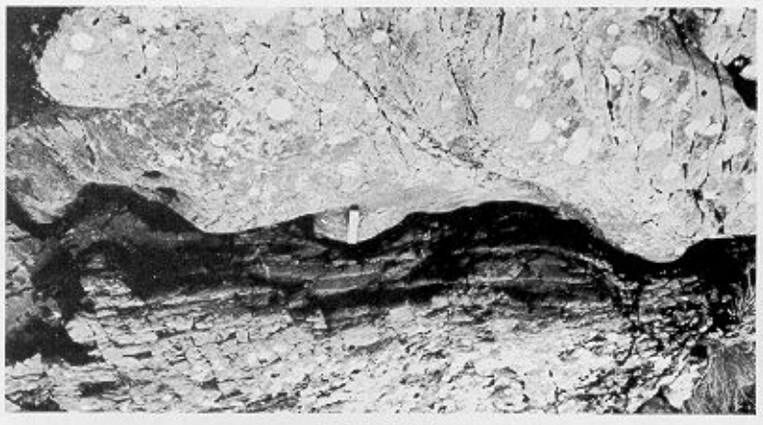

Figure 14
Bottom structures of the Cooper Island Formation. The scale is 10 cm long.

2. *Petrography*

a. *Argillaceous sediments.* The clastic sandstone units of the Cooper Island Formation are moderately to poorly sorted immature sub-quartzose sandstones (<75% detrital grains are quartzose), which fall in the arkosic (feldspathic) greywacke and arkosic arenite field of Pettijohn and others (1972). A predominance of angular quartz, feldspar and lithic fragments (0.1–0.8 mm grain-size) derived from a granitic, metamorphic and volcanic terrain are set in a partially recrystallized quartzo-feldspathic groundmass. Modal analyses are given in Table IV.

Plagioclase (oligoclase-andesine) and quartz are the commonest crystal fragments. Cloudy, sericitized, saussuritized, twinned and untwinned feldspar fragments, often enclosing zircons, are present. Potash feldspar (microcline) and perthite, although entirely absent from some rocks, form up to 3% of thin section M.4131.4. Quartz shows some undulose extinction.

Occasional biotite, chlorite and muscovite plates up to 3.0 mm wide (Fig. 15a) are bent and deformed between crystal

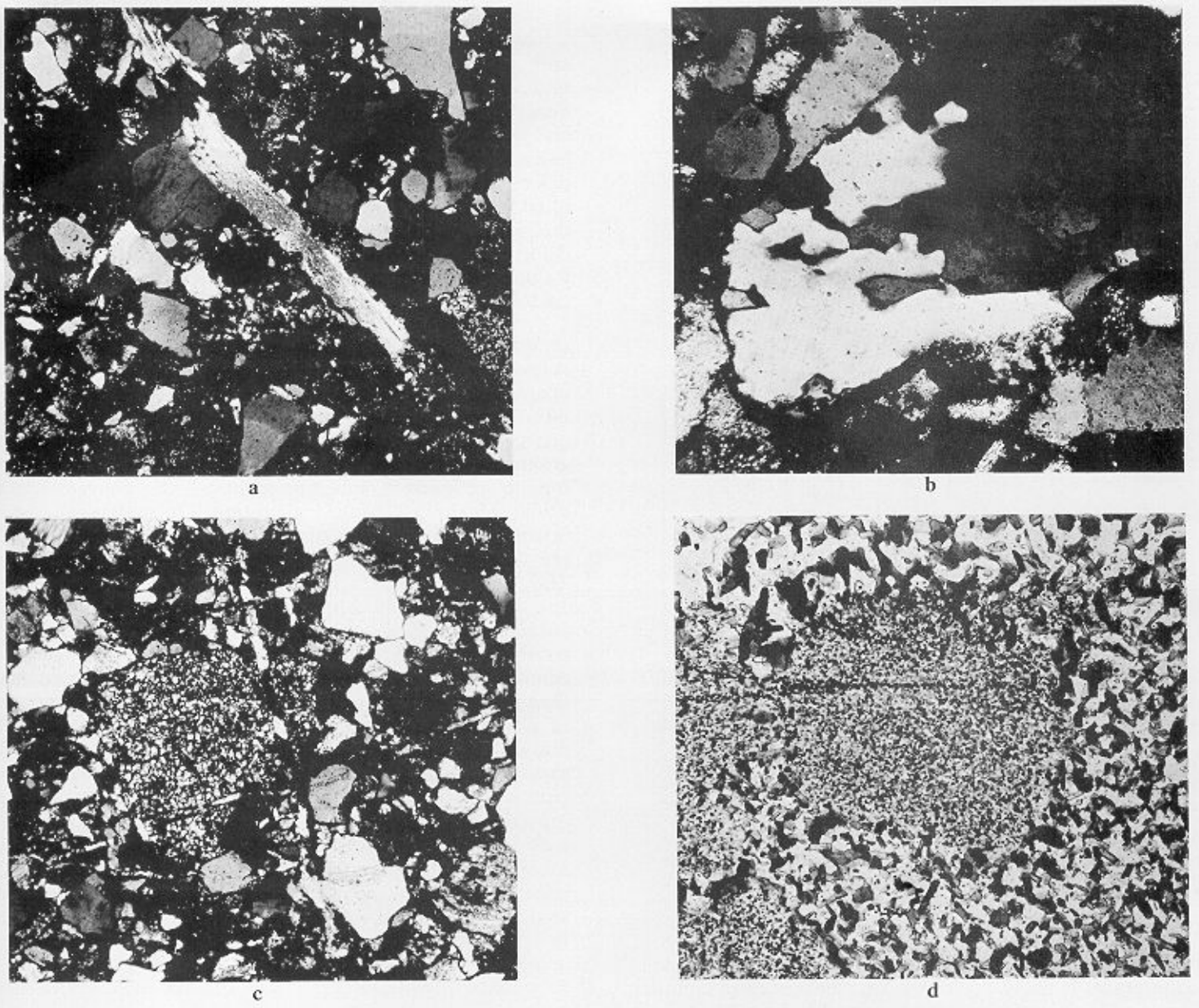

FIGURE 15

a. Detrital mica in a sub-quartzose sandstone of the Cooper Island Formation. (M.4131.4; X-nicols; ×40)
b. Composite quartz clast in a sandstone of the Cooper Island Formation. (M.4131.13; X-nicols; ×160)
c. Felsite fragment in a sandstone of the Cooper Island Formation. (M.4131.13; X-nicols; ×40)
d. Cordierite porphyroblast packed with fine-grained inclusions. (M.1970.4B; ordinary light; ×160)

and rock fragments. Biotite laths are pale coloured and partially replaced by chlorite. Subsidiary rounded, heavy mineral fragments include epidote, sphene, garnet, opaque minerals, zircon and apatite.

Medium-grained (0.25–0.60 mm) polycrystalline quartz, quartz-plagioclase, quartz–plagioclase–perthite and quartz–plagioclase–muscovite are the most abundant lithic fragments. Well-developed angular and irregular crystal margins (Fig. 15b) within the polycrystalline fragments indicate an igneous and metamorphic origin for the clasts. Metamorphic fragments also include sheared quartz-plagioclase-gneisses, mica-bearing quartzo-feldspathic schists, chlorite- and muscovite-schists, quartzites (polycrystalline quartz) and fine-grained granoblastic quartz-plagioclase-potash feldspar-muscovite-gneissic fragments. The origin of the granoblastic fragments with well-deformed triple junctions is uncertain. These may have been derived from recrystallized sedimentary quartzites, vein quartz or segregations from a fine-grained gneissic terrain. In spite of

TABLE IV
MODAL ANALYSES OF SANDSTONES FROM THE COOPER ISLAND FORMATION

	M.4131.15	*M.4131.13*	*M.4131.4*
Quartz	23	24	25
Plagioclase	30	36	17
Perthite	<1	<1	3
Biotite	3	3	4
Epidote	1	–	–
Opaque minerals	<1	<1	<1
Muscovite	<1	<1	<1
Garnet	<1	<1	<1
Sphene	<1	<1	<1
Calcite	–	–	–
Chlorite	2	1	2
Lithic fragments			
Granite/gneiss	13	12	11
Felsite	2	2	8
Metamorphic	7	5	4
Sedimentary	1	1	2
Matrix	16	14	23

Rock modes were determined using a Swift point counter set at a point interval of 0·5 mm. The vertical distance between each traverse was also 0·5 mm. 1 000 points were counted per thin section.

the uncertainties, a metamorphic and igneous origin for most of the clastic grains is likely. Volcanic fragments are not common but occasional microcrystalline quartz–feldspar felsic fragments (Fig. 15c) may be derived from acidic volcanic rocks. Broken phenocrysts were recorded within some of these clasts. Re-worked penecontemporaneous sedimentary fragments form a small proportion (<2%) of the lithic fragments.

The matrix is composed of fine-grained crystal and lithic fragments partly replaced and overgrown by sericite, epidote, chlorite, and opaque granules partially replaced by sphene and leucoxene. Prehnite, epidote–quartz, quartz–albite and chlorite veins cut the rocks.

The predominance of quartz and plagioclase crystal fragments, biotite and muscovite crystals, and granitic, granitic gneiss and metamorphic lithic fragments suggest that the sediments were derived from an eroded continental fragment comprising acid plutonic and gneissic metamorphic rocks with some schists, quartzites and occasional acid volcanic rocks. The biotite and muscovite flakes may have been derived from a metamorphic or igneous terrain. Assemblage: quartz–sericite–chlorite–epidote.

b. *Arenaceous sediments*. The siltstones and mudstones are similar to the above but are mainly composed of angular quartz and feldspar crystal fragments and aligned pale biotite, muscovite and chlorite with accessory opaque and epidote minerals. Variation in the concentration of the micaceous plates, and bands of opaque granules define the original bedding of the laminated units. Small-scale graded beds and syn-sedimentary deformation structures are present. The micaceous plates are often bent around the angular quartz and feldspar fragments; this indicates that the micas are detrital in origin and were deformed during compaction. The quartz and feldspar fragments are characterized by an undulose extinction. Detrital epidote, sphene and zircon are common in the fine-grained units.

c. *Banded hornfelses*. Banding and bedding laminations are defined by variations in the concentration of biotite, chlorite and opaque minerals. Disorientated biotite, which may form up to 80% of the biotite-rich bands, is scattered in a granoblastic quartz–oligoclase groundmass peppered by fine-grained opaque granules, apatite and zircon. Secondary chlorite, epidote and sericite are found in some thin sections, often concentrated along veins of hydrothermal alteration. Intensely altered, disorientated cordierite poikiloblasts (Fig. 15d), up to 2 mm long, are found mainly concentrated within the biotite-rich layers. They are packed with inclusions of recrystallized groundmass and opaque laminae. Although the optical properties (colourless, parallel extinction, biaxial positive, low relief and low birefringence) are not diagnostic, the intense alteration to penninite, muscovite, sericite and a yellow alteration mineral, pinite, and the high proportion of inclusions are characteristic of cordierite. Secondary muscovite is aligned parallel to the margins of the crystal. Chlorite with epidote inclusions is the main ferromagnesian mineral in some bands. As it co-exists with biotite, it is probably of secondary origin. Disorientated ragged crystals of epidote, zoisite and clinozoisite are common also with scattered euhedral and anhedral opaque minerals (altered to sphene and leucoxene), zircon and apatite. The opaque minerals often define a lamination which may be orientated at an angle to the banding (cross lamination).
Primary assemblage: quartz–oligoclase–biotite–cordierite–apatite.
Secondary assemblage: chlorite–sericite–epidote–sphene–pinite.

3. *Structural and metamorphic history*

The sediments exposed on the north-east promontory probably lie on the inverted limb of a major fold, the orientation of which is unknown. Slight variation in the dip and strike of the strata (Fig. 8, inset G) is the result of open folds. A penetrative fabric is not developed; the flaky minerals, chlorite and muscovite, are aligned parallel to bedding in some specimens. A 5 m zone of more intense deformation is found within the sediments of the north-east promontory. The folds are mainly small-scale angular kink folds of variable orientation and dimension. Late small-scale faulting and brittle deformation considerably disrupt the bedding of these rocks.

Banding within the scattered metasedimentary lenses and enclaves, which occur throughout the remainder of the island, is more variable in orientation (Fig. 8, inset G) and the rocks have supported more extensive recrystallization.

The metamorphic facies of these rocks is difficult to access as

the clastic sediments were derived from a metamorphic and plutonic terrain. The cloudiness, sericitization and saussuritization of the feldspars may be a primary feature inherited from the metamorphic terrain. The secondary sericite, chlorite and epidote present in the matrix are not diagnostic of a metamorphic facies but indicate a low grade of metamorphism for the rocks of the north-east promontory.

The mineral assemblage and textures of the banded hornfelses indicate contact thermal metamorphism up to the biotite–cordierite zone of the hornblende-hornfels facies (Turner, 1968) with retrogression to a chlorite–epidote assemblage.

C. Novosilski Glacier Formation

Low-grade epiclastic and volcaniclastic sediments and porphyritic felsites of the Novosilski Glacier Formation, intruded by basic and acidic rocks, crop out at a number of localities in the Novosilski, Spenceley and Risting Glacier basins and within the dislocation zone (Fig. 3). Within the northern part of the zone, the epiclastic sediments are closely associated with, and probably grade into, the volcaniclastic sediments and porphyritic felsites. The true relationship is uncertain as all are affected by a strong mylonite fabric which has destroyed previous contact relations. The sediments outside of the dislocation zone have suffered low-grade metamorphism, whereas within the zone they were metamorphosed up to the biotite grade of greenschist facies and were deformed prior to intrusion of the igneous rocks, mylonitization, retrogression and further deformation.

1. *Field description*

The epiclastic sediments are predominantly thin-bedded, pale green and grey sub-quartzose sandstones with interlaminated black mudstone and shale horizons. Within the dislocation zone, lenses of sandstone and shale units, unaffected by the mylonite fabric, co-exist with white, pale and grey iron-stained massive volcaniclastic rocks and areas of pale grey massive porphyritic felsites with a strong schistose mylonite fabric.

2. *Petrography*

a. *Epiclastic sediments.* In thin section the rocks are similar to the sediments of the Cooper Island Formation. They are poorly sorted immature sub-arkosic arenites and sub-quartzose greywackes derived from a plutonic and metamorphic terrain. Angular quartz and plagioclase crystal fragments are the most abundant detrital fragments; remaining crystal fragments include biotite, muscovite (0.9 mm long), chlorite, epidote, sphene, apatite, opaque minerals (generally altered to sphene and leucoxene), (?) garnet and zircon. The lithic fragments are mainly polycrystalline medium-grained (0.25–0.60 cm) quartz, quartz–plagioclase, and fine-grained granoblastic quartz, quartz–feldspar and quartz–mica fragments. The presence of recrystallized rock fragments, porphyroblastic quartz crystals with fine-grained inclusions, myrmekitic intergrowth, sheared gneissic and schistose fragments and aggregates of biotite suggests that the rocks were derived from a granitic and granite-gneiss terrain. Rare microcrystalline felsic clasts, generally clouded with sericite or opaque granules, may be derived from acid volcanic rocks.

Recrystallization was not an important process in these sediments but sericite, epidote and opaque granules make identification and differentiation of the matrix minerals difficult. Detrital biotite is pale coloured and partially replaced by chlorite. Marginal recrystallization of some of the clasts has also occurred.

Similar clastic sediments crop out within the northern part of the dislocation zone. In some thin sections (M.2413.3 and 2417.1) poorly orientated biotite is common in the matrix. Where deformation is intense, the biotite is orientated around the detrital clasts. Some biotites are pale coloured and partially replaced by chlorite. Further evidence of retrogression is indicated by partial and complete replacement of the matrix minerals and some clasts by veins and irregular patches of sericite (Fig. 16a).

b. *Volcaniclastic sediments.* Within the dislocation zone a gradation exists from clastic sediments with a small proportion of volcanic fragments to volcaniclastic sediments with up to 75% volcanic clasts. Quartz and feldspar crystal fragments (up to 3 mm) often show euhedral shapes (phenocrysts) and partially resorbed crystal margins (Fig. 16b). The feldspars are twinned oligoclase-andesine crystals up to 1 cm long, some of which have a cross-hatched albite-twin pattern, whilst others are partially replaced by potash feldspar and perthite (Fig. 16c). Phenocrysts of potash feldspar may be of primary or secondary origin. The acidic volcanic fragments, which are variable in texture and composition, are microcrystalline and porphyritic rhyolites and dacites. The dacitic clasts contain aligned and disorientated feldspar microlites with interstitial quartz. Also present are polycrystalline mosaic quartz, feldspar spherulites, medium-grained granitic and gneissose clasts, allanite, sphene, zircon and epidote crystal fragments. Euhedral allanite crystals, which are not recorded in the clastic sediments, are a characteristic accessory of the volcaniclastic sediments.

The matrix, similar to that of the epiclastic sediments, contains orientated and disorientated biotite, muscovite and chlorite laths. The biotite crystals are often concentrated in irregular aggregates within the matrix (M.3784.3; Fig. 16d). Within the schistose rocks, detrital clasts, phenocrysts and biotite aggregates (M.2414.2) are surrounded by a strong chlorite, muscovite and occasionally a biotite schistosity. Disorientated biotite also surrounds some phenocrysts and detrital clasts within the fabric.

c. *Porphyritic felsites.* These rocks are similar to the volcaniclastic sediments described above. They contain quartz and feldspar phenocrysts in an even-textured microcrystalline matrix. As potash feldspar (indicated by staining) is common within the matrix, the felsites are mainly rhyolites; some dacites were recorded. Some felsites are partially recrystallized to granular mosaics of polygonal quartz. A strong chlorite, muscovite and biotite schistosity is present in some specimens.

3. *Structure and metamorphism*

Outside the dislocation zone the clastic sediments have not been extensively recrystallized. Chlorite and sericite define a weak fabric which passes around and is deflected by the detrital clasts. The secondary assemblage (chlorite–sericite–epidote) is not diagnostic but indicates a sub-greenschist- or low greenschist-facies metamorphism.

Within the dislocation zone the strong schistosity, which is sub-parallel to the margins of the zone and occurred after intrusion of the igneous rocks, is related to formation of the mylonites and will be discussed below.

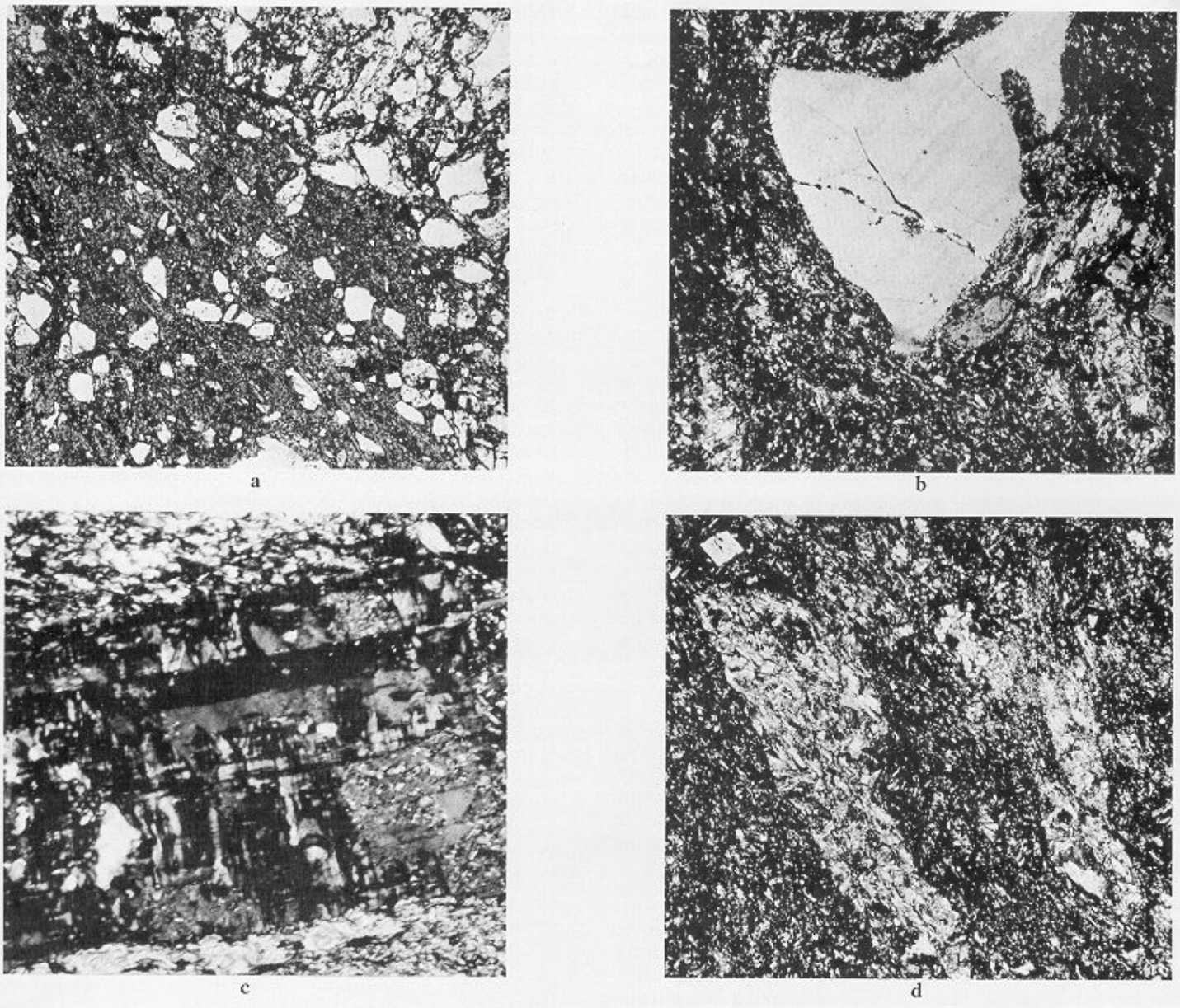

FIGURE 16
a. Sericite replacing the groundmass of a sub-quartzose sandstone of the Novosilski Glacier Formation. (M.2413.3; ordinary light; ×40)
b. Partially resorbed quartz phenocryst in a volcaniclastic sediment of the Novosilski Glacier Formation. (M.3784.3; X-nicols; ×40)
c. Microcline replacing a plagioclase phenocryst in a volcaniclastic sediment of the Novosilski Glacier Formation. (M.2415.1; X-nicols; ×160)
d. Clusters of biotite within a volcaniclastic sediment of the Novosilski Glacier Formation. (M.3784.3; X-nicols; ×40)

Within the weakly mylonitized volcaniclastic and epiclastic rocks biotite is an important constituent. It may represent detrital biotite inherited from a metamorphic or igneous terrain or may be metamorphic in origin due to thermal or regional metamorphism of the sediments prior to mylonitization; the clusters may represent pseudomorphs of former detrital clasts. However, as biotite is common within a recrystallized matrix of these rocks and was not present as fine-grained crystals within similar clastic sediments outside of the dislocation zone, it is unlikely it is detrital in origin. It is thus concluded that these rocks have been metamorphosed up to the biotite grade of the greenschist facies and that the aggregates of biotite represent disjointed biotite-rich laminae. The orientation of the biotites indicates that these rocks had been deformed and that a crenulated cleavage was present prior to the mylonitization. Partial retrogression to a chlorite–epidote–sericite assemblage accompanied mylonitization.

D. Discussion

The clastic sediments of the Novosilski Glacier and Cooper Island Formations are petrographically similar and are probably part of the same sedimentary sequence. They were both derived from a granitic and granite-gneiss metamorphic terrain and from acidic volcanic rocks.

On Cooper Island, a gradation exists from the clastic sediments of the north-east promontory to the banded hornfelses found elsewhere on the island. The latter are recrystallized sediments petrographically similar to the undeformed gneisses of the Salomon Glacier Formation; this suggests that the Salomon Glacier, Cooper Island and Novosilski Glacier Formations may be correlated and that variable degrees of deformation and metamorphism affected the formations during a single orogenic event prior to intrusion of the basic rocks.

Although these rocks may have a similar origin, there is some variation in the sedimentary facies. The form of the laminated sediments, the massive poorly sorted immature sub-quartzose sandstone units and associated sedimentary structures suggest that the Cooper Island Formation sediments represent part of a turbidite sequence; these massive sandstone units were not seen in the Novosilski Glacier Formation sediments. The sedimentary structures and banding of the least-deformed Salomon Glacier Formation gneisses also indicate that they may have been deposited by turbidity currents.

It is thus concluded that the sediments and metasediments, which form the country rock of the intrusive rocks, were derived from a continental fragment comprising outcrops of metamorphic and acidic igneous rocks (essentially plutonic but with minor volcanic rocks) and deposited in an offshore basin. These rocks suffered varied degrees of polyphase deformation and recrystallization about an east–west axis (D2) and subsequent asymmetric folding about north-east–south-west axes (D3). The Salomon Glacier Formation suffered intense deformation, recrystallization and migmatization up to a high-temperature amphibolite facies, whereas clastic sediments of the Cooper Island Formation retained their sedimentary character with low-grade, sub-greenschist-facies metamorphism and lesser degrees of deformation.

As the deformed and metamorphosed sediments are intruded by plutonic acid and basic rocks, the oldest of which has been dated as early Jurassic (Tanner and Rex, 1979), it is concluded that the sediments originally formed part of a continental margin assemblage that was deformed during a late Palaeozoic or, at the latest, an early Mesozoic (Gondwanide) orogeny and that they now form part of the pre-Jurassic basement of South Georgia.

III. GABBROS

Gabbroic rocks, which vary in composition from feldspathic leucogabbros to ultramafic rocks, are the most abundant igneous rocks of the complex. They range from small intrusive bodies to large irregular plutons. The larger plutons, which frequently exhibit cumulate layering, are mainly exposed in the south of the complex.

1. *Field relations*

Faulted contacts and chilled margins against the deformed gneisses of the Salomon Glacier Formation and sediments of the Novosilski Glacier Formation are present throughout the complex. The gabbros are intruded by basic and acidic dykes, irregular acid–basic intrusive breccias, migmatitic granites, and quartz and feldspar veins.

The relationship to the larger granitoid (Trendall Crag granodiorite) and quartz-diorite bodies is complex, as contact relations are in most cases destroyed by the later intrusive breccias and migmatites. It was previously suggested (Bell and others, 1977) that the gabbros were emplaced at the same time as the basic dykes which cut the Trendall Crag granodiorite (inferring that the gabbros are younger than the granodiorites). However, to the north of Bogen Glacier (Fig. 5) the contact zone is cut by basic dykes without the formation of intrusive breccias; this indicates an original intrusive contact where the Trendall Crag granodiorite intrudes and assimilates the basic rocks; diorites and ocellar hybrids are formed by contamination of the basic magma along this contact zone.

Dating of intercumulus hornblende (Tanner and Rex, 1979) within the gabbros (201±7 and 186±9 Ma) and a Rb-Sr isochron age for the Trendall Crag granodiorite (186±30 Ma) are not conclusive due to the high error obtained on the Rb-Sr isochron in confirming this relationship; they support a close association in time of the acid and basic magmas, and indicate that magmatic activity commenced during the early Jurassic. However, these dates must be interpreted with care for the following reasons: the origin of hornblende is difficult to establish within any particular rock (hornblende appears as an intercumulus phase, by late-stage autometasomatism and by widespread post-consolidation amphibolitization of the gabbro); the higher age (201 Ma) may be complicated by the formation of a gabbroic pegmatite and subsequent diffusion of radiogenic argon within the sample (dating of a biotite within a similar pegmatite gives a K-Ar age of 149±6 Ma); some of the rocks used in the Rb-Sr isochron are hybrid rocks formed by mixing of the acid and basic magmas; petrographically similar gabbroic plutons intrude both the Larsen Harbour Formation (inferred age 130–150 Ma; Tanner and Rex, 1979) and the Drygalski Fjord Complex. These points suggest three possible alternatives:

i. There was more than one period of gabbro emplacement.
ii. The ages are in error and all the gabbros formed after formation of the Larsen Harbour Formation (130–150 Ma).
iii. The ages of the gabbros are correct and the Larsen Harbour Formation formed prior to 186 Ma.

Due to the concentration of dates in the early Mesozoic and the correlation of basic dykes with the formation of the Larsen

Harbour Formation, the author concludes that gabbroic activity began during the early Jurassic and that it was continuous over a period of time with some emplacement of plutons at higher levels in the complex after formation of the Larsen Harbour Formation.

On the eastern margin of the complex the gabbros are affected by the mylonite shear zone. Minor ductile shear zones also cut the gabbros in the Hamilton Bay area.

2. *Lithology*

The gabbros are mainly medium-grained (1–2 mm), pale green to dark grey and black massive rocks of variable composition (troctolites, olivine-gabbros, hornblende-pyroxene-gabbros, two-pyroxene gabbros, norites, leucogabbros and metagabbros). The more basic lithologies weather to a pale brown colour. A mottled clump texture is found on weathered surfaces where large intercumulus poikilitic ferromagnesian minerals occur in a medium-grained green groundmass. Bulbous exfoliation weathered surfaces are formed in the Trendall Crag area.

FIGURE 17
Layered gabbro. The scale is 10 cm long.

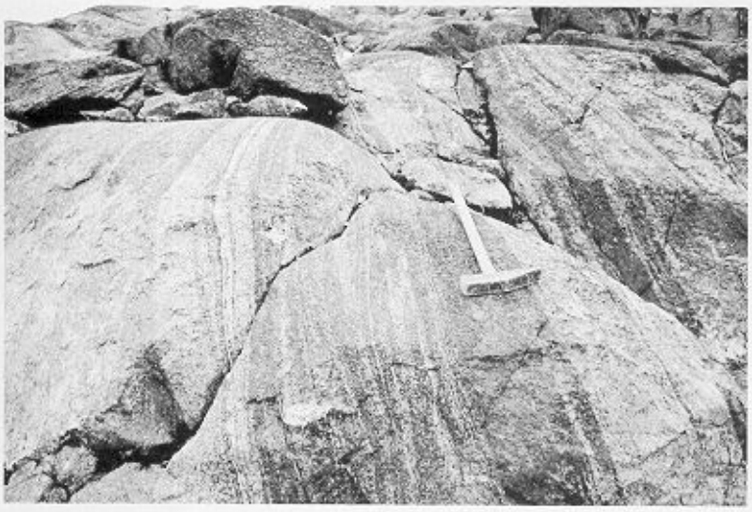

FIGURE 18
Layered gabbro. The hammer shaft is 60 cm long.

Many of the larger plutons, as well as displaying cumulate rhythmic layering (Figs 17 and 18), are composite bodies; intrusive contacts are present between different phases and enclaves of variable grain-size and composition, sometimes layered, are found within the intrusions. In the Hamilton Bay area, knolls of feldspathic gabbro crop out alongside knolls of metagabbro. Contacts are not exposed but these may be faulted, as deep gullies separate many of the knolls. Ultramafic inclusions are enclosed within the feldspathic leucogabbros in this area. Coarse gabbroic pegmatites cut the layered and massive gabbros and coarse-grained crystal segregations of feldspar and ferromagnesian minerals occur in some intrusions.

3. *Petrography*

The gabbroic rocks consist of variable amounts of plagioclase, augite, hypersthene, olivine and hornblende with accessory apatite, zircon, quartz, and opaque minerals, ilmenite, magnetite and spinel. Alteration minerals include serpentine, mica, epidote, chlorite, sphene and tremolite-actinolite. In the cumulate rocks, stumpy prisms of plagioclase, augite and olivine are in contact along triple junctions (Fig. 19a). They are often enclosed within large poikilitic augite (Fig. 19b), hypersthene and hornblende crystals. There is a marked variation in grain-size between the enclosed crystals and those outside. Excluding the poikilitic crystals, there is sometimes a bimodal grain-size distribution; fine crystals of feldspar and ferromagnesian minerals fill the interstices between the larger stumpy prisms. An alignment of the elongated crystals is present in some thin sections.

Plagioclase varies in composition, An_{55-80}. Poikilitic plates were not recorded but inclusions occur in the margins of some crystals.

Rounded olivine crystals, which may form up to 70% of the troctolites and olivine-gabbros, display characteristic fractures which are often filled with antigorite and lined with secondary magnetite granules. Feldspar and augite inclusions are enclosed within the margins of some crystals. Some olivines are uniformly rimmed (corona structure) by single or multiple zones of orthopyroxene, pale green and brown hornblende and hornblende–spinel symplectites (Fig. 20).

Augite and pleochroic hypersthene (light green to pink) occur as stumpy rounded crystals and as large poikilitic sheets enclosing olivine, feldspar, augite, hypersthene and opaque minerals. A schiller structure, defined by lines of opaque granules, is found in some augite crystals. Alteration patches of optically continuous light brown hornblende form within some pyroxene crystals and light green, brown or colourless rims of hornblende (uralitization) surround them. Fine biotite crystals are found within, and are aligned normal to, some amphibole rims.

In the hornblende-pyroxene-gabbros, a pleochroic brown hornblende (brown to brown-green) forms large prisms and poikilitic crystals similar to the pyroxenes described above.

Opaque minerals, magnetite, skeletal ilmenite and green spinel are important accessory minerals and form up to 8% of some gabbros. They occur as inclusions, symplectic intergrowths and as irregular crystals moulded around the other crystals. Euhedral apatite prisms are common as inclusions in some thin sections.

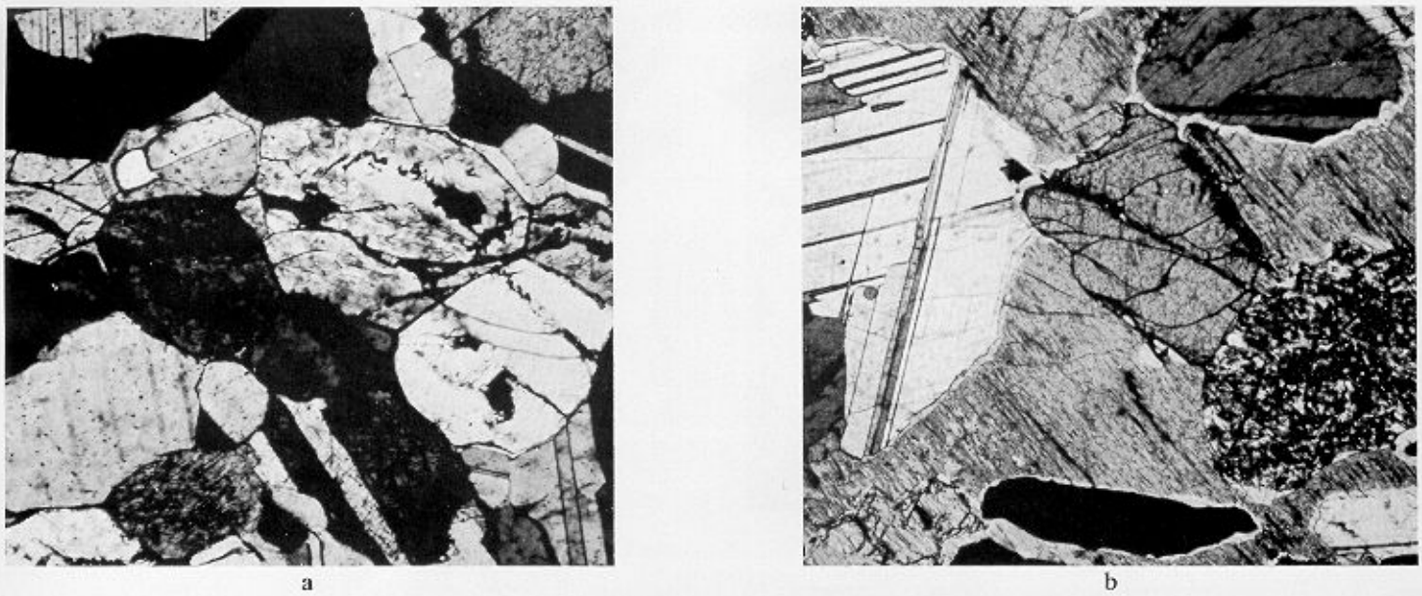

a b

FIGURE 19
a. Cumulus feldspar, olivine and pyroxene in a layered gabbro. (M.2053.2C; X-nicols; ×40)
b. Intercumulus pyroxene enclosing cumulus feldspar, olivine and pyroxene. (M.2053.2C; X-nicols; ×40)

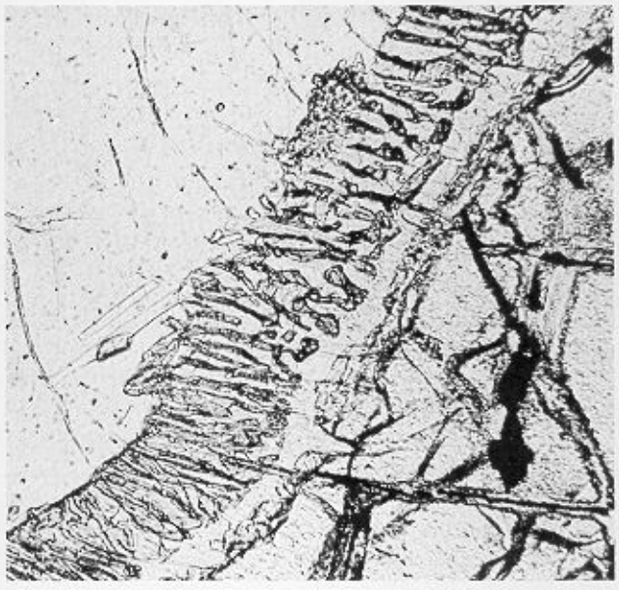

FIGURE 20
Amphibole–spinel symplecite surrounding olivine in a cumulate gabbro. (M.2149.6B; X-nicols; ×160)

4. *Layering*

The rhythmic layering of the cumulate gabbros, which is of variable strike and is steeply inclined (Fig. 8), varies in thickness from thin laminations less than 1 cm thick to massive bands up to 1 m thick. Thin feldspathic laminae (Fig. 21) are found in massive melagabbro and thin ferromagnesian-rich laminae in feldspathic gabbros. Sharp and gradational contacts separate successive layers, the regular nature of which is most striking. Contacts may be straight (Fig. 17) with layers continuing for up to 100 m. Irregular wavy contacts (Fig. 18) with lensing of the lithologies also exist. East of peak 520 m (Fig. 8), an area of irregular layering (Fig. 22), folding (Fig. 23), minor unconformities (Fig. 24) and cross bedding exists; large angular blocks (Fig. 25) of layered gabbro are found in more massive gabbro. Discontinuous layering (Fig. 26) was observed in some localities; lenses of feldspathic gabbro and fine-grained ferromagnesian-rich bands exist in a massive laminated gabbro. Small fine enclaves with cumulate textures were recorded in the Hamilton Bay area.

In thin section, the layered gabbros show a well-developed cumulate texture (Fig. 19a) with co-existing cumulus and post-cumulus crystalline material. A detailed analysis of cumulus and post-cumulus phases is given in Table V.

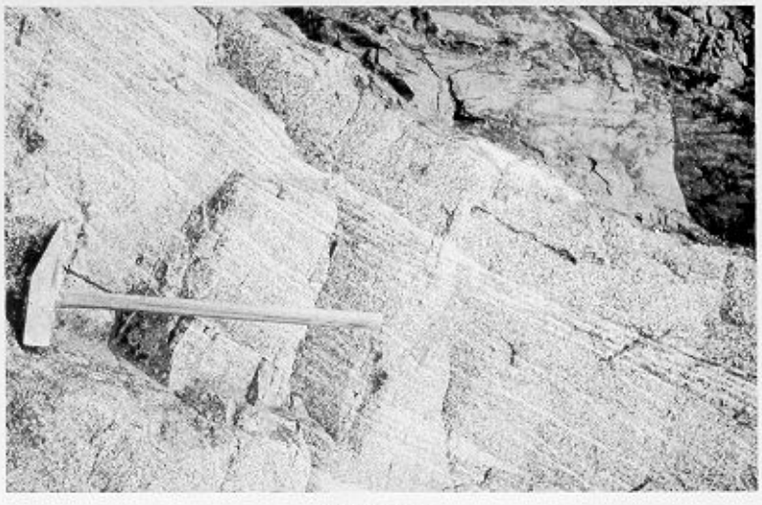

FIGURE 21
Fine laminations in a layered gabbro. The hammer shaft is 60 cm long.

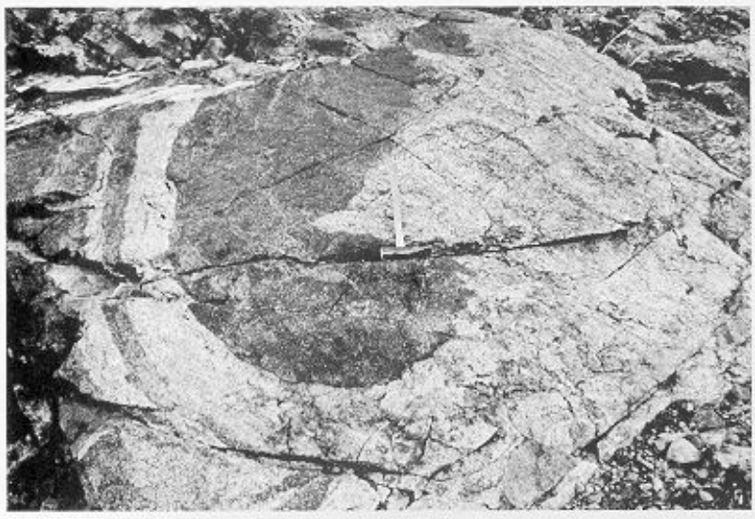

FIGURE 22
Irregular layering of the gabbro. The hammer shaft is 60 cm long.

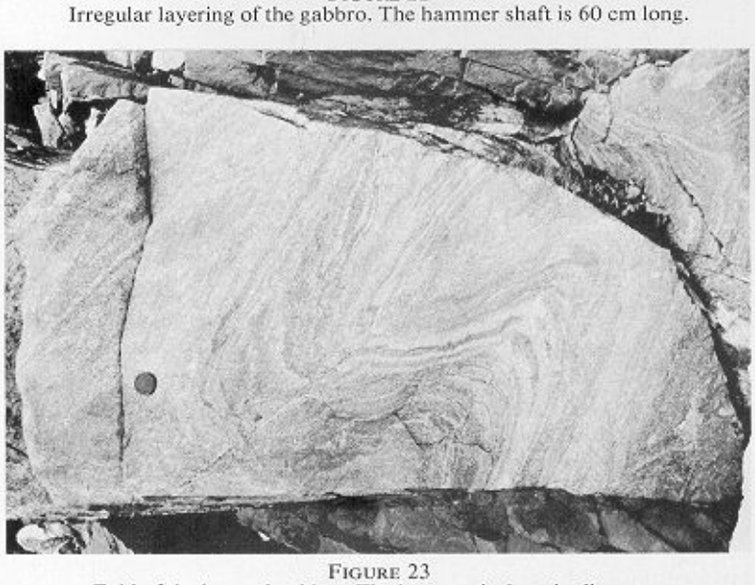

FIGURE 23
Fold of the layered gabbro. The lens cap is 6 cm in diameter.

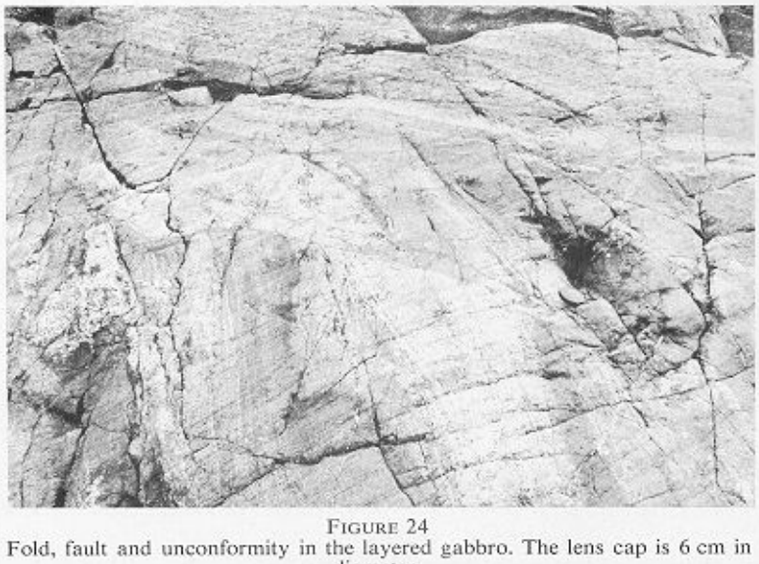

FIGURE 24
Fold, fault and unconformity in the layered gabbro. The lens cap is 6 cm in diameter.

FIGURE 25
Block of layered gabbro in a massive gabbro. The hammer shaft is 60 cm l

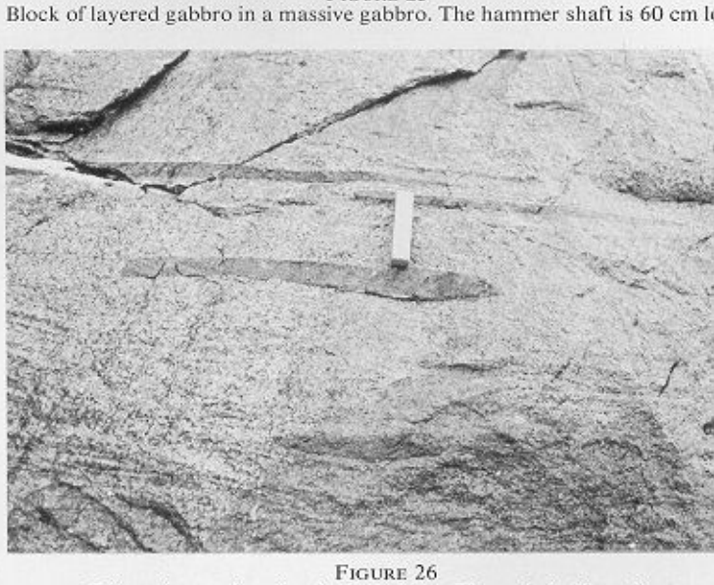

FIGURE 26
Discontinuous layering in the gabbro. The scale is 10 cm long.

a. *Cumulus phases*. Augite, plagioclase, olivine and hypersth are the commonest cumulus phases with plagioclase found in analysed layers. Successive layers are separated by the follo ing criteria:

i. Marked changed in the proportions of the cumu minerals (ratio contact). The terms in parentheses w proposed by Wyllie (1967).
ii. The appearance and disappearance of a cumulus min phase, e.g. olivine (phase contact).
iii. A sharp change in the grain-size of the cumulus mine (form contact).

Fine-grained bands alternate with medium-grained bands ferromagnesian-rich layers occur within a feldspathic gabb Ratio contacts are by far the most abundant. As well as va tions in the cumulus phases between successive bands, va tions in the concentration of the minerals within a single la result in gradations from a ferromagnesian-rich base to a m

TABLE V

MODAL ANALYSES OF CUMULUS AND POST-CUMULUS MINERAL PHASES OF THE LAYERED GABBROS

Specimen number	*Cumulus phases*				*Post-cumulus phases*				*Total rock name*
	Plagioclase	*Olivine*	*Augite*	*Hypersthene*	*Augite*	*Hornblende*	*Hypersthene*	*Opaques*	
Hamilton Bay gabbro									
M.2122.9	49	–	39	–	–	9	3	–	Hornblende-pyroxene-gabbro
M.2148.5A	57	2	37	–	–	2	1	1	Gabbro
M.2148.5B (1)	26	–	60	–	–	4	10	–	Melagabbro
(2)	74	–	22	–	–	4	10	–	Leucogabbro
M.2149.1 (1)	93	–	7	–	–	–	–	–	Anorthosite
(2)	55	–	39	–	–	6	?	–	Hornblende-pyroxene-gabbro
M.2149.6A	27	43	22	–	–	2	6	–	Mela-olivine-gabbro
M.2174.17	52	26	–	–	19	3	–	–	Olivine-gabbro
M.2120.9*	30	–	60	10	–	–	–	–	Melagabbro
M.2122.2*	60	–	30	–	–	5	5	–	Gabbro
M.2125.10*	50	–	40	5	–	5	?	–	Gabbro
M.2135.2*	70	–	–	–	12	8	10	–	Hornblende-pyroxene-gabbro
M.2148.5B*	60	–	40	–	–	–	–	–	Gabbro
M.2149.5*	70	–	20	–	–	10	–	–	Leucogabbro
M.2149.6B*	40	30	–	–	25	5	–	–	Olivine-gabbro
M.2174.1A*	10	80	–	–	5	–	5	–	Troctolite
M.2174.1B*	45	45	–	–	5	5	?	–	Troctolite
M.2174.1C*	40	40	–	–	20	–	–	–	Olivine-gabbro
M.2185.9*	50	50	–	–	–	–	–	–	Olivine-gabbro
Salomon Glacier gabbro									
M.1676.2	46	2	–	1	–	32	19	–	Pyroxene-hornblende-norite
M.1691.1	56	–	1	24	–	4	10	5	Norite
M.1696.1	45	–	25	19	–	2	–	9	Two-pyroxene gabbro
M.4179.2*	60	–	20	20	–	–	–	–	Two-pyroxene gabbro
Trendall Crag and Drygalski Fjord gabbros									
M.2033.3	50	–	22	17	–	1	–	10	Two-pyroxene gabbro
M.2034.5*	60	–	30	–	5	5	–	–	Gabbro
M.2040.8	82	–	18	–	–	–	–	–	Leucogabbro
M.2053.2A	63	10	–	–	7	11	9	–	Olivine-hornblende-norite
M.2053.2B (1)	65	16	1	–	6	6	6	–	Hornblende-pyroxene-olivine-gabbro
(2)	40	4	–	–	23	22	10	1	Hornblende-pyroxene-olivine-gabbro
(3)	40	29	27	–	–	4	–	–	Hornblende-pyroxene-olivine-gabbro
M.2053.2B (1)	65	–	29	–	–	3	1	2	Gabbro
(2)	20	–	9	–	4	39	24	4	Melahornblende-norite
M.2053.2C (1)	65	17	3	–	3	8	3	1	Hornblende-pyroxene-olivine-gabbro
(2)	38	30	20	–	–	12	–	–	Hornblende-pyroxene-olivine-gabbro
M.2054.3	50	25	25	–	–	–	–	–	Olivine-gabbro
M.1696.1	45	–	25	19	–	2	–	9	Two-pyroxene gabbro

Rock modes were determined using a Swift point counter set at a point interval of 0·5 mm. The vertical distance between each traverse was also 0·5 mm. 1 000 points were counted per thin section.

* Percentages were estimates due to alteration of gabbros.

[face page 23.

feldspathic top (mineral-graded layers). Layers characterized by uniform proportions (isomodal layers) are more common. Size-graded layers are not present and chemical-graded layers have not been investigated.

b. *Post-cumulus phases.* Augite, hypersthene and hornblende are the main post-cumulus phases and occur as large poikilitic crystals (Fig. 19b) enclosing the cumulus crystals (heteradcumulate of Wager and Brown (1968)). They are usually randomly distributed within the layers but in isolated instances define a lamination.

In many cases, poikilitic crystals are not formed but post-cumulus overgrowth of the cumulus minerals may have occurred, forming triple junctions and interlocking crystal margins (adcumulates). Contacts between the cumulus phase and post-cumulus growth are not evident in thin section. Inclusions within the margins of some of the crystals suggest that post-cumulus overgrowth has occurred.

The bimodal size distribution of some of the cumulates may be explained by nucleation and crystallization of new minerals from intercumulus liquids with the new fine-grained crystals filling the voids between the cumulus crystals (orthocumulates).

The embayed and corroded margins of the cumulus minerals enclosed within some of the poikilitic crystals may indicate that post-cumulus replacement is an important phenomenon. Olivine is often surrounded and embayed by orthopyroxene and orthopyroxene by augite.

The above textural variation in the post-cumulus mineral phases may be dependent on the composition of the trapped magma, rates of diffusion, rates of burial, original porosity and depositional and post-depositional processes (Wyllie, 1967).

It is not certain whether some of the opaque minerals are cumulus or post-cumulus phases. The opaque minerals occur as inclusions in the post-cumulus poikilitic crystals but more commonly as interstitial material moulded around the cumulus phases.

c. *Origin of layering.* Various mechanisms have been postulated to explain the origin of rhythmic layering of cumulate gabbros (Wager and Brown, 1968). In a basic magma chamber, fractional crystallization and gravitational settling are inevitable but will produce a continuous pile of cumulates without necessarily producing layering. Layering may, however, be produced by the action of a mechanical agency, rhythmic in nature, such as convection or turbidity currents. Rhythmic layering may also be produced by bursts of discontinuous nucleation or variation in the nucleation rate of the cumulate phases as a result of changes in the physico-chemical state of the magma. These changes may be initiated by repeated injection of parental magma into a chamber. O'Hara (1977) has shown that multiple injection with continual removal of evolved melts may be a realistic model of magma-chamber processes and can produce the mineral layering observed in many gabbros.

In accessing the origin of a layered series, the character and abundance of isomodal, mineral and size-graded layers and phase, ratio and form contacts are important. Phase contacts are most likely a product of changes in the crystallization history of the magma, whereas ratio contacts may be a product of a mechanical sorting or as a result of physico-chemical changes affecting nucleation; form contacts are most likely due to mechanical disturbances (Wyllie, 1967). Within the Drygalski Fjord Complex the occurrence of layers of various grain-size support a mechanical sorting agency perhaps associated with some form of current activity. Minor unconformities, irregular laminations and layer boundaries, lensing of layers and the orientation of the platy minerals support current action. The high occurrence of thick cumulates with sharp ratio contacts separating layers of variable proportions of two or three cumulus minerals of similar grain-size and density suggest repetitive changes in the supply of crystalline products. Bursts of discontinuous nucleation of the cumulus phases will produce a periodic repetitive supply of crystalline products which may be followed by differential gravitational settling of pyroxene and olivine relative to plagioclase. Dependent on the distance of the nucleation zone above the pile of settled minerals, the layer will be mineral graded or isomodal as a result of either complete or partial separation of the cumulus phases. Continuous mineral grading may result from settling overlap of crystals formed in a later nucleation cycle.

It is thus concluded that the layering is a product of currents in a magma chamber associated with fractional crystallization, different crystal settling rates and discontinuous nucleation of the cumulus phases. The variation in nucleation rate is most likely related to multiple injections of parental magma within the chamber.

Various theories are possible (Goode and Kreig, 1967) to explain the variation in dip and strike of the layered series (Fig. 8):

i. Folding of horizontal cumulates.
ii. Flow differentation of an intrusive magma.
iii. Multiple injections.
iv. Differential viscous flow along steep contacts of an inhomogeneous crystal mush derived from horizontal layering.

In the Drygalski Fjord Complex, the dip and strike of the layering (Fig. 8) indicate large-scale folding of former horizontal cumulates; to the east of Bogen Glacier, the dip and strike of the layering of the gabbros is similar to the dip and strike of the banding of the metasediments (Fig. 8). The lensing of the lithologies, the discontinuous layering, angular blocks of layered gabbros within a massive gabbro, unconformities, multiple intrusions and the occurrence of gabbroic pegmatites within the hinge zones suggest that deformation was in part synchronous with magmatic activity. The layering was disrupted and possibly re-intruded as a crystal mush during a deformation event (? D3 event). Within parts of the Hamilton Bay and Trendall Crag gabbros (Fig. 8) there is great variation in the dip and strike of the layering. This may be due to tectonic disturbance of a more ductile, less crystallized crystal mush during the deformation; with a higher degree of crystallization the banding remained intact and deformed in a more competent manner similar to the metasediments. As well as stretched and fragmented layers, a mineral alignment fabric is developed in some localities in the Hamilton Bay area. Multiple injections of parental magma may also disrupt the layering within the chamber.

d. *Crystallization history.* Due to the post-cumulative movements, which affect the banding, it is not possible to establish a sequence of crystallization within the gabbros as a whole or within individual plutons; however, certain trends were noted. Feldspar is found as a cumulus phase throughout the

layered series. Olivine, found with feldspar, augite and hypersthene, occurs in the western part of the Hamilton Bay gabbro and in the Trendall Crag gabbro.

Orthopyroxene, augite and hornblende are common intercumulus phases throughout the complex and indicate the composition of residual liquid phases after nucleation and precipitation of the cumulus phases. If the intercumulus liquid is supersaturated with respect to the cumulus phases, adcumulus crystal growth will be expected, the amount of which can be estimated by comparing the size of crystals enclosed within a poikilitic crystal with those outside. 300% enlargement was recorded in the Bushveld Igneous Complex (Goode, 1977) but this may be an overestimate as enclosed cumulus phases can be resorbed by intercumulus liquids.

It was not possible to establish the overall composition of the magma or large-scale patterns of layering (macro-layering) within the layered series. Intrusive contacts indicate more than one pulse of magmatic activity.

FIGURE 27
Gabbro-pegmatite. The scale is 10 cm long.

5. *Ultramafic inclusions*

A number of ultramafic bodies cut by basic dykes are exposed in the Hamilton Bay gabbro (Fig. 5). They are irregular in shape, up to 40 m wide, and are enclosed as large xenoliths within a massive recrystallized gabbro. Contacts are mainly sheared but veining and stoping by the surrounding gabbros occurs.

The rocks are coarsely granular lherzolites (olivine-hypersthene-augite), pyroxene-hornblende-peridotites (augite-hornblende-olivine) and picrites (feldspar-olivine-augite) in composition, black in colour and altered in thin section; original cumulate textures are not evident in thin section. The primary minerals are replaced by irregular aggregates of serpentine, talc, chlorite, epidote, muscovite and actinolite (alteration described in detail below). Numerous cracks, which are filled with serpentine and lined with opaque granules, cut the olivine crystals. These fractures are often aligned parallel to the margins of the ultramafic bodies and may have formed as a result of shearing during emplacement of the ultramafic rocks.

The origin of the ultramafic bodies is uncertain. They may represent cumulates formed originally at the base of the layered mafic series and included as xenoliths within the gabbros, or they may be locally derived boudinaged ultramafic cumulates. Alternatively, hydration may have occurred at depth due to percolating hydrothermal fluids introduced along fracture zones. This may have been followed by subsequent intrusion of the lighter hydrated serpentinite high into the gabbro pile.

6. *Pegmatites*

Pegmatitic gabbroic veins and isolated crystal aggregates (up to 3 cm long) occur with some gabbroic bodies and intrude and brecciate the layered series (Fig. 27). The pegmatites are variable in composition; crystal aggregates of augite, hypersthene, green-brown pleochroic hornblende, biotite, chlorite, andesine and labradorite crystals are found within pools of interstitial quartz with accessory apatite, zircon and opaque minerals. Alteration and replacement textures, similar to those in the gabbros, are common in the pegmatites. The augite is often surrounded by brown-green hornblende fringes and is replaced by aggregates of tremolite-actinolite laths.

The pegmatites probably crystallized from late-stage magmatic or hydrothermal fluids percolating through the layered series, perhaps during large-scale movements of the layering or during localized fracturing of a consolidated layered series.

7. *Recrystallization*

Replacement of the original anhydrous minerals by hydrous mineral phases has taken place to a variable extent within the complex. A new fabric was not developed and igneous textures are preserved. Primary minerals are pseudomorphed by secondary minerals resulting in metagabbros with some alteration and rocks in which the primary minerals are completely replaced by aggregates of pistacite–clinozoisite–zoisite–actinolite–chlorite–serpentine–talc–muscovite–hornblende. The alteration, although widespread, is concentrated within the Hamilton Bay gabbro.

Plagioclase is variably replaced by aggregates of epidote minerals (pistacite, clinozoisite and zoisite) with scattered muscovite and irregular patches of calcite and prehnite. Recrystallization of the plagioclase to (?) albite has occurred in a few altered rocks. Olivine, the most altered mineral, is generally traversed by a network of cross-fibre serpentine (chrysotile) and magnetite-filled cracks. Complete replacement by irregular aggregates of antigorite, orange-yellow iddingsite and talc or muscovite is common. The distinction between talc and muscovite is uncertain; the abnormal high birefringence and unusual colours suggest talc. Altered olivine may be surrounded by irregular aggregates of actinolite. A colourless amphibole accompanied by opaque granules is usually a distinctive alteration phase of olivine. In some cases, however, the alteration of olivine is difficult to distinguish from that of orthopyroxene.

Augite is pseudomorphed by irregular aggregates or single crystals of colourless or pale green actinolite, penninite or brown-green hornblende (Fig. 28). Hypersthene, which is more susceptible to alteration than augite, is replaced by talc or muscovite, actinolite and antigorite. Opaque granules are altered to sphene and leucoxene, and occasionally surrounded by biotite, chlorite and epidote.

As well as the replacement minerals, biotite, chlorite and

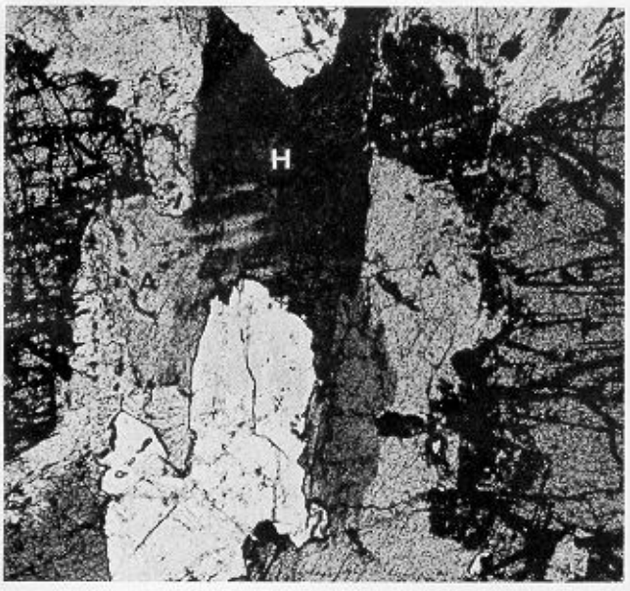

FIGURE 28
Pyroxene surrounded by pale actinolite (A) and dark hornblende (H). (M.4134.7; ordinary light; ×40)

hornblende are found scattered in some thin sections. The chlorite flakes often contain sphene and epidote granules. Pistacite occurs within some biotite flakes.

Amphibole, chlorite, feldspar, epidote, opaque and prehnite-filled veins cut the gabbros.

The alteration of the gabbros may be due to a number of processes:

i. Deuteric effect of the late-stage gabbroic fluids (auto-metasomatism).
ii. Sub-solidus reactions.
iii. Dynamic regional metamorphism.
iv. Post-consolidation hydrothermal and metasomatic alteration due to:
   a. meteoric ground waters;
   b. metamorphic fluids;
   c. sea-water (ocean-floor metamorphism);
   d. magmatic fluids of later intrusions.
v. Contact thermal metamorphism of later intrusions.

The role of amphiboles within the gabbros is important in accessing the metamorphic facies and type of alteration. Amphiboles are the commonest hydrous mineral and occur as:

i. Large poikilitic crystals of brown hornblende enclosing cumulus crystals.
ii. Prisms of green and brown hornblende.
iii. Thin rims of brown and green hornblende surrounding pyroxene.
iv. Brown hornblende patches replacing augite.
v. Aggregates of actinolite laths.

The hornblende prisms, poikilitic crystals and reaction rims co-exist with actinolite. Gabbros devoid of hornblende also exist.

As the poikilitic hornblende is similar to the poikilitic pyroxene, it is proposed that these are intercumulus minerals and that crystallization passed into the hornblende stability field during the post-cumulate crystallization of the layered gabbros. Similarly, the biotite and hornblende prisms in the gabbroic pegmatites probably crystallized directly from late-stage hydrous fluids which percolated through the layered series.

The replacement structures and reaction rims of brown hornblende have previously been described (Stern and others, 1976) as a characteristic of ocean-floor metamorphism of gabbros up to amphibolite facies, and by Grapes and others (1977) as initial stages in the dynamic metamorphism of cumulate amphibole-free pyroxene-gabbros to amphibolites. As the gabbros in the Drygalski Fjord area intrude metasediments, ocean-floor metamorphism is ruled out. However, the sequence outlined by Grapes and others could apply to these rocks. The hydrous minerals indicate a retrogressive metamorphism from a high-temperature assemblage to a low-temperature assemblage. The initial stages of this retrogression are indicated by sub-solidus reactions (corona structure) between olivine, plagioclase and pyroxene with the formation of thin rims of orthopyroxene, amphibole and spinel–amphibole symplectites, and replacement of augite by brown or green-brown hornblende (amphibolite facies). The pyroxenes are subsequently replaced by aggregates of actinolite which is accompanied by saussuritization of the feldspar (epidote-amphibolite facies). The presence of chlorite often pseudomorphing actinolite, muscovite and albite as replacement minerals indicates some recrystallization in the greenschist facies. The assemblages indicate retrogressive metamorphic processes with widespread amphibolitization of the gabbros, disequilibrium conditions and partial adjustment of the igneous assemblage to a greenschist-facies assemblage. The irregular distribution of the alteration and lack of a tectonic fabric indicate that the alteration is a result of sub-solidus hydrothermal metamorphism. This may be due to the introduction of hydrous fluids associated with any one of the following: the intrusion of the Trendall Crag granodiorite, the migmatitic granites, the intrusive breccias or late-stage fluids introduced by infiltration along deep fractures or dyke zones during uplift and cooling. Hornblende is thus both magmatic and metamorphic in origin and the exact distinction between them is not always obvious. It appears as an intercumulus phase, as a late-stage reaction phase (autometasomatism), and as a post-consolidation phase associated with hydrothermal metamorphism. Some alteration may be due to a contact-thermal effect of basic dykes.

The spinel–amphibole symplectites are an unusual feature. They have been recorded by Grapes and others (1977) and occur in metaperidotites of Connemara (Ahmed and Leake, 1978) and in the Belhelvie troctolites, Aberdeen (Hatch and others, 1968), and are believed to be due to the action of liquid residues at high temperature.

IV. DIORITES AND QUARTZ-DIORITES

1. *Field relations*

Dioritic rocks, which are found in the Trendall Crag area and on Cooper Island (Fig. 5), are a small proportion of the basic rocks of the Drygalski Fjord Complex. They crop out along gabbro–granitoid contact zones and form small remnant bodies up to 50 m wide within the Trendall Crag granodiorite. The diorites are intruded and assimilated by the granodiorites, cut by basic dykes and acid–basic intrusive breccias; rounded quartz ocelli (up to 0.8 cm) rimmed by opaque minerals and amphibole laths are developed within dioritic enclaves of the granodiorites and along the granite–diorite contact zones. To the east of Bogen Glacier (Fig. 5), diorite and quartz-diorite dykes cut the metasediments. The Cooper Island body is strongly jointed, with granitic veins forming a characteristic reticulate network along the joint sets (Fig. 29a and b). The sub-horizontal granitic veins have sharp lower contacts and irregular fretted upper margins; occasional plumes of granite join successive veins.

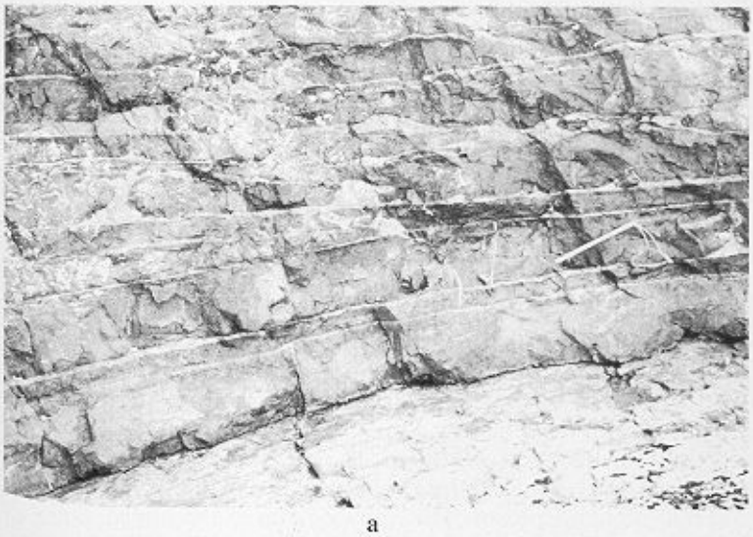

a

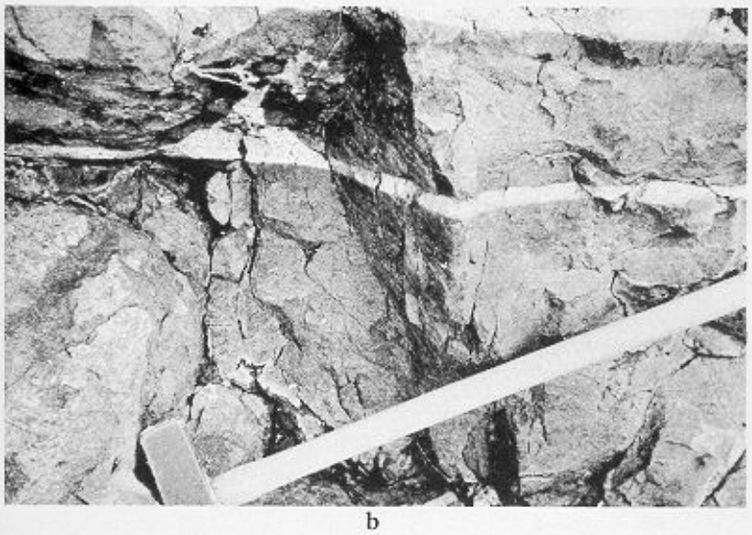

b

FIGURE 29

a. Granitoid veins in a diorite on Cooper Island. The hammer shaft is 60 cm long.
b. A granite vein illustrating an irregular upper margin in a diorite on Cooper Island. The hammer shaft is 60 cm long.

In the hand specimen the rocks are medium-grained (0.5–2.0 mm) dark and compact rocks with occasional quartz and feldspar phenocrysts. In contrast to the quartz ocelli described above, irregular quartz-filled inclusions (up to 10 cm), also rimmed by opaque minerals and amphibole laths, are found to the north of Storey Glacier. The size and shape of these, some of which are pale blue in colour, suggest that they may be relict quartzites.

2. *Petrography*

The intermediate rocks are diorites and quartz-diorites. The principal minerals are plagioclase, augite, amphibole, biotite and quartz with accessory apatite, sphene and opaque minerals and alteration minerals, actinolite, epidote, clinozoisite, zoisite, muscovite and chlorite. Prehnite and epidote veins cut the intermediate rocks.

Euhedral and anhedral twinned and zoned plagioclase crystals are variable in composition (An_{5-70}) and grain-size (0.5–5.0 mm). Although they are mainly andesine crystals, some have labradorite-bytownite cores surrounded by wide mantles of lower relief, normally zoned andesine-albite. Large andesine and oligoclase porphyroblasts, often zoned with patchy extinction and feldspar inclusions (high-relief labradorite) are found in some thin sections; some are extensively altered to albite and are replaced by aggregates of epidote, zoisite, clinozoisite and sericite. Potash feldspar, although uncommon, is present in some diorites.

Colourless and pleochroic (α = light brown; β = bottle-green; γ = green-brown) hornblende occurs as euhedral prisms, irregular crystals often poikilitic and as fine-grained crystal aggregates occasionally cored by augite. Extensive colour variation exists within the individual prisms and within the patchwork aggregates; rims of bottle-green hornblende surround colourless prisms, and patches of green and brown hornblende occur within the crystals. The crystal aggregates are often associated with and replaced by aggregates of pale green and bottle-green actinolite and pale green chlorite. The pale green actinolites have a characteristic lamellar structure parallel to 110; these are not found in the hornblendes and may represent exsolution lamellae (Ross and others, 1968).

Biotite occurs as poikilitic crystals, up to 3 mm long, and as aggregates of disorientated biotite plates. The biotite, often altered to chlorite and prehnite, is closely associated and intergrown with the green and brown hornblende; it may show deformation strain lamellae. Penninite, which contains high-birefringence epidote and which is surrounded by opaque granules, also forms large crystals up to 2 mm long.

Quartz, which has an uneven distribution throughout the diorites and quartz-diorites, forms large poikilitic crystals, composite ovoids and interstitial patches between the subhedral plagioclase and amphibole prisms. The quartz ovoids (termed "ocelli" by Rosenbusch (1887)) are up to 2 cm wide and are mantled by narrow rims of pale green amphibole laths (Fig. 30). Small pools of interstitial quartz may be optically continuous

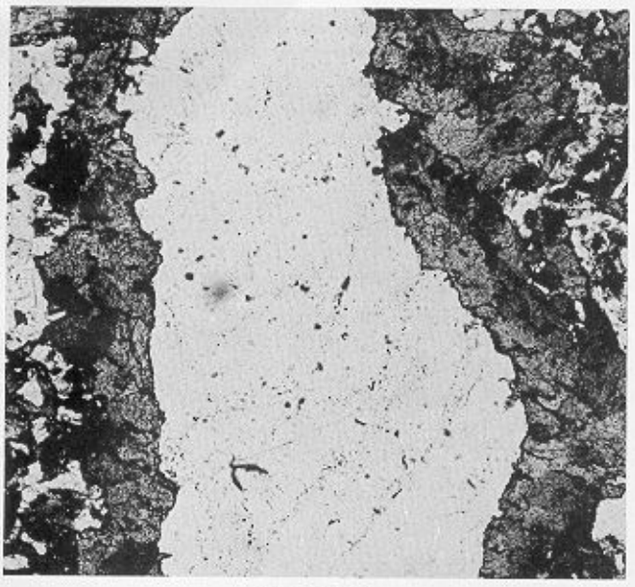

FIGURE 30
Ocellar quartz surrounded by amphibole in a diorite. (M.2050.F; ordinary light; ×40)

over large distances (up to 2 cm). Granophyric intergrowths with plagioclase and green hornblende are common in some thin sections. Quartz may show an undulose extinction and deformation strain lamellae.

Anhedral opaque minerals, haematite often surrounding pyrite, magnetite and ilmenite, are common accessory minerals; they are enclosed within amphibole and surrounded by aggregates of epidote, clinozoisite, zoisite and sphene. Euhedral zircon and sphene, and elongate apatite needles, up to 2 mm long, are enclosed within plagioclase and quartz. The slender apatite needles, which may be aligned and fragmented, are a characteristic and abundant accessory of these rocks.

The (?) quartzite inclusions, rimmed by pale green amphibole laths are composite quartz crystals; potash feldspar and plagioclase are present within the margins of the inclusions.

3. *Discussion*

The origin of the diorite and quartz-diorite is complex and will be discussed in more detail together with the geochemistry of these rocks. The situation of the diorites along the granite–gabbro contact zones suggests, however, a close relationship between the rocks and the origin of the diorites. They may have formed by differentiation of the basic magma, by contamination of the basic magma by the nearby acid magma, or by crystallization from a primary intermediate magma. The presence of quartz ocelli and the mineralogical and textural features (outlined below) suggest a hybrid origin for some of these rocks.

In general, hybrid rocks are characterized (Wells and Bishop, 1955; Joplin, 1959; Angus, 1962; French, 1966) by the presence of:

i. Poikiloblastic quartz, amphibole and biotite.
ii. Unevenly zoned plagioclase prophyroblasts.
iii. Sporadic distribution of interstitial pools of optically continuous quartz.
iv. Replacement textures and mineral disequilibrium assemblages; pyroxene–hornblende–biotite–chlorite replacements are common and cores of labradorite are rimmed by oligoclase and albite.
v. Mineral intergrowths; quartz–plagioclase and plagioclase–amphibole symplectites are present.
vi. Partial or open prisms of hornblende (Wells and Bishop, 1955).
vii. Abundant minute apatite needles enclosed within quartz and plagioclase.

Although the intermediate rocks of the complex exhibit some of these characteristics, the feldspars, which may contain high-anorthite cores, are mainly slightly altered, normally zoned and twinned andesine crystals which are in equilibrium with a dioritic assemblage. Similarly, hornblende occurs as euhedral prisms with sharp crystal outlines with quartz and andesine. It thus appears that some of the dioritic rocks, although partially retrogressed to an actinolite–epidote–chlorite assemblage, are primary rocks which may have formed by crystallization from a dioritic liquid formed by differentiation of the basic magma. The textures in some intermediate rocks close to the gabbro–granite contact zone may have formed by some *in-situ* metasomatic transfer with the country rock or granitoids. The network of acidic veins in the Cooper Island diorite mentioned above may have formed by *in-situ* differentiation of the basic magma during crystallization.

V. BASIC DYKES

1. *Field relations*

Basic dykes were intruded at various stages during the history of the complex. The concentration of dykes increases towards the western margin where they form up to 80% of the outcrop. They are commonest in the granites and metasediments but also cut the gabbros. Most dykes were intruded prior to, and were affected by, the migmatization event; a small percentage of later dykes intrude the migmatites.

The dykes, which have a prominent chilled margin against the country rock, generally occur as single units 1–2 m wide, but dykes up to 10 m wide were recorded. They are mainly straight-sided and are continuous along strike at a constant width and dip. However, thinning and displacement of the dykes (Fig. 31) does occur; large 10 m dykes may suddenly thin and continue as a single or a number of narrow veinlets, or die out completely. Enclaves of country rock are common in some dykes and at station M.2429, bordering Novosilski Glacier (Fig. 3), enclaves of amygdaloidal lava fragments were recorded. Multiple dykes previously described by Trendall (1959) (Fig. 32) are present in the Trendall Crag area. These represent re-

FIGURE 31
Displaced basic dyke. The pencil is 16 cm long.

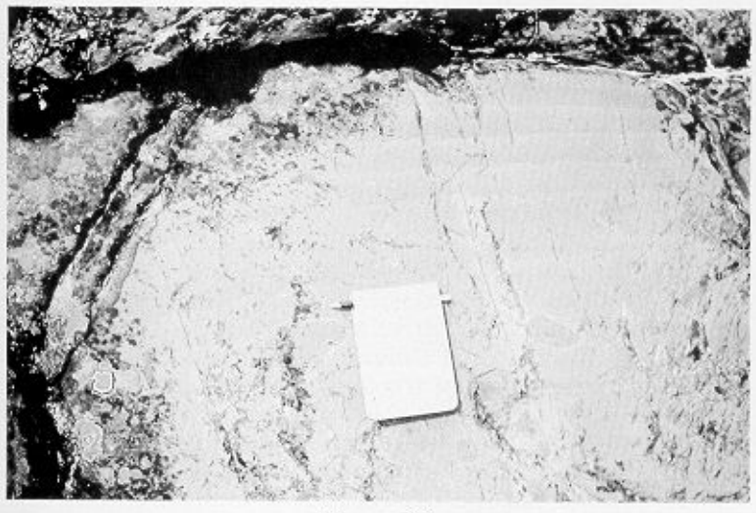

FIGURE 32
Multiple basic dyke. The notebook is 16.5 cm long.

FIGURE 33
Fragmented basic dyke in an altered gabbro. The pencil is 16 cm long.

intrusion of magma along a previously established plane of weakness with successive phases intruding in the centre of the preceding dyke; up to five separate intrusions were recorded in one instance. As well as relict dykes, which are discussed below, basic dykes in the Hamilton Bay area are fragmented, sheared and intruded by numerous quartz and feldspar veins (Fig. 33).

A statistical analysis of the dyke orientations supports the bimodal distribution (north-west and north-east trending sets) recorded by Trendall (1959) but indicates that the overall pattern is more complex. The main trends, which cut each of the major rocks units (Fig. 34a and b), are recorded in Table VI. Excluding the Mount Baume area, the north-easterly set varies from 047° to 073° and is the dominant trend in the gabbros. The north-westerly set varies from 283° to 329° and is dominant in the metasediments and granites. Equal proportions of both sets cut the granites and sediments. The Cooper Island granophyre, which has a dominant north-westerly dyke trend, is an exception. The angle between the dyke trends in any rock type varies from 90° to 34°. The lowest figures were recorded in the gabbros. In the Mount Baume area, in the north-west part of the

TABLE VI
DETAILS OF THE DYKE-TREND ANALYSES FROM WITHIN THE MAJOR ROCK TYPES

Locality and rock type	*Number*	*Dyke trends*	*%**
Cooper Island granophyre	48	047° 68° SE 310° SV*	20 6
Cooper Island Formation	61	041° 66° SE 063° 56° SE 20% 052° 61 SE 287° 83° N 307° SV 16% 297° SV	10 10 8 8
Hamilton Bay gabbro	125	019° SV 103° SV 078° SV 064° 58° SE 16% 058° SV 045° SV	4 4 4 4 8
Salomon Glacier gabbro	39	060° 69° NE 090° SV 298° 69° SW	18 4 6
Salomon Glacier Formation	52	069° 78° SW 329° 82° W	10 10
Trendall Crag gabbro and Drygalski Fjord gabbro	46	073° SV 107° SV	22 6
Trendall Crag granodiorite	267	074° SV 320° 65° NE	10 14
Mount Baume area	40	358° SV 343° SV 122° SV 83° SV 66° SV 10% 75° SV	18 10 4 6 4

*The values are the percentage number of dykes within each trend (computed from stereo nets).
SV Sub-vertical dip (> 86°).

complex, the dyke pattern is different from the above. North-west (302°) and north-east (076°) dyke trends are recorded but the majority of dykes form an almost north–south (352°) trend.

The cross-cutting relationships of the dyke trends are complex with up to three relationships recorded at any one locality. In the Trendall Crag granodiorite, dykes varying in strike by up to 15° were recorded within a dyke trend. However, in general the north-easterly trend is younger than the north-westerly trend but exceptions were found throughout the complex. In most cases it was not possible to recognize an age relationship between dyke suites, as single dykes cutting the host rocks were mostly observed. Both sets are cut by the migmatites but again, due to the sporadic development of the migmatites, it was not possible to relate every dyke to this event. Where relationships are known, the basic dykes which cut the migmatites fall in a more easterly (070°) trend (Fig. 35a). A few post-migmatite north-westerly trending dykes are cut by and cross-cut this trend. Pre-migmatization dykes are more varied in orientation and fall in the north-easterly and north-westerly trends (Fig. 35b).

The displacements of single basic dykes (Fig. 31) may be a primary or a secondary feature (Kaitaro, 1952). A primary origin is usually due to the opening of initial compound fissures, which may be orientated perpendicular to or oblique to the general trend. A secondary origin may be related to faulting, the form of which, unless a three-dimensional picture is obtainable, is very difficult to analyse; displacements may be simultaneous with dyke intrusion with subsequent healing of fractures. As chilled margins are present in the complex, it is unlikely that the offsets are caused by late faulting of the dykes.

Where two dykes cut at an angle (λ) less than 90°, a prominent offset was recorded. The relationship ($\cos \lambda = X/Y$; Goodspeed, 1940) between the width (Y) of the cross-cutting dyke and the amount of displacement (X) of the early dyke indicates that the basic dykes are dilation rather than replacement dykes and that the offset formed as a result of spreading rather than shearing along the margins of the dyke.

2. *Petrography*

The dykes, often porphyritic, vary in composition from olivine-dolerites to quartz-diorites of fine and medium grain-size with variable amounts of alteration. The phenocrysts are usually randomly distributed but may be aligned along the margins or concentrated in the centre of the dyke. They can be subdivided into a number of ill-defined groups which are dependent on the mineral assemblage and the extent of alteration.

a. *Dolerites*. The least-altered dykes, which are common in some areas, are dolerites and olivine-dolerites. They show a well-developed ophitic texture with twinned and occasionally zoned feldspar enclosed or partially enclosed in pyroxene, olivine and hornblende with accessory opaque minerals, apatite and quartz. Feldspar (An_{55-60}), augite and opaque phenocrysts, up to 1 cm wide, were recorded in some dykes. Olivine, which may enclose small droplets of pale green or brown spinel, is often clouded with opaque granules; it may form up to 20% of the olivine-dolerites. Augite and pigeonite (identified by a very low 2V) are the main ferromagnesian minerals. Pigeonite shows an hour-glass structure and undulose extinction in some dykes. Altered hypersthene was recorded in one dyke. Patches of pleochroic brown hornblende surround and partially enclose pyroxene in some dyke rocks. Feldspar generally shows a simple zoning pattern from a high anorthite core (An_{65}) to a more albite-rich margin of variable composition (An_{5-30}).

b. *Diorites and quartz-diorites*. The intermediate dykes, which are invariably altered, are similar to the above and show an ophitic texture. Zoned feldspar laths (up to An_{42}) are generally enclosed within pleochroic brown-green hornblende. Quartz, which may form up to 15% of the dyke rocks, occurs interstitially to the hornblende and feldspar. Apatite is a common accessory and is enclosed within hornblende, feldspar or quartz.

As in the gabbroic rocks, it is uncertain in many cases whether the brown-green hornblende is a primary or secondary mineral; however, as it is generally present with a dioritic or quartz-dioritic assemblage, it is probably of primary origin.

Dykes which have been intruded by veinlets of granitoid rocks (intrusive breccia) are partially recrystallized to an amphibolite (quartz–oligoclase–hornblende–K-feldspar) assemblage. On Cooper Island (M.1972.3), irregular pools of interstitial quartz (Fig. 36), rounded quartz-filled ocelli and irregular veins of granite are found together with disorientated aggregates of hornblende, actinolite, chlorite and epidote. In some cases, the ocelli are bridged by slender actinolite and chlorite laths up to 5 mm long, some of which are bent and deformed. These laths are only present with the ocelli and are in strong contrast to the fine-grained laths of the dyke rock. Clusters of amphibole and chlorite are a characteristic of these dykes; brown-green hornblende surrounds irregular aggregates of mainly pale green or colourless actinolite.

Dyke rock M.4146.5 is partially replaced by a granular mosaic of potash feldspar, quartz and oligoclase with euhedral green hornblende prisms and biotite.

c. *Metabasites*. The above dykes show variable amounts of alteration but many are completely replaced by an actinolite ± biotite–muscovite–epidote–chlorite ± serpentine ± talc assemblage, which is generally associated with primary feldspar. The olivine shows intital alteration to serpentine (antigorite) and magnetite. In more altered sections, olivine is replaced by an aggregate of colourless actinolite, talc, biotite and opaque granules. Complete pseudomorphs of antigorite are also common. Orthopyroxene, fringed with actinolite, is altered to actinolite and muscovite. Augite, which often contains opaque granules, is surrounded by brown-green hornblende and partially replaced by blue-green actinolite, or by actinolite and biotite, or by aggregates of penninite often associated with actinolite and epidote. Remnant cores of augite are often surrounded by successive rims of actinolite and chlorite. Actinolite and biotite usually form disorientated aggregates of pale green and brown crystals, respectively. Opaque granules are generally altered to leucoxene and sphene; skeletal ilmenite, which is common in the altered dykes, may be surrounded by biotite. Calcite is occasionally found, usually associated with chlorite psuedomorphs. Sericitization and saussuritization of the feldspar are common. Phenocrysts may be completely pseudomorphed by epidote. Some alteration to prehnite is also present. Recrystallization of the feldspar is not common but untwinned secondary albite occurs in some of the more altered dyke rocks. Veins of prehnite, epidote and chlorite transgress the more altered dykes.

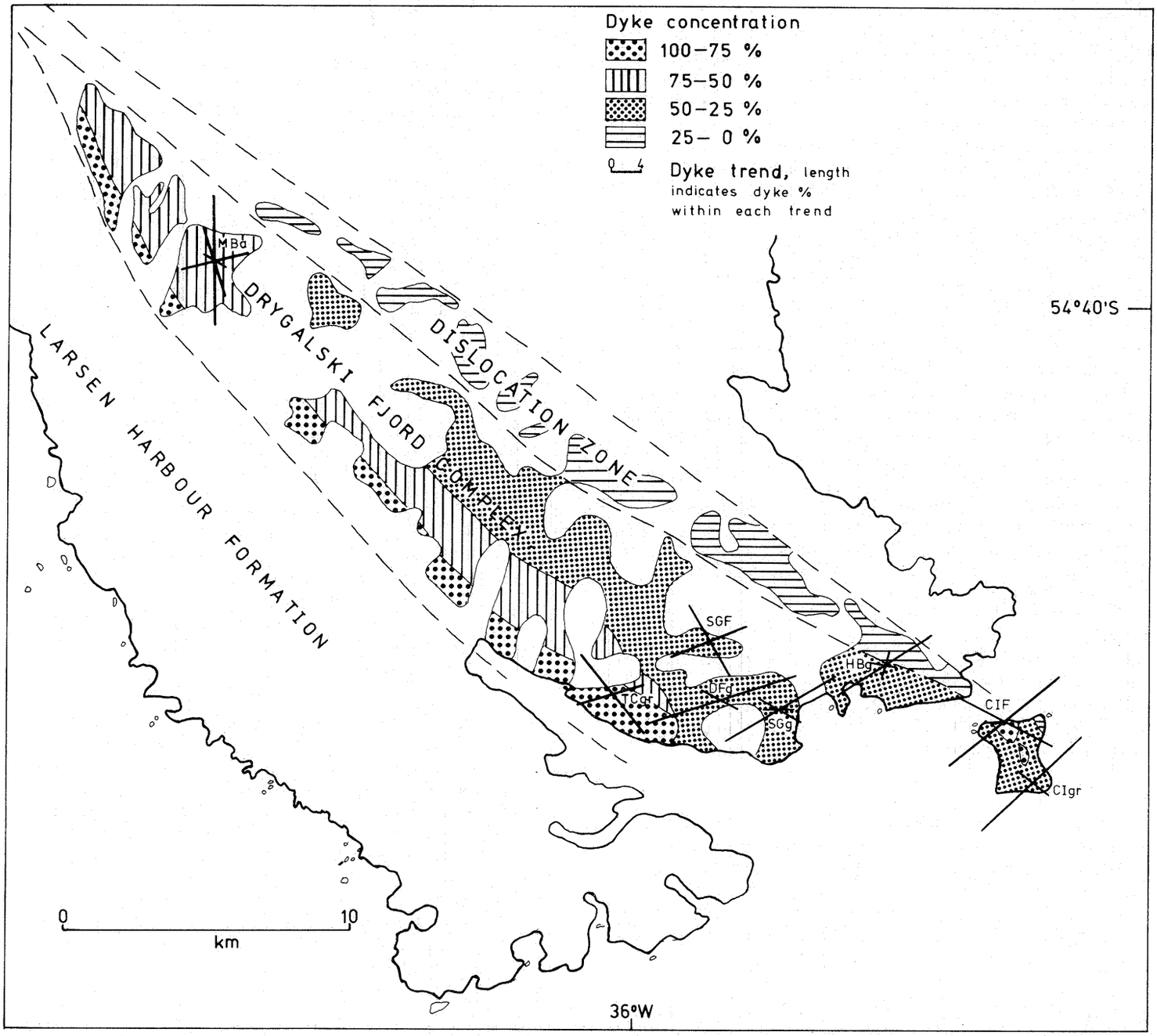

a

FIGURE 34

a. Map showing the trends and concentrations of the basic dykes within the Mount Baume area (MBa), Trendall Crag granodiorite (TCgr), Drygalski Fjord gabbro (DFg), Salomon Glacier gabbro (SGg), Hamilton Bay gabbro (HBg), Salomon Glacier Formation (SGF), Cooper Island Formation (CIF) and Cooper Island granophyre (CIgr).

b. Equal area projections of the dyke trends within the rock units of Fig. 34a. The numbers of dykes are shown in brackets, and the contour intervals are 0–2, 2–6, 6–10, 10–13 and 13–22% area.

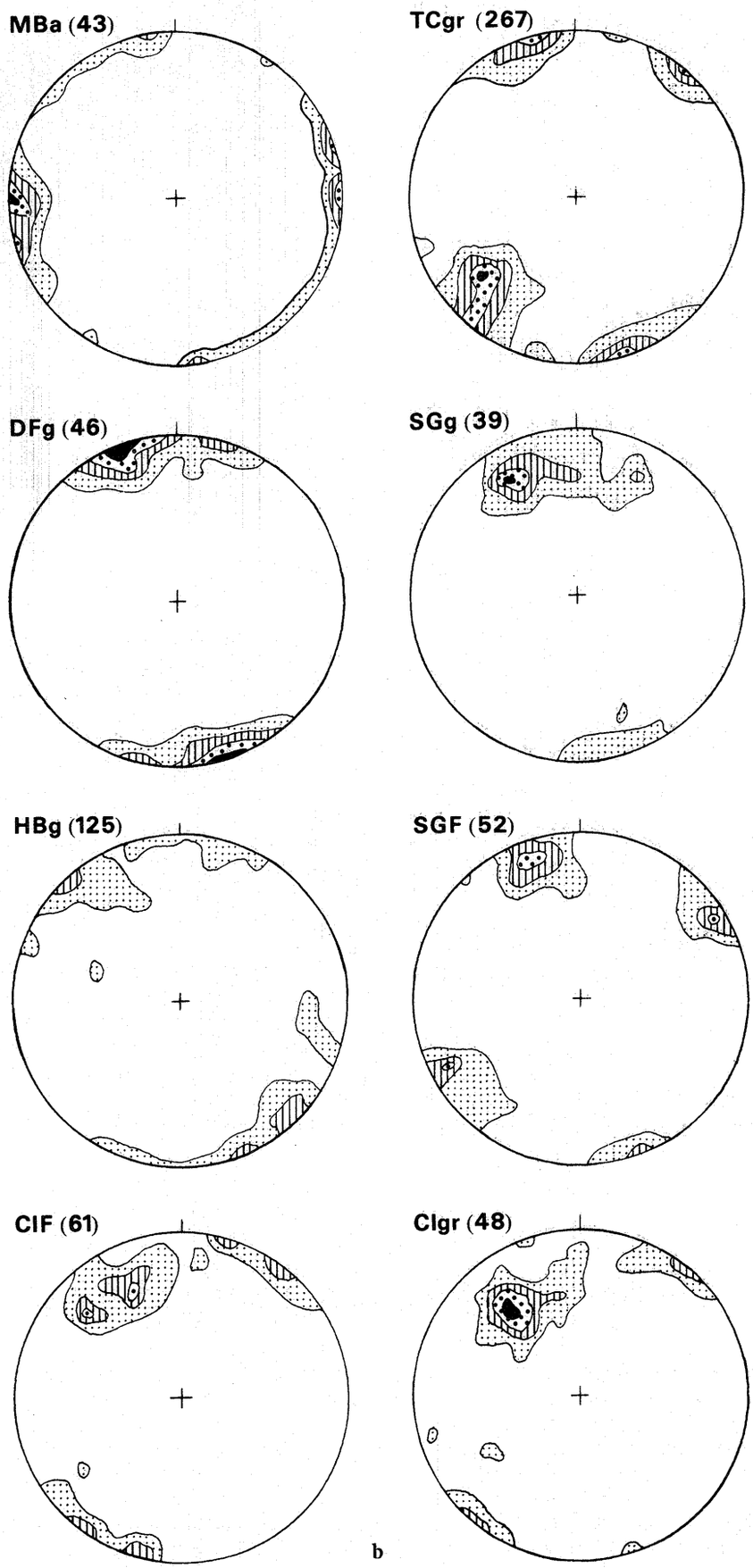

b

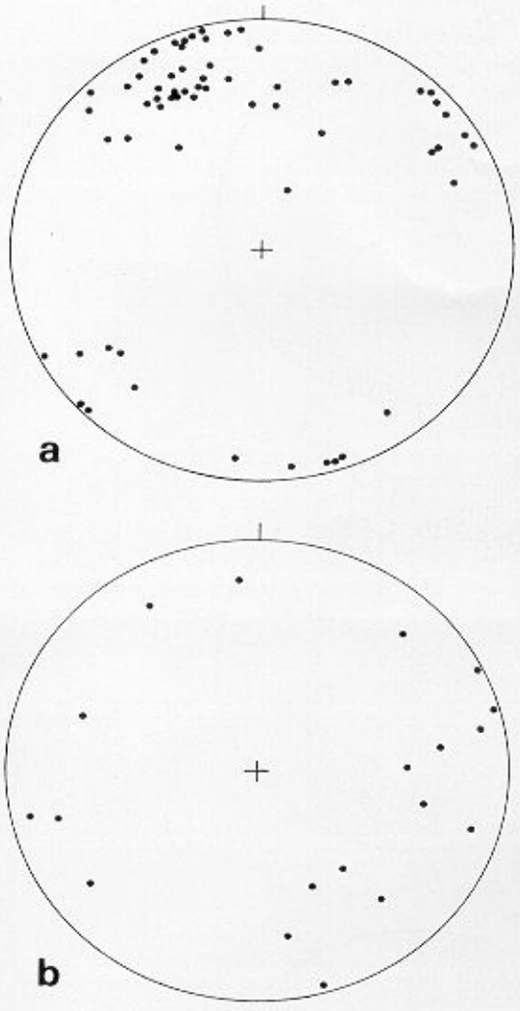

FIGURE 35
a. Equal-area projection showing poles to basic dykes which cut the migmatites.
b. Equal-area projection showing poles to basic dykes which are cut by the migmatites.

3. *Discussion*

There is no correlation between the amount of alteration, dyke composition, grain-size and trend of the dykes. Altered dykes of variable grain-size occur in the latest dyke sets which cut the migmatites and intrusive breccias. The amount of alteration appears to be dependent on the geographical location; unaltered dykes cut unaltered gabbros, whereas altered dykes are common in areas of recrystallized gabbro. Altered dykes also cut unaltered gabbros. Dykes associated with the migmatites show extensive alteration and some recrystallized assemblages.

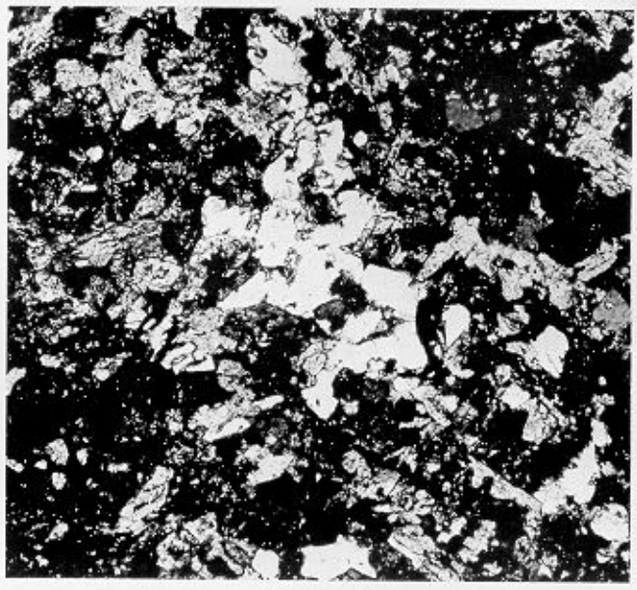

FIGURE 36
Irregular pools of interstitial quartz in a partially assimilated basic dyke. (M.1972.3; X-nicols; ×40)

The irregular distribution of the alteration and the lack of a penetrative foliation, excluding the shear zones, indicate that alteration was probably hydrothermal. The dykes exhibiting most alteration probably acted as conduits for hydrothermal fluids.

The presence of interstitial quartz, quartz ocelli and brecciating veinlets suggests that some of the diorite and quartz-diorite assemblages may have formed by metasomatic contamination by the intrusive breccias and migmatitic granites. The clusters of amphibole laths have previously been reported from, and may be a characteristic of, altered dioritic assemblages (Wells and Bishop, 1955).

VI. GEOCHEMISTRY OF THE BASIC ROCKS

FORTY-FIVE gabbros, one quartz-gabbro pegmatite, 41 basic dyke rocks, 12 intermediate rocks and four ultramafic rocks were analysed for major- and trace-element geochemistry (Tables VII and VIII). The ultramafic rocks came from the Hamilton Bay area, whereas the gabbros and dykes are from the Cooper Island, Hamilton Bay, Drygalski Fjord and Mount Baume areas of the complex. Basic dyke samples were taken from the different dyke trends and different compositional groups (26 dolerites, 11 diorites and quartz-diorites) (Table VIII). A number of altered dykes (four) and gabbros (three) were included to investigate the effects of the widespread metamorphism and recrystallization. Seven of the intermediate rocks were taken from the gabbro–granodiorite contact zone (contact diorites) in the Trendall Crag area; the remaining ones came from intermediate bodies in the Trendall Crag area and on Cooper Island. Chemical analyses of all rocks described in this

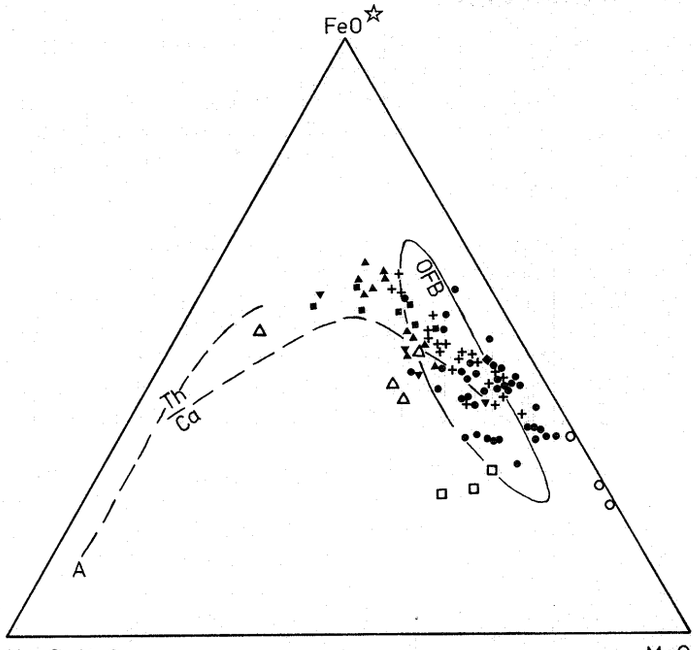

FIGURE 37
AFM triangular diagram of the basic rocks of the Drygalski Fjord Complex. FeO*, total iron as FeO; OFB, ocean-floor basalt field of Bailey and Blake (1974); tholeiitic (Th) and calc-alkaline (Ca) fields from Irvine and Barager (1971); line A indicates the variation trend of the acidic rocks of the Drygalski Fjord Complex.
o Ultramafic rocks.
• Gabbros.
▾ Quartz-gabbros, diorites and quartz-diorites.
◆ Quartz-gabbro pegmatite.
+ Dolerite dykes.
▲ Diorite and quartz-diorite dykes.
△ Recrystallized dykes.
▪ Contact diorites.
□ Metagabbro.
These symbols are used throughout this section.

report were carried out by X-ray fluorescence methods at the University of Birmingham, using techniques described elsewhere.

A. Chemical Character and Fractionation Trends

Using the AFM diagram (Fig. 37), the basic rocks predominantly fall in the tholeiitic field and show a marked iron-enrichment trend, parallel to the FeO–MgO boundary, characteristic of tholeiitic rocks (Irvine and Barager, 1971; Thompson, 1973). There is some scatter into the calc-alkaline field, which may be due to the mobility of the major elements and slight alkali enrichment during alteration as shown by the metagabbros. The C.I.P.W. normative values, which were calculated with an assumed $Fe_2O_3/FeO = 0.15$ (Tables VII and VIII), indicate that the basic dykes are olivine- and quartz-tholeiites with normative olivine, quartz, hypersthene and diopside; the gabbros are sub-alkaline olivine-tholeiites which plot in the olivine–diopside–hypersthene field (Fig. 38) of the normative tetrahedron. The metagabbros have been displaced into the nepheline-normative alkali olivine-basalt field. In considering normative feldspar in the olivine–plagioclase–pyroxene system (Fig. 39), the samples are scattered around the presumed olivine–plagioclase cotectic line (Miyashiro and others, 1970; Shido and others, 1971).

Although the majority of the basic rocks analysed are gabbroic in composition and show a narrow range of SiO_2 values, some, including the gabbroic pegmatite, contain interstitial quartz; others are dioritic and quartz-dioritic in composition and show a wider range of SiO_2 values (Fig. 40). As many of these rocks have been metamorphosed, recrystallized and intruded by quartz-rich magmatic phases, the origin of the dioritic assemblages is uncertain; the SiO_2 values may thus not be a primary feature of the rocks and the Fe*/Mg ratio

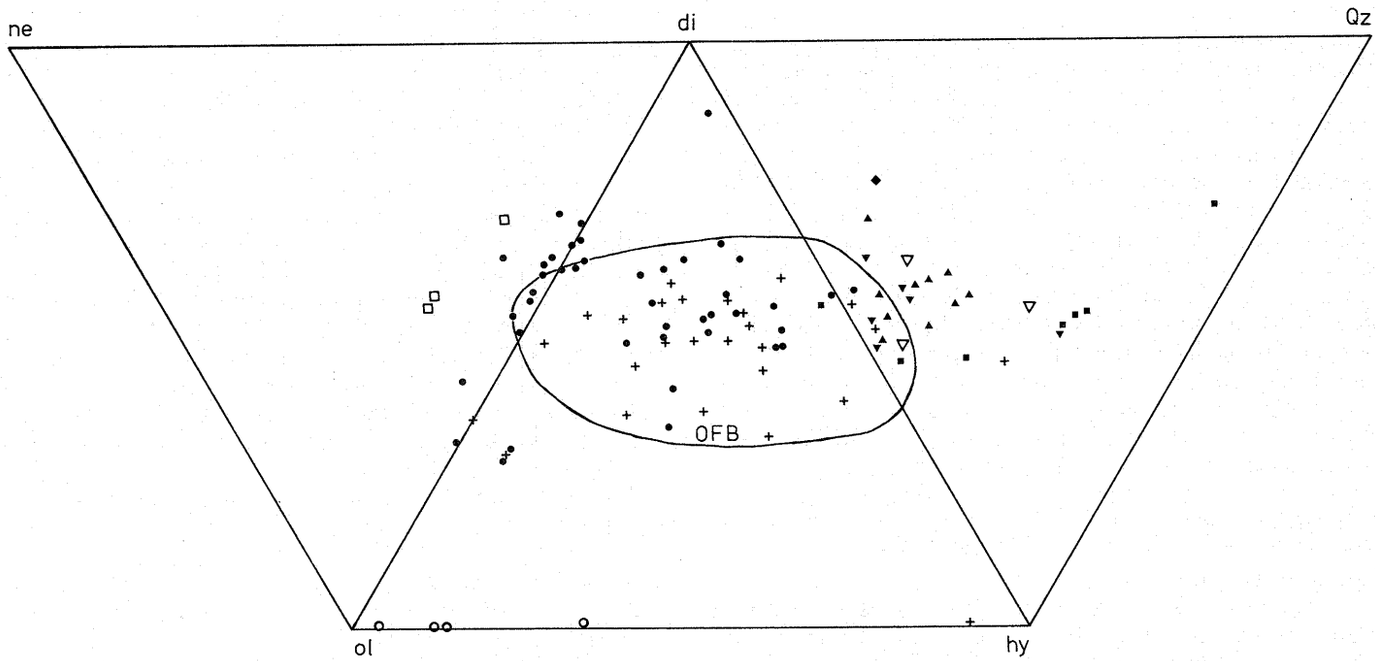

FIGURE 38
Normative di–ol–hy–Qz–ne tetrahedron of the basic rocks of the Drygalski Fjord Complex. Ocean-floor basalt (OFB) field from Saunders and others (1979).

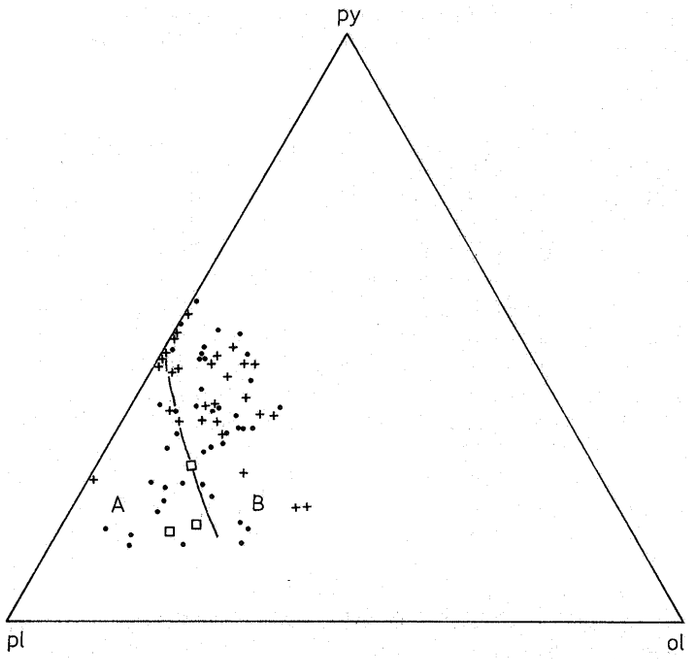

FIGURE 39
Normative py–pl–ol triangular diagram for the basic rocks of the Drygalski Fjord Complex, showing the plagioclase-tholeiite (A) and olivine-tholeiite (B) fields of Miyashiro and others (1970).

(Fe* = total iron as Fe^{2+}) is used here an an indicator of fractionation (Miyashiro and others, 1969, 1970, 1971; Shido and others, 1971; Saunders and others, 1979). Zircon was not used as a fractionation index, as many of the gabbros are cumulates and have low Zr contents.

1. *Gabbroic rocks*

a. *Major elements*. The basic rocks display a wide range of Fe*/Mg ratios (0.25–4.30 with a single partially assimilated dyke with a value of 13.2) due to the marked increase in Fe_2O_3 and decrease in MgO during fractional crystallization of the magma. As Fe*/Mg increases (Fig. 40), there is a marked increase in the concentration of the major oxides, TiO_2, FeO*, Na_2O, K_2O and P_2O_5, and a marked decrease in the concentration of Al_2O_3, MgO and CaO. Although there is some overlap, there is a significant difference between the dykes and gabbros with the dykes being more fractionated (have a higher Fe*/Mg ratio with more Fe*, TiO_2, Na_2O and K_2O and less Al_2O_3, MgO and CaO) than the gabbros. The least-fractionated gabbros crop out in the Hamilton Bay area. The high concentration of MgO is due to the separation and accumulation of olivine and pyroxene in cumulate gabbros in the early stages of fractionation. Titanomagnetite was not an important cumulus phase in these gabbros, as indicated by the low TiO_2 and FeO values and by petrographic evidence. However, some fractionated ferrogabbros with high TiO_2 (4.75 and 2.35%) and FeO* values crop out in the Mount Baume area.

The ultramafic rocks are similar to the least-fractionated gabbros, having a high concentration of MgO due to the accumulation of olivine, and a low concentration of TiO_2, Na_2O, K_2O and P_2O_5. In contrast to the gabbros, they have abnormally low concentrations of Al_2O_3 and CaO (absence of feldspars) and high concentrations of Fe*.

The metagabbros are similar to the above and, with the exception of Na_2O and K_2O, fall within the above trends; there is a marked increase in Na_2O and K_2O with a slight decrease in CaO for a given Fe*/Mg ratio.

b. *Trace elements*. As the Fe*/Mg ratio increases, there is a marked decrease in the concentration of Ni and Cr and an increase in Ce, La, Zr, Nb, Y and Zn (Fig. 40). Rb, Sr and Ba show a wide range of values for a given Fe*/Mg ratio; the ultramafic rocks have low (below detection limits) concentrations of Rb (< 3 ppm) and Sr (< 3 ppm). There is an increase in the Ba/Sr and Rb/Sr ratios from gabbros to dykes (Tables VII and VIII).

As in the major elements, the dykes, although they show some overlap with the gabbros, are in general more fractionated than the gabbros. The incompatible elements, Zr, Ce, La and Y, are in much lower abundances in the gabbros than in the dykes, with only a small number of samples, from Cooper Island and the Mount Baume area, having concentrations similar to those in the basic dykes. This agrees with the cumulate nature of the gabbros; the incompatible elements are largely concentrated in the intercumulus liquids and the most-fractionated rocks. The strong negative relationship between Ni and Cr and the Fe*/Mg ratio in both dykes and gabbros is most striking and supports fractionation involving olivine, clinopyroxene and possibly chrome spinel; Ni partitions strongly into olivine and both Ni and Cr into clinopyroxene (Leeman, 1976). The high Cr values are probably due to the chrome-spinel symplectites present in some gabbros. The ultramafic rocks have extremely high Ni and Cr values. The wide range of Ni and Cr values for a given Fe*/Mg ratio is due to the presence of widespread feldspar-rich cumulates.

Although considerable scatter exists, there is an increase in Rb values and a decrease in the K/Rb ratio with increase in K_2O from gabbros to dykes with many of the gabbros and some dykes falling below the detection limits (< 3 ppm) for Rb (Fig. 41). It was suggested by Saunders and others (1979) that hydrothermal activity, which caused recrystallization of the dykes, was accompanied by loss of Rb and K from the dykes and some gabbros in the Sarmiento Complex. This was not found in the Drygalski Fjord Complex, where the dykes are richer in K_2O and Rb than the gabbros and where the altered gabbros show a wide range of Rb and K values, the majority of which are enriched in Rb and K (Figs 40 and 41); this variation of K_2O and Rb in the metagabbros may indicate a marked mobility but not necessarily a loss of K_2O or Rb during alteration. The difference between the Sarmiento Complex and the Drygalski Fjord Complex observations may reflect an important difference in the hydrothermal regime at each site. At Sarmiento, the presence of an active spreading centre encouraged mobilization and depletion of the alkalis.

In the absence of a complete rare-earth element analysis of the dykes and gabbros, chrondite-normalized La, Ce and Y values have been plotted (Fig. 42). Y is used in place of Ho as it has a similar ionic radius and charge to Ho, and closely parallels the behaviour of the heavy rare-earth elements. The dykes and gabbros are mainly slightly light rare-earth element enriched although some gabbros, mainly from the Mount Baume area, and dykes are enriched in the heavy rare-earth elements; a few

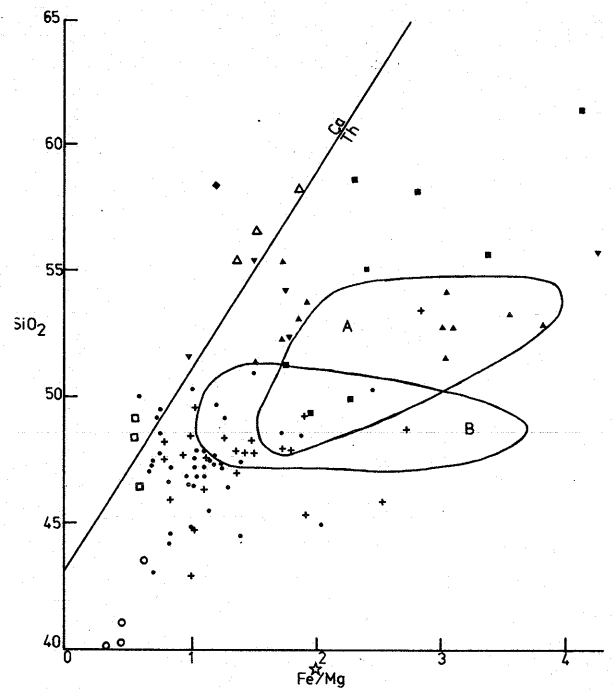

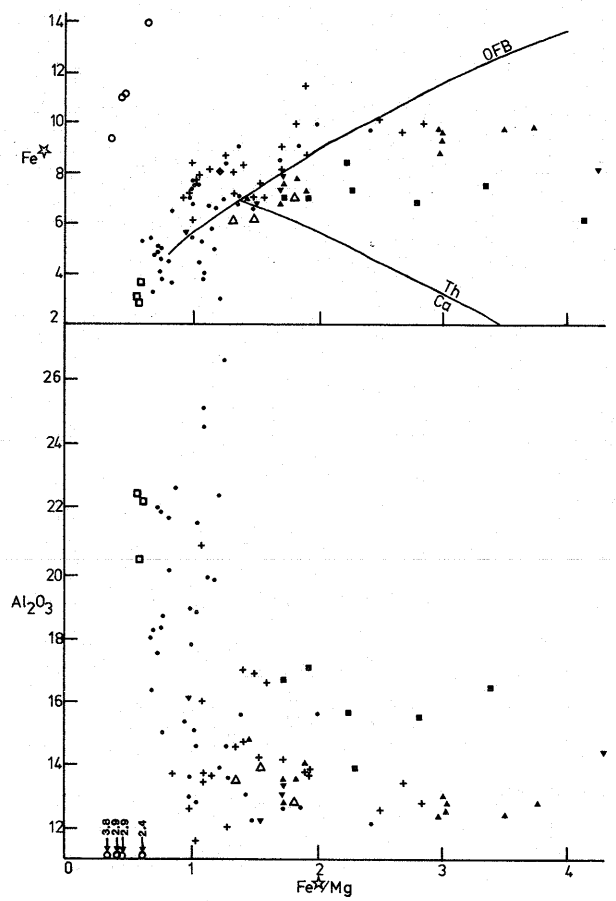

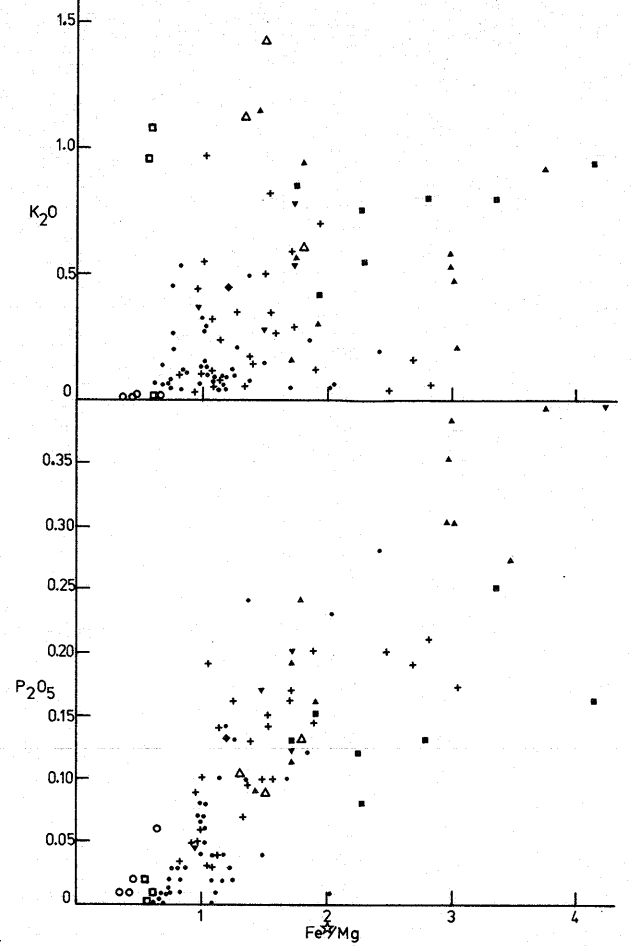

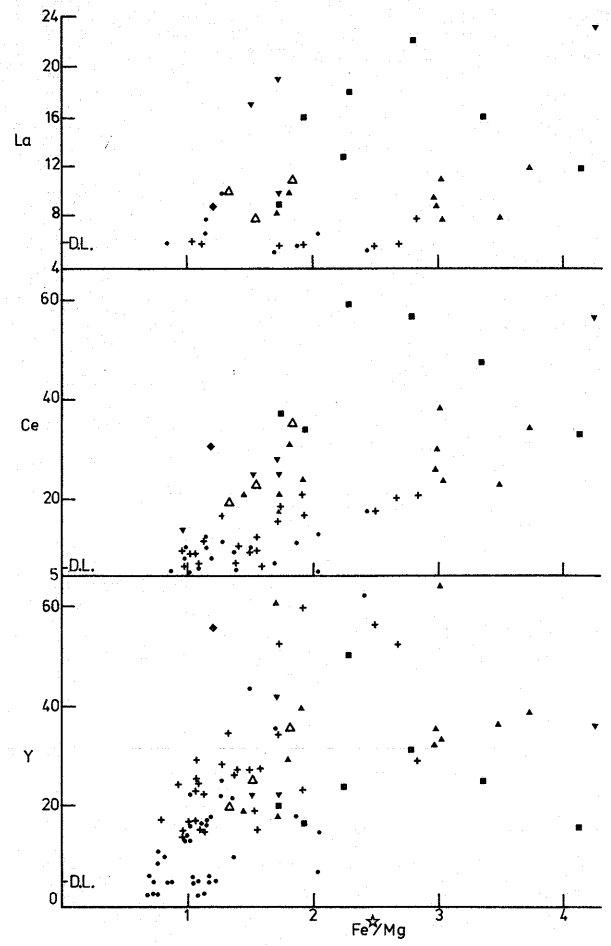

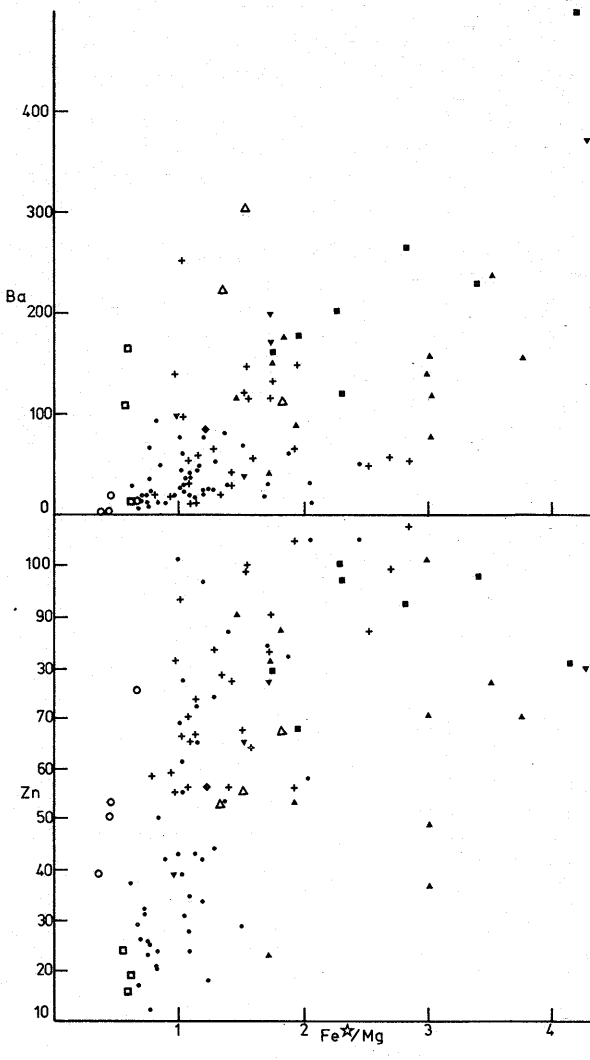

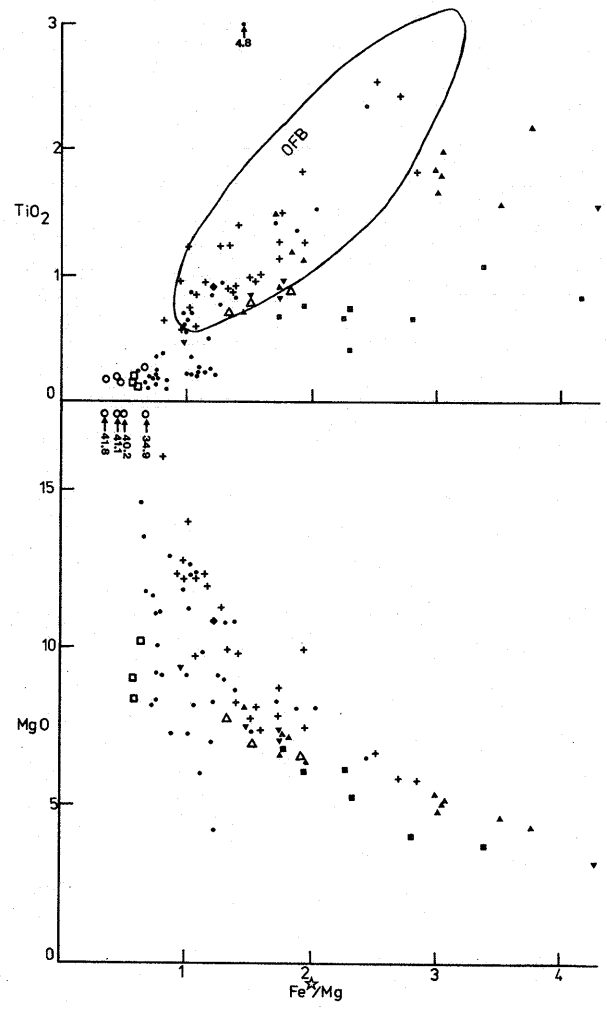

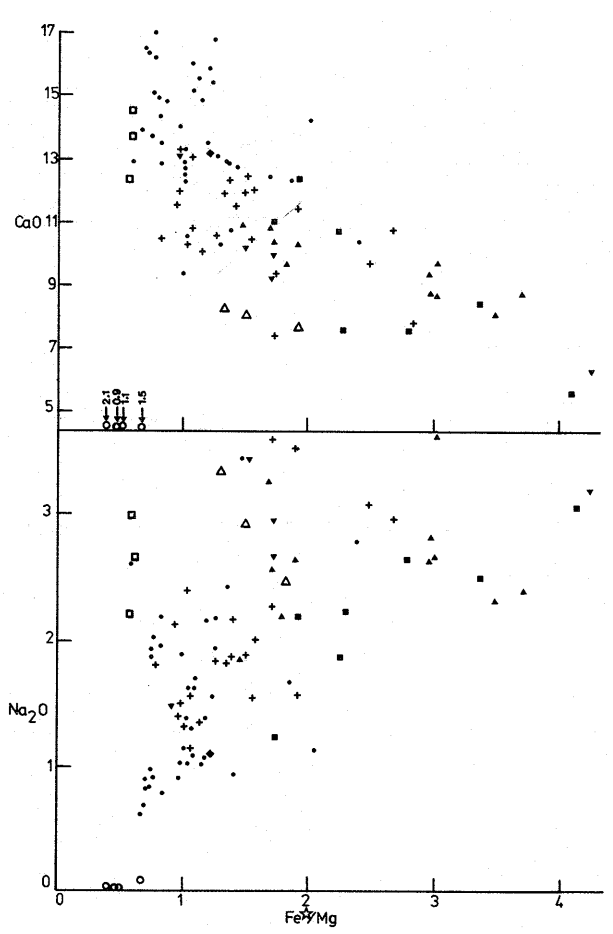

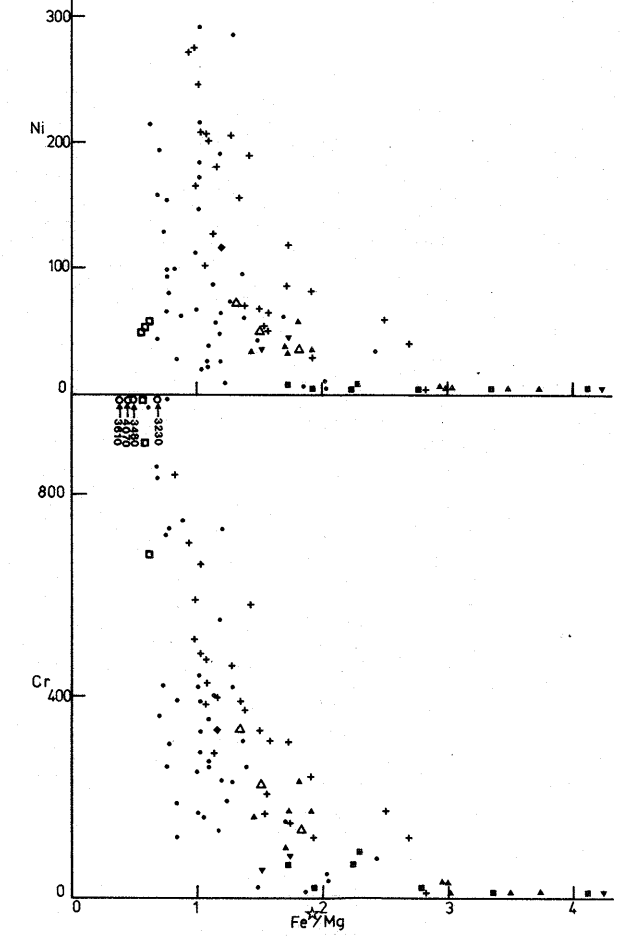

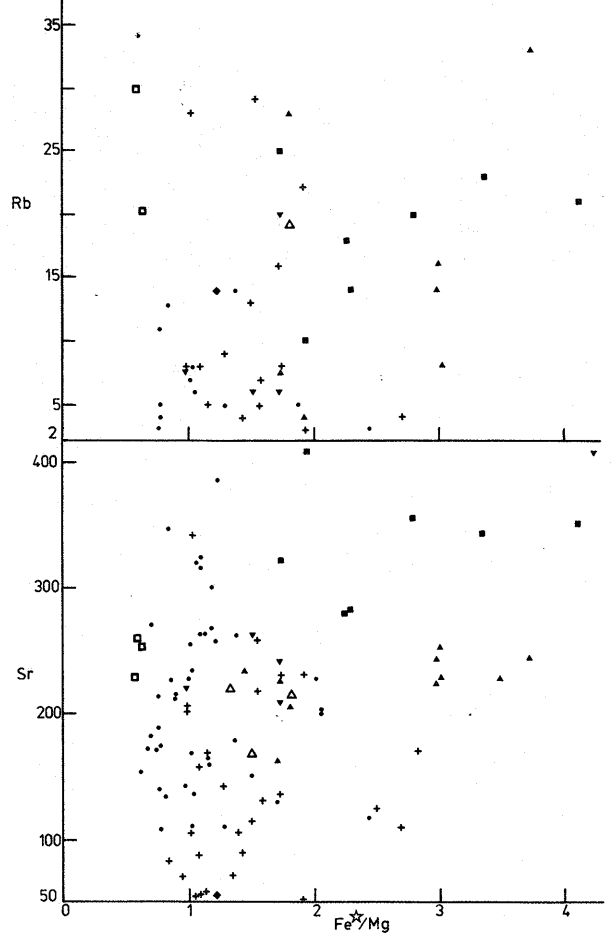

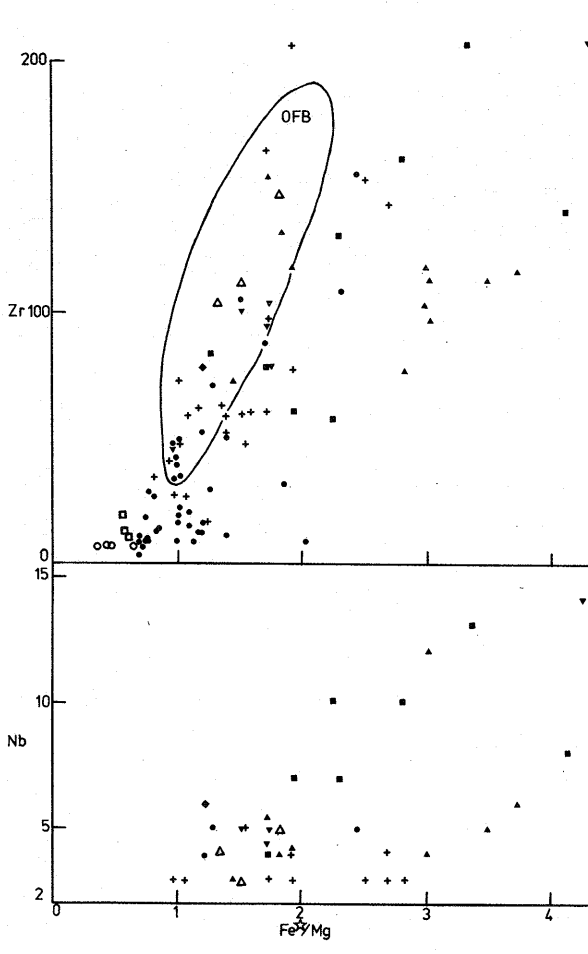

FIGURE 40
Plots of the major- (weight %) and trace-element (ppm) abundances for the basic rocks of the Drygalski Fjord Complex against the Fe*/Mg ratio (Fe* is total iron as Fe^{2+}). The boundary between the calc-alkaline (Ca) and tholeiitic (Th) fields is from Miyashiro (1973); "A" encloses island-arc tholeiite and "B" mid-ocean ridge basalt field (Saunders and others, 1979); the ocean-floor basalt field (OFB) and trend is taken from Saunders and others (1979); D.L., lower limit of detection.

[face page 36

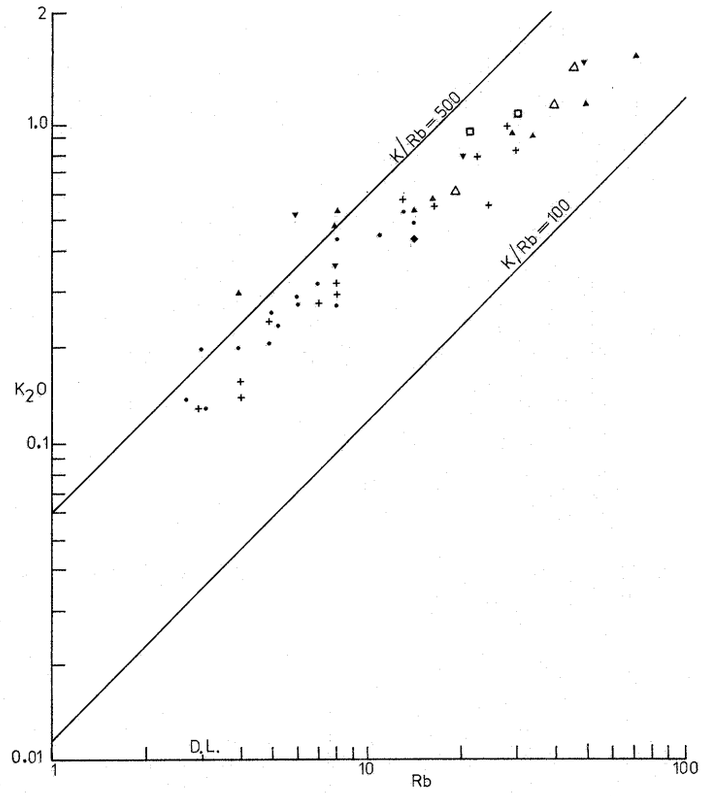

FIGURE 41
K_2O versus Rb variation diagram for the basic rocks of the Drygalski Fjord Complex. D.L., lower limit of detection.

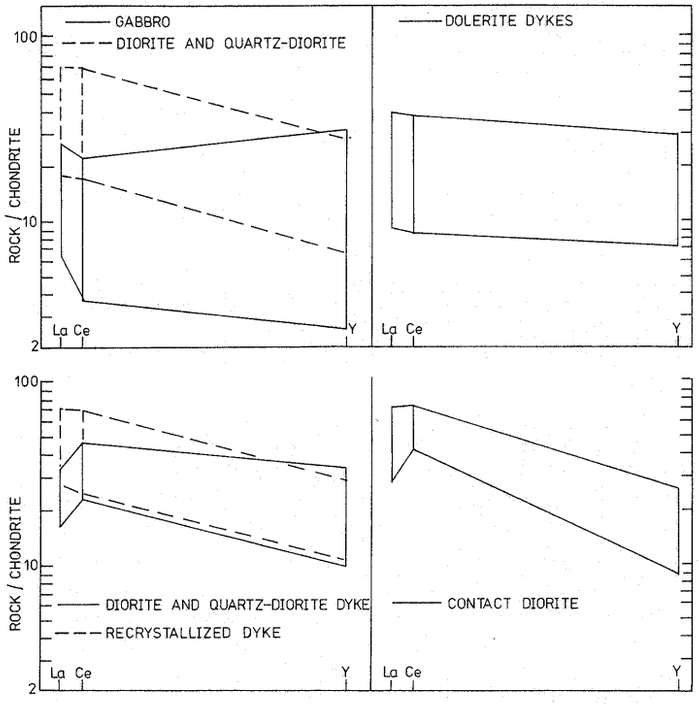

FIGURE 42
Simulated rare-earth patterns for the basic rocks of the Drygalski Fjord Complex based on XRF values for La, Ce and Y.

have similar concentrations (flat trend) of the light and heavy rare-earth elements. The dykes have higher total rare-earth element abundances than the gabbros with the most fractionated dykes and gabbros being most enriched in the rare-earth elements relative to the least-fractionated dykes and gabbros. Many of the gabbros analysed have Ce and La values below the detection limits of the University of Birmingham XRF equipment. This is commonly found in cumulate gabbros.

2. *Diorites and quartz-diorites*

With few exceptions, which will be discussed below, the intermediate rocks have a similar fractionation trend and are more fractionated than the gabbroic rocks. The lower Mg values and higher Fe* values result in higher Fe*/Mg ratios than the gabbroic rocks. Similarly, the diorites have higher TiO_2, Na_2O, K_2O, P_2O_5, Zr and Ba, and lower Al_2O_3, MgO, CaO, Cr and Ni values than the gabbroic rocks. They show overall enrichment in rare-earth elements relative to the gabbroic rocks and are relatively enriched in light rare-earth elements (Fig. 42). These trends indicate that the SiO_2 values are primary features of the rocks and that many of the intermediate rocks did not develop by recrystallization or metasomatism of the basic rocks.

In some cases, the basic dykes and gabbros were affected by intrusive breccias, and these rocks, including the gabbroic pegmatite, show high SiO_2 contents without a significant increase in Fe*/Mg, Fe*, TiO_2 or P_2O_5 values. They are enriched in mobile alkali elements Na_2O, K_2O and CaO, and trace elements La, Ce, Y and Zr. This may be due to recrystallization and an enrichment caused by the magmatic fluids of the intrusive breccias (metasomatism).

The dioritic and quartz-dioritic rocks, which crop out along the gabbro–Trendall Crag granodiorite contact zone, follow for the most part the trends of the above dioritic dykes and intrusions (Fig. 37). Although they show a marked increase in Fe*/Mg ratio, some have slightly lower values of Fe*, TiO_2, P_2O_5, MgO and Y, and higher values of Al_2O_3, SiO_2, K_2O, Ce, La and Sr for the given Fe*/Mg ratio relative to the above. The lower TiO_2 and P_2O_5 values may be due to earlier fractionation of apatite and sphene, both of which are common in the gabbros. The high Zr values and the fact that, in general, they follow the fractionation trends indicate that they also have formed by fractional crystallization of a tholeiitic magma without any significant magma mixing. The (?) hybrid textures discussed earlier and the relative increase in some elements are probably due to some exchange of SiO_2 and K_2O and associated elements with the country rock or the Trendall Crag granodiorite.

3. *Discussion*

With the exception of some of the quartz-dioritic and dioritic rocks discussed above, the fractionation trends and, in particular, the wide range of Fe*/Mg values and small variations in the SiO_2 values are characteristic of tholeiitic differentiation trends (Nockolds and Allen, 1953; Miyashiro, 1972, 1973). The fractional crystallization is controlled by separation of olivine and plagioclase with a marked initial decrease in Cr and Ni contents due to the early precipitation of olivine; plagioclase fractionation mainly affects Sr values. Clinopyroxene and primary brown hornblende are important in the middle stages of fractionation (Thompson, 1973) and Fe–Ti oxides, which gave

TABLE IX

AVERAGE CHEMICAL ANALYSES OF BACK-ARC BASIN, OCEAN BASIN, LOW-POTASSIUM THOLEIITES AND CALC-ALKALINE BASALTS

	1	2	3	4	5	6	7	8	9	10	11	12	13	14	15	16	17	18	19	20	21	22
SiO_2	51·21	49·00	47·79	50·94	48·97	48·98	45·46	49·36	48·8	48·6	50·62	49·6	49·5	49·6	49·21	48·56	52·83	49·0	50·94	46·96	49·44	72·47
TiO_2	1·25	1·04	0·35	1·37	1·66	1·63	2·19	0·92	0·6	1·0	1·26	1·5	1·2	1·5	1·39	0·24	0·83	0·8	0·74	0·78	1·33	0·33
Al_2O_3	14·25	16·31	17·41	15·31	14·62	12·52	10·44	15·66	16·8	16·4	16·77	16·6	15·5	15·7	15·81	18·69	16·69	18·6	18·42	18·77	16·12	14·17
Fe_2O_3*	11·74	10·04	7·73	12·00	12·72	12·5	12·76	8·87	7·7	9·3	8·32	9·5	10·8	8·44	10·20	–	8·39	10·6	10·56	9·11	12·65	–
MnO	–	0·18	0·17	0·19	0·18	0·24	0·21	–	0·1	0·2	0·15	0·1	0·1	0·2	0·16	0·11	0·16	0·2	–	0·14	0·23	0·08
MgO	8·19	8·14	10·82	5·84	6·5	8·5	17·66	7·54	8·4	9·5	7·53	6·8	6·7	9·3	8·53	9·26	9·74	5·1	5·47	8·06	7·46	1·39
CaO	10·31	12·82	14·13	10·22	11·71	10·0	9·92	13·10	12·9	12·2	10·95	11·4	11·3	11·2	11·14	12·67	8·15	9·0	11·70	13·52	10·03	1·48
Na_2O	2·35	2·11	1·54	2·40	1·95	2·73	1·27	3·11	2·2	2·3	3·08	3·2	2·7	2·7	2·71	1·88	3·24	3·0	2·10	1·99	2·5	5·55
K_2O	0·53	0·18	0·19	0·23	0·41	0·29	0·16	0·37	0·2	0·2	0·42	0·42	0·3	0·08	0·26	0·07	0·26	0·6	0·27	0·37	0·42	0·24
P_2O_5	0·18	0·09	0·03	0·29	0·14	0·21	0·04	0·05	0·06	0·09	0·18	0·2	0·1	0·03	0·15	0·02	–	0·14	0·05	0·14	0·20	0·06
Cr	235	236	494	115	152	249	778	200	–	520	257	230	300	730	296	900	–	35	62	130	150	<20
Ni	76	69	140	27	30	62	239	52	–	226	69	70	90	163	123	200	–	20	27	48	48	22
Zn	73	61	37	–	–	–	–	46	–	–	68	–	–	–	122	–	–	–	–	87	43	–
Rb	16	4	4	8	12	9	3	5	–	1	5	5	–	–	1·3	–	–	4	11	13	6	–
Sr	186	225	184	191	140	166	105	154	–	142	195	190	150	176	123	110	–	250	137	451	410	89
Y	31	19	8	32	21	33	14	22	–	–	28	–	–	29	32	25	–	–	–	10	22	–
Zr	94	53	22	122	53	100	33	–	–	–	109	–	–	47	100	<10	–	50	69	49	73	200
Nb	3	3	<3	3	1	3	1	<3	–	–	4	–	–	–	3	–	–	–	–	2	3	–
Ba	116	58	39	92	96	139	49	49	–	34	61	40	–	14	12	10	–	95	58	139	88	200
La	6	6	<6	9	4	26	13	<6	–	–	8	–	–	–	–	–	–	–	–	4	6	–
Ce	19	10	<6	22	10	18	8	6	–	–	16	–	–	–	–	–	–	–	–	12	18	–
Fe*/Mg	2·14	1·46	0·84	2·38	2·27	1·72	0·84	1·40	1·07	0·89	1·29	1·21	1·45	1·06	1·10	–	0·86	1·88	2·25	1·32	2·21	–
K/Rb	308	398	398	239	277	267	443	730	–	1 660	639	697	–	–	2 158	–	–	1 203	204	236	581	–
Rb/Sr	0·11	0·06	0·06	0·04	0·09	0·05	0·03	0·03	–	0·01	0·03	0·03	–	–	0·01	–	–	0·02	0·08	0·03	0·01	–
Ba/Sr	0·63	0·39	0·39	0·48	0·69	0·84	0·47	0·32	–	0·24	0·31	0·21	–	0·08	0·10	0·09	–	0·38	0·42	1·14	0·21	2·25
Zr/Nb	31	17·6	–	41	53	33·3	33	14·2	–	–	27·3	–	–	–	3·33	–	–	–	–	25·0	24·3	–
n	40	18	21	34	22	6	5	3	5	14	6	6	10	2	33	1	5	7	9	26	2	1

n Number of samples.
Fe* Total iron as Fe^{+2}.
Fe_2O_3* Total iron as Fe_2O_3.

Drygalski Fjord Complex
1. Basic dykes.
2. Gabbros (Fe*/Mg>1).
3. Gabbros (Fe*/Mg<1).

Back-arc basins
4. Basic dykes, Sarmiento Complex (Saunders and others, 1979).
5. Gabbros, Sarmiento Complex (Saunders and others, 1979).
6. Basic dykes, Tortuga Complex (Suárez, 1977).
7. Gabbros, Tortuga Complex (Suárez, 1977).
8. Wheeler Glacier gabbros, Larsen Harbour Formation (Mair, in press).
9. Gabbros, Lau Basin (Hawkins, 1976).
10. Basalts, Lau Basin (Hawkins, 1976).
11. Basalts, East Scotia Sea (Saunders and others, 1982).
12. Basalts, Mariana Basin (Hart and others, 1972).
13. Basalts, North Fiji Basin (Hawkins, 1977).

Ocean basins
14. Gabbros, Mid-Atlantic Ridge (Miyashiro and others, 1970; Thompson, 1973).
15. Basalts, Mid-Atlantic Ridge (Melson and Thompson, 1971).
16. Gabbros, Romanche Fracture Zone (Melson and Thompson, 1971).

Low-potassium tholeiites
17. Gabbros, Mount Stuart Batholith (Erikson, 1977).
18. Basalts, Tongan Islands (Jakes and Gill, 1970; Ewart and Bryan, 1972).
19. Basalts, South Sandwich Islands (Baker, 1976).

Calc-alkaline basalt series
20. Gabbros, Antarctic Peninsula (West, 1974; Singleton, 1976; Dewar, 1970; Smith, 1977; Saunders and others, 1982).
21. Basalts, South Shetland Islands (Weaver and others, 1982).

Ocean basin
22. Diorite, Mid-Atlantic Ridge (Aumento, 1969).

Iface page 38.

the high TiO_2 values of some of the Mount Baume area gabbros, are important in the later stages of fractional crystallization.

As there is considerable chemical overlap between the dykes, gabbros and some diorites, and they show a continuous tholeiitic fractionation trend, it is concluded that the dykes and gabbros are co-magmatic with both being derived from a single olivine-tholeiitic magma by fractional crystallization; the gabbros formed by crystal accumulation, whereas the more fractionated liquids, enriched in incompatible elements, were intruded as diorites and a basic dyke suite.

B. Tectonic Environment

1. *Discrimination diagrams*

The quartz- and olivine-tholeiites of the Drygalski Fjord Complex may have been generated in a number of different tectonic environments; tholeiitic basalts occur as ocean-floor basalts and marginal back-arc basin basalts at constructive plate margins; low-potassium tholeiites and calc-alkaline basalts occur at converging plate margins; and tholeiitic basalts are found within continental plates (Miyashiro, 1975).

There have been many attempts using geochemistry to differentiate between the above tectonic environments; Ti, Zr, Y, Cr and Nb, which are the most immobile elements during low-grade metamorphism (Cann, 1970; Pearce and Cann, 1973; Pearce and others, 1975; Floyd and Winchester, 1975), have been used with particular success. As the gabbros are cumulates and may be depleted in Zr or enriched in Ti due to crystal accumulation, they are not considered.

Using the Ti–Zr–Y triangular diagram (Fig. 43a) of Pearce and Cann (1973), the basic rocks (excluding gabbros) mainly fall within the low-potassium tholeiite and ocean-floor basalt overlapping fields with some spread of the dioritic rocks into the calc-alkaline field; the only conclusion that can be drawn is that they are not within-plate basalts. Similarly, on the Ti–Zr discriminating diagram (Fig. 43b) (Pearce and Cann, 1973) there is a wide distribution of the points with the analyses falling in a number of different fields. The discriminating plots of Floyd and Winchester (1975) support the tholeiitic nature of the rocks but do not discriminate between oceanic and continental tholeiites. Island-arc tholeiites were not considered in constructing these plots.

As well as the above immobile elements, Sr and K_2O have been used in discriminating plots (Pearce and Cann, 1973; Pearce and others, 1975) but these must be interpreted with caution due to the mobility of these elements. Using the TiO_2–K_2O–P_2O_5 diagram (Pearce and others, 1975), the dykes predominantly fall in the ocean-floor basalt field (Fig. 44a), ruling out the presence of continental tholeiites. The wide spread of data which results from the Ti–Zr–Sr plot (Fig. 44b) is of little use in determining the origin of the basic rocks.

In conclusion, the discriminating plots are not conclusive but indicate that the basic rocks are associated with a plate margin, have tholeiitic trends and are similar to ocean-floor basalts formed at a spreading axis. The possibility of the rocks being low-potassium tholeiites formed in an immature island arc cannot at this stage be ruled out.

2. *Comparison with basic rock suites*

The data given in Table IX are averages based on available analyses for marginal basin basalts (Sarmiento and Tortuga

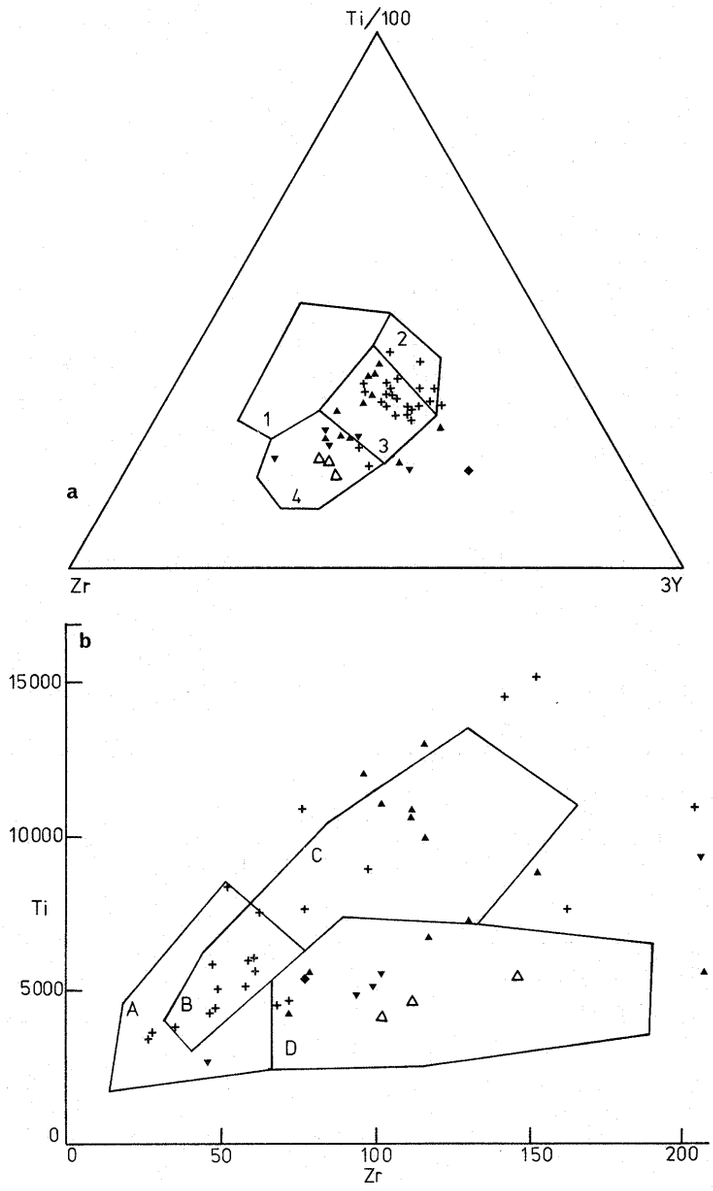

FIGURE 43

a. Basic rocks plotted on the Ti/100–Zr–3Y triangular diagram of Pearce and Cann (1973). 1, within-plate basalts; 2, 3, low-potassium tholeiites; 3, ocean-floor basalts; 3, 4, calc-alkaline basalts.

b. Basic rocks plotted on the Ti–Zr diagram of Pearce and Cann (1973). A, B, low-potassium tholeiites; B, D, calc-alkaline basalts; B, C, ocean-floor basalts.

Complexes from South America, North Fiji Plateau, east Scotia Sea, and Lau and Marianas basins from the western Pacific Ocean), oceanic tholeiites from mid-ocean ridges, island-arc tholeiites, and calc-alkaline basalts. Only those rocks which represent liquid compositions are included. As the dykes of the Drygalski Fjord Complex display a wide range of values due to crystal fractionation, and as ocean-floor and marginal basin basalts show considerable variation, care must be taken in making comparisons and in establishing averages of this kind. The figures are purely used as guide lines, as in many cases the rock associations, variation trends and ratios are more important in establishing a tectonic environment than a particular analysis.

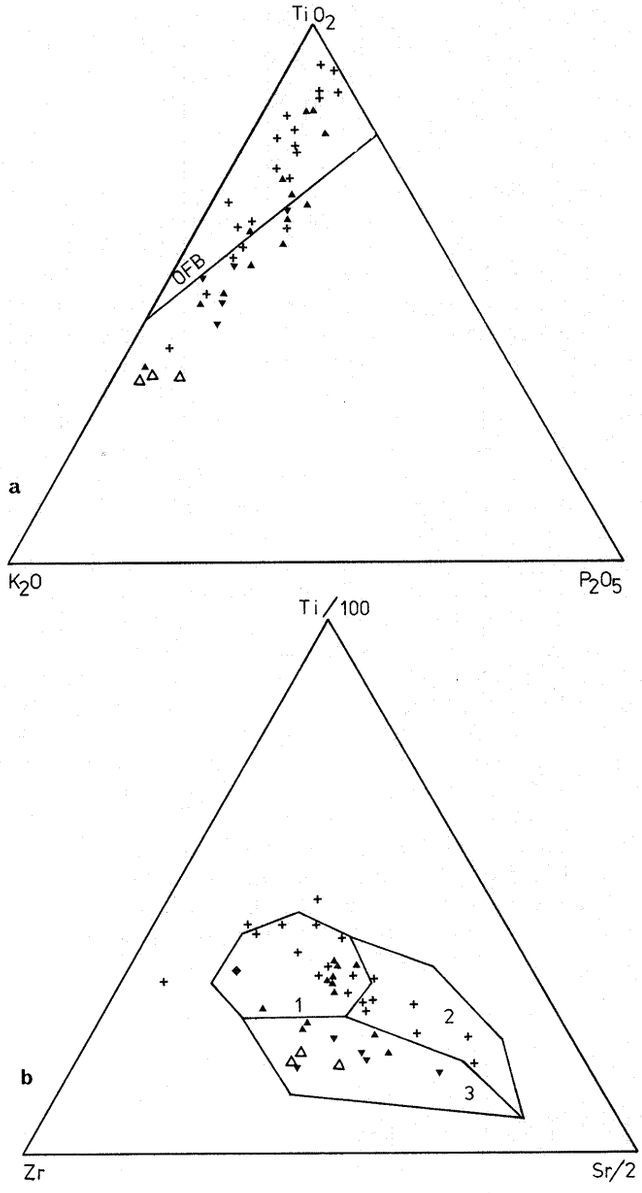

FIGURE 44

a. Basic rocks plotted on the TiO_2–K_2O–P_2O_5 triangular diagram (Pearce and others, 1975). OFB, ocean-floor basalt field.
b. Basic rocks plotted on the Ti/100–Zr–Sr/2 triangular diagram of Pearce and Cann (1973). 1, ocean-floor basalts; 2, low-potassium tholeiites; 3, calc-alkaline basalts.

Although there are some differences, the dykes of the Drygalski Fjord Complex are similar to the dykes of the Tortuga Complex (Suárez, 1977*a*; Stern, 1979) and the Sarmiento Complex (Saunders and others, 1979), which are believed to be part of the same back-arc basin system (Dalziel and others, 1975; Suárez and Pettigrew, 1976; Storey and others, 1977). The dykes of the Drygalski Fjord Complex have lower values of incompatible elements (TiO_2, Zr, Y, La and Ce) than the dykes of the Sarmiento and Tortuga Complexes, which may indicate that the former are less fractionated than the latter. The Drygalski Fjord Complex dykes are also richer in K_2O and Rb. This may be due to the difference in the amount of alteration and the hydrothermal regime at each site. At Sarmiento and Tortuga, the hydrothermal activity was probably closely associated with and controlled by an active spreading centre. This encouraged mobilization and scavenging of alkalis, alkali earths and perhaps even silica. As the dykes of the Drygalski Fjord Complex were emplaced within continental crust, the amount of water available was probably limited.

In comparison with basalts formed by sea-floor spreading in large ocean basins (mid-ocean-ridge basalts (Melson and Thompson, 1971; Thompson and others, 1972)), the Drygalski Fjord Complex dykes compare favourably, both being depleted in lithophile elements; mid-ocean-ridge basalts have characteristically low K_2O and Rb values (Engel and others, 1965; Cann, 1971) and $Ce_N/Y_N < 1$ (Engel and others, 1965). However, similar to the Sarmiento and Tortuga Complexes, the dykes of the Drygalski Fjord Complex are enriched in some lithophile elements (K, Rb and Ba, the most mobile elements), depleted in Ni, have lower K/Rb ratios and higher Rb/Sr, Fe*/Mg and Ba/Sr ratios than mid-ocean-ridge basalts. The dykes of the Drygalski Fjord Complex have very similar Zr, Y, Ce, La and P, the most immobile elements, to the mid-ocean-ridge basalts. The Y/Nb ratios (<3 for mid-ocean-ridge basalts (Pearce and Cann, 1973)) and the Zr/Nb ratios (10–40 for depleted mid-ocean-ridge basalts (Erlank and Kable, 1976)) are also similar to mid-ocean-ridge basalts (Table VIII). Although most ocean-floor basalts are "depleted" in lithophile elements, they are chemically varied and may have less-depleted characteristics in certain elements; those from lat. 45°N show strong enrichment in K, Rb, Ba, Sr, Ce and La (Erlank and Kable, 1976) in a similar way to the Drygalski Fjord Complex dykes. In the same way, the dykes of marginal basins (Lau (Hawkins, 1976), Mariana (Hart and others, 1972) and North Fiji basins (Hawkins, 1977)) and the Scotia Sea (Saunders and Tarney, 1979; Saunders and others, 1982*a*) are chemically varied and may be transitional between ocean-floor basalts and island-arc tholeiites due to additional involvement of fluids arising from the subduction zone (Saunders and Tarney, 1979; Weaver and others, 1979). The Drygalski Fjord Complex dykes resemble those more closely than mid-ocean-ridge basalts. The Mariana, South Sandwich Islands and Fiji back-arc basin basalts are enriched in Ce, La, P, Ba, Rb and K_2O, depleted in Ni, and have lower K/Rb ratios. The Lau basin basalts are an exception to this and most closely resemble the mid-ocean-ridge basalts, being depleted in the lithophile elements.

Although the Drygalski Fjord Complex dykes display some of the characteristics of ocean-floor and marginal basin basalts, it is important to consider whether they are part of a magmatic arc related to calc-alkaline or island-arc tholeiitic plutonic activity above a subduction zone. Low-potassium tholeiites are characteristic of some primitive island arcs (Tonga Islands (Ewart and Bryan, 1972; Ewart and others, 1973)). In comparing average analyses for a given Fe*/Mg ratio, the island-arc tholeiites are significantly lower in TiO_2, Ni, Cr, P_2O_5 and Zr and enriched in Al_2O_3 and Sr compared to the Drygalski Fjord Complex rocks and mid-ocean-ridge basalts. However, similar to the Drygalski Fjord Complex, they are enriched in K_2O, Ba and Rb (this may be due to alteration in the Drygalski Fjord Complex basic rocks). The high Ni, Cr and Zr values and low Fe*/Mg ratios and Al_2O_3 values of the Drygalski Fjord Complex dykes are not a characteristic of island-arc tholeiites. In the same way, the calc-alkaline volcanic rocks of the South

Shetland Islands are enriched in Sr, Ba, K_2O and Rb, and depleted in Ti and Ni with high Ce_N/Y_N ratios.

The Drygalski Fjord and Sarmiento Complex dykes show overall and light rare-earth element enrichment compared to some "depleted" mid-ocean-ridge basalts (Erlank and Kable, 1976). The Mariana basin basalts, although they display poor trends (Hart and others, 1972) are 2–4 times more enriched in rare-earth elements than the mid-ocean-ridge basalts. In contrast, the island-arc tholeiites are depleted with variable light rare-earth element concentrations (Jakes and Gill, 1970). Chondrite-normalized Ce/Y ratios of mid-ocean-ridge basalts are generally less than 1 (Engel and others, 1965; Frey and others, 1974). Due to the light rare-earth element enrichment,

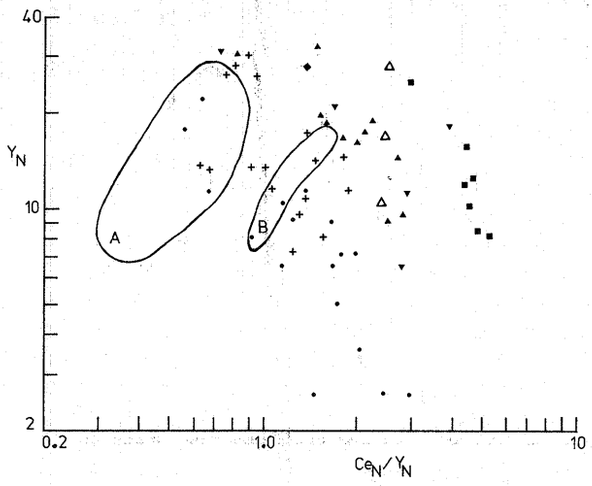

FIGURE 45
Chondrite-normalized Y versus Ce_N/Y_N diagram for the basic rocks of the Drygalski Fjord Complex. The ocean-floor basalt field (A) and Scotia Sea marginal-basin basalt field (B) are taken from Saunders and others (1979).

the dykes of the Drygalski Fjord Complex (Fig. 45) and of back-arc basins have Ce_N/Y_N ratios greater than 1; however, they still fall within the range of transitional "enriched" mid-ocean-ridge basalts (O'Nions and Gronvold, 1973).

Although the dykes and gabbros of the Drygalski Fjord Complex are both quartz- and olivine-normative, mid-ocean-ridge basalts are rarely quartz-normative (Chayes, 1972). However, the basalts of the South Sandwich Islands spreading centre are both quartz- and olivine-normative (Saunders and Tarney, 1979). Green (1973) has suggested that under water-saturated conditions, partial melting of pyrolite mantle could yield quartz-normative basalt at pressures up to 20 kbar. On considering the normative olivine–plagioclase–pyroxene system, the Drygalski Fjord Complex dykes, like the Lau basin basalts, are both olivine- and plagioclase-tholeiites, whereas the North Fiji plateau and Mariana basin basalts are plagioclase-tholeiites and the Tortuga Complex basalts are mainly olivine-tholeiites.

It is thus concluded that the dykes and gabbros of the Drygalski Fjord Complex are slightly enriched in alkalis and have a composition intermediate between a calc-alkaline basalt suite and abyssal tholeiites, and that the initial magma formed by partial melting of the mantle and developed by accumulation and fractional crystallization along tholeiitic trends. They are most similar to documented marginal basin tholeiites and to the dykes and gabbros of the nearby Larsen Harbour Formation (Mair, in press, *b*), which are slightly enriched in large-ion lithophile elements compared to the depleted mid-ocean-ridge basalts. With the exception of the Lau basin and Tortuga Complex basalts, none of the marginal basin basalts is as depleted in large-ion lithophile elements as ocean-floor basalts. The transitional nature of marginal basin basalts between ocean-floor basalts and island-arc basalts may be due to the potential involvement of fluids arising from the subduction zone (Saunders and Tarney, 1979; Weaver and others, 1979).

VII. ACID AND ASSOCIATED ROCK TYPES

AS WELL as the migmatitic granites, which are described later, acidic rocks form about 15% of the complex. Two coarse-grained bodies, the Trendall Crag granodiorite and the Cooper Island granophyre, which form mappable units (Fig. 5) are intruded by intrusive breccias, pegmatites and aplites. Trondhjemite, tonalite, granodiorite and granite dykes intrude and form lenses within the gabbros and metasediments of the Salomon Glacier Formation. In the northern part of the complex and on Cooper Island, porphyritic felsites (rhyolites and dacites) and porphyritic microgranites form lenses and dykes within the numerous basic dykes and sediments; in the dislocation zone, porphyritic felsites are interbanded with silicic volcaniclastic sediments of the Novosilski Glacier Formation.

A. TRENDALL CRAG GRANODIORITE

1. *Field relations*

This is a composite body of variable composition (tonalite, granodiorite, granite) which crops out over 6 km^2 on the north side of Trendall Crag (Fig. 5). It was previously termed the Trendall Crag granite (Storey and others, 1977) but, as granodiorite forms the bulk of the exposure, the pluton is renamed the Trendall Crag granodiorite. More than one intrusive phase was recognized in the field; enclaves of granodiorite and tonalite occur in a later granite.

The pluton intrudes and assimilates the older gabbro bodies with the formation of marginal diorites and quartz-diorites by contamination of the basic magma. Dioritic enclaves with quartz ocelli are found within the margins of the body. To the north of Storey Glacier (Fig. 5), rafts of banded gneiss with relict sedimentary structures are found within and form the country rock of the pluton. Areas of aligned basic and meta-sedimentary enclaves and a flow lamination are found within the margins of the pluton. Masses of ptygmatic veins, which occur within the metasediments, may be associated with emplacement of the pluton; irregular patches of migmatitic granite (Fig. 46) also occur within the gneissic country rock. The complexly deformed metasediments of structural area B are spatially removed from the Trendall Crag granodiorite but dykes of

FIGURE 46
Migmatites in the country rock of the Trendall Crag granodiorite. The scale on the hammer shaft is 20 cm long.

FIGURE 48
Basic dyke intruded by veinlets of Trendall Crag granodiorite. The scale is 10 cm long.

similar granodiorite, which cut the F3 folds of the layered migmatite, suggest a post-D3 origin for the Trendall Crag granodiorite.

A complex suite of basic dykes, which form up to 80% of the outcrop (Fig. 47), was emplaced after cooling of the granodiorite; the granite is preserved as remnant lenses between these dykes. Subsequent re-mobilization of the Trendall Crag granodiorite, and emplacement of intrusive breccias, pegmatites, aplites and basic dykes occurred. During the re-mobilization, minor veinlets of granite intruded the chilled margins of the earlier cross-cutting basic dykes (Fig. 48).

2. *Petrography*

The rocks, which are variable in composition, are coarse-grained quartz-andesine-potash feldspar-biotite-granodiorite, tonalite and granite, which have subsidiary amounts of amphibole, chlorite and epidote and accessory sphene, zircon, apatite, allanite and opaque minerals.

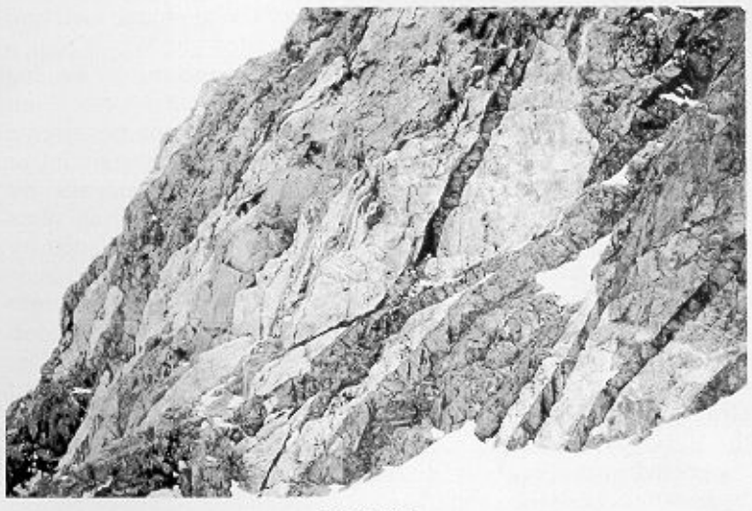

FIGURE 47
Trendall Crag granodiorite and basic dykes. The rucsac in the foreground (right) is 1 m long.

Quartz, which may form up to 25% of the rock, occurs as composite sub-rounded ovoids (6 mm in diameter) with irregular interpenetrating boundaries and as interstitial pools partially or completely enclosing the other crystals and forming poikilitic crystals up to 7 mm across. Plagioclase (An_{5-40}), which may form up to 50% of the rock, is mainly andesine (An_{40}) euhedral to subhedral in shape with a range in grain-size of 1–5 mm. Complex twins and oscillatory and simple zoning of the feldspars are found; narrow zones of low-relief feldspar (albite) occur at the margins of the crystals. Sericitization and saussuritization have taken place. Feldspars, partially devoid of twinning, have a characteristic patchy extinction with irregular patches of optically continuous quartz and potash feldspar enclosed within the plagioclase (Fig. 49a). Albite also occurs interstitially with the quartz.

Potash feldspar, which may be absent, forms up to 15% of the tonalite and granodiorite. It occurs as interstitial patches (Fig. 49b), irregular in shape and moulded around the other mineral phases, and as poikilitic crystals (up to 5 mm) enclosing plagioclase and biotite. Minor apophyses intrude the quartz ovoids and plagioclase crystals. Polysynthetic twins, characteristic of microcline, perthitic flame intergrowths and myrmekite are recorded. In the granites, subhedral plates of microcline and perthite (up to 5 mm) form up to 40% of the rock; interstitial potash feldspar also occurs. Antiperthitic intergrowths of irregular inclusions of potash feldspar, often aligned along cleavage planes, are found in the plagioclase.

Biotite is the most abundant ferromagnesian mineral, often forming up to 25% of the granitoids. It is is found as large flakes and poikilitic sheets (6 mm long, pleochroic; various shades of brown-green but usually light brown to dark brown) often altered to penninite, prehnite and yellow to pale green pistacite. Inclusions of quartz, feldspar, opaque minerals, and accessory zircon and apatite are found within the biotite. Biotite also occurs as clusters of fine-grained crystals between the ovoidal quartz and subhedral plagioclase crystals; these biotites, which

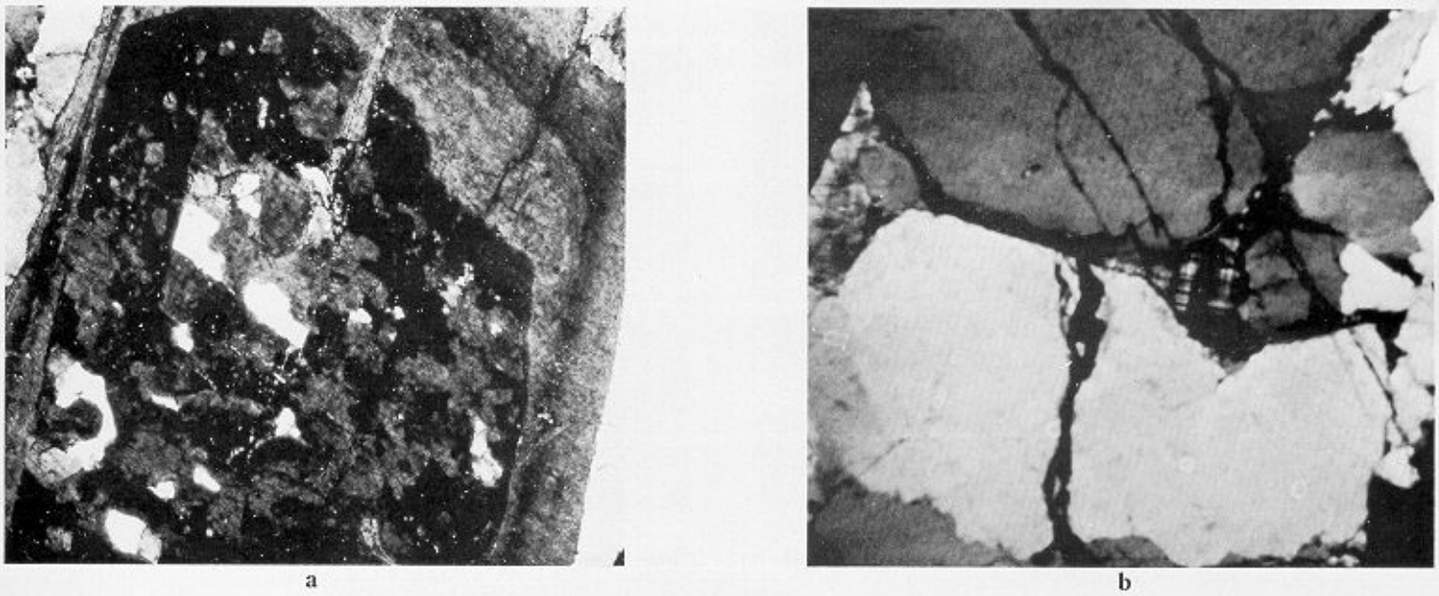

a b

FIGURE 49
a. Zoned plagioclase with inclusions of optically continuous quartz. (M.2050.A; X-nicols; ×40)
b. Quartz and interstitial microcline. (M.1801.1; X-nicols; ×40)

may represent remnant sedimentary enclaves, are usually associated with granular zircon, sphene, opaque minerals and granoblastic quartz and plagioclase. The margins of the plagioclase crystals and quartz ovoids are frequently rimmed by a thin layer of fine-grained biotite.

Amphibole, which may form up to 15% of the rock, is variable in composition. Colourless and pale-coloured (light green to bottle green) tremolite-actinolite laths and poikilitic prisms of pleochroic hornblende (α = green; β = brown-green; γ = dark green) are found. Rims of green hornblende may surround the colourless tremolite. Alteration products, penninite, epidote and clinozoisite, are found usually associated with biotite and amphibole.

Accessory sphene, zircon, acicular apatite and opaque minerals (skeletal ilmenite) are common as inclusions in the ferromagnesian minerals. Occasional (1.0 mm) euhedral crystals of a pleochroic mineral with strong absorption colours and colour zoning (allanite; parallel extinction, high relief, characteristic cracks and twinning parallel to 100) are present. The colour zoning varies from light brown to dark red-brown pleochroic to various shades of yellow. Pleochroic haloes are not present around the allanite or zircon enclosed in biotite.

Minor irregular mylonite shear zones (0.5 cm wide), peppered by granular opaque minerals, transgress the Trendall Crag granodiorite. Deformed biotite, chlorite and feldspar twin lamellae are present. Brittle deformation is indicated by extensive cracking of the feldspar and ovoidal quartz crystals. These have been filled by secondary quartz and potash feldspar.

The marginal rocks are similar to the quartz-diorites described previously. Poikilitic biotite, amphibole and chlorite laths, granophyric intergrowths and interstitial quartz and potash feldspar are characteristic features. Remnant cores of pyroxene within the amphibole are pitted with opaque minerals, partially replaced by colourless tremolite and surrounded by rims of brown-green hornblende. Porphyroblastic andesine crystals enclose high-relief plagioclase crystals (mainly labradorite).

3. *Discussion*

The origin of the Trendall Crag granodiorite is uncertain and will be discussed in more detail together with the geochemistry of the rocks. The metasedimentary enclaves, clots of fine-grained biotite and migmatites suggest a close association with the metasediments. The flow lamination, the alignment of mafic and sedimentary inclusions in the margins of the body, and the ptygmatic veins indicate that the Trendall Crag granodiorite may be a forceful intrusion. An anatectic origin by melting of the metasediments at depth, collection of the anatectic melt and intrusion of the granitic melt into the banded gneisses is thus a possible origin for these rocks. Assimilation and *in-situ* melting of the metasediments and gabbros may have occurred as a result of the intruding anatectic melt forming some of the migmatitic features and marginal hybrid rocks. Subsequent granitic intrusions may be formed from the granodioritic magma by contamination by percolating hydrothermal fluids rich in silica and potash feldspar (plagioclase crystals partially replaced by potash feldspar). Oldershaw (1969), in a study of the Lochnagar granite, has described a similar contamination of a granodiorite magma and *in-situ* formation of granites by interfacial diffusion and ionic displacement by permeating hydrothermal fluids. The field observations, which indicate a re-activation of the Trendall Crag granodiorite and subsequent intrusion of the granite into the basic dykes (which formerly chilled against the granite) is supported in thin section by irregular interlocking recrystallized boundaries and the abundance of secondary quartz, potash feldspar and plagioclase. The potash feldspar and secondary minerals may have been introduced metasomatically during the

re-heating event which also formed many of the migmatitic granite features.

Alternatively, the Trendall Crag granodiorite may have formed by differentiation from the large volume of gabbroic magma, which intruded the metasediments during the same time period as the granodiorites. Partial melting of the metasediments, as a result of the high heat flow associated with intrusion of the basic magma, would result in contamination of the acidic differentiates and the close association of the Trendall Crag granodiorite, metasediments and gabbros.

B. Cooper Island Granophyre

1. *Field relations*

A pale grey-white leucocratic granitoid pluton, cut by basic dykes, crops out over 5 km^2 on Cooper Island (Fig. 5). As granophyric textures are characteristic of this rock, the pluton is named the Cooper Island granophyre. It intrudes and assimilates sediments of the Cooper Island Formation and is closely associated with the gabbros on Cooper Island. Quartz-diorites and ocellar diorites crop out along the granophyre–gabbro contact zones; isolated rounded fine-grained basic enclaves are enclosed within the granophyre. Porphyritic rhyolite and dacite dykes, which cut the Cooper Island Formation, may represent the sub-surface equivalent of the granophyre. Intrusive breccias, which are not seen within the granophyre, are emplaced within the hornfelsed sediments, marginal diorites and gabbroic country rock of the granophyre. Although the intrusive breccias cut most basic dykes, they may represent a marginal volatile-rich phase of the granophyre.

2. *Petrography*

The Cooper Island granophyre is mainly a leucocratic trondhjemite and tonalite body which displays complex plagioclase (60%)–quartz (30%) granophyric textures (Fig. 50); ferromagnesian minerals which may form up to 5% of the rock are replaced by epidote, tremolite-actinolite, chlorite and muscovite assemblages with accessory zircon, opaque minerals and sphene. Granite crops out in the southern part of the island.

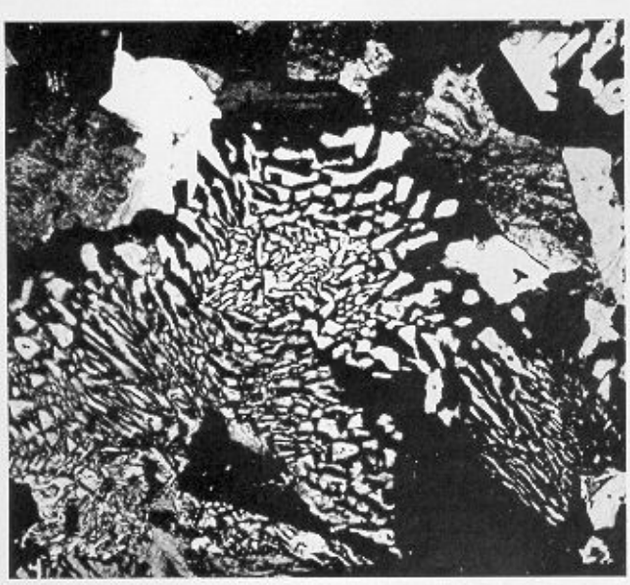

Figure 50
Granophyric intergrowths in the Cooper Island granophyre. (M.2013; X-nicols; ×40)

Quartz and plagioclase crystals vary from subhedral crystals (up to 1.5 mm wide) surrounded by optically continuous quartz–plagioclase intergrowths (up to 3 mm wide) to complete granophyric intergrowths (up to 5 mm wide). Plagioclase, which displays repeated albite twinning, is characteristically clouded with extensive sericitization and saussuritization. It is variable in composition, mainly biaxial negative andesine crystals (An_{33}); albite and potash feldspar also form granophyric intergrowths with quartz. The form of the graphic texture varies from a regular tartan pattern to quartz patches with irregular interpenetrating boundaries. In its most regular form, the quartz appears as sub-parallel elongated prisms and rods, which pass through the feldspar and present characteristic hexagonal cross-sections. The prisms may merge and diverge along their length, often portraying a dendritic pattern. A single quartz crystal may form a graphic texture with more than one crystal and quartz rods may protrude into other minerals or extend as euhedral crystals into cavities.

Radiating sheaves of epidote (mainly pistacite) closely associated with irregular patches of actinolite, spherulitic penninite and muscovite are the commonest ferromagnesian minerals. In some cases, the original prismatic shape of the primary ferromagnesian mineral, which is pseudomorphed by the above secondary minerals, is preserved. Sphene, a common accessory, occurs as subhedral crystals and as disseminated patches surrounding opaque minerals. Dark red haematite aggregates are often associated with the sphene.

3. *Discussion*

The origin of graphic textures, which are a characteristic feature of these rocks, is uncertain. Brown (1963) favoured high-level crystallization for the origin of granophyres exposed on Skye. As the proportion of quartz to feldspar (3 : 7) is fairly constant in graphic granites, Vogt (1921) suggested that the structure resulted from crystallization of a eutectic or cotectic mixture of the two components with one of the two phases growing in optical continuity with an earlier phase. Despite this, an origin by replacement of feldspar by quartz has been favoured by many authors (Schaller, 1927; Walhlstrom, 1939); Jahns and others (1963) experimentally produced a graphic texture from basalt by aqueous vapour transport and re-deposition of Si, Na and K. Barker (1970) favoured a polygenetic origin for complex intergrowth patterns with an origin for a particular sample dependent on the textural characteristics and field relations of the rock.

On Cooper Island, the rock shows signs of recrystallization (irregular interpenetrating boundaries) and alteration (epidote and chlorite minerals). The irregular form of some of the intergrowths and the veinlets of quartz that penetrate the feldspar crystals suggest a secondary origin for much of the quartz. As the matrix of the intrusive breccias is similar to the granophyric texture of the pluton and, as the intrusive breccias, which cut most of the basic dykes and crop out in the country rock of the pluton, are not seen to cut the Cooper Island granophyre (which is cut by numerous basic dykes), the granophyric texture may be a secondary feature which formed at the same time as the intrusive breccias by the passage of quartz and feldspar-rich hydrothermal fluids. The marginal hybrids, quartz ocelli and granitic veins forming the reticulate pattern of the nearby diorite

body may be related to this event or to the initial intrusion of the granitoid body.

However, as some of the granophyric texture is in optical continuity with the enclosed quartz and plagioclase crystals, it is most likely that the texture is a primary feature and that the composition of the magma was close to the quartz–plagioclase cotectic during crystallization.

C. Tonalite, Granodiorite and Granite Dykes

1. *Field relations*

Throughout the southern part of the complex, isolated medium- to coarse-grained granitoid dykes cut the layered gabbros and metasediments. Granite and alkali-feldspar granite dykes, similar to the agmatitic veins, cut the metasediments. To the east of Hamilton Bay, a suite of pale-coloured leucocratic tonalite and granite dykes which cut the gabbros produce a characteristic black-and-white striping of the exposure. The dykes, which are of irregular orientation, are up to 5 m wide and are mainly sub-vertical. Basic dykes and trains of angular basic fragments (relict dykes) cut the tonalite and granite dykes. In the northern part of the complex, pale-coloured trondhjemite lenses are found within the gabbros and basic dykes.

2. *Petrography*

Quartz and plagioclase are the main minerals present in the dykes cutting the gabbros. Quartz, with an undulose extinction, exists as irregular crystals, up to 5 mm in length, and forms up to 40% of the rock. It often contains numerous inclusions of the other mineral phases. Plagioclase is mainly subhedral (2–3 mm), biaxial positive, oligoclase (An_{15}) with well-developed twins. Extensive alteration, sericitization and cracking of plagioclase have taken place. Disseminated actinolite, chlorite and epidote minerals exist in the cracks and along the margins of the feldspar. Deformed twin lamellae are a common feature. A small amount of potash feldspar occurs as interstitial blebs and as antiperthitic intergrowths with plagioclase in the trondhjemites and tonalites. Subhedral poikilitic microcline and perthite crystals are present in the granites. The ferromagnesian minerals (5% of the rock) occur as disseminated and irregular crystals of green pleochroic (bottle green to brown-green) actinolite, biotite, chlorite (penninite) and epidote interstitial to quartz and feldspar. Pyroxene, partially altered to actinolite and chlorite, is also present. Irregular opaque minerals, sphene, allanite and euhedral zircon are scattered throughout the rock. Chlorite and epidote veins, which are often aligned, cut the dykes.

The trondhjemite lenses from the northern part of the complex are medium-grained granophyric intergrowths of quartz and plagioclase with interstitial epidote, chlorite, actinolite and prehnite and accessory opaque minerals and sphene. The alteration minerals may form large irregular areas of the groundmass (pseudomorphs).

The granitic dykes within the metasediments are characterized by medium- to coarse-grained quartz, andesine and potash feldspar intergrown crystals with numerous fine-grained quartz, plagioclase and biotite inclusions. Myrmekitic intergrowths are common in the plagioclase inclusions. Aggregates of fine-grained biotite and biotite up to 5 mm wide are partially altered to epidote, chlorite and sericite.

D. Porphyritic Microgranites

1. *Field relations*

A number of characteristic porphyritic microgranite dykes cut the metasediments and some basic dykes within the southern part of the complex and occur as enclaves within the Trendall Crag granodiorite. They are distinguished from the porphyritic rhyolites and dacites by their fine- to medium-grained granoblastic texture, characteristic quartz-filled ovoids (? ocelli) and recrystallized texture; the rock was termed a "bird's-eye granite" in the field due to the conspicuous transparent quartz ovoids which are set in a dull grey groundmass. Occasional rounded and assimilated basic dyke enclaves are found within the microgranites.

2. *Petrography*

They are variable in composition, mainly granite but some granodiorite is present. Composite quartz, plagioclase, occasional biotite and hornblende (α = green; β = brown-green; γ = dark green) phenocrysts are found in a medium-grained matrix of quartz, potash feldspar, plagioclase, biotite and hornblende with secondary actinolite, epidote and chlorite and accessory opaque minerals, sphene, zircon and apatite.

The quartz phenocrysts are large (7.0 mm) ovoids formed of more than one crystal (Fig. 51). Outlines tend to be rounded with irregular embayments and recrystallized margins. Euhedral crystal shapes, which may be cracked and infilled with secondary quartz, also exist. The plagioclase phenocrysts, which tend to be euhedral, are mainly high-relief, biaxial positive, andesine crystals and isolated labradorite crystals which may be xenocrysts. Glomerophenocrysts, composed of a number of welded feldspar fragments, also exist. A low-relief albitic overgrowth, grading into the groundmass, occurs in some thin sections. Many of the feldspars display simple and complex zoning patterns. Patchy extinction, replacement textures (quartz and potash feldspar veinlets intrude the phenocrysts and form antiperthitic intergrowths), sericitization and saussuritization are also common features. Mats of fine-grained actinolite, chlorite

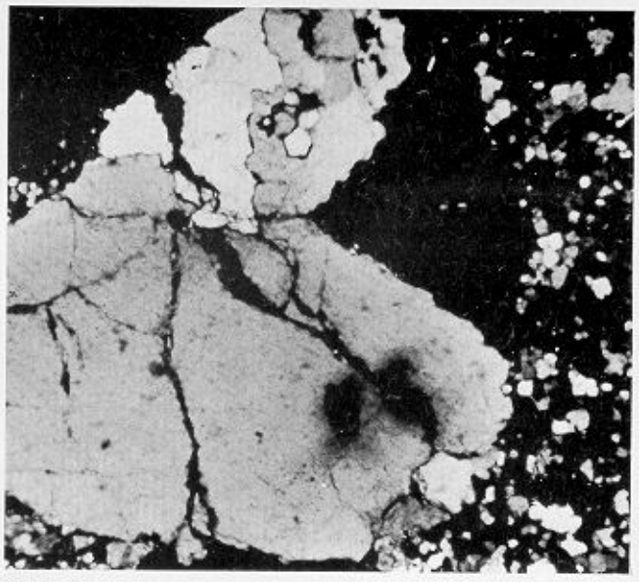

Figure 51
Ovoidal quartz in a porphyritic microgranite. (M.2040.10Q; X-nicols; ×40)

and epidote pseudomorph former hexagonal crystals (ferromagnesian phenocrysts) in some altered thin sections.

The groundmass is a fine-grained network of irregular interlocking quartz and potash feldspar crystals with scattered pleochroic biotite (α = light brown; β = dark brown; γ = black), plagioclase (zoned oligoclase and andesine crystals), pleochroic hornblende (α = light green; β = bottle-green; γ = brown-green), chlorite and actinolite with accessory opaque minerals, zircon and apatite. Euhedral epidote is found in some of the poikilitic biotite crystals. Sphene also occurs as a granular mass surrounding anhedral opaque minerals (ilmenite altering to sphene). Dark red to black haematite and dark brown limonite were also observed.

Secondary quartz and potash feldspar are found interstitially in the amphibolite enclaves (zoned feldspar laths, actinolite and biotite), some of which contain porphyritic feldspars (labradorite).

3. *Discussion*

The quartz ovoids, although lacking the ferromagnesian rims, are similar to the quartz ocelli found within the hybrid diorite rocks. Relict xenocrysts, basic enclaves and the recrystallized granoblastic and replacement textures indicate a complex history for these rocks. They may represent hybrid rocks formed at depth and intruded after some of the basic dykes but prior to the migmatization event, which may have formed the characteristic recrystallized texture. Alternatively, as enclaves of these rocks are enclosed within the Trendall Crag granodiorite, they may represent the hypabyssal equivalent of the more deep-seated granodiorite with the quartz ovoids representing former recrystallized phenocrysts.

E. Porphyritic Felsites

1. *Field description*

Within the northern part of the complex, in the Novosilski, Risting and Spenceley Glacier basins, felsites similar to the microgranitoid lenses described above form the country rock between the numerous basic intrusives and dykes; massive felsites up to 10 m wide are present in some instances. Contacts with basic rocks are usually abrupt but gradational contacts occur. A number of flow-banded felsite dykes cut basic rocks. The felsites are slightly porphyritic of black and white dense cherty aspect; they are often discoloured by a reddish iron staining. Irregular pale grey and dark colour banding occurs in some localities, indicating a possible extrusive origin for some of these rocks. Sample M.2424.3, from the east side of Risting Glacier, has an uneven texture which may indicate a volcaniclastic rock. Within the complex, the relationship of the felsites to the clastic sediments and coarse-grained gabbro bodies is not exposed.

Within the northern part of the dislocation zone, porphyritic felsites intruded by isolated basic dykes form the bulk of nunatak M.3783 (Fig. 3). They are pale, uniform grey and white, massive, slightly prophyritic rocks, which in some cases show a well-developed schistose fabric related to the formation of the dislocation zone. They are closely related to the volcaniclastic felsites, which crop out within the same nunatak and more extensively within the northern part of the dislocation zone where the volcaniclastic sediments are interbanded with the clastic sediments of the Novosilski Glacier Formation.

Flow-banded and massive felsite dykes and irregular bodies intrude the hornfelsed metasediments on Cooper Island. The flow-banding, defined by epidote-rich laminae, is well defined in the margins of the dykes; folded laminae were observed in some cases. The rocks are light-coloured, pale green and white porphyritic rocks of dense cherty aspect which contain occasional rounded basic fragments. In most cases, basic dykes cut the felsites; however, at station M.1960 (Fig. 5) a basic dyke, which cuts the felsites with a chilled margin, is partially absorbed on one side of the dyke. This body grades into the intrusive breccias which cut most basic dykes, suggesting possible re-mobilization of the felsites.

A porphyritic spherulitic rhyolite body, up to 20 m wide, intrudes the overturned epiclastic sediments on the northern promontory of Cooper Island. The rock is light coloured, pale green in colour with conspicuous white phenocrysts up to 6 mm long.

2. *Petrography*

Quartz and plagioclase phenocrysts, which form up to 10% of the rock, are set in a spherulitic felsic groundmass. The quartz phenocrysts (4 mm in diameter), which tend to be euhedral in shape, may have an irregular overgrowth of secondary quartz. The feldspar phenocrysts, often completely sericitized, are twinned, biaxial negative, andesine (An_{33}) crystals which are sometimes zoned. The phenocrysts may be embayed by the groundmass, corroded, altered and rimmed by opaque minerals; some are completely pseudomorphed by aggregates of epidote, sericite and tremolite-actinolite. The groundmass is composed of quartz–feldspar spherulites (Fig. 52a) with ragged aggregates of zoisite, clinozoisite, chlorite, epidote, tremolite, actinolite, sericite, prehnite and biotite, and accessory zircon, sphene, apatite and opaque minerals. The colourless and pale to dark green pleochroic tremolite-actinolite laths are often clustered to form radial sprays. Biotite, partially altered to secondary chlorite and epidote, may occur as disorientated aggregates of fine-grained laths. The spherulites are defined by radiating sheaves of quartz showing an undulose extinction and a radial arrangement of feldspar microlites. The composition of the microcrystalline felsic groundmass is both rhyolitic and dacitic (as indicated by staining) in composition. The spherulites, which have a refractive index less than the recrystallized quartz, are microcrystalline aggregates of potash feldspar and quartz; intergrowths of plagioclase and quartz are also present. Recrystallization of the spherulites occurs in some cases; the cloudy undulose spherulites are replaced by clear granoblastic quartz and feldspar. Veins of epidote, clinozoisite, penninite and prehnite transgress the rock. Irregular patches of prehnite, often replacing plagioclase, are common within the groundmass of the felsites on Cooper Island. Opaque minerals, identified as skeletal ilmenite, are scattered in the groundmass. They are usually preserved as an aggregate of granules surrounded by disseminated dusty sphene and occasionally rimmed by biotite or epidote. Euhedral opaque minerals (pyrite) are also present throughout the rock. Break-down of the ilmenite, with the formation of secondary sphene, has probably occurred; the iron is taken up by secondary pyrite and incorporated in a biotite crystal lattice. In one thin section (M.2442.2), trains of fine granules (light brown, high relief, isotropic), often hexagonal in shape, which may be garnet, occur throughout the rock. In most cases, the

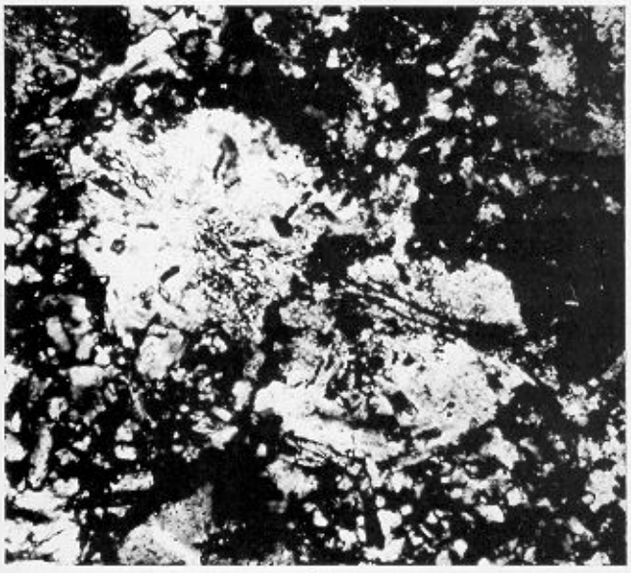

a

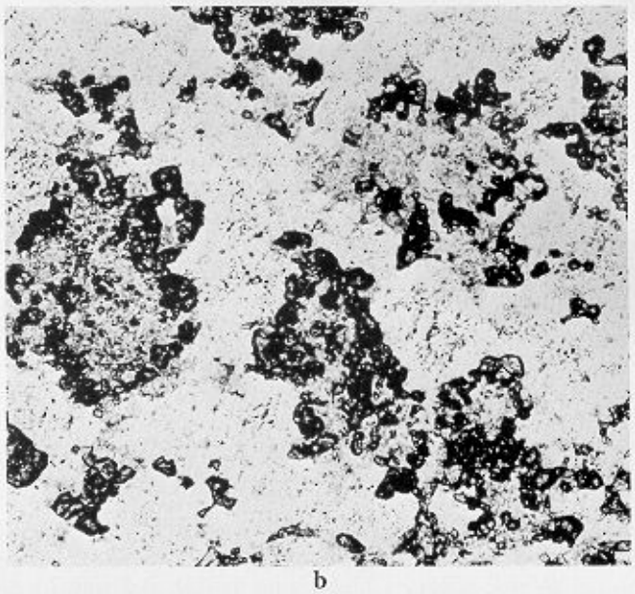

b

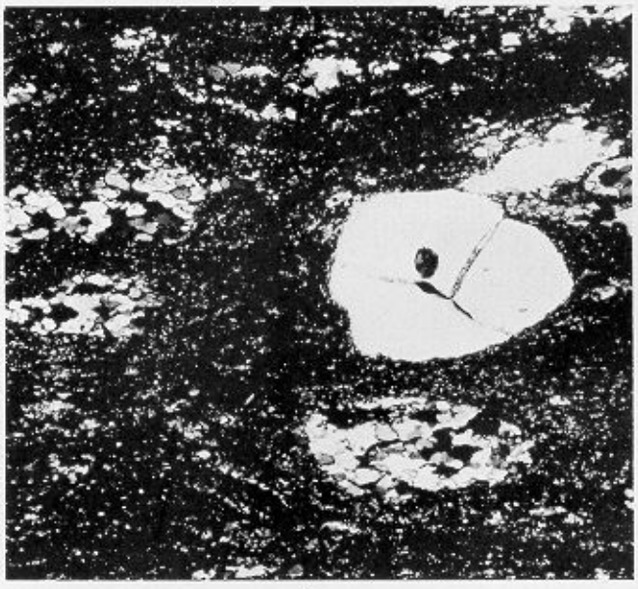

c

FIGURE 52
a. Spherulites in a porphyritic felsite. (M.1656.2; X-nicols; ×40)
b. (?) Garnets defining a circular outline in a recrystallized porphyritic felsite. (M.2442.3; ordinary light; ×40)
c. Patches of recrystallized mosaic quartz in a porphyritic felsite. (M.3783.1A; X-nicols; ×40).

granules define a circular pattern (Fig. 52b) which may outline former spherulites. Colourless, high-relief granules of a possible epidote mineral (low birefringence) are closely associated with the above (?) garnets. The texture of this rock is non-spherulitic with the occurrence of recrystallized quartz and feldspar.

On Cooper Island, the quartz and feldspar phenocrysts of the porphyritic rhyolite, exposed on the north-east promontory, form up to 60% of the rock. The feldspars (up to 6.0 mm) are mainly brown and clouded with dusty inclusions; some twinned andesine crystals occur. The groundmass is similar to that of the felsites described above and is spherulitic with cryptocrystalline quartz and feldspar aggregates.

Within the dislocation zone, euhedral quartz and plagioclase phenocrysts (up to 5 mm), which often show resorbed margins characteristic of volcanic rocks, are set in a microcrystalline rhyolitic and dacitic groundmass. The plagioclase crystals (An_{36}) in some cases show partial replacement by potash feldspar. The felsic groundmass is mainly a low-relief (less than quartz) microcrystalline feldspar with patches of recrystallized mosaic quartz (Fig. 52c).

3. *Discussion*

The felsites and microgranites, which form the country rock in the northern part of the complex and intrude the sediments on Cooper Island, may represent the sub-surface and surface equivalent of the larger granitoid bodies in the southern part of the complex. As has been discussed previously, the porphyritic felsites within the northern part of the dislocation zone may be part of the pre-Jurassic basement rocks of the Novosilski Glacier Formation.

The presence of a metamorphic assemblage (garnet-biotite) in some of these rocks indicates that they may have been thermally metamorphosed by the numerous basic dykes cutting the felsites. Subsequent partial retrogression to a chlorite–epidote–sericite assemblage is common.

F. Intrusive Breccias

1. *Field relations*

Throughout the southern part of the complex and on Cooper Island, medium-grained granitoids packed with enclaves of different rock types (Fig. 53) were emplaced late in the history of the complex. They intrude the gabbro, Trendall Crag granodiorite and basic dyke suites, but are cut by some basic dykes, aplites and pegmatites. They are found within well-defined areas; they crop out along the margins of the granitoid bodies, along acid–basic contact zones and within basic dyke zones. The term "intrusive breccia" (Bowes and Wright, 1961) is used here to describe these rocks, as they were emplaced as breccias with mixed acid and basic enclaves, which were derived from different localities and suspended in a granitoid matrix. These intrusive breccias are in strong contrast to the numerous areas of *in-situ* migmatization, brecciation and net-veining by migmatitic granite which occur without any large-scale displacement of the basic and acid country rocks. The intrusive breccias and migmatites have a similar time relationship to the other rock types and probably both formed at the same time.

The intrusive breccias vary in form from a single dyke-like body packed with enclaves to irregular areas with isolated enclaves (Fig. 54). The enclaves are variable in size, shape, lithology and amount of displacement. Coarse-grained gabbro, amphibolite and basic dyke fragments are the most abundant; isolated metasediment and coarse-grained granodiorite (Fig. 54) were identified. They vary in shape from angular to sub-rounded and are in various stages of assimilation. Large areas of granodiorite, often devoid of enclaves and with remnant partially assimilated enclaves, also exist.

Figure 53
Intrusive breccia packed with enclaves of different rock types. The hammer shaft is 80 cm long.

Figure 54
Intrusive breccia with partially assimilated basic enclaves and an enclave of Trendall Crag granodiorite. The scale is 10 cm long.

2. *Petrography*

The granitoid matrix is variable in composition: quartz-diorite, tonalite and granodiorite. Euhedral to subhedral plagioclase crystals, biotite and amphibole are completely and partially enclosed in irregular pools of quartz and potash feldspar with accessory zircon, apatite, sphene and opaque minerals.

The plagioclase crystals (40–60% of the rock) of variable composition (up to An_{52}) display simple and complex zoning patterns, secondary overgrowths of albite and irregular extinction patterns. Five zones of moderate relief were recorded in one crystal; high-relief cores are often sericitized and saussuritized.

Quartz, which may show an undulose extinction, forms irregular pools and poikilitic crystals (up to 5 mm) enclosing and replacing the feldspar and ferromagnesian minerals.

Poikilitic crystals and interstitial patches of microcline and flame perthite form up to 15% of some thin sections but are entirely absent from others. Minor apophyses of quartz and potash feldspar intrude, replace and form antiperthitic intergrowths with plagioclase. Myrmekitic intergrowths of quartz and plagioclase occur in some plagioclase crystals, generally where they are in contact with potash feldspar.

The ferromagnesian minerals may form up to 40% of the rock. Irregular prisms and poikilitic crystals of pleochroic (α = light green-brown; β = bottle-green; γ = dark brown-green) hornblende and radiating acicular needles of light green to bottle-green pleochroic actinolite and a colourless amphibole (tremolite) also occur. Pleochroic biotite crystals (α = light brown; β = dark brown; γ = black) and poikilitic sheets are common in some thin sections. Sericite, epidote, zoisite, clinozoisite and penninite occur as secondary alteration products. Scattered anhedral opaque minerals are usually closely associated with the amphibole.

The basic amphibolite enclaves show various stages of assimilation. Recrystallized feldspar, poikilitic quartz, biotite, amphibole and interstitial potash feldspar are present.

3. *Discussion*

The mode of brecciation and origin of the granitic matrix of the intrusive breccias is uncertain. Large distances must be involved in the ascent of the liquid as, in most cases, up to five different lithologies occur in close juxtaposition. In thin section the secondary matrix of quartz and potash feldspar, which encloses and replaces the plagioclase and ferromagnesian minerals, indicates that the rocks may have intruded as enclaves and crystal fragments suspended in a quartz and potash feldspar-rich hydrothermal fluid. On Cooper Island there is a marked size sorting of the enclaves which may have taken place after intrusion of the breccia and prior to solidification. The variation in plagioclase composition may indicate that some of the crystals may be xenocrysts inherited from assimilated basic rocks; albite rims may have crystallized from the hydrothermal fluids.

The granitoid matrix may be responsible for the initial brecciation of the country rock (gabbro, granite and basic dykes) with forceful intrusion of the magma along distinct zones. Alternatively, the initial brecciation (explosion breccia) may have occurred during a period of gas streaming from a more deep-seated magma prior to emplacement of the liquid; subsequent upward migration of the granitoid matrix along the brecciated channels formed the intrusive breccia. The roundness and assimilated margins of the enclaves support magmatic erosion over long distances.

G. Granite Pegmatites

Throughout the complex, minor pale-coloured pegmatitic veinlets (1–10 cm wide) cut the above rock types. They are later than the intrusive breccias but are cut by occasional basic dykes.

In thin section, a mosaic network of quartz, potash feldspar and plagioclase crystals (up to 1 cm long) forms typical pegmatitic graphic textures. Scattered irregular opaque minerals and occasional euhedral columnar prisms of iron-rich tourmaline, schorlite (strong absorption, pleochroic, light green to dark green, uniaxial negative, diagonal twin plane), the margins of which are altered to epidote and biotite, also exist. The pegmatites probably represent the classical situation of late-stage hydrothermal fluids percolating through the complex.

H. Aplitic Veins

Associated with the pegmatites are a number of white to buff-coloured aplitic veins and dykes. These occur late in the history of the complex and cut the porphyritic rhyolites, intrusive breccias and most basic dykes.

The composition varies from fine-grained intergrowth of quartz and plagioclase (oligoclase) with minor amounts of potash feldspar and aplites with up to 30% microcline intergrown with plagioclase and quartz. Some phenocrysts up to 2 mm with irregular recrystallized margins are present. Coarse-grained graphic intergrowths of quartz and plagioclase (6 mm), similar to the pegmatites, also occur. Scattered ragged laths of epidote, clinozoisite, zoisite and chlorite, and accessory apatite and zircon, are found throughout the aplites. Subhedral crystals (up to 1.0 mm) of a high-relief, slightly brown-coloured garnet with poorly developed fracture patterns are found in one thin section (M.1257). The garnet shows a slight alteration rim of chlorite and may represent xenocrysts incorporated in late-stage fluids.

VIII. GEOCHEMISTRY OF THE ACID ROCKS

1. *Introduction*

A detailed geochemical analysis of some of a wide variety of acid rocks (Table X) which exist within the Drygalski Fjord Complex has been carried out. They form a diverse group, outlined below, which displays marked differences in composition, texture, form, field relations and chemistry.

a. *Trendall Crag granodiorite.* The seven samples, tonalites, granodiorites and granites, are part of the composite pluton which intruded the Trendall Crag gabbro in the southern part of the complex. The more basic members of the analysed suite are hybrid rocks which contain pyroxene and plagioclase of the gabbroic country rock.

b. *Cooper Island granophyre.* Eight samples, granites and trondhjemites, from the pale leucocratic altered pluton on Cooper Island were analysed.

c. *Microgranitoid dykes and lenses.* A diverse group (nine samples), trondhjemites, tonalites, granodiorites, granites and

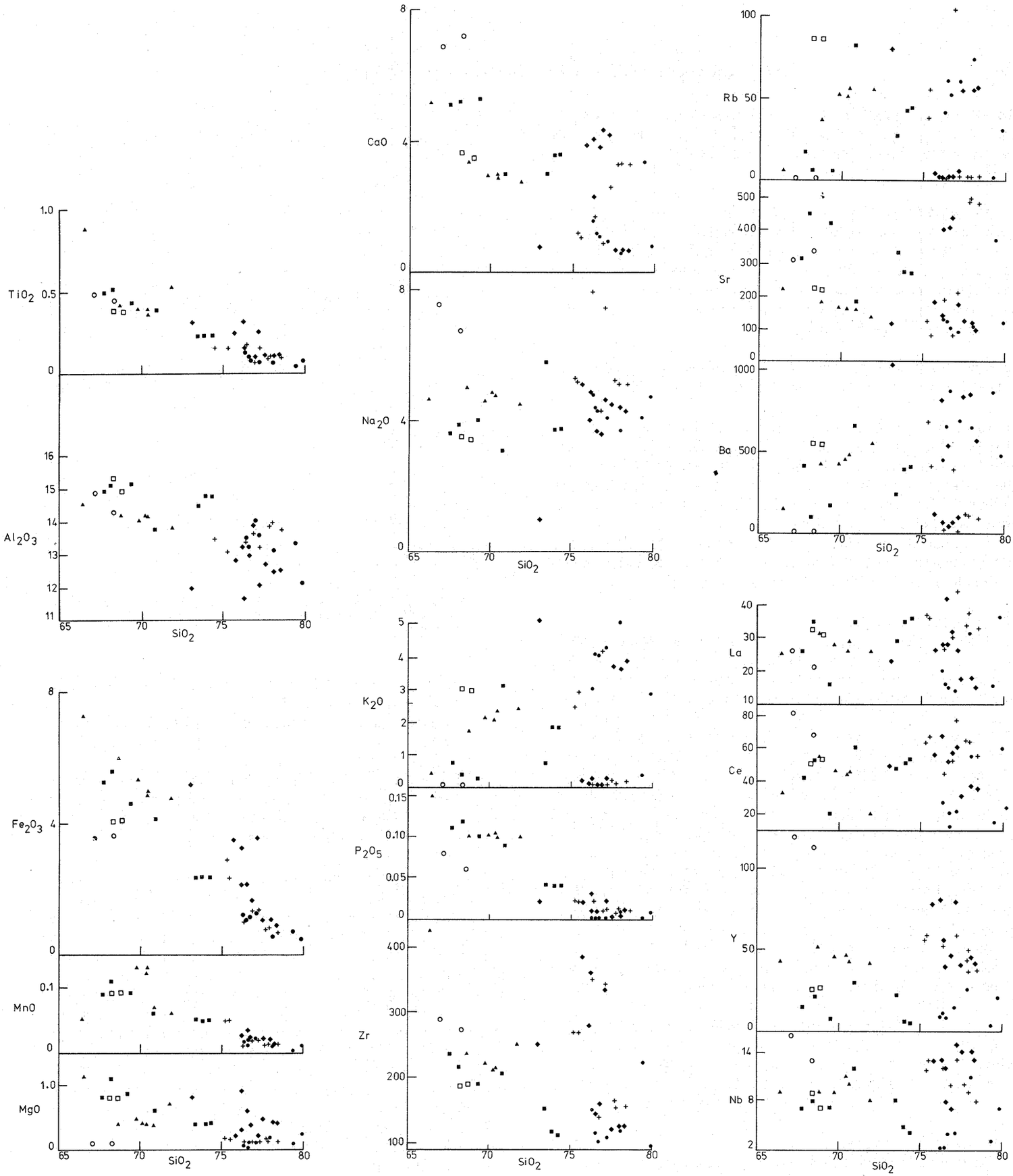

FIGURE 55

Plot of the major- (weight %) and trace-element (ppm) concentrations in the granitoid rocks of the Drygalski Fjord Complex against SiO_2.

- ▪ Trendall Crag granodiorite.
- + Cooper Island granophyre.
- • Granitoid dykes within the gabbros.
- ○ Granitoid dyke (M.3787).
- ◆ Porphyritic felsite.
- □ Porphyritic microgranite.
- ▲ Intrusive breccia granitoid matrix.

The above symbols are used on all diagrams in this section.

alkali-feldspar granites, from acid dykes which intrude the gabbros at Hamilton Bay and Trendall Crag, and from pale lenses within the gabbros at Spenceley Glacier (M.3787), were analysed.

d. *Porphyritic felsites.* The analysed samples (ten) are mainly dacites with some rhyolites. They were taken from dykes and lenses within the basic dykes, which intrude the gabbros in the northern part of the complex, and from dykes which intrude the hornfelsed metasediments on Cooper Island. Three rhyolites were analysed from the intrusive porphyry on the north-east promontory of Cooper Island.

e. *Porphyritic microgranite.* Two samples were analysed from a microgranite dyke within the southern part of the complex.

f. *Intrusive breccias.* Six samples of granitoid matrix and six enclaves (not illustrated on Fig. 55) from the intrusive breccias were analysed from within the Trendall Crag granodiorite and basic dykes on the north side of Trendall Crag. The granitoids, although they contain a considerable amount of potash feldspar, are dacitic in composition.

The analysis was carried out to investigate the origin of the acid rocks and their relationship to the basic, dioritic and metasedimentary rocks with which they are closely associated.

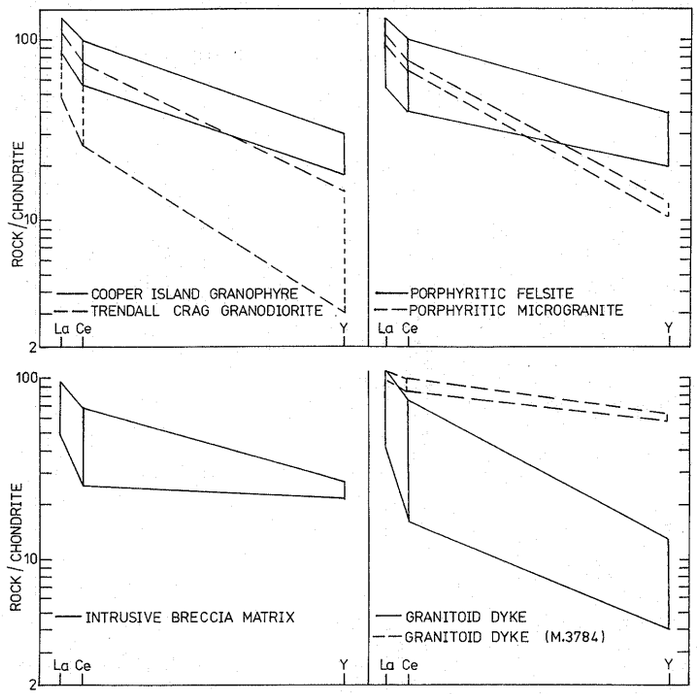

FIGURE 56
Simulated rare-earth patterns of the granitoid rocks of the Drygalski Fjord Complex using XRF values for La, Ce and Y.

2. *Chemical trends*

The diversity in composition, form and field relations of the acid rocks is reflected in the chemistry of the rocks. With the exception of a few major and minor elements, they do not form well-defined trends when the major and minor elements are plotted against SiO_2 (Fig. 55). There is a marked decrease in TiO_2, Al_2O_3, MnO, Fe_2O_3, MgO, P_2O_5 and Zn (not illustrated) with increasing SiO_2. The remaining trace and major elements do not show well-defined trends. This is reflected in the variation in composition of the acid rocks and, in particular, in the concentration of potash feldspar and composition of plagioclase. For a given SiO_2 content, there is considerable variation in K_2O content. Many of the samples are dacitic in composition with K_2O less than 0.25% whilst others, often within the same group of rocks, have up to 5% K_2O. There is a corresponding variation in Rb and Ba contents with samples enriched in K_2O being enriched in Rb and Ba also (K, Rb, Ba and Sr are mobile elements). There is a wide variation in Y, Nb, Sr and Zr contents; some, the porphyritic felsites, granitoid dykes and Cooper Island granophyres, are relatively enriched in Y, Nb, Sr and Zr relative to the remainder of the acid rocks.

Using Y as a heavy rare-earth element, there is considerable variation in the rare-earth element pattern of the acid rocks (Fig. 56). The Trendall Crag granodiorites, granitoid dykes and porphyritic microgranites are depleted in Y relative to the porphyritic felsites and the Cooper Island granophyre.

3. *Origin of the granitic rocks*

As there is considerable variation in the chemistry of the acid rocks, it is quite likely that they may have been derived from different sources (outlined below) within the proposed island-arc–back-arc basin system of southern South Georgia. The acid rocks may be:

i. Calc-alkaline rocks of part of a pre-marginal basin remnant magmatic arc or part of a syn- or post-marginal basin island-arc magmatic suite.
ii. Derived by fractional crystallization of the basic dykes or gabbros of the Drygalski Fjord Complex or Larsen Harbour Formation.
iii. Derived by partial melting of the metasedimentary rocks due to high heat flow associated with the opening of the back-arc basin and emplacement of the basic rocks.
iv. Derived by a combination of the above.

a. *Trendall Crag granodiorite.* Despite the close association of the Trendall Crag granodiorites, gabbroic and intermediate rocks (formed along the contact zone), the low Y and Zr values of the granitoid rocks and their depletion in heavy rare-earth elements preclude the possibility that the acid rocks are differentiates of the basic magma. Similarly, the initial $^{87}Sr/^{86}Sr$ ratio (0.7086; age 186 Ma; Tanner and Rex, 1979), although high for mantle-derived rocks (Brown, 1977), precludes a single origin by partial melting of the metasedimentary country rock (Salomon Glacier Formation) during emplacement of the basic rocks. However, with the exception of K_2O, Rb and Ba values, the rocks show calc-alkaline trends (Fig. 55) that are similar to the calc-alkaline plutons of the Antarctic Peninsula (Saunders and others, 1982*b*) and South America (Suárez, 1977*b*; Stern and Stroup, 1982); some of the Trendall Crag rocks are depleted in K_2O, Rb and Ba.

It thus appears likely that the Trendall Crag granodiorites are mantle-derived rocks, which were probably generated under conditions of high P_{H_2O} resulting in the calc-alkaline trends. They may be related to subduction of Pacific oceanic floor prior to formation of the back-arc basin but, as these rocks have a

similar age to the basic rocks and form a very small proportion of the rocks of the Drygalski Fjord Complex, an origin by partial melting of the mantle rocks as a result of the opening of the back-arc basin is suggested here. The initial $^{87}Sr/^{86}Sr$ ratio (higher than pure mantle-derived rocks) and field evidence suggest that partial melting of continental crust (not necessarily metasediments) also played a small but significant role in the development of these rocks.

b. *Cooper Island granophyre.* As the considerable variation in the major (K_2O) and trace elements (Rb, Sr and Ba) of these rocks may be due to the widespread alteration and metamorphism (the ferromagnesian minerals are completely replaced by aggregates of chlorite, epidote and prehnite), it is necessary to consider the elements Ce, Zr, Y, Nb and Ti which are assumed immobile during greenschist-facies metamorphism (Pearce, 1975) when considering the origin of these rocks. Relative to calc-alkaline rocks (Nockolds and Allen, 1953; Saunders and others, 1982*b*), the granophyres are variably enriched in Zr, Y, Nb and rare-earth elements, and have low Ce_N/Y_N and high Fe*/Mg ratios. These characteristics disagree with subduction-related tectonics or an origin by partial fusion of the metasediments but suggest that the rocks were derived by extreme fractionation of the basic rocks. There is, however, a considerable range in Zr values at the 74–76% SiO_2 level. The high values (350 ppm) are similar although slightly less than similar differentiates (plagiogranites) of the Sarmiento Complex (Saunders and others, 1979), whereas the lower values are more characteristic of the re-mobilized continental fragments (granophyres and trondhjemites) of the Sarmiento Complex, the Tobifera Formation (Bruhn and others, 1978) and the Taupo volcanics of New Zealand (Ewart and others, 1968). Both the Tobifera Formation and the Taupo volcanics are derived by partial melting of metasediments (Bruhn and others, 1978). Average analyses of some of these rocks are given in Table XI. Similarly, the Y values of the Cooper Island granophyres are lower than the recorded Y values of the Sarmiento acid differentiates (plagiogranites) but are more enriched than the Sarmiento Complex granophyres and trondhjemites. As the Cooper Island granophyres may be more differentiated than the Sarmiento Complex rocks (higher Fe*/Mg ratios), it is not unreasonable that the rocks are more depleted in Y and Zr. The high K_2O, Rb and Ba values of some of the granophyres are in strong contrast to most documented oceanic plagiogranites (acid differentiates of ophiolite sequences (Coleman and Peterman, 1975; Saunders and others, 1979)). As K_2O, Rb or Ba are not partitioned early in the fractional crystallization of a tholeiitic magma, one would expect late-stage differentiates to be enriched in these elements (the basic rocks of the Drygalski Fjord Complex have low primary values of these elements). It thus appears that the silicic differentiates of ophiolite complexes with high Na/K ratios (Thayer, 1967; Engel and Fisher, 1975) have been leached of these elements due to the hydrothermal activity (Saunders and others, 1979). In contrast, differentiates of continental tholeiites (Wager and Mitchell, 1951; McBirney, 1975; Eales and Robey, 1976; Jamieson and Clarke, 1970) and sub-aerial lavas on Iceland (Carmichael, 1964), which have not suffered an open hydrothermal system, have a high K_2O content due to interaction with meteoric ground water (Taylor and Coleman, 1977). The high K_2O values of some of the Cooper Island granophyres support an origin by differentiation of a tholeiitic magma emplaced within a continental margin. Some of the high values of K_2O may be due to contamination by meteoric ground water or due to assimilation of the metasediments. Depending on the level of Zr and Y in the sediments and the amount of assimilation, this may dilute the Zr and Y values of the acid differentiates, giving values more characteristic of some of the Cooper Island granophyres and slightly atypical of differentiates of tholeiitic magma.

c. *Porphyritic felsites.* As the felsites show a wide variation of Zr and Y content and have similar trace- and major-element patterns to the Cooper Island granophyre, a similar origin is suggested for these rocks. The felsites (M.4130) from Cooper Island are least enriched in Zr and Y and probably represent re-mobilized continental material, whereas the felsites from the Novosilski and Spencely Glacier areas have similar concentrations to the plagiogranites of the Sarmiento Complex.

d. *Porphyritic microgranites.* In contrast to the Cooper Island granophyre and the felsites, these rocks are similar to the Trendall Crag granodiorites and have values characteristic of the calc-alkaline trends of the Antarctic Peninsula and southern South America.

e. *Granitoid dykes.* With the exception of the dacitic microgranitoid lenses from the Spenceley Glacier area (M.3787), the dykes which intrude the gabbros in the Hamilton Bay and Trendall Crag areas from a uniform group similar to the agmatitic veins within the Salomon Glacier Formation. Despite their close association with the gabbros, the high K_2O values, accompanied by low Y and Zr contents, preclude an origin by fractionation of the basic rocks. It is more likely that, as in the agmatites, they are derived by partial melting of blocks of metasediment suspended in the gabbro magma. Although the geochemistry leads to this conclusion, there is a marked absence of metasedimentary residues and the rocks are petrographically similar to documented plagiogranites (Coleman and Peterman, 1975; Saunders and others, 1979).

In contrast, the lenses within the Spenceley Glacier gabbros, although highly altered, have Y and Zr values as high as the Sarmiento plagiogranites. They are similarly depleted in K_2O, Rb and Ba (Fig. 55) and have low Ce_N/Y_N and flat chondrite-normalized rare-earth element enriched trends (Fig. 56).

f. *Intrusive breccias.* Although the granitic matrix is slightly enriched in Y, the chemical characteristics are not diagnostic in determining the origin of these rocks. If the acid and basic rocks are cogenetic and the acid matrix was derived by fractional crystallization from the basic magma, it is difficult to envisage a process that will mechanically re-mix early-formed basic rocks and derivative melt. Similar quartz-diorites and enclaves have been interpreted (White and Chappell, 1977; Price and Sinton, 1978) as a mixture of melt and residue left after partial melting has occurred in igneous rocks of the lower crust. A similar origin for these rocks is supported by the high abundances of Na_2O, P_2O_5, Ce, La, Y, Zr and Nb in the basic enclaves. These may be due to the presence of plagioclase, apatite and zircon in original residues left after partial melting in the lower crust. Conversely, the petrographic evidence indicates that the metamorphic assemblages of the enclaves are retrogressive with no prograde minerals or pseudomorphs indicative of high

TABLE XI

REPRESENTATIVE ANALYSES OF ACIDIC ROCKS FROM SOUTH AMERICA, ANTARCTIC PENINSULA AND NEW ZEALAND

	1	2	3	4	5	6	7	8	9	10	11	12	13
SiO_2	70·66	77.4	75·3	59·98	73·22	66·42	73·23	73·2	78·32	65·5	71·16	69·52	59·64
TiO_2	0·38	0·13	0·27	0·61	0·24	0·95	0·31	0·31	0·13	1·01	0·38	0·32	0·82
$A1_2O_3$	14·27	12·13	13·5	17·42	13·43	12·15	12·10	13·60	12·33	15·86	13·80	15·65	17·07
Fe_2O_3*	3·94	1·52	1·87	6·89	2·48	7·60	3·82	2·96	1·12	4·53	3·17	3·06	8·10
MnO	0·03	0·03	–	0·18	0·06	0·14	0·06	0·03	0·02	0·18	0·11	0·07	0·14
MgO	1·23	1·12	0·25	3·23	0·44	1·32	0·24	0·48	0·33	1·68	0·53	0·84	1·89
CaO	0·84	0·67	1·49	5·94	2·07	6·62	7·47	5·12	0·40	3·87	1·19	2·52	5·07
Na_2O	4·40	2·69	4·12	3·45	3·75	2·19	2·07	2·79	3·19	5·30	4·92	4·29	3·21
K_2O	4·23	3·53	3·39	1·66	3·38	0·01	0·01	0·85	4·41	1·98	3·71	3·17	2·80
P_2O_5	0·09	0·03	–	0·16	0·06	0·19	0·05	0·07	0·01	0·31	0·07	0·11	0·31
Cr	21	–	–	–	–	8	6	13	6	1	3	<1	11
Ni	7	–	–	–	–	3	5	7	<1	1	<1	6	1
Zn	66	–	–	–	–	50	15	18	41	93	64	22	95
Rb	168	117	108	57	123	1	1	28	119	52	127	118	103
Sr	146	126	125	326	193	234	298	230	60	426	145	261	682
Y	28	–	–	18	–	78	108	33	32	48	46	22	29
Zr	313	159	160	92	146	375	516	178	108	309	422	165	334
Nb	12	12	6	13	20	13	14	9	8	11	18	13	13
Ba	1 068	872	870	484	812	18	5	3 020	670	579	834	560	801
La	39	–	–	–	–	27	28	37	42	25	31	13	26
Ce	65	–	–	–	–	55	69	73	64	60	77	32	55
Na_2O/K_2O	1·04	0·76	1·22	2·08	1·11	219	207	3·28	0·72	2·68	1·33	1·35	1·15
Fe/Mg	3·71	–	–	–	–	5·7	29·0	7·15	3·04	3·13	6·94	4·22	3·74
K/Rb	209	251	250	242	229	–	–	252	508	316	242	233	226
Rb/Sr	1·15	0·93	0·86	0·18	0·64	–	–	0·12	1·98	0·12	0·88	0·45	0·15
Ba/Sr	73	6·9	7·0	1·5	4·2	0·08	0·04	13·1	11·17	1·36	5·75	2·15	1·17
$(Ce/Y)_N$	6·6	–	–	7·1	–	2·1	1·8	20	4·09	2·56	3·42	3·55	4·63
Zr/Nb	26	12·3	28·6	7·1	7·3	30	30	6·4	–	–	–	12·70	26·7
n	8	13	6		6	2	3	1	1	1	1	1	1

n Number of samples.
Fe_2O_3* Total iron as Fe_2O_3.

1. Tobifera Formation (Saunders and others, 1979).
2. Tobifera Formation (Bruhn and others, 1978).
3. Taupo volcanic zone (Ewart and others, 1968).
4. Average composition of Patagonian Batholith (Stern and Stroup, 1982).
5. Patagonian Batholith (SiO_2 = 72–75 wt %) (Stern and Stroup, 1982).
6. Plagiogranite (D3, A25), Sarmiento Complex (Saunders and others, 1979).
7. Plagiogranite (PA28A, PA28W, PA23J), Sarmiento Complex (Saunders and others, 1979).
8. Granophyre (PA37B), Sarmiento Complex (Saunders and others, 1979).
9. Rhyolite, South Shetland Islands (Weaver and others, 1982).
10. Dacite, Antarctic Peninsula (Weaver and others, 1982).
11. Rhyodacite, Antarctic Peninsula (Weaver and others,1982).
12. Adamellite, Antarctic Peninsula (Saunders and others, 1982).
13. Tonalite, Antarctic Peninsula (Saunders and others, 1982).

temperatures associated with partial melting of basic rock. Alternatively, the silicic matrix may have formed by differentiation of the basic magma, collection of the acid magma and reintrusion of the less dense acidic magma into the overlying cooler basic and acid rocks along fracture zones or basic dyke conduits. The angular nature of some enclaves, together with the rounded partially assimilated enclaves, indicate varying temperatures of the country rock or varying times of suspension within the granitoid matrix.

4. *Discussion*

It is thus concluded that the granitoid rocks of the Drygalski Fjord Complex are variable in origin (Fig. 57). The relationships between the above rocks and the basic rocks is indicated on Zr–Y and Ce–Y plots (Fig. 58a and b). The diagrams support the conclusion that the Trendall Crag granodiorite, the porphyritic microgranites, and many of the microgranitoid dykes and diorites are unrelated to the basic rocks. The Cooper Island granophyre, the porphyritic felsites and dykes (M.3787) lie close to the trend of the basic rocks and support an origin by differentiation of the basic magma; the variation may be due to contamination by partial melting of metasediments, into which the acid rocks were emplaced. The diagram also indicates that the granitoid matrix of intrusive breccias may be related to the differentiation of the basic magma.

The importance of plagioclase and augite fractionation is indicated on the CaO and Y plot (Fig. 58c) (Lambert and Holland, 1974), which shows a marked increase in Y with a corresponding increase in Ca. In contrast, the Trendall Crag

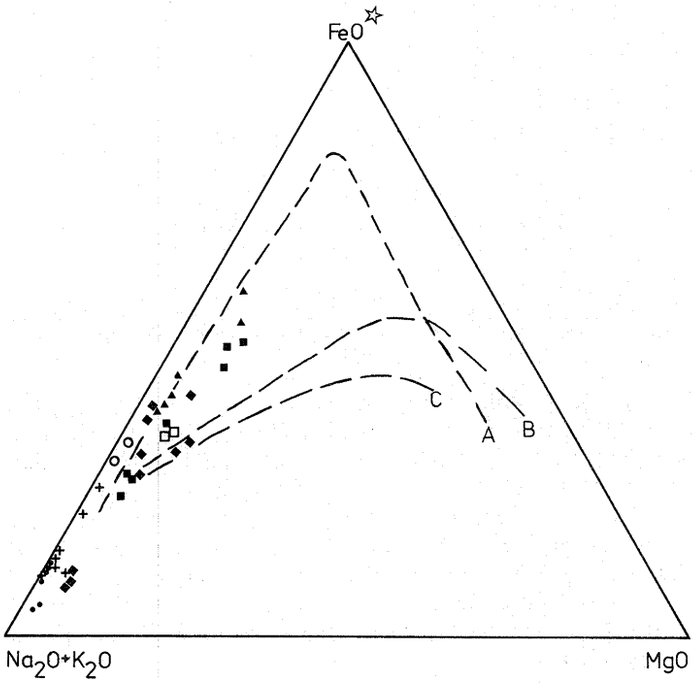

FIGURE 57
AFM triangular diagram of the granitoid rocks of the Drygalski Fjord Complex. The dashed line (A) indicates the differentiation trend of the Skaergaard intrusion (Wager and Deer, 1939); line B indicates the differentiation trend of the Patagonian batholith (Stern and Stroup, 1982); line C indicates the differentiation trend of the Antarctic Peninsula plutons (Saunders and others, 1982*b*).

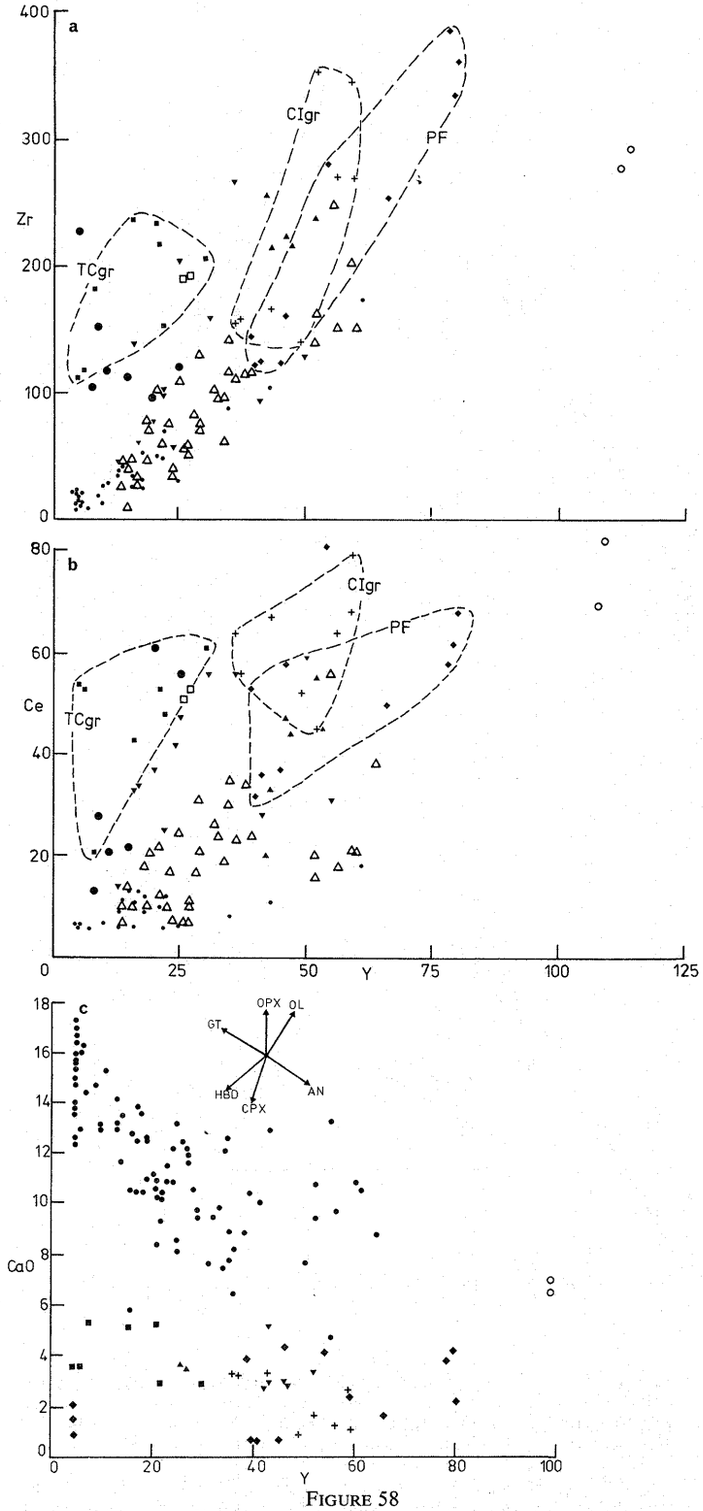

FIGURE 58
a. Plot of Zr versus Y for the gabbros (●), basic dykes (△), intermediate rocks (▾) and granitoid rocks of the Drygalski Fjord Complex. The dashed lines enclose the fields for the Trendall Crag granodiorite (TCgr), the Cooper Island granophyre (CIgr) and the porphyritic felsites (PF).
b. Plot of Ce versus Y for the gabbros (●), basic dykes (△), intermediate (▾) and granitoid rocks of the Drygalski Fjord Complex.
c. Plot of CaO versus Y for the basic (●) and granitoid rocks of the Drygalski Fjord Complex. The inset illustrates the variation-trend direction associated with crystallization of garnet (GT), orthopyroxene (OPX), olivine (OL), plagioclase (AN), clinopyroxene (CPX) and hornblende (HBD) (Lambert and Holland, 1974).

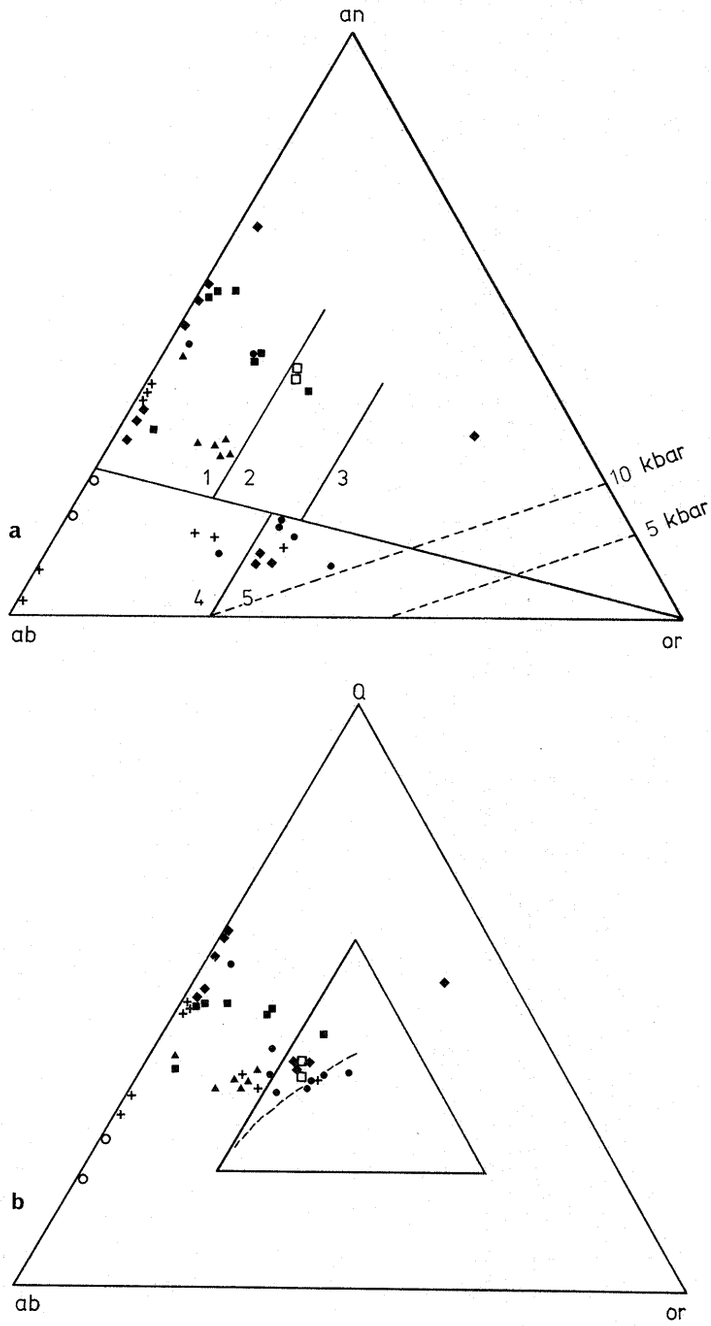

FIGURE 59

a. Normative an–ab–or diagram for the granitoid rocks of the Drygalski Fjord Complex. 1, dacites; 2, rhyodacites; 3, quartz-latites; 4, quartz-keratophyres; 5, rhyolites (fields after O'Connor (1965)). The dashed line indicates the position of the thermal trough at 10 and 15 kbar (Kleeman, 1965).

b. Normative Q–ab–or diagram for the granitoid rocks of the Drygalski Fjord Complex. The inner triangle indicates the field of granitic composition (Tuttle and Bowen, 1958). The dashed line indicates the locus of the ternary eutectic as a function of increasing P_{H_2O} (Luth and others, 1964).

granodiorite shows a decrease in Y values relative to CaO, possibly due to the importance of hornblende fractionation (cf. the Patagonian Batholith; Stern and Stroup, 1982), resulting in derivative liquids impoverished in Y relative to Ca.

Although the majority of the granitoid dykes fall within the field of granitic composition and lie close to the minimum melting composition (Tuttle and Bowen, 1958) on the ternary Q–ab–or plot, this diagram (Fig. 59a and b) provides no help in understanding the genesis of granitic rocks (Winkler, 1976). At any given pressure, late differentiates of calc-alkaline magmas and early anatectic melts of gneisses consisting of quartz, potash feldspar and plagioclase are not located near the minimum melting or eutectic composition. The exact position of a melt is determined by both alkali-feldspar and plagioclase co-existing with quartz, melt and vapour at any temperature and water pressure. The concentration of points along the quartz–albite boundary indicates the scarcity of potash feldspar in many of the acid rocks.

The variation of the Ce_N/Y_N ratio with Y (Fig. 60) supports the origin of some of the acid rocks by differentiation of the

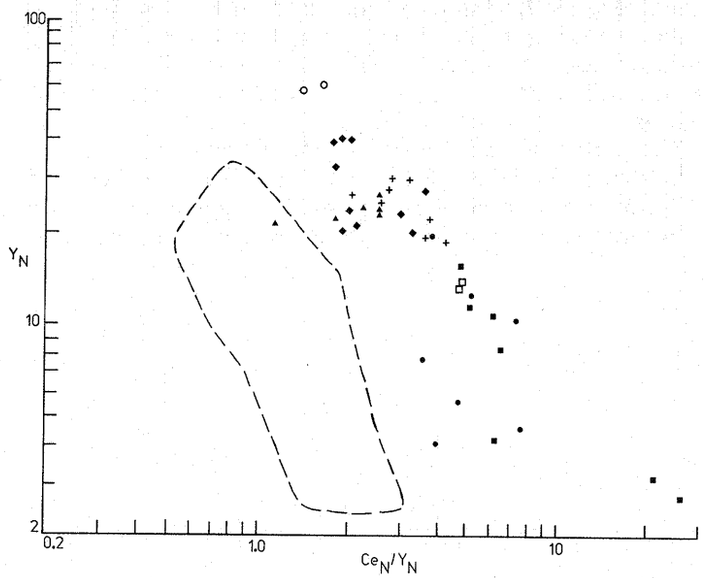

FIGURE 60

Chondrite-normalized Y versus Ce_N/Y_N diagram for the granitoid rocks of the Drygalski Fjord Complex. The dashed line enclosed the field of the basic rocks.

basic magma (with increase in Y_N content, the Ce_N/Y_N ratio remains constant in these rocks). Partition-coefficient data (Arth and Hanson, 1975) indicates that the Ce/Y ratio remains constant with fractionation of olivine, decreases slightly with significant fractionation of plagioclase, and increases with fractionation of clinopyroxene; a significant increase in the Ce/Y ratio with a decrease in the Y content (as seen in the Trendall Crag granodiorites) can only be achieved by fractionation of garnet and hornblende (Arth and Hanson, 1975; Saunders and others, 1979).

IX. RELICT DYKES

1. *Field description*

Aligned chains of angular or rounded and partially assimilated fine-grained basic enclaves (relict dykes) are locally abundant in the migmatites, gabbros and granites. Within the gabbros (Fig. 61) and granites (Fig. 62) to the east of Bogen Glacier and within the Trendall Crag granodiorite, aligned chains of angular basic fragments are found within coarse-grained gabbro, quartz-diorite and granodiorite. In the Trendall Crag area, the dykes show conflicting age relationships; continuous basic dykes, which have chilled margins against the granodiorite, are fragmented in places by veins of the plutonic rock invading the dyke (Fig. 63); some of the angular fragments have chilled margins on one of their faces; veinlets of granite may also intrude continuous dykes (Fig. 48). In some cases within the metasediments (Fig. 64), granites and gabbros (Fig. 65), the basic dykes are fragmented and net-veined *in situ* by a fine-grained granitic matrix (neosome). All gradations exist from basic dykes with minor granitic veinlets with irregular fretted margins (Fig. 65) and trains of angular fragments disrupted by agmatitic veins (Fig. 66) to remnant traces of partially

FIGURE 61
Relict dyke in a massive gabbro cut by granitic veins. The scale is 10 cm long.

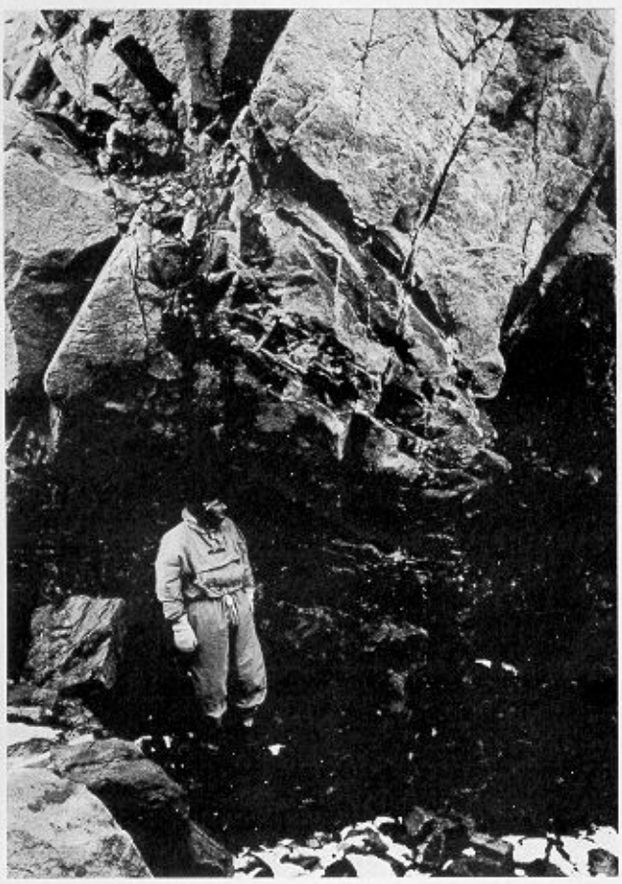

FIGURE 62
Relict dyke in a coarse-grained granite.

FIGURE 63
Basic dykes brecciated and net-veined by granitic veins. The hammer shaft is 35 cm long.

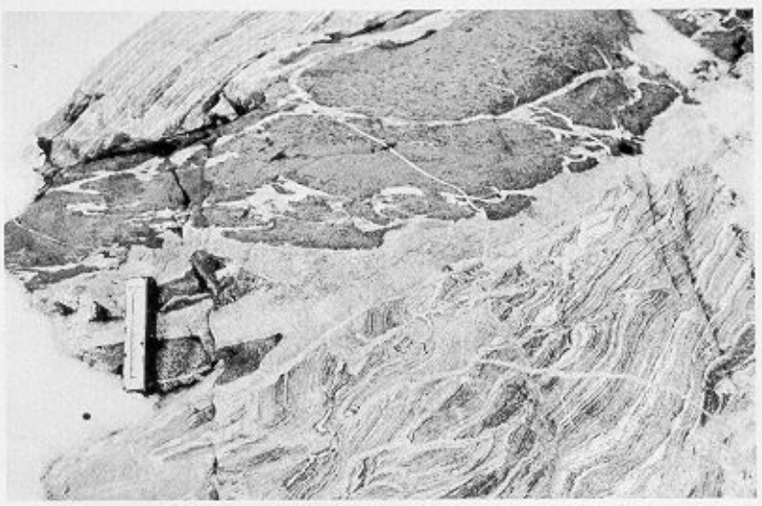

FIGURE 64
Basic dyke net-veined by granitic veins in metasediments. The scale is 10 cm long.

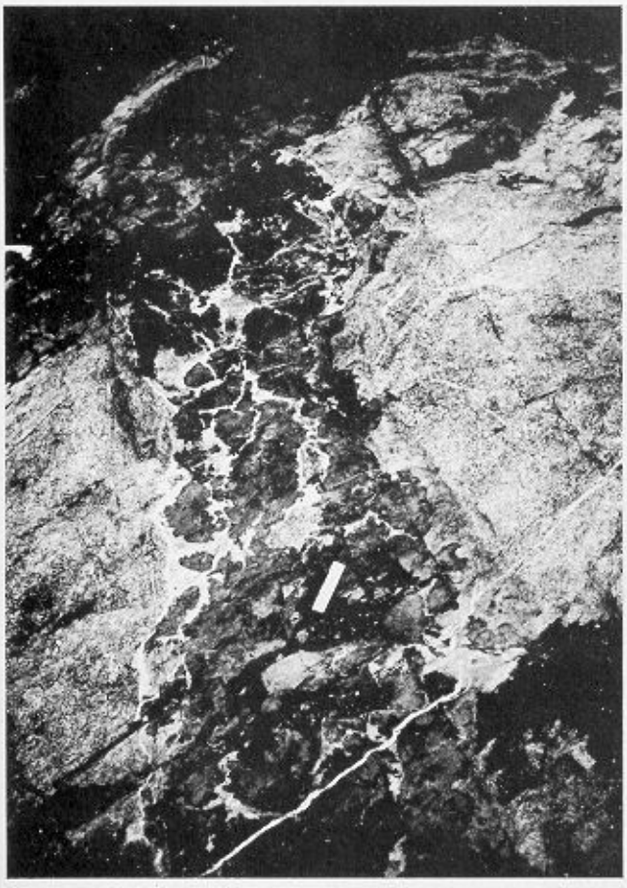

FIGURE 65
Basic dyke net-veined by granitic veins in a gabbro. The scale is 10 cm long.

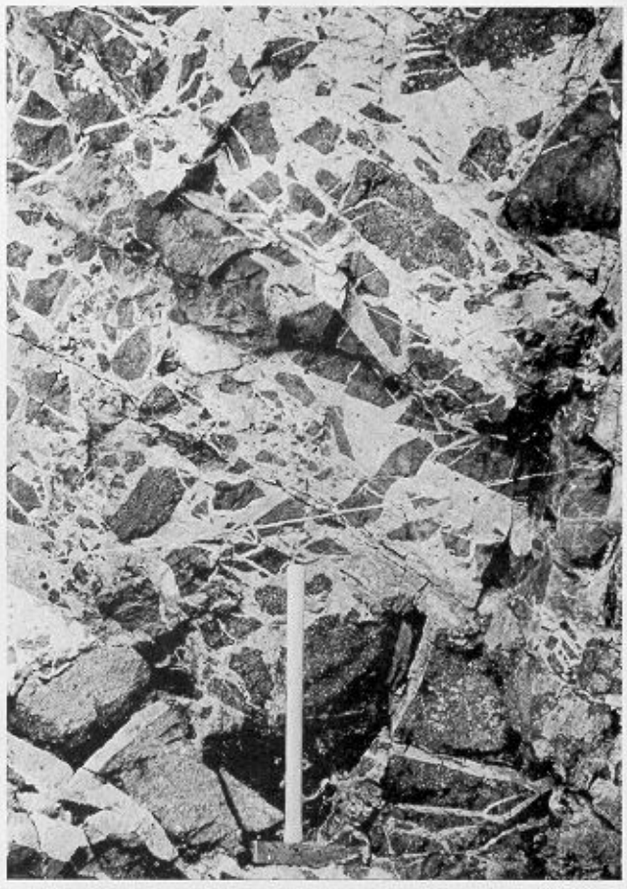

FIGURE 67
Angular basic fragments cut by granitic veins in an intrusive breccia. The hammer shaft is 60 cm long.

FIGURE 66
Basic dyke cut by granite veins in the metasediments.

FIGURE 68
A fragment of Trendall Crag granodiorite cut by a basic dyke and surrounded by intrusive breccia packed with basic enclaves. The hammer shaft is 60 cm long.

FIGURE 69
Mineral lineation in a net-veined basic dyke. The pencil is 10 cm long.

assimilated basic enclaves. The granitic veins preferentially net vein the dykes, leaving the country rock intact. Where trains of angular basic fragments with sharp contacts against granitic neosome are present, some rotation and small displacements of the basic fragments have taken place but, in general, the rocks can be fitted together to form larger basic bodies. In some cases, considerable disruption of the basic bodies has occurred and irregular areas of acid–basic breccia exist (Figs 67 and 68); angular and sub-rounded, partially assimilated basic fragments are set in a granitic neosome. The amount of displacement is unknown and the acid–basic breccias may have intruded. These rocks, although similar to the intrusive breccias described previously, are characterized by enclaves of uniform lithology. Many of the net-veined basic dykes have acted as shear zones and a mineral-alignment fabric is developed in the acid and basic components (Fig. 69).

Quartz and feldspar veins, aplites, pegmatites, occasional basic dykes and ductile shear zones cut the relict dykes.

2. *Petrography*

a. *Basic enclaves.* Partial and complete recrystallization of the basic dyke assemblages has taken place within the basic enclaves. Some are pseudomorphed and replaced by secondary hornblende, chlorite, tremolite and actinolite assemblages similar to those of the metabasites described previously, whilst others are completely replaced by fine-grained, melanocratic, green pleochroic amphibole, andesine (An_{32}), quartz- and biotite-amphibolite assemblages. Remnant pyroxene cores and feldspar xenocrysts (labradorite phenocrysts of basic dykes) are preserved within some amphibolites. Clusters of amphibole laths with opaque minerals, which may surround the felsic veins or occur within the amphibolites, are a characteristic of these rocks.

b. *Felsic neosome.* The felsic neosome, which net veins and brecciates the basic dykes, is composed of leucocratic rocks which are similar in composition but are more varied in texture than the basic enclaves. Some are similar to the migmatitic granite and will be discussed later, whilst others are quartz-diorite and tonalite with a similar texture to the granitoid matrix of the intrusive breccias. Granulose quartz, disorientated feldspar, biotite and hornblende prisms, andesine phenocrysts (to 3 mm) some of which are zoned, accessory sphene and opaque minerals, secondary chlorite and sericite, and irregular pools of quartz are characteristic of the fine-grained felsic neosome. The coarse-grained veins have irregular, often poikilitic, ragged prisms of biotite and hornblende (up to 5 mm), clusters of pale green to colourless actinolite laths, subhedral zoned andesine and interstitial quartz with irregular recrystallized boundaries. In the Trendall Crag area, the granitic veins are replaced by chlorite, tremolite-actinolite assemblages with sericitization, saussuritization and partial replacement of the plagioclase by quartz.

c. *Re-activated granites and gabbros.* The re-activated Trendall Crag granodiorite, which fragments the basic dykes, is similar in composition to the granodiorite described previously but contains recrystallized grain boundaries, interstitial quartz, potash feldspar and replacement textures. The gabbroic rocks containing fine-grained basic enclaves on the east of Bogen Glacier are quartz-gabbros and diorites with a primary igneous texture. Poikilitic augite and brown-green hornblende, occasionally cored by pyroxene, enclose andesine and labradorite crystals. Interstitial quartz, opaque minerals, apatite and zircon are common. Secondary chlorite, epidote, and sericite are present also.

3. *Discussion and origin*

Aligned chains of basic enclaves are a common feature of igneous complexes and have previously been interpreted (Goodspeed, 1955) as:

i. Basic magma intruded into semi-consolidated acidic country rock (syn-plutonic dyke).
ii. Basic dykes brecciated by acid veins subsequent to their intrusion (relict dyke).

In the former case, as in the Austurhorn net-veined complex in Iceland (Blake, 1966), pillows of basic magma, each with a chilled margin, are formed on contact with the cooler acid magma. In some cases, the chilled margin may be broken down and replaced by a transitional or crenulated margin due to heating of and re-absorption by the acid magma. Because the basic dykes in the Drygalski Fjord Complex have chilled margins against the country rock, it is unlikely that they are syn-plutonic dykes. What is more likely is that they are relict dykes, which were originally intruded into cooler consolidated or semi-consolidated country rock with the formation of chilled margins. Where basic dykes intrude granitic rocks, as in the Trendall Crag area, it is possible that the relict dykes are replacement dykes (Goodspeed, 1952); the dykes may have formerly intruded metasediments which were subsequently selectively granitized and replaced by the Trendall Crag granodiorite. It is, however, very unlikely that basic dykes could act as such efficient barriers and that a magmatic process should be so selective so as to cut away all the country rocks leaving the basic dykes in most places unaffected by the granitization (Roddick and Armstrong, 1959). It is more likely that the basic dykes intruded consolidated or semi-consolidated country rock (granite and metasediment) with the formation of chilled

margins, and that brecciation took place subsequent to formation by emplacement of later granitic veins, and by partial melting and re-activation of the granites and metasediments during the migmatization event. The granitic veins which are concentrated within the dykes may have arisen by metamorphic differentiation or by partial melting and segregation of the felsic component, leaving the melanocratic portion with clusters of hornblende. In some cases, where minor veinlets occur in the basic rocks and an *in-situ* brecciation (indicated by irregular margins) has taken place, metamorphic differentiation is the most likely process. However, in most cases the amount of granitic material is too great for metamorphic differentiation (Watterson, 1965) and the dykes have been fragmented, with some movement of the angular fragments, by granitic veins introduced from an external source along fractures in the dykes. The granitic veins probably formed by partial melting of the metasediments during migmatization and were concentrated along basic dykes due to the inhomogeneity of the country rock. The origin, by partial melting, is supported in thin section by the similarity of the neosome with the migmatitic granite.

Some of the granitic veins within the gabbroic and basic dyke rocks may represent acid differentiates of the basic magma. The acidic rocks may have separated at depth and re-intruded into the overlying rocks along basic dyke conduits.

Although there is some evidence of re-mobilization of the metasediments and granitoid rocks, the gabbroic matrix, to the east of Bogen Glacier appears to be a primary igneous rock, quartz-gabbro and quartz-diorite in composition, which formed by differentiation of the basic magma.

It is thus concluded that, in most cases, the basic dykes intruded consolidated granite, gabbro or metasediment. However, in some cases the granite, gabbro and metasediment were consolidated and, although chilled margins may have formed, the basic dykes were displaced prior to their consolidation.

X. MIGMATITES

THE term "migmatite" was initially introduced by Sederholm (1907) but this term and its correct application have since been much discussed and criticized. This report will use Mehnert's (1971, p. 8) definition of a migmatite as "a megascopically composite rock consisting of two or more petrographically different parts, one of which is the country rock generally in a more or less metamorphic stage [paleosome], the other is of pegmatitic, aplitic, granitic or generally plutonic appearance [neosome]." The migmatite nomenclature used here is purely descriptive. Trendall (1959) previously used the term "migmatite" to describe the cataclastically deformed gneisses north-west of Cooper Bay (described below as part of the dislocation zone).

Migmatites, with complex migmatitic structures, are found throughout the Salomon Glacier Formation gneisses. They were not observed in the sediments of the Novosilski Glacier or Cooper Island Formations. The most striking aspect of these migmatites is the gradation in migmatitic structures from a single gneissic parent through a series of complex paleosome–neosome relations to a final single granitic phase (migmatitic granite). The megascopic structures are attributed to two migmatization events which probably represent a single prograde cycle but are separated in time by intense deformation and intrusion of basic and acidic rocks.

A. First Migmatization Event

The layered migmatites described previously and found throughout the gneisses of the Salomon Glacier Formation formed during this event. It is probable that they have originated by selective recrystallization and metamorphic differentiation during a prograde metamorphic event (Scheumann, 1937) associated with the D1 event. This may be superimposed on original heterogeneities in the sedimentary rocks. The migmatitic segregations are folded by F2 and F3 folds which are, in turn, cut by acid and basic intrusions prior to the second migmatization event.

B. Second Migmatization Event

1. *Field description*

The structures formed during this event are superimposed on the layered migmatites. They represent a more advanced stage in the migmatization process and are best exposed to the east of Bogen Glacier (Fig. 5). Basic dykes, which cut the folded layered migmatites, were affected by the second migmatitic structures. All gradations exist from the layered migmatites and basic dykes cut by irregular veins of a migmatitic granitic neosome to large areas (up to 10 m wide) of medium-grained granite (neosome) with nebulitic gneissose and basic enclaves and relict ghost structures. The first three structures described below form a gradation in a single prograde migmatization sequence.

a. *Diktyonitic structure.* Narrow veins of granitic neosome, which exhibit small-scale shear movements (5 cm) and an aligned biotite fabric, interlace the folded layered migmatites. As they often occur axial planar to the pre-existing F3 folds of the layered migmatites, the migmatization may be related in time to the formation of these folds or may be utilizing the pre-existing weakness in the folded country rock. Veins and small irregular patches of granitic neosome (a few centimetres wide), without a fabric, are also developed at random throughout the layered migmatites and may represent the initial stage in the formation of the migmatitic granite.

b. *Schollen structure.* With more extensive development of the neosome, fragments of the paleosome are left suspended in a granitic matrix (Fig. 70). The fragments, which may be rounded, are often partially dissolved showing indistinct borders. As intrusion of basic dykes occurred prior to the second migmatization event, many of the enclaves are remnants of brecciated basic dykes. There are all gradations from basic dykes intruded by a fine network of veins (Fig. 64) to dykes completely disrupted by the granitic neosome. In the final schollen structure (Fig. 71), enclaves of basic dykes, *para*gneiss and layered

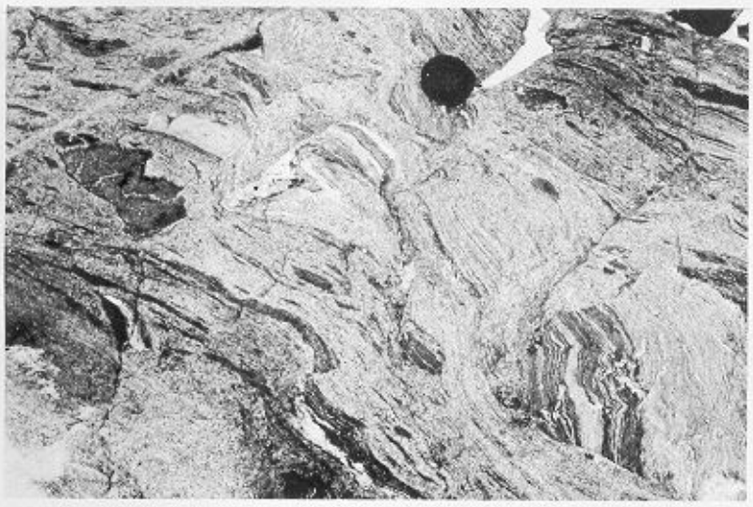

FIGURE 70
Fragments of layered migmatite (paleosome) in a granitoid matrix (neosome). The lens cap is 6 cm in diameter.

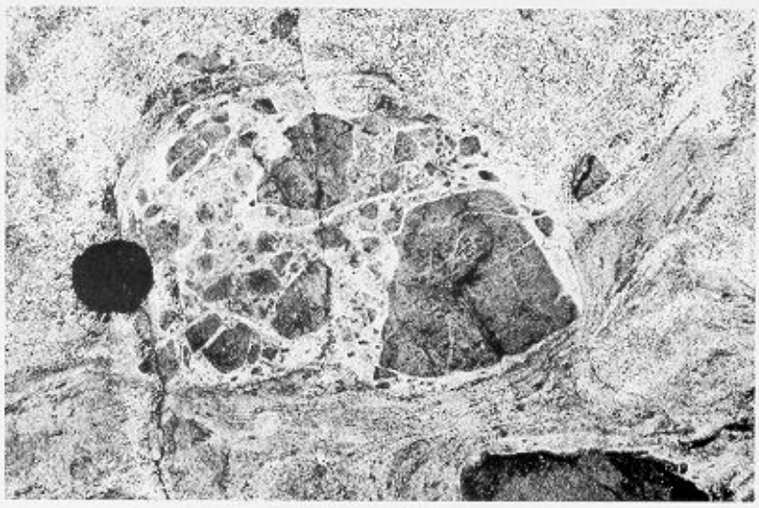

FIGURE 72
Fragmented and partially assimilated basic enclave. The lens cap is 6 cm in diameter.

FIGURE 71
Basic and metasedimentary fragments in a granitic matrix (schollen structure). The hammer shaft is 35 cm long.

migmatites occur randomly distributed and orientated in a granitic matrix. Larger enclaves are brecciated *in situ* with veins of granitic neosome intruding and assimilating the basic fragments (Fig. 72).

c. *Nebulitic structure.* This state has been reached in small areas of the layered migmatites. It represents the final stage of the migmatization process when the paleosome and neosome can no longer be identified as separate units. The former paleosome can be recognized by identifying the cloudy dissimilarities that are present in the otherwise homogeneous rock. Neosomes of the layered migmatites are occasionally preserved as indistinct ghost structures in the nebulitic granite. Areas of medium-grained more homogeneous granite (often up to 5 m wide) exist within, and form gradational contacts with, the nebulitic granite and schollen structure.

d. *Agmatitic structure.* This structure occurs extensively throughout the Salomon Glacier Formation gneisses and layered migmatites. Angular fragments of layered migmatite with well-defined abrupt margins are brecciated by relatively narrow veins of pale-coloured, medium-grained granitic and aplitic neosome. In some cases, the fragments can be restored to their former position by closure of the fracture but, in other cases, rotation and movement of the fragments has occurred. A gneissic fabric parallel to the margins of the vein, which may exist, was probably formed by laminar flow of a granitic liquid in the fracture (Mehnert, 1971). Cross-cutting relationships are recorded indicating more than one pulse of activity. Agmatitic veins may also cut the above migmatization structures. On a larger scale, similar pale-coloured granitic dykes (up to 5 m wide), with fragments of wall rock, brecciate the layered migmatites.

e. *Ptygmatic structure.* Well-developed ptygmatic structures occur in the *para*gneisses in the Trendall Crag area. Highly disharmonic folds are developed in cross-cutting granitic veins. As variation in thickness and trend of the ptygmatic veins occur, detailed measurements were not attempted. In some cases, the folding is not continuous but may die out along the length of the veins or occur at sporadic intervals. The ptygmatic veins are best developed in a region where the boudinaged planar fabric of the layered migmatites does not occur. Thus the age of the ptygmatic veins is not certain but they do cut a vague migmatitic banding of the gneisses. As they mainly occur in the peripheral regions of the Trendall Crag granodiorite, they may be associated with the formation of this granite.

The origin of ptygmatic structures is perhaps one of the most controversial in literature on migmatites. In principle, two groups of hypotheses can be distinguished:

i. The folding was of primary origin, simultaneously with the formation of the vein (Godfrey, 1954).
ii. The folding was of secondary origin; the formation of vein and folding are products of independent processes (Kuenen), 1938).

The latter appears to be the most generally accepted theory, having been supported by the experimental work of Ramberg (1960). The ptygmatic veins are interpreted as having resulted from differences in competence between the competent vein and the incompetent host rock with ptygmatic veins forming as a result of compression of such a heterogeneous system.

A number of structures, described below, developed as a result of laminar flow of the mobile neosome. The neosome developed a gneissic fabric at the same time as the migmatization event.

f. *Banded gneissic neosome.* The layered migmatite fabric, which developed during the first event and was folded prior to intrusion of the basic dykes, has been granitized and re-orientated, producing a gneissic fabric (Fig. 73). Folded layered migmatites occur as enclaves in the newly developed non-folded gneissic fabric. With a more advanced stage of granitization, a true granitic gneissic neosome (Fig. 74) formed with the laminar gneissic flow fabric around the basic and migmatitic enclaves. Flow folds (Fig. 75) indicate the extent of the mobile environment during granitization. In the migmatitic granites, a relict fabric is occasionally preserved (Fig. 76) from the former layered migmatites, indicating *in-situ* granitization. The granitic neosome that has developed is devoid of a fabric.

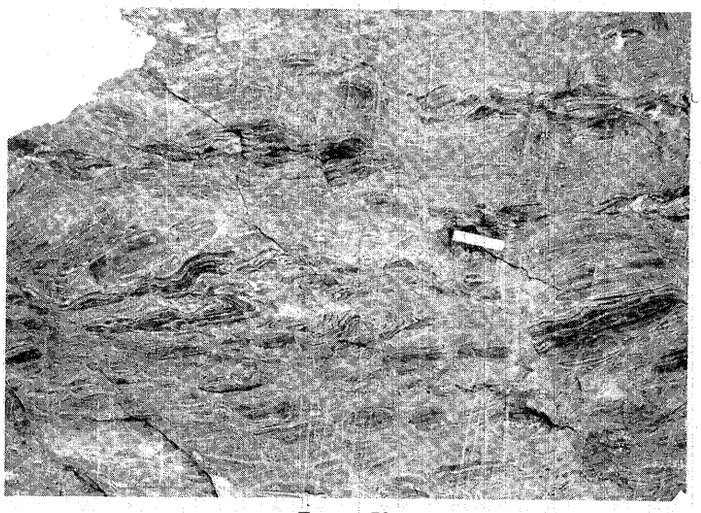

FIGURE 73
Gneissose neosome with enclaves of folded layered migmatite. The scale is 10 cm long.

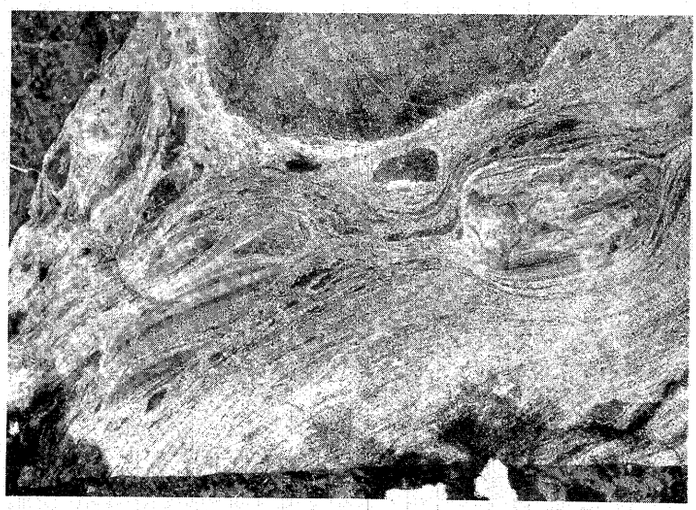

FIGURE 74
Gneissose neosome surrounding metasedimentary enclaves. The scale is 10 cm long.

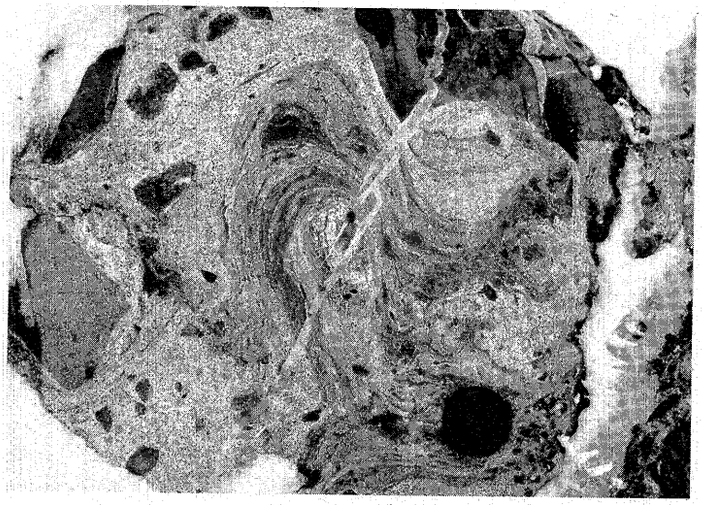

FIGURE 75
Ductile flow fold of migmatitic granite. The lens cap is 6 cm in diameter.

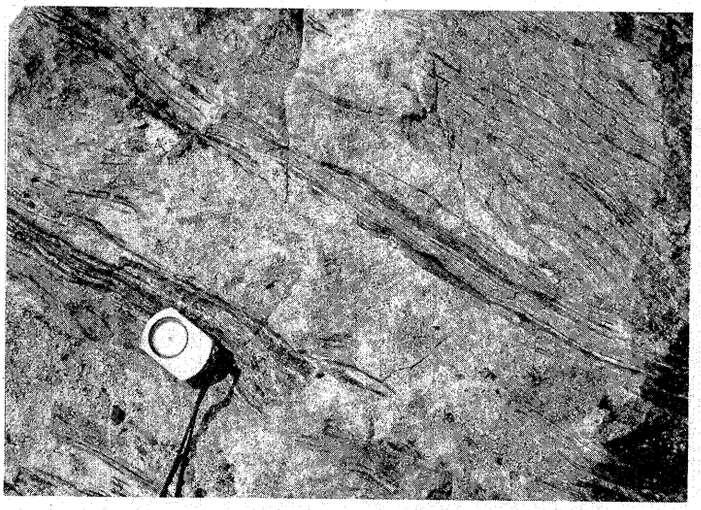

FIGURE 76
Relict fabric of a layered migmatite in a migmatitic granite. The compass dial has a diameter of 4.25 cm.

g. *Schlieren structure.* This structure occurs in the migmatites which show signs of high mechanical mobility and greater granitization than in the granitic gneisses described above. The schlieren appear as light and dark streaks of elongated shape in a migmatitic granite with a gneissic fabric.

2. *Petrography*

As indicated above, the migmatitic granite and granitic gneiss vary from small patches and veins of granitic rock with sharp

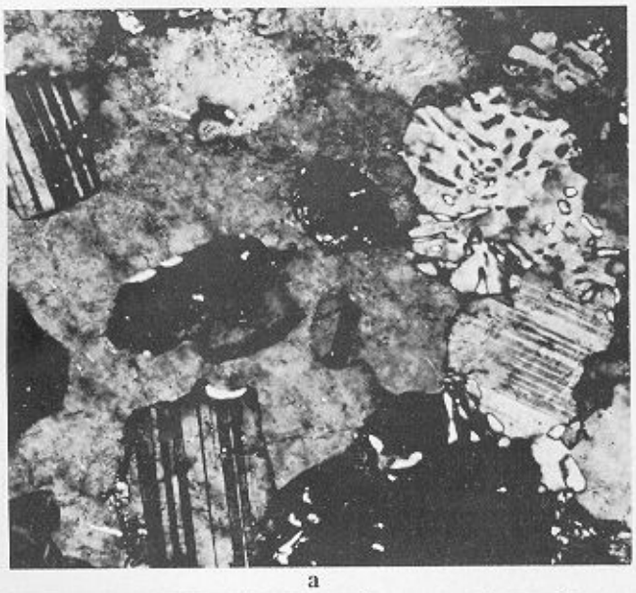

a

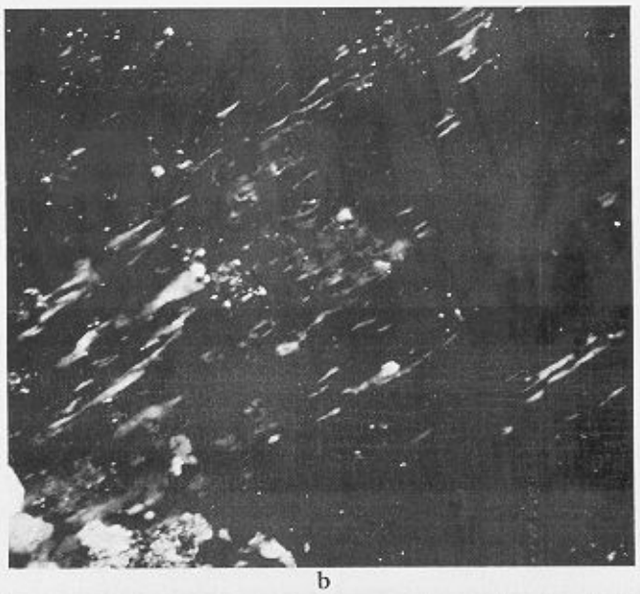

b

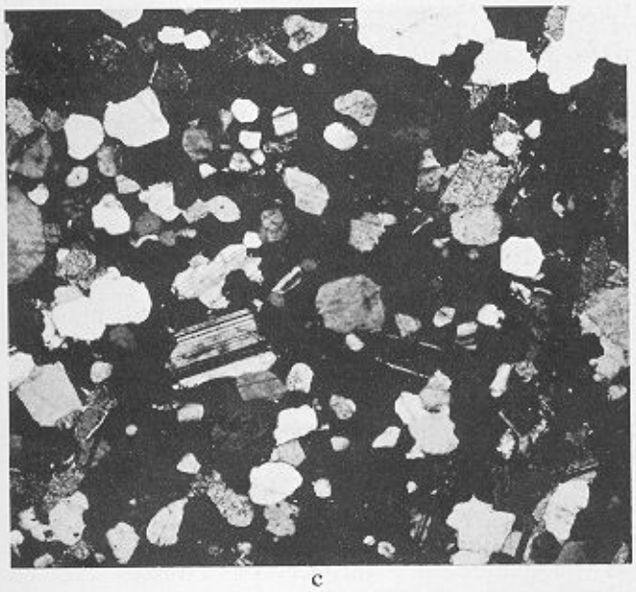

c

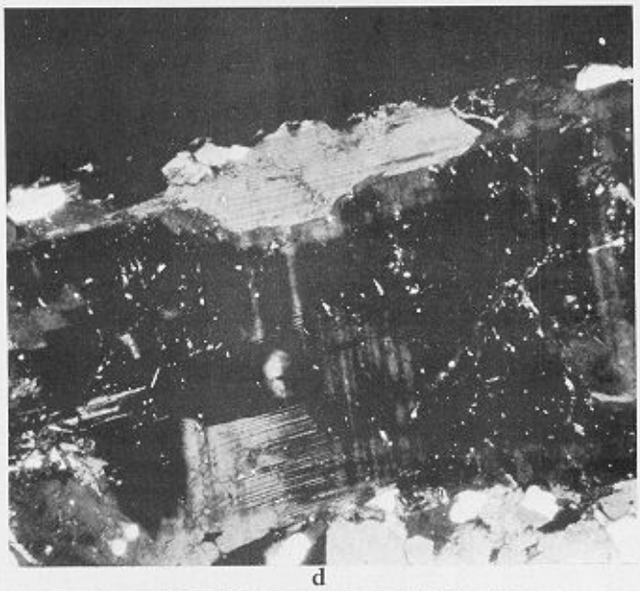

d

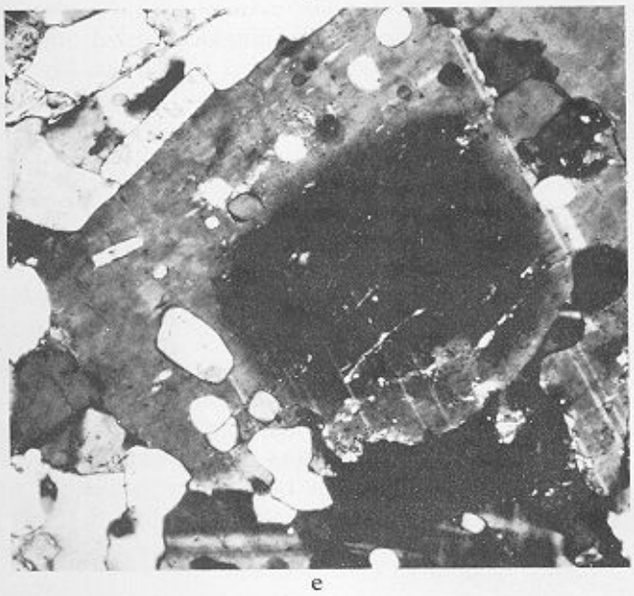

e

f

FIGURE 77

a. Poikiloblastic potash feldspar enclosing quartz and plagioclase. Myrmekitic intergrowths occur in some inclusions. (M.1682.2b; X-nicols; ×160)
b. Flame perthite in a migmatitic granite. (M.1659.5A; X-nicols; ×160)
c. Poikiloblastic quartz (black) enclosing quartz, plagioclase and biotite in a migmatitic granite. (M.1695.2; X-nicols; ×40)
d. Uneven extinction pattern of plagioclase in a migmatitic granite. (M.1683.10; X-nicols; ×40)
e. Quartz inclusions in the margins of plagioclase in a migmatitic granite. (M.1683.11; X-nicols; ×40)
f. Biotite strain lamellae in a migmatitic granite. (M.1694.2; X-nicols; ×160)

and gradational contacts developed at random in the layered migmatites to large masses of granitic rock with nebulitic gneissose enclaves and relict ghost structures. In thin section the migmatitic granite has similar textural features but varies in composition from tonalite to granodiorite and granite.

The migmatitic granite shows great variation in grain-size. Fine-grained granoblastic quartz, twinned albite-oligoclase and unorientated biotite occur interstitially and are enclosed within coarse-grained (up to 1.0 cm) quartz, oligoclase, potash feldspar and biotite with accessory zircon, apatite, sphene and opaque minerals. Potash feldspar (microcline and perthite), which may be absent, forms up to 50% of some migmatitic granite. It occurs as irregular interstitial blebs and large (up to 1.0 cm) poikilitic crystals (Fig. 77a) packed with various amounts of fine-grained inclusions. Flame perthitic intergrowths (Fig. 77b) of albite occur in some thin sections. The quartz and oligoclase crystals vary from subhedral shapes devoid of inclusions to poikilitic crystals (Fig. 77c) with irregular interpenetrating boundaries and corroded inclusions of the fine-grained minerals described above. Biotite (10–15%) and subsidiary muscovite vary in grain-size and are randomly distributed and orientated throughout the rock. Some biotite has a lighter-coloured pleochroic rim. Retrogressive alteration lamellae of chlorite (penninite) and prehnite often occur within the biotite. Laths of penninite often contain granules of epidote and sphene and may be scattered in the migmatitic granite. In thin section (M.1682.7) the ferromagnesian mineral is an acicular colourless amphibole identified as tremolite. Clusters of disorientated tremolite laths and fine acicular needles form up to 20% of the rock. Biotite and xenomorphic poikilitic muscovite also occur. Fine-grained granules of a xenomorphic opaque mineral are scattered throughout the thin section. These appear to be closely associated and are usually enclosed in the tremolite. There is a marked absence of potash feldspar poikiloblasts. An enclave of quartz-oligoclase-biotite-chlorite-*para*gneiss occurs in this neosome. Epidote-filled joints transgress the rock; sericitization and saussuritization of the feldspar and some development of calcite have taken place.

Myrmekitic intergrowths (Fig. 77a) are common in the migmatitic granite. They occur in the fine-grained plagioclase as a ramifying network of vermicular quartz. They are only found in plagioclase crystals in partial contact or completely enclosed in poikiloblastic potash feldspar. They do not occur in all plagioclase crystals found in this situation. The occurrence of the intergrowth may be compositionally controlled but there is an undoubted association with potash feldspar.

The areas of medium-grained migmatitic granites of similar texture and composition, and with gradational contacts to the above, are characterized in thin section by subhedral plagioclase crystals often porphyritic and up to 5 mm in length. These feldspars, which form up to 30% of the rock, are variable in composition (albite to andesine), twinned, non-twinned and often zoned. The nature of the zoning varies from normal to complex, regular and irregular oscillatory patterns. The normal zoning indicates a more sodium-rich margin but it was not possible using optical methods to denote the changes in composition of the oscillatory zoning; narrow zones of high-relief feldspar often occur near the margins. As well as the zoning, irregular patterns of uneven extinction (Fig. 77d) are often found in these crystals. The feldspars are mainly devoid of inclusions except in the margins of some crystals (Fig. 77e). Some feldspars with inclusions and irregular penetrating margins often have a euhedral high-relief core indicating a poikilitic regrowth. Corroded margins also occur with quartz and microcline veinlets intruding the euhedral feldspars. Antiperthitic inclusions of potash feldspar are often found. They may form irregularly distributed tricuspate blebs and veinlets often aligned along the cleavage. Sericitization and saussuritization of the plagioclase have also occurred. Some large 4 mm biotite crystals have black pleochroic sigmoidal lamellae (strain lamellae) in a brown pleochroic background (Fig. 77f). Minor kink bands of the biotite cleavage and an undulose extinction of the blastic quartz grains indicate deformation.

Some of the migmatitic granitoids are quartz-dioritic in composition. Scattered irregular poikilitic patches of green, pleochroic hornblende (α = yellow-green; β = brown-green; γ = dark green) and colourless poikilitic laths of tremolite are present. A core of high-relief, high-birefringence, biaxial positive pyroxene (augite) was identified. The amphiboles are predominant in migmatitic granite with basic enclaves. An irregular, green, slightly pleochroic (olive-green to brown-green) mineral (0.3 mm) with strong absorption and uniaxial negative character (tourmaline) also occurs.

In some thin sections, the ferromagnesian minerals are chlorite, epidote and sericite; the feldspars are partially replaced by prehnite and sericite. Prehnite and epidote veins are common.

Enclaves of *para*gneiss and amphibolite (brecciated basic dykes) are found in these rocks. Contacts are gradational with poikilitic quartz and feldspar crystals of the granite being replaced by blastic overgrowths on the fine-grained granoblastic quartz and feldspar of the *para*gneissic enclaves. Interstitial quartz, potash feldspar and albite occur between the andesine and amphibole of the amphibolites. Poikiloblastic crystals of the above and biotite may be developed in the amphibolites.

The agmatitic veins and granite dykes within the metasediments are leucocratic granite similar to the fine- to medium-grained migmatitic granite. Crystal outlines are characteristically irregular with poikilitic microcline and perthite (up to 2 mm) forming intergrowths with plagioclase and quartz, and enclosing fine-grained oligoclase, quartz and biotite. Myrmekitic intergrowths are common within enclosed plagioclase. Plagioclase crystals (up to 1.5 mm), which are sometimes zoned, also enclose quartz and biotite within their margins. Biotite, the main ferromagnesian mineral, encloses zircon with pleochroic haloes and is partially altered to chlorite and epidote.

3. *Discussion and origin of the migmatitic granites*

Before discussing the origin of the migmatites it may be useful to outline possible origins of a granitic rock (outlined by Mehnert (1971)).

i. Magmatic origin.
ii. Anatectic origin, where complete or partial melting of the rock, without any addition of components, produced the granitic rock; an anatectic melt may crystallize *in situ* or intrude the surrounding rocks.
iii. Metasomatic origin, where addition of components was supplied from an external source.

The petrographic study of the migmatites and metasediments has indicated a number of well-defined changes which can be traced from the metasediments to the migmatitic granite:

i. Increase in grain-size of the common components.
ii. Occurrence of quartz, plagioclase, potash feldspar and biotite poikiloblasts.
iii. Occurrence and increase in the concentration of potash feldspar.
iv. Disorientation of the gneissic banding.
v. Decrease in the concentration of biotite.

The strong contrast in grain-size and abundance of poikilitic crystals packed with fine-grained inclusions, which are present in a migmatitic granite, do not favour a magmatic origin for these rocks. The fine-grained inclusions (quartz, oligoclase and biotite) are similar to those in the *para*gneisses and it is therefore proposed that they represent remnants of the *para*gneisses (paleosome), and that the poikiloblasts and coarser crystals (neosome) have crystallized from fluids formed by partial melting of the metasediment (anatectic or palingenetic origin) or from fluids introduced metasomatically into the rock.

The most conspicuous change in the petrography during the granitization is the marked increase in the concentration of potash feldspar. The metasediments are essentially tonalitic and granodioritic in composition, whereas in composition the migmatites are tonalites, granodiorites and granites. Potash feldspar is mainly concentrated within the neosome of the layered migmatites. The increase in potash feldspar is, in part, balanced by a decrease in the biotite content. The melting of the biotite may release sufficient potassium to form the potash feldspar-forming solutions. As potash feldspar forms up to 50% of the neosome, occurs interstitially and poikiloblastically to the other mineral phases and forms replacement anti-perthitic intergrowths with earlier feldspars, it appears that the potassium content of the rocks is not balanced and that the potassium has been introduced to the Salomon Glacier Formation gneisses by alkali-bearing solutions. The validity of this conclusion will be discussed with a detailed geochemical analysis of the *para*gneisses and granitized rocks. The proportion of quartz and plagioclase appears constant, thus indicating that blastic growth of these minerals occurred from solutions produced by the melting of the *para*gneiss. The origin of the alkali-bearing solutions is not certain. Metasediments with a high potassium content may exist in the area. An external source associated with an earlier magmatic activity must not be ruled out.

Kilinc (1973), investigating the formation of migmatites by experimental studies in partial melting in the presence of chlorite-bearing aqueous solutions, discovered that partial melting of a shale produced potassium-rich leucocratic veins, whereas the partial melting of a greywacke produced migmatites with sodium-rich leucocratic veins. Suk (1972), in discussing the origin of the south Bohemian migmatites, emphasized the importance of the original composition of the metasediments and the dependence of the mobilizate on the mineral facies of the paleosome. In the lower-amphibolite facies, the metatect is mainly quartz–albite in composition, characteristic of syn-orogenic migmatites (layered migmatites of the Salomon Glacier Formation) and quartz–plagioclase–potash feldspar in the upper-amphibolite facies, characteristic of the late-tectonic migmatites (second migmatization event). The above is supported by the following observations of Suk (1964) and Krupicka (1968): potash feldspar is more abundant in the neosome than in the paleosome; it is released on formation of cordierite (garnet) from biotite and from the primary feldspars; the total volume of the feldspars is constant; only a small decrease in the sodium and calcium content of the plagioclase is reflected in the formation of potash feldspar at the expense of plagioclase.

As cordierite and garnet are not recorded in the Salomon Glacier Formation gneisses, it is probable that most of the potash feldspar has appeared from alkali-bearing fluids produced at depth, where melting in the upper-amphibolite facies may have taken place. As a result of experimental and field evidence, Brown (1973) has correlated the composition of migmatitic granites with temperature, depth and confining pressure (Fig. 78).

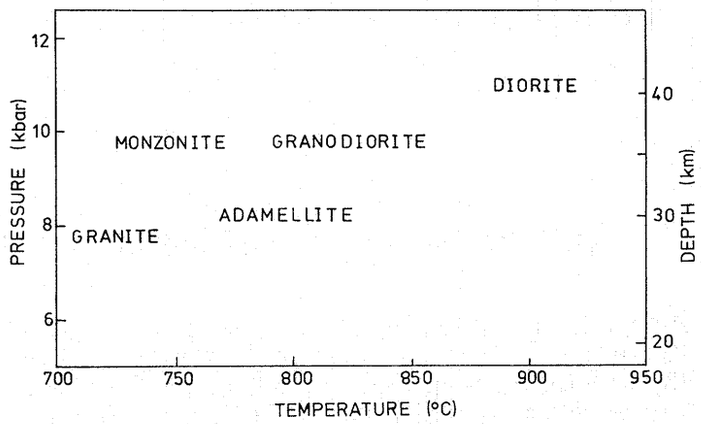

FIGURE 78
A diagram illustrating the relationship between the composition of an anatectic melt, temperature, depth and confining pressure during formation of migmatites (Brown, 1973) as deduced from experimental results.

Thus, an anatectic and metasomatic origin for the migmatitic rocks is most likely. The problem arises in anatectic migmatites as to whether the anatectic melt crystallized *in situ* or intruded the rocks as a magma. In the Salomon Glacier Formation migmatites, some *in-situ* granitization occurred, as indicated by the preservation of undisturbed relict gneissic fabrics (Fig. 76) in the margins of the migmatitic granite. This may be a marginal feature due to an aureole of metasomatism and anatexis around an intrusive anatectic melt. Randomly distributed basic dyke and *para*gneissic enclaves and laminar flow fabrics in the migmatitic granite indicate that a mobile liquid or part-liquid existed but the extent of movement of the anatectic melt cannot be evaluated. The sharp contacts of the agmatitic granite suggest that the rocks intruded as anatectic melts formed at depth and modified by percolating hydrothermal fluids into the *para*gneisses. An origin by penetration of metasomatic fluids along weaknesses in the metasediments may also be a possible *in-situ* origin for some of these agmatitic structures.

The origin of the coarser-grained migmatitic granites with euhedral zoned plagioclase crystals, often porphyritic and up to 5 mm in length, is more complex. The phenocrysts are not in equilibrium with the groundmass, as corrosion and replacement by potash feldspar has occurred. Secondary overgrowths of albite also occur. These may represent porphyroblasts that have grown *in situ* in the *para*gneisses. Mehnert (1962) has indicated that the idiomorphic shape and lack of inclusions in feldspar porphyroblasts are characteristic of high-grade migmatites

(anatexis), whereas poikiloblastic crystals with xenomorphic outline are characteristic of low-grade migmatites (palingenesis). These rocks may thus have intruded prior to the second migmatization event as porphyroblastic crystals suspended in a granitic liquid produced by high-grade migmatization at greater depth in the sedimentary pile, probably during intrusion of the Trendall Crag granodiorite. Some of the zoned plagioclase crystals may be xenocrysts incorporated in the rising melt. These rocks may then have been intruded by basic dykes, subjected to *in-situ* migmatization with recrystallization, blastic growth of the groundmass and introduction of potash feldspar. This event may have re-mobilized the existing granite, which subsequently intruded and fragmented the former cross-cutting basic dykes forming the relict dykes.

The complex structures in the Salomon Glacier Formation gneisses and layered migmatite have thus arisen by a combination of *in-situ* anatexis, *in-situ* metasomatism by potash feldspar-rich hydrothermal fluids, and intrusion of a melt or partial melt produced by anatexis at depth. The sharp contacts of the migmatitic granite with the metasediments are characteristic of the intrusive anatectic melts, whereas the gradational contacts and re-mobilization structures are characteristic of *in-situ* anatexis and metasomatism. Some anatectic melts, which may have intruded prior to the second migmatization event (dykes associated with the intrusion of the Trendall Crag granodiorite), are cut by basic dykes and subsequently reheated and metasomatized with resulting fluids brecciating the cross-cutting basic dykes and forming gradational contacts with the country rocks. Many agmatitic granites cut the *in-situ* migmatites, indicating a late intrusion of anatectic melts.

XI. GEOCHEMISTRY OF THE METASEDIMENTS, MIGMATITES AND SEDIMENTS

A CHEMICAL programme was carried out in order to investigate the relationship between the unmetamorphosed sediments of the Cooper Island and Novosilski Glacier Formations and the metamorphosed sediments of the Salomon Glacier Formation; the metasediments and the (?) anatectic migmatites and agmatites of the Salomon Glacier Formation; the Cooper Island Formation and the remaining sediments on South Georgia (Ducloz Head, Sandebugten, Cumberland Bay and Cooper Bay Formations).

The major- and trace-element concentrations (Table XII) of seven banded *para*gneisses, 15 layered migmatites, 15 migmatitic granitoids, eight agmatitic granitoids, three granitic dykes and one quartz-diorite dyke are plotted against SiO_2 (Fig. 79) in order to show their chemical variation. The granite and quartz-diorite dykes, similar to the agmatitic veins, cut the migmatized Salomon Glacier Formation with sharp well-defined boundaries. In contrast, the migmatitic granitoids are gradational into, and have diffuse boundaries with, the layered migmatites. Enclaves of metasediment and migmatitic granitoid from the same specimen were analysed.

1. *Metasediments and migmatites*

The metasediments, layered migmatites and migmatitic granitoids, show a well-marked linear variation trend when the major and trace elements are plotted against SiO_2. With an increase in the SiO_2 value, from the biotite-rich metasediment to the felsic neosome of the layered migmatite, there is a marked decrease in TiO_2, Al_2O_3, MgO, Fe_2O_3, Cr, Ni, Zn, Y and Nb and Ga (not illustrated) values, with a slight decrease in MnO and P_2O_5 values, and a slight increase in Na_2O concentrations. A variation trend is not so well defined for K_2O, CaO, La, Ce, Ba, Rb, Sr and Zr. Within the above trends, there is a marked similarity in major- and trace-element concentrations in the banded gneisses, layered migmatites and migmatitic granites. The variation of Ba, Sr and Zr within the metasediments is mirrored by a similar variation within the migmatites. The similarity is again brought out on AFM (Fig. 80), Ce_N/Y_N versus Y_N (Fig. 81), normalized an–ab–or–Qz (Fig. 82) and rare-earth element (Fig. 83) diagrams. This similarity confirms the petrographic evidence, which indicates that metasomatism played a minor and insignificant role in the development of the migmatitic granites and layered migmatites, and that the migmatitic granites developed by *in-situ* partial melting of the metasediments and that the layered migmatites developed by *in-situ*

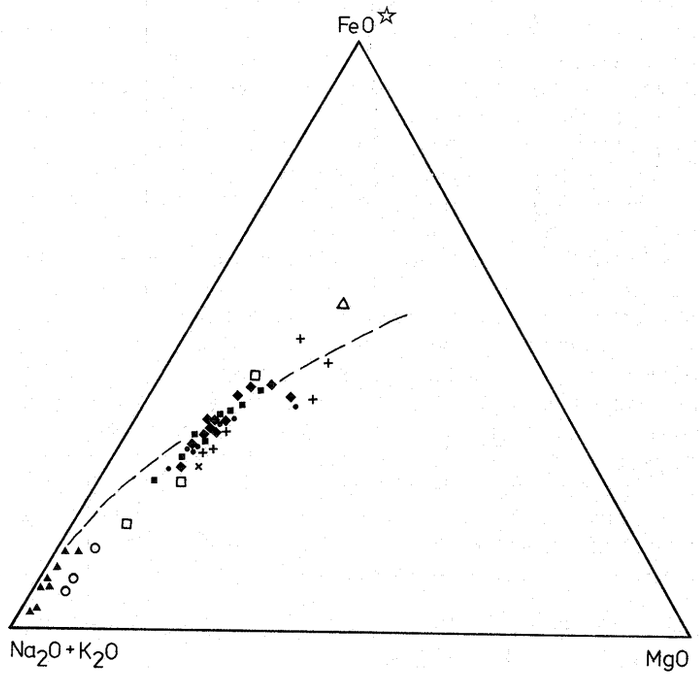

FIGURE 80
AFM triangular diagram for the sediments, metasediments and migmatites of the Drygalski Fjord Complex and the sediments of the Ducloz Head Formation. The dashed line indicates the calc-alkaline differentiation trend of the Mount Lassen suite (Nockolds and Allen, 1953).

TABLE XIII

CHEMICAL ANALYSES OF THE SEDIMENTS OF THE DUCLOZ HEAD FORMATION

	1	2	3	4	5	6	7	8
SiO_2	72·11	76·79	76·61	72·38	68·06	60·78	67·08	44·70
TiO_2	0·08	0·07	0·31	0·32	0·39	0·77	0·81	0·20
Al_2O_3	12·62	13·52	12·89	13·22	15·46	19·09	10·15	3·70
Fe_2O_3*	1·35	0.80	0·92	1·68	3·41	6·63	8·65	4·85
MnO	–	–	–	–	–	–	–	–
MgO	0·51	0·50	0·50	0·66	1·42	1·92	2·69	2·08
CaO	3·55	0·20	0·35	3·56	0·97	0·35	2·12	35·90
Na_2O	4·05	5·38	6·43	3·36	4·20	2·00	1·58	0·50
K_2O	3·24	3·77	2·03	2·98	3·38	4·05	1·88	0·58
P_2O_5	0·01	0·01	0·01	0·09	0·12	0·09	0·09	0·10
TOTAL	97·52	101·04	99·87	98·25	97·41	95·68	95·05	92·61
	C.I.P.W. NORMS*							
Q	30·12	29·14	29·83	33·89	25·59	28·03	39·88	0·00
C	0·00	0·21	0·00	0·00	3·41	11·50	1·94	0·00
Z	0·03	0·02	0·03	0·03	0·05	0·04	0·00	0·00
or	19·65	22·06	12·02	17·97	20·58	25·21	11·78	0·00
ab	35·16	45·07	54·50	28·96	35·56	17·78	14·17	0·00
an	6·86	1·03	0·32	12·40	4·42	1·34	10·66	6·66
di	6·09	0·00	1·17	4·30	0·00	0·00	0·00	24·87
wo	1·67	0·00	0·00	0·00	0·00	0·00	0·00	51·08
hy	0·00	2·19	1·71	1·33	7·74	13·15	18·13	0·00
mt	0·24	0·14	0·16	0·31	0·61	1·20	1·58	0·91
il	0·16	0·13	0·25	0·62	0·76	1·54	1·63	0·41
ap	0·02	0·02	0·02	0·22	0·29	0·22	0·22	0·26
	COORDINATES OF TRIANGULAR DIAGRAMS							
A	80·8	88·2	86·4	74·5	62·8	43·4	24·8	14·4
F	13·5	6·9	8·5	17·7	25·4	42·8	55·9	58·0
M	5·7	4·9	5·1	7·8	11·8	13·8	19·3	27·6
an	11·1	1·5	18·0	20·9	7·2	3·0	29·1	—
ab	57·0	66·1	81·5	48·8	59·4	40·1	38·7	—
or	31·9	32·4	0·5	30·3	33·4	56·9	32·3	—
	TRACE ELEMENTS (ppm)							
Cr	<10	<10	<10	18	20	60	30	10
Ni	<6	<6	<6	<6	7	15	47	21
Zn	60	<6	<6	22	29	78	199	50
Rb	89	60	29	96	111	176	28	11
Sr	52	26	35	239	356	89	88	89
Y	32	24	26	14	22	32	20	18
Zr	130	99	141	148	218	188	69	68
Nb	9	10	11	7	9	15	<3	<3
Ba	724	548	304	547	756	470	462	81
La	41	21	36	23	29	35	<6	<6
Ce	84	49	77	46	58	81	11	18
Pb	27	8	<9	14	17	11	<9	<9
Th	22	11	11	9	14	17	<9	<9
Ga	16	8	9	14	21	29	16	6
W	404	341	513	517	507	34	16	<5

* Fe_2O_3/FeO was asssumed to be 0·15 for norm calculations.
Fe_2O_3* Total iron as Fe_2O_3.

1. M.4090.2 Volcaniclastic sandstone, coastal member.
2. M.4093.4 Volcaniclastic tuff, coastal member.
3. M.4097.8 Volcaniclastic tuff, coastal member.
4. M.4104.4 Sandstone, coastal member.
5. M.4110.3 Sandstone, coastal member.
6. M.4118.7 Shale, coastal member.
7. M.4087.2 Tuff, inland member.
8. M.4087.5 Tuff, inland member.

facing page 66.

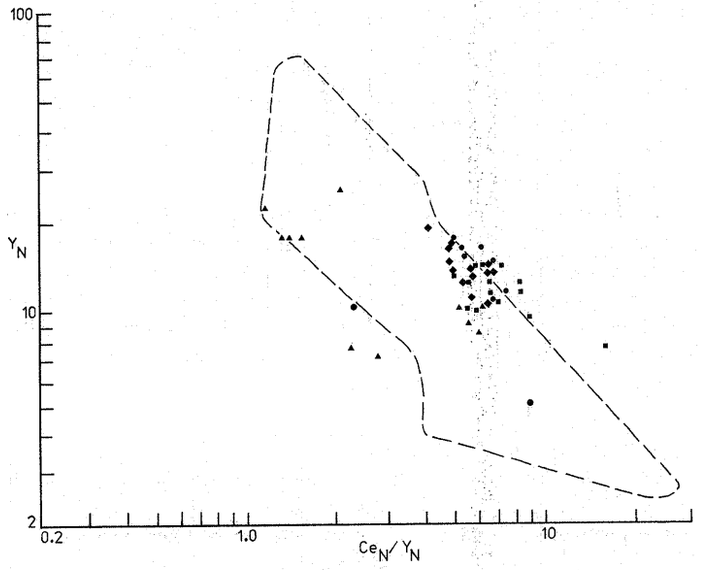

FIGURE 81
Chondrite-normalized Y versus Ce_N/Y_N diagram for the sediments, metasediments and migmatites of the Drygalski Fjord Complex. The dashed line indicates the boundary of granitoid rocks of the Drygalski Fjord Complex.

metamorphic segregation. There is, however, a significant difference in the concentration of K_2O; it is more enriched in the banded gneisses than in the migmatitic granites. This is due to potassium being held within the biotite-rich schlieren and enclaves of paleosome within the granitic neosome.

The analysed neosome and paleosome of a layered migmatite host rock show no significant variation from the above trend. The segregated neosome, being predominantly quartz, has a high SiO_2 content and is depleted in most major and trace elements. An altered retrogressed layered migmatite showed no chemical variation from the trend of the unaltered metasediments and migmatites.

2. *Agmatitic granitoids and dykes*

The chemistry of the agmatitic granitoids and dykes is remarkably different from that of the metasediments and migmatites above. Although there is no overlap between the migmatites and agmatites, the latter sometimes lie along the continuation of the variation trend of the metasediments and migmatites. The agmatites and dykes, with the exception of the quartz-diorite dyke ($SiO_2 = 60\%$), are enriched in SiO_2 and for most elements form a compact group. The majority are depleted in TiO_2, MgO, MnO, Fe_2O_3, P_2O_5, CaO, La, Ce, Cr, Ni, Zr, Zn and Sr, and enriched in K_2O and Y relative to the migmatites and metasediments. The majority fall in the rhyodacite field (O'Connor, 1965) of the an–ab–or diagram (Fig. 82a) and form a tight cluster at the Na_2O+K_2O apex of the AFM diagram (Fig. 80).

Although there is no overlap between the chemistry of the agmatites and metasediments, it does not necessarily follow, as suggested previously, that the agmatites have not arisen by partial melting of the metasediments at depth, segregation of the anatectic fluids and intrusion of the melt into the overlying metasediments. As the agmatites are depleted in most elements and lie close to minimum melt-eutectic composition determined by experimental work (Von Platen, 1965; James and Hamilton, 1969), an origin by partial melting at depth is quite possible. However, in contrast to the migmatitic granites, an *in-situ* partial-melt origin is ruled out by the sharp contacts of the agmatitic veins with the country rock, and in every case where

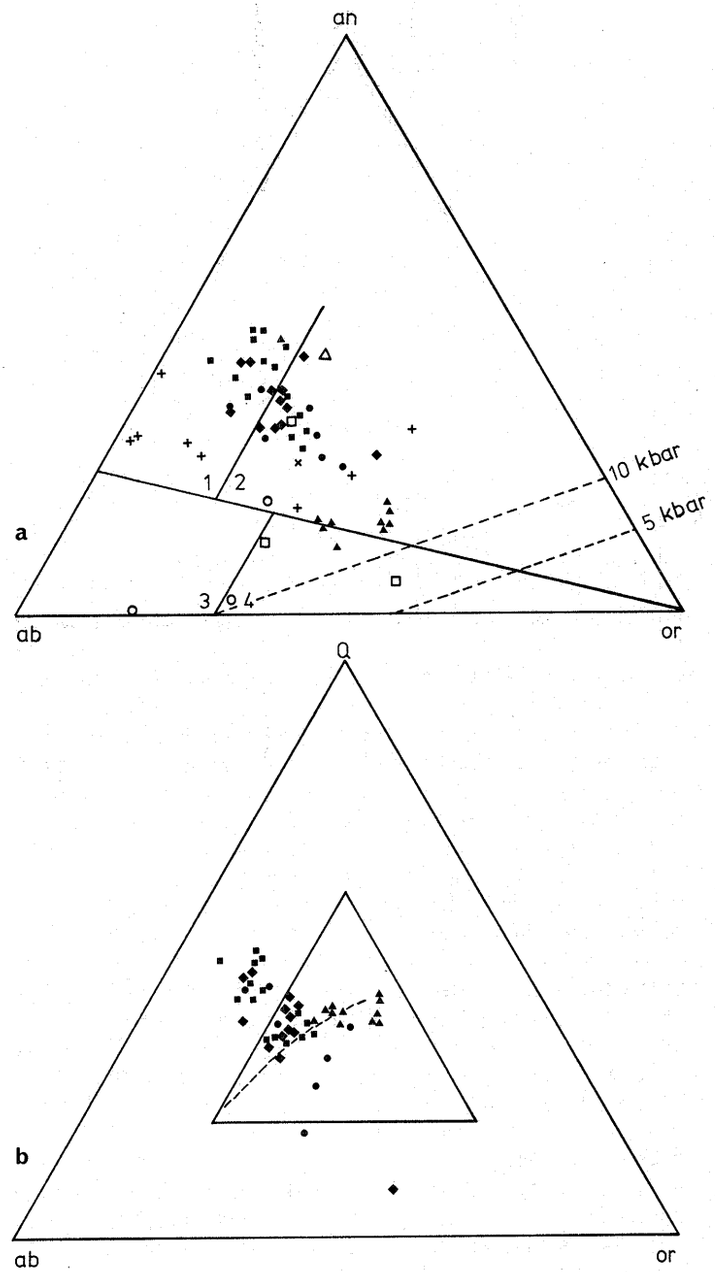

FIGURE 82
a. Normative an–ab–or diagram for the sediments, metasediments and migmatites of the Drygalski Fjord Complex and sediments of the Ducloz Head Formation. 1, dacites; 2, rhyodacites; 3, quartz-keratophyres; 4, rhyolites (O'Connor, 1965). The dashed line indicates the position of the thermal trough at 10 and 15 kbar (Kleeman, 1965).
b. Normative Q–ab–or diagram for the sediments, metasediments and migmatites of the Drygalski Fjord Complex. The inner triangle indicates the field of granitic composition (Tuttle and Bowen, 1958). The dashed line indicates the locus of the ternary eutectic as a function of increasing P_{H_2O} (Luth and others, 1964).

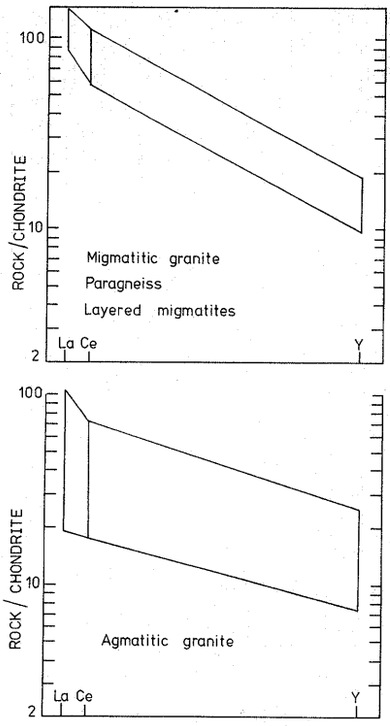

FIGURE 83
Simulated rare-earth element patterns for the sediments, metasediments and migmatites of the Drygalski Fjord Complex using XRF values for La, Ce and Y.

metasediments and agmatitic veins were analysed from the same sample there was no relationship between the agmatitic veins and the metasediment. The petrographic evidence supports an origin by partial melting of the metasediments. The Y and Zr values of the agmatites may have been produced by contamination by extreme differentiates of the nearby basic magma.

Although it was assumed that the acid rocks depleted in Y were derived by partial melting of the metasediments, they may have been derived by fractional crystallization of a calc-alkaline magma (also impoverished in Y). The latter are characterized by a low Sr/Ba ratio due to plagioclase fractionation (Sr preferentially enters intermediate plagioclase (Drake and Weill, 1975) and is depleted after this stage); a low K/Rb ratio due to the concentration of Rb in felsic portions relative to K_2Q (most of the K is partitioned at an early stage into hornblende (Gast, 1968)); and a low Ba/Rb ratio as Ba is concentrated earlier than Rb and becomes depleted in a magma late in the differentiation sequence (Taylor, 1965). As these ratios are high in the agmatitic granites, it precludes an origin by extreme differentiation of a calc-alkaline magma and supports an origin by partial melting of the metasediments and re-intrusion of the partial melt into the overlying sediments.

3. *Cooper Island and Novosilski Glacier Formations*

Within the Cooper Island Formation there is considerable variation in SiO_2 content; it varies from the SiO_2-rich coarse sandstone bands to the SiO_2-depleted black shale bands. When the major and trace elements are plotted against SiO_2 (Fig. 79), the variation trend is remarkably similar to the variation trend of the metasediments and migmatites. For a given SiO_2 value, they have similar concentrations of SiO_2, Al_2O_3, P_2O_5, MgO, MnO, Fe_2O_3, La, Ce, Cr, Ni, Ga, Y and Nb. Although there is considerable variation, some of the sediments of the Cooper Island Formation are depleted in the mobile elements K_2O, CaO, Ba and Rb, and enriched in Na_2O and Sr relative to the metasediments. There is some variation in the Zn and Zr values of the Cooper Island Formation.

The Novosilski Glacier Formation sandstone, although enriched in SiO_2, has concentrations of most major and trace elements similar to the Cooper Island Formation (Fig. 79).

The geochemistry thus supports the petrographic evidence, which indicates that the metasediments of the Salomon Glacier Formation are the metamorphosed equivalent of the Cooper Island and Novosilski Glacier Formations.

4. *Ducloz Head Formation*

a. *Coastal member.* There is considerable variation and spread of the limited number of samples (six) analysed (Table XIII) from the coastal member of the Ducloz Head Formation (Fig. 79). The volcaniclastic sediments are similar to the agmatites discussed above. As these rocks have low Zr and Y contents, they are, as suggested previously (Storey, in press), similar to the Tobifera Formation and were probably derived by partial melting of metasediments or by fractionation of a calc-alkaline magma. These values preclude an origin by tholeiitic differentiation from a basic magma. The epiclastic sediments are similar to the sediments of the Cooper Island and Novosilski Glacier Formations, thus supporting the hypothesis that they may have been derived from a similar source.

b. *Inland member.* Of the two analysed specimens (Table XIII), one (M.4087.5) is enriched in CaO (35.9%); the other sample is different from the variation trend of the coastal member and metasediments (Fig. 79). It is enriched in TiO_2, MgO, Fe_2O_3, Ni and Zn, and depleted in Al_2O_3, P_2O_5, Na_2O, Ca, Ce, Rb, Sr, Nb and Zr, relative to the coastal member. The inland member is equivalent to the lower tuff member of the Annenkov Island Formation.

Clayton (1982) has suggested that there are few significant chemical differences between the Cumberland Bay and Cooper Bay Formations, and that the Sandebugten Formation sediments were derived from a different source to the Cooper Bay Formation. This is in strong contrast to the petrographic evidence and the conclusions of Stone (1980) and of the author, who suggested that the Cooper Bay Formation is most similar to the Sandebugten Formation. The conclusions of Clayton are based on averages compared using the *t*-test. However, the samples analysed from the Cooper Bay Formation were predominantly the pelitic members (low SiO_2 values) of the formation and these (using the *t*-test) are closer to the more basic Cumberland Bay Formation than to the acidic members of the Sandebugten Formation. The individual acid members of the Cooper Bay Formation compare favourably with the Sandebugten Formation and confirm the petrographic evidence that the Cooper Bay and Sandebugten Formations were derived from similar sources.

5. *Discussion*

For most major and trace elements, the sediments and metasediments of the Drygalski Fjord Complex have similar varia-

tion trends to those of the Cumberland Bay, Sandebugten and Cooper Bay Formations. It has previously been established (Stone, 1980; Clayton, 1982) that the Cumberland Bay Formation sediments were derived from a calc-alkaline volcanic source and show typical calc-alkaline differentiation trends (Nockolds and Allen, 1953; Gill, 1970). Thus, it is not unreasonable to suggest, as mentioned previously, that the sediments and metasediments of the Drygalski Fjord Complex were derived from a calc-alkaline source. It is also quite possible, however, that the similar trends could be derived by erosion of former continental crust (i.e. older calc-alkaline material) but not necessarily a neighbouring arc sequence.

XII. COOPER BAY DISLOCATION ZONE

WEST of Cooper Bay, a zone of mylonitized rocks previously referred to as the Cooper Bay mylonite zone (Bell and others, 1977) (Fig. 2) separates the complex from tightly folded sediments of the Cooper Bay Formation. It consists of a narrow belt, trending north-west and less than 1 km wide, of mylonitized sedimentary, igneous and metamorphic rocks (Fig. 3) and was originally located by Douglas (1930), who described it as the contact zone of the igneous complex. Trendall (1959) described well-foliated acid gneisses, quartz-diorites and migmatites from the zone and Stone (1980) has described the Cooper Bay sediments and mylonites in some detail. The zone of mylonitized rocks forms part of a larger tectonic break now defined as the Cooper Bay dislocation zone (Tanner, 1982*b*) which stretches from Hauge Reef to Cooper Island (Fig. 2).

A marked topographic depression, occupied by Spenceley, Twitcher and Quensel Glaciers, separates the zone of mylonitized rocks from the Cooper Bay Formation. Mylonites occur on both sides of this line but the predominance of igneous rocks, and in particular the occurrence of feldspar porphyroblasts in the metasediments of the dislocation zone, has been used to separate the zone from the volcaniclastic sediments and metabasites of the Cooper Bay Formation. Also, the metasediments (Novosilski Glacier Formation) of the dislocation zone have had a different structural history and are different petrographically from the volcaniclastic sediments of the Cooper Bay Formation. To the south-west a similar marked depression separates the dislocation zone from the non-mylonitized metasediments and igneous rocks of the complex.

Within the dislocation zone, narrow bands of laminated green and white mylonite and ultramylonite (Zeck, 1974) separate areas of weakly mylonitized and undeformed gabbro, metagabbro, basic dykes, quartz-diorite, granodiorite, porphyritic felsite and folded metasedimentary rocks. The early history of these rocks is similar to that of the remainder of the complex. In the southern part, large gabbro bodies cut by basic dykes intrude folded metasedimentary rocks of the Salomon Glacier and Novosilski Glacier Formations. Quartz-diorite, granodiorite and porphyroblastic gneiss intrude, net vein and form migmatitic relationships with the basic rocks, many of which have recrystallized to actinolite–chlorite–epidote assemblages (metabasites). Potash feldspar metasomatism is an important process within this zone; plagioclase phenocrysts and porphyroblasts are completely or partially replaced by perthite. Occasional late basic dykes cut the granitic rocks. Porphyritic textured rhyolites and volcaniclastic rhyolites of the Novosilski Glacier Formation crop out in the northern part of the zone.

The zone has had a complex structural history: a mylonite fabric is superimposed on pre-magmatic tectonic structures, resulting in a sequence of metabasites, mylonite granitoid gneisses, quartz-feldspar-mylonites and ultramylonites; where deformation is intense, the original sedimentary or igneous nature of these rocks is destroyed. The mylonite fabric, which is mainly developed in quartz-bearing rocks, is due to the ductile behaviour of quartz and the brittle behaviour of feldspar during deformation. Retrogression from biotite grade of greenschist facies to chlorite–epidote assemblages accompanied mylonitization. As well as the mylonite fabric, minor conjugate shear zones, conjugate faults and post-mylonitization folding and planar fabrics are common within the zone. The folding, which is mainly concentrated along the margins of the zone and within narrow schistose shear zones, varies from tight and open folds devoid of a fabric to intense crenulation folds with conjugate planar fabrics.

The dislocation zone has some of the characteristics of a ductile shear zone (Wakefield, 1977) with a period of migmatization, growth of feldspar prophyroblasts, potash feldspar metasomatism and a superimposed ductile mylonite fabric which formed by pure and simple shear during an intense compressional event. The mylonite fabric lacks an overall sigmoidal form similar to that described by Ramsay and Graham (1970) for schistosity in ductile shear zones. This relationship is present on a small scale within the zone which has led the author to suggest the term *composite* ductile shear zone to describe this zone. The lack of an overall sigmoidal trend may be due to later faulting or due to the post-mylonitization folding of the mylonite fabric. The amount and sense of movement within this zone is not certain but there is undoubted vertical movement on a north-easterly directed reverse fault, which has resulted in the complex being at the same level as the Cooper Bay Formation; large transcurrent movements are not ruled out. The present sharp topographic boundaries of the zone may be the late fault zones which were responsible for the vertical movement.

A. NON-MYLONITIZED ROCKS

1. *Basite and metabasite*

The gabbro and basic dykes, which crop out in the southern part of the mylonitized zone, are similar to, and form part of, the same intrusive phase as those described previously. They are pale to dark green medium-grained rocks, which have suffered extensive recrystallization, intrusion and brecciation by

medium- to coarse-grained quartz-diorite, tonalite and granodiorite. All gradations exist from cumulate-layered gabbro, with pyroxene partially and completely replaced by actinolite, to recrystallized actinolite–chlorite–epidote–muscovite assemblages (metagabbros). Medium-grained hornblende-gabbro, with a cumulate texture, also crops out within this zone. The green-brown pleochroic hornblende forms triple junctions with stumpy cumulus plagioclase crystals (M.678).

2. *Diorite and quartz-diorite*

Medium- and coarse-grained diorite and quartz-diorite, which are often porphyritic, form small intrusive bodies within the metasediments of the southern part of the dislocation zone and form irregular veins and patches within the basite and metabasite described above (Fig. 84). In the latter case, angular

FIGURE 84
Quartz-diorite net-veining a metabasite in the dislocation zone. The scale on the hammer shaft is 20 cm long.

and partially assimilated enclaves of gabbro, basic dyke and metabasite are suspended in a mainly coarse-grained quartz-diorite matrix.

The intermediate rocks contain up to 60% plagioclase with hornblende and biotite, and interstitial quartz and accessory opaque minerals, sphene and apatite. The feldspars, which often form phenocrysts up to 5 mm long, are mainly andesine (biaxial positive and negative) crystals. Zoning, patchy birefringence and optically continuous intergrowths of quartz and potash feldspar are common in some andesine crystals. Sericitization and saussuritization of the feldspar are mainly restricted to high-anorthite cores of some of the zoned crystals. Partial replacement by albite is present in some of the altered rocks. Pleochroic hornblende (α = light-brown; β = brown-green; γ = dark brown) is the main ferromagnesian mineral. It forms ragged prisms and large (up to 5 mm) poikilitic crystals enclosing apatite, opaque minerals and plagioclase. Similar poikilitic biotite crystals and aggregates of fine-grained biotite are present in some quartz-diorites. The irregular outline of biotite and hornblende prisms is a characteristic of these intermediate rocks. Quartz, which may form up to 15% of the rocks, occurs interstitially and as poikilitic prisms enclosing plagioclase and hornblende. Anhedral opaque minerals, including some haematite, are enclosed within hornblende and biotite with sphene closely associated with, and rimming, skeletal ilmenite. Acicular apatite, which forms slender prisms up to 2 mm long, is a common accessory enclosed within plagioclase, quartz and hornblende. The long needles are often fragmented along their length.

Similar to the basic rocks, the diorite and quartz-diorite are partially replaced by an actinolite–epidote–chlorite–muscovite–albite assemblage. Disorientated aggregates of pale green actinolite laths replace hornblende. Chlorite, often interlaminated with biotite, may contain epidote inclusions. Zoisite, clinozoisite, epidote and sericite replace plagioclase, whilst some feldspars are partially recrystallized to secondary albite.

Enclaves of basic rock, which occur within the diorite and quartz-diorite, are generally partially replaced by an actinolite–epidote–chlorite assemblage.

3. *Granodiorite, tonalite and granite*

These rocks, similar to the intermediate rocks, are emplaced as small (up to 10 m wide) bodies and intrude, brecciate and form migmatitic structures within the metasediment and metabasic rocks, within the southern part of the dislocation zone. They are often porphyritic and generally display a gneissic fabric. Folded metasedimentary enclaves are common within the small intrusive bodies. Euhedral to subhedral porphyritic plagioclase crystals up to 1 cm long, quartz, potash feldspar, perthite and biotite plates with subsidiary amphibole are present in a groundmass of fine- to medium-grained quartz, biotite and plagioclase with accessory euhedral allanite, opaque minerals altered to sphene, apatite and zircon. These rocks are similar in composition to the Trendall Crag granodiorite. The feldspar phenocrysts are mainly low-relief (less than quartz), twinned, biaxial negative oligoclase with occasional andesine crystals. Zoning, patchy birefringence, patchy sericitization and saussuritization, which are mainly concentrated within the high-relief areas, are common. Inclusions of biotite and chlorite are found within the margins of some crystals. Potash feldspar (biaxial negative microcline) and perthite (low relief, biaxial positive) with flame intergrowths replace plagioclase in some thin sections; poikilitic potash feldspar crystals enclose plagioclase (Fig. 85) with biotite; myrmekitic intergrowths are present in thin section M.1332. Fine- to medium-grained biotite, with alteration chlorite lamellae, is the main ferromagnesian mineral. Some large pleochroic plates of biotite and green pleochroic hornblende are also present. Euhedral zircon with pleochoric haloes and numerous apatite crystals, often concentrated in lenses, are enclosed in biotite. Fine granules of sphene often occur at the margins of biotite and as alteration rims around enclosed opaque minerals (ilmenite). Zoisite, clinozoisite, chlorite, tremolite and calcite are found in the groundmass.

4. *Porphyritic felsites*

Porphyritic acid volcanic rocks intruded by isolated basic dykes form the bulk of the nunatak at station M.3783 in the northern part of the dislocation zone (Fig. 3). They are uniform pale grey and white massive, slightly porphyritic rocks with, in some cases, a well-developed schistose fabric which is believed to be related to mylonitization. They are closely related to volcaniclastic textural rhyolites which crop out within the same

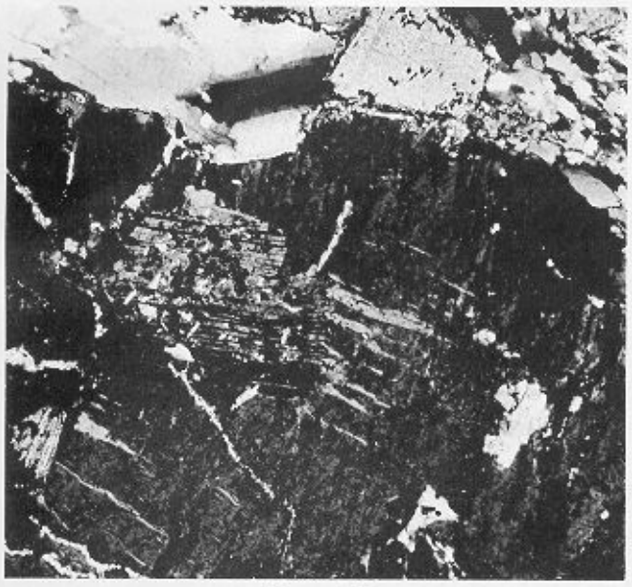

FIGURE 85
Potash feldspar enclosing plagioclase within a porphyritic granodiorite in the dislocation zone. (M.2172.5A; X-nicols; ×40)

nunatak and also more extensively within the northern part of the dislocation zone.

5. *Sediment, metasediment and migmatite*

A complex range of sediments and metasediments of various degrees of metamorphism, migmatization, deformation and mylonitization are found within the dislocation zone. Non-mylonitized lenses of folded gneiss and layered migmatite of the Salomon Glacier Formation and sediments and volcaniclastic rhyolites of the Novosilski Glacier Formation occur together with laminated green and black retrogressed clastic sediments, mylonites and ultramylonites.

a. *Salomon Glacier Formation.* On the east side of Salomon Glacier, a lens of partially mylonitized folded gneisses of the Salomon Glacier Formation crops out within the dislocation zone.

b. *Novosilski Glacier Formation.* In the southern part of the dislocation zone, lenses and enclaves of folded and deformed pale brown laminated metasediment are found within the intermediate and acid rocks. They contain detritial quartz and feldspar crystal fragments and quartz–feldspar lithic clasts, which are surrounded by orientated and disorientated biotite, muscovite and chlorite in a recrystallized matrix of mosaic quartz. The biotite, partially altered to chlorite, is commonly associated with ragged epidote; opaque minerals, which tend to be drawn out along a biotite fabric, are partially altered to sphene and leucoxene. Haematite is present in some thin sections.

As these sediments were deformed and metamorphosed up to the biotite grade of the greenschist facies prior to the emplacement of the igneous rocks and contain detrital quartz and feldspar crystal and lithic fragments, they are included within the Novosilski Glacier Formation. They have not been recrystallized to the same extent as the gneiss of the Salomon Glacier Formation, within which all the detrital clasts have been destroyed.

As well as the above metasediments, pale green fine-grained sandstone and black shales of the Novosilski Glacier Formation (Fig. 86) crop out along the eastern margin of Salomon Glacier.

Fine- to medium-grained quartz and feldspar crystals and quartz–feldspar lithic fragments are set in a fine-grained recrystallized quartz-rich matrix with interstitial biotite, chlorite, epidote and disseminated opaque minerals, apatite and zircon. Biotite, which is pale-coloured and partially altered to chlorite, often defines a lamination together with the disseminated opaque minerals. The lamination is folded about tight crenulations; biotite and chlorite is, in some cases, aligned along the crenulation cleavage planes.

Although these sediments have been metamorphosed up to the biotite grade of the greenschist facies, the subsequent partial retrogression to a chlorite–epidote assemblage has resulted in the pale green and black colour.

c. *Porphyroblastic feldspar rock.* Within the pale brown metasediments of the Novosilski Glacier Formation of the southern part of the dislocation zone there is widespread development of white feldspar porphyroblasts and poikiloblasts up to 1 cm long. They overgrow and replace the crystal and lithic clasts of the metasediments and produce a characteristic porphyroblastic rock. The feldspars are mainly oligoclase but some are partially replaced by potash feldspar. Some flame perthites may be primary porphyroblasts.

B. Mylonitized Rocks

The term mylonite was introduced by Lapworth (1885) to describe cataclastic rocks from the Moine thrust in Scotland which he believed were formed solely by crushing and brittle deformation. Christie (1960), who subsequently studied these rocks, pointed out that recrystallization is common within those mylonites and used the term blastomylonite, which was intro-

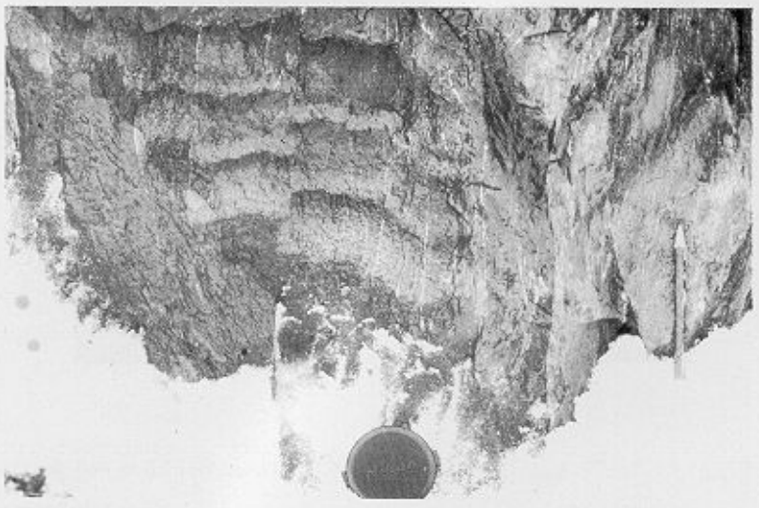

FIGURE 86
Graded sedimentary units of the Novosilski Glacier Formation and a mylonite fabric (right-hand side of the photograph).

duced by Sander (Hobbs and others, 1976) to describe mylonites formed by cataclasis and subsequently recrystallized. As it is now generally accepted that many of the features of mylonites result from ductile deformation accompanied by recrystallization, much of the cataclastic terminology is not strictly applicable. However, as recommended by Bell and Etheridge (1973) and Hobbs and others (1976), the term *mylonite* is used here in a general sense to describe rocks in zones of intense deformation no matter whether the deformation is cataclastic or ductile, and the term *blastomylonite* is used to refer to rocks that have been completely recrystallized during or after the deformation. Using the nomenclature of Zeck (1974), many of the rocks in the dislocation zone are hemimyloblastites where incomplete cataclasis is accompanied by recrystallization.

1. *Mylonitic granitoid gneisses*

The porphyritic, quartz-diorite, granodiorite, tonalite and porphyroblastic feldspar rock show extensive shearing which has resulted in characteristic lenses of mylonitic granitoid gneiss within the metabasic rocks. The fabric is defined by an alignment of biotite, chlorite, muscovite, epidote and opaque granules; streaks of ribbon quartz surround relict feldspar augens (Fig. 87a) and lenses of apatite. The amount of deformation of the quartz varies from an initial flattening and elongation of the quartz phenocrysts to recrystallized mosaics of elongated quartz aggregates. All gradations exist from an initial recrystallization of the margins of elongated quartz grains (mortar structure) and the division of flattened quartz into a number of ribbon-shaped deformation bands (Fig. 87b) to polygonal mosaic quartz. The flattened quartz grains show an

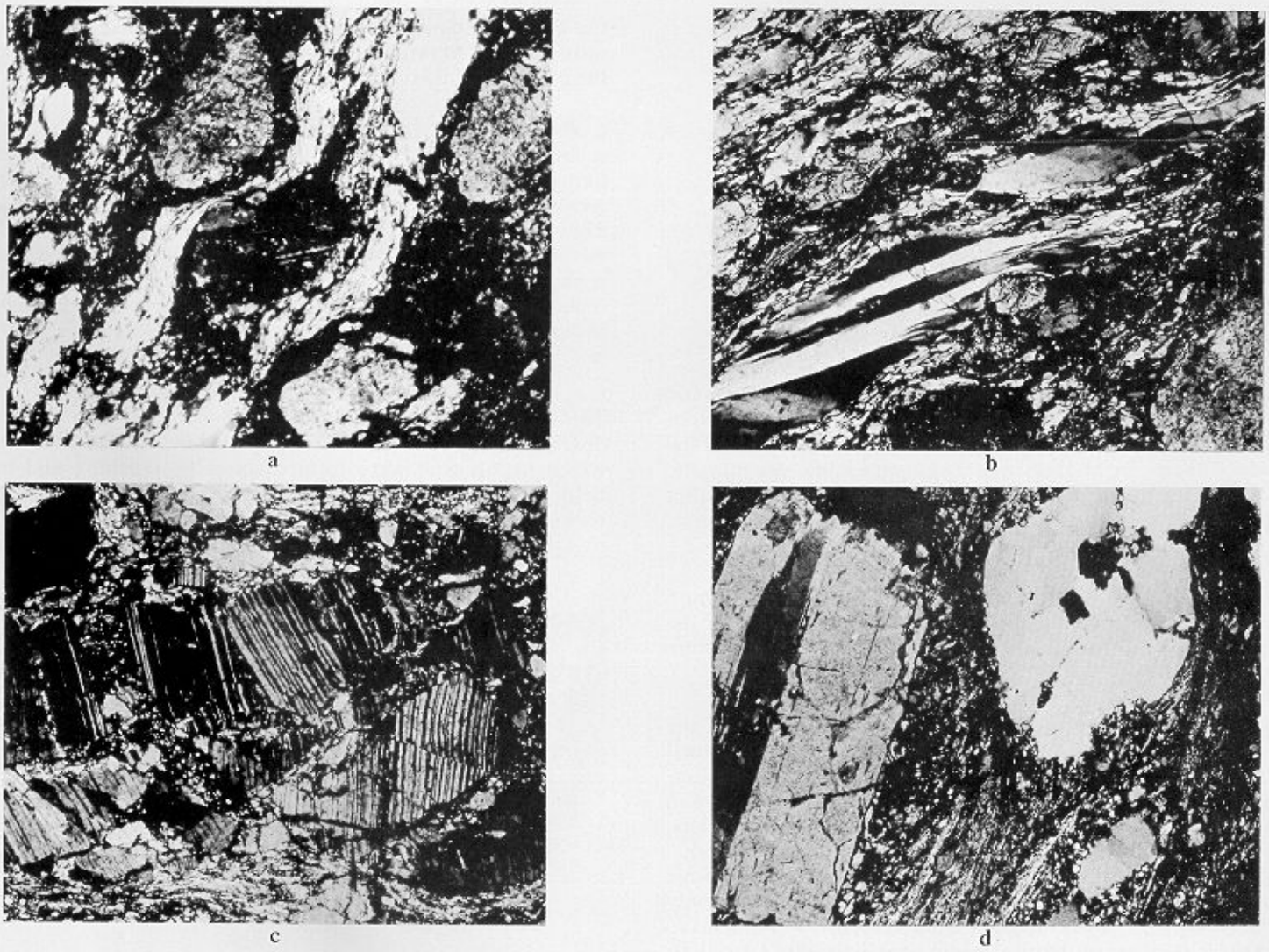

FIGURE 87
a. Feldspar augen and ribbon quartz. (M.2143.1A; X-nicols; ×20)
b. Undulose extinction and deformation bands in ribbon quartz. (M.2185.B; X-nicols; ×40)
c. Strained and fractured feldspar in a mylonite. (M.1932.1; X-nicols; ×40)
d. Quartz and feldspar phenocrysts surrounded by a mylonite fabric in a volcaniclastic sediment of the Novosilski Glacier Formation. (M.3784.5; X-nicols; ×40)

undulose extinction and deformational lamellae generally inclined at an angle to the elongated quartz ribbons (Fig. 87b). Where deformation is intense, ribbons of inequant and polygonal strain-free quartz define the fabric. Recrystallization of the bent and sheared ribbon quartz has taken place with formation of strain-free polygonal quartz grains. Serrated grain boundaries are characteristic of initial marginal recrystallization of the elongated grains. In some cases, the alignment of the ferromagnesian minerals is not complete and patches of fine-grained disorientated biotite, muscovite, epidote and amphibole still exist.

In most cases, the feldspar is unaligned and unaffected by the deformation, most of which has been absorbed by the more ductile quartz crystals. In zones of more intense deformation, some flattening and re-orientation of the feldspar augen occurred, and kink bands and deformation twin lamellae traverse the feldspar (Fig. 87c). In some cases, the margins of the feldspar porphyroblasts appear to overgrow and cut across the mylonitic fabric. For example, in thin section M.2138.2, former aligned chlorite laths which formerly surrounded a feldspar porphyroblast are partially enclosed within it. The feldspars characteristically have irregular margins with partial inclusion of the groundmass; this indicates some syn-tectonic growth of the feldspars.

Biotite, which shows deformation and strain lamellae, is often aligned parallel to the mylonite banding. Marginal alteration of the larger plates to muscovite and chlorite is a common feature.

2. *Mylonitic basites*

A mylonite fabric is not well developed in the basic rocks. However, some basic dykes show intense deformation with an alignment of the ferromagnesian minerals and trains of epidote and opaque granules. Some hornblende prisms are partially recrystallized to elongated ribbons of colourless and pale green tremolite-actinolite laths. The feldspars, like those in the acid rocks, are virtually unaffected by the mylonitization.

3. *Mylonitic sediments and metasediments*

A fabric similar to that of the granitoid gneisses is imprinted on the folded gneisses and sediments of the Salomon Glacier and Novosilski Glacier Formations which crop out in the southern part of the dislocation zone. Elongated quartz ribbons and aggregates of mosaic quartz are present, mainly in the quartzo-feldspathic horizons of the laminated sediments. Where mylonitization is intense, the pre-existing folds are obliterated and a new mylonite foliation is present. Intrafolial folds within the mylonite foliation may represent remnants of the pre-existing folds.

Within the northern part of the zone, the rocks have not been intensely mylonitized. However, the volcaniclastic sediments and felsites of the Novosilski Glacier Formation have a strong sub-vertical schistosity which is parallel to the margins of the zone. The fabric is defined by an alignment of sericite, muscovite, biotite and chlorite around the quartz and feldspar phenocrysts (Fig. 87d). The quartz phenocrysts, unlike the quartz grains in the southern part of the zone, have not been intensely flattened; most of them have retained their original shape and show an undulose extinction and deformation strain lamellae. Both the quartz and plagioclase phenocrysts are fractured due to brittle deformation during mylonitization. There is some flattening and development of ribbon quartz within the matrix of these rocks.

4. *Mylonites and ultramylonites*

Along the margins of the dislocation zone and within zones of intense deformation, discontinuous bands of pale green, white and black laminated hemimylonites, mylonites and ultramylonites of uncertain origin are exposed. These rocks display many of the mesoscopic features of classical mylonites: discontinuous colour banding, lineations, intrafolial folds and a finer grain-size than the surrounding rocks into which they grade.

The mylonite foliation is defined by alternating quartz- and epidote-rich bands. The quartz-rich bands are composed of elongated quartz ribbons and granular aggregates of recrystallized mosaic quartz. Disseminated sphene, opaque granules and aligned chlorite, sericite, biotite and actinolite laths are present within some of the epidote-rich bands. Remnant clasts are mainly plagioclase crystal fragments but colourless to light green tremolite-actinolite laths (former basic rocks) and accessory zircon, allanite and apatite are found in some bands. Within some thin sections there is a great variation in the grain-size of feldspars. This is due to the presence of large feldspar porphyroblasts and detrital crystal fragments of former metasedimentary rocks. The feldspars are often partially replaced by perthite or microcline, partially flattened, strained, fractured and re-orientated within the mylonitic groundmass. Some are cut by deformation strain and twin lamellae, which are often defined by fine granules of recrystallized feldspar. Recrystallization of the margins of some of the feldspar has also taken place; remnant augen are surrounded by polygonal feldspar grains. There is a marked absence of a stretching lineation within the mylonitic foliation plane.

C. Structural History

The dislocation zone (Fig. 88) has a complex structural history with a complex array of minor structures that can be subdivided as follows:

i. Pre-mylonite folds of the gneisses and sediments of the Salomon Glacier and Novosilski Glacier Formations.
ii. Penetrative mylonite foliation and schistosity.
iii. Conjugate minor shear zones and associated mylonite fabric.
iv. Post-mylonite folds and associated planar fabrics.
v. Late-stage faults.

1. *Pre-mylonite folds*

The gneisses and sediments of the Salomon Glacier and Novosilski Glacier Formations were folded, deformed and intruded by basic, acidic and migmatitic rocks prior to the mylonitization event. The early folds, which are partially granitized and overgrown by feldspar porphyroblasts, are affected by the mylonitization, re-aligned parallel to the fabric and drawn out along the fabric (isoclinal folds). The interfolial isoclinal folds within some retrogressed pale green, black and white laminated mylonites may represent pre-mylonite fold hinge zones.

2. *Mylonite foliation*

The main penetrative fabric in the southern part of the zone is the mylonite foliation; in the northern part it is represented by a

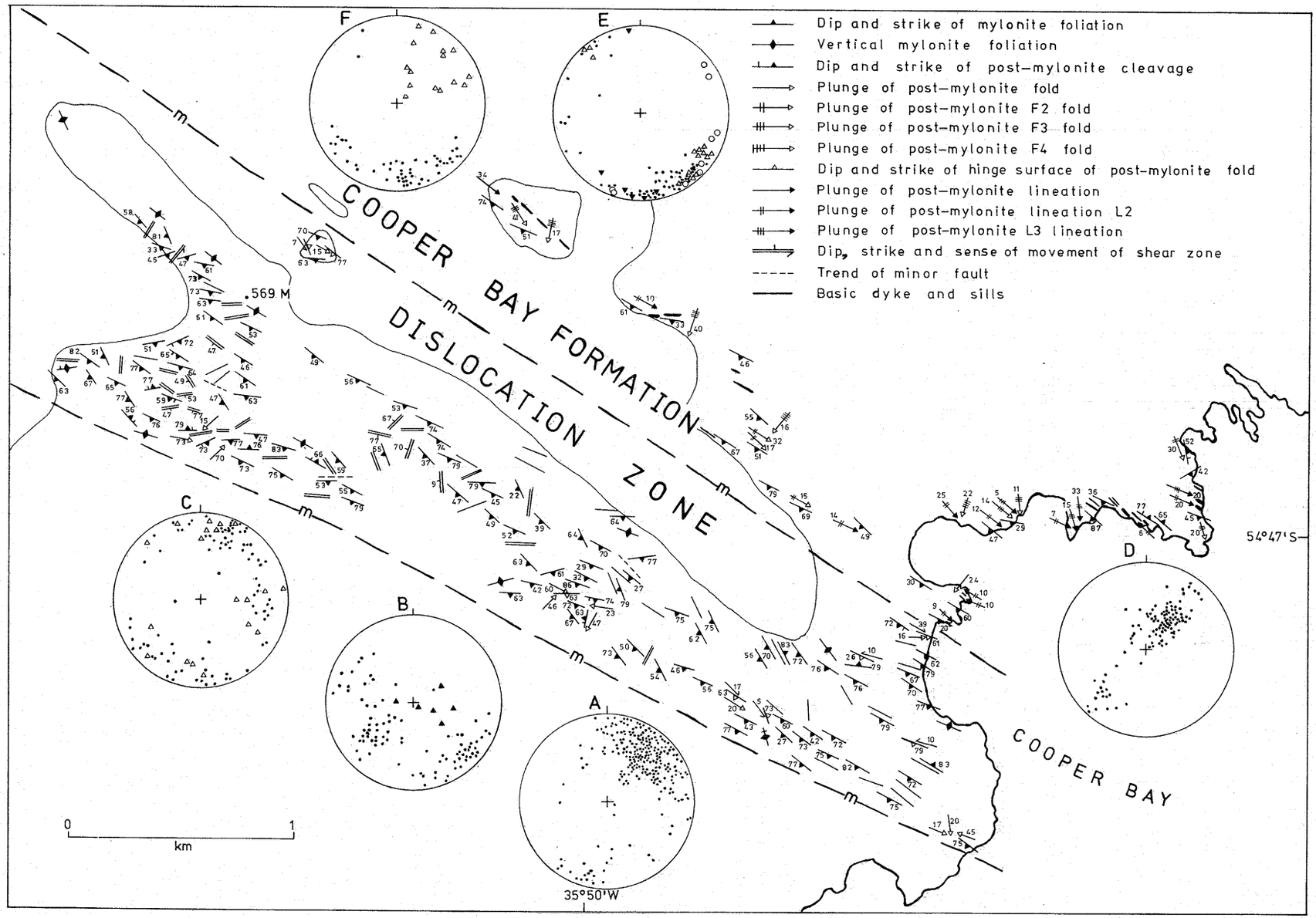

FIGURE 88
Structural map of the southern part of the Cooper Bay dislocation zone and part of the Cooper Bay Formation. Insets are equal-area projections of the structural data.
A. Poles to mylonite fabric (·).
B. Undifferentiated (·) and second (▲) post-mylonite fold hinges.
C. Poles to post-mylonite cleavage (·) and fold hinge surface (△).
D. Poles to mylonite fabric.
E. Undifferentiated (·), L3 (○), L4 (▼) and quartz-rodding lineation (△).
F. Post-mylonite fold hinges (·) and poles to F2 planar surfaces (△).
A–C refer to the Cooper Bay dislocation zone.
D–F refer to the Cooper Bay Formation.

schistosity devoid of ribbon quartz, in the volcaniclastic sediments. The fabric is a strong planar fabric trending north-west and, although it is mainly sub-parallel to the margins of the dislocation zone, there is considerable variation in the dip and strike of the fabric (Fig. 88). This is in part due to a combination of an initial variation in the orientation of the fabric, which was deflected around the more resistant gabbro and basic dykes, and in part due to the later folding. Due to the difference in response between the acid and basic rocks during mylonitization, the mylonite foliation is mainly present within the acidic rocks. The basic rocks are present as undeformed lenses within the granitoid gneisses and mylonites. The difference in the fabric from the northern to the southern part of the dislocation zone is due to the difference in intensity of deformation, temperature and pressure during mylonitization. The northern part of the dislocation zone represents a higher structural level, where the fabric is represented by an alignment of the flaky minerals, chlorite, sericite and biotite with only slight cataclasis within the matrix. There is no significant flattening of the quartz phenocrysts.

3. *Minor shear zones*

Minor shear zones are restricted in occurrence and generally crop out south of peak 569 m (Fig. 88). They are zones of intense deformation aligned both normal and parallel to the margins of the dislocation zone which shows both sinistral and dextral displacement. The mylonitic foliation, which is developed within these shear zones, has a characteristic sigmoidal relationship (Fig. 89) as described by Ramsay and Graham (1970) for schistosity in ductile shear zones. Although the relationship of these zones to the mylonite foliation is uncertain, similar ductile shear zones are found within the Drygalski Fjord Complex.

FIGURE 89
Sigmoidal fabric within a minor shear zone in the dislocation zone. The hammer shaft is 60 cm long.

4. *Post-mylonite folds and associated planar fabrics*

Folding of the mylonite fabric is mainly concentrated within the minor shear zones, along the margins of the dislocation zone and along the ridge west of the dislocation zone. With the exception of folded sedimentary enclaves, the earliest folds are interfolial isoclinal folds of uncertain origin within the mylonite lamination. These may be associated with the formation of the mylonite fabric or may be sheared-out remnants of the pre-mylonite folds.

a. *F1 folds*. Ductile post-mylonite folds of the mylonite lamination vary from close (Fig. 90) and tight similar folds (wavelength up to 10 cm) to small-scale crenulation folds with an

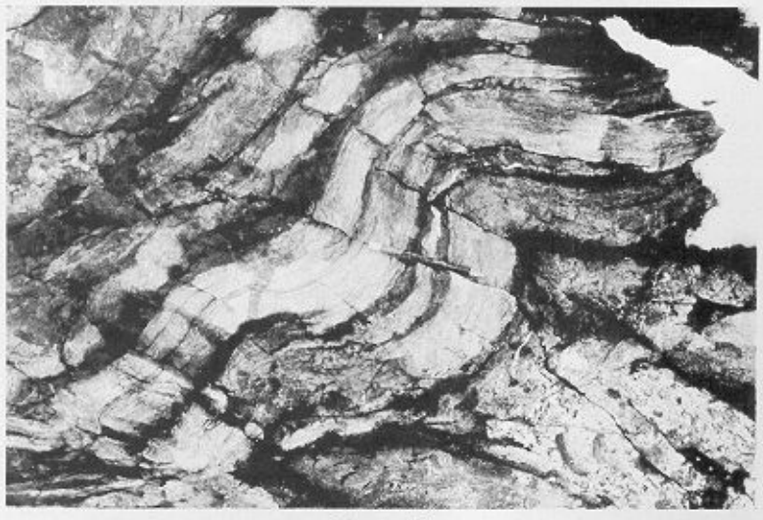

FIGURE 90
Folding of the mylonite fabric in the dislocation zone. The pencil is 16 cm long.

associated crenulation cleavage. Although there is some scatter in the orientation of the fold hinges of the post-mylonite folds (Fig. 88), they form two main groups plunging gently to the south-east and south-west. The hinge planar surfaces and cleavage planes similarly form two groups, one of which is steeply inclined westward, whilst the other is steeply inclined to the north and south. A crenulation lineation, parallel to the fold hinges, is developed on both sets of folds. In thin section, the quartz- and epidote-rich mylonite foliation is folded about the noses of the folds. There is some re-alignment of the flaky minerals, chlorite and sericite, and ribbon quartz has been aligned axial planar to these folds. This gives some indication of the intense compression during the formation of these folds. Chlorite, muscovite and biotite are also aligned parallel to crenulation cleavage surfaces within the crenulation folds. Although the relationship between the two groups of fold

orientations is uncertain, they may represent a single fold phase that has been re-folded about a later fold axis. However, as two cross-cutting crenulation cleavages, producing a diamond-shaped interference pattern, are present in some localities, the folds, which have a similar style and crenulation lineation, may be conjugate pairs formed during a single deformation event.

b. *F2 folds.* A further more brittle phase of deformation is superimposed on the F1 folds of the mylonite lamination. Within schistose zones of intense deformation the gently plunging crenulation lineation and F1 fold hinges are folded about steeply plunging hinge zones. The folds, like the F1 folds, are tight similar folds with steeply inclined axial planar surfaces. Boat-shaped folds are developed in some instances due to the interference of the F1 and F2 fold phases. The brittle nature of the deformation has resulted in disruption of quartz-rich mylonitic laminations and the development of a fracture cleavage. In thin section, the ribbon quartz of the S1 fabric has recrystallized in the noses of the F2 folds to give a granular equidimensional quartz mosaic.

A late-stage open fold about a north-east axis is also present within the dislocation zone. This may account for some of the spread of the planar and linear data from the dislocation zone (Fig. 88).

XIII. MINOR SHEAR ZONES

MINOR acid–basic shear zones (Fig. 91), up to 2 m wide, cut the Hamilton Bay and Salomon Glacier gabbros. They are defined by elongated pale white acid lenses within a fine-grained schistose basic rock. The schistosity and pale white acidic veins, which are often folded, are aligned sub-parallel to the margins of the zones and have a sigmoidal form across the shear zones. The acid lenses probably developed by segregation banding associated with the shearing. Isolated aligned pods of gabbro (Fig. 92) and granite are often caught up within the shear zone and occasional basic dykes cut the zones.

FIGURE 91
Deformed basic dykes within an acid–basic shear zone in the Hamilton Bay gabbro. The lens cap is 6 cm in diameter.

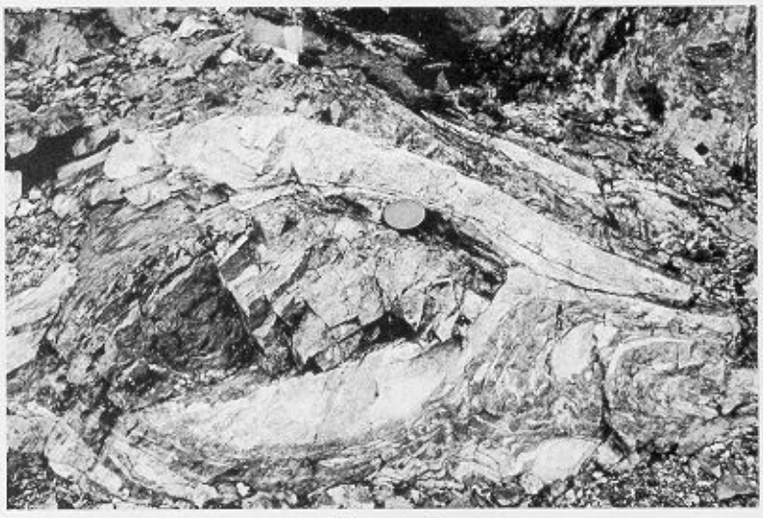

FIGURE 92
Lens of gabbro in an acid–basic shear zone. The lens cap is 6 cm in diameter.

The zones are variable in strike and dip. An analysis of the trends (Fig. 93) indicates a dominant south-westerly trend (220°), dipping shallowly to the north-west (20°) and steeply (70°) to the south-east. The direction of shearing was, in a few cases, indicated by basic dykes which are cut by the shear zone and bent in the direction of movement within the zone (Fig. 91). Both dextral and sinistral movement directions are present. It was not possible to establish the amount of movement within any of these zones.

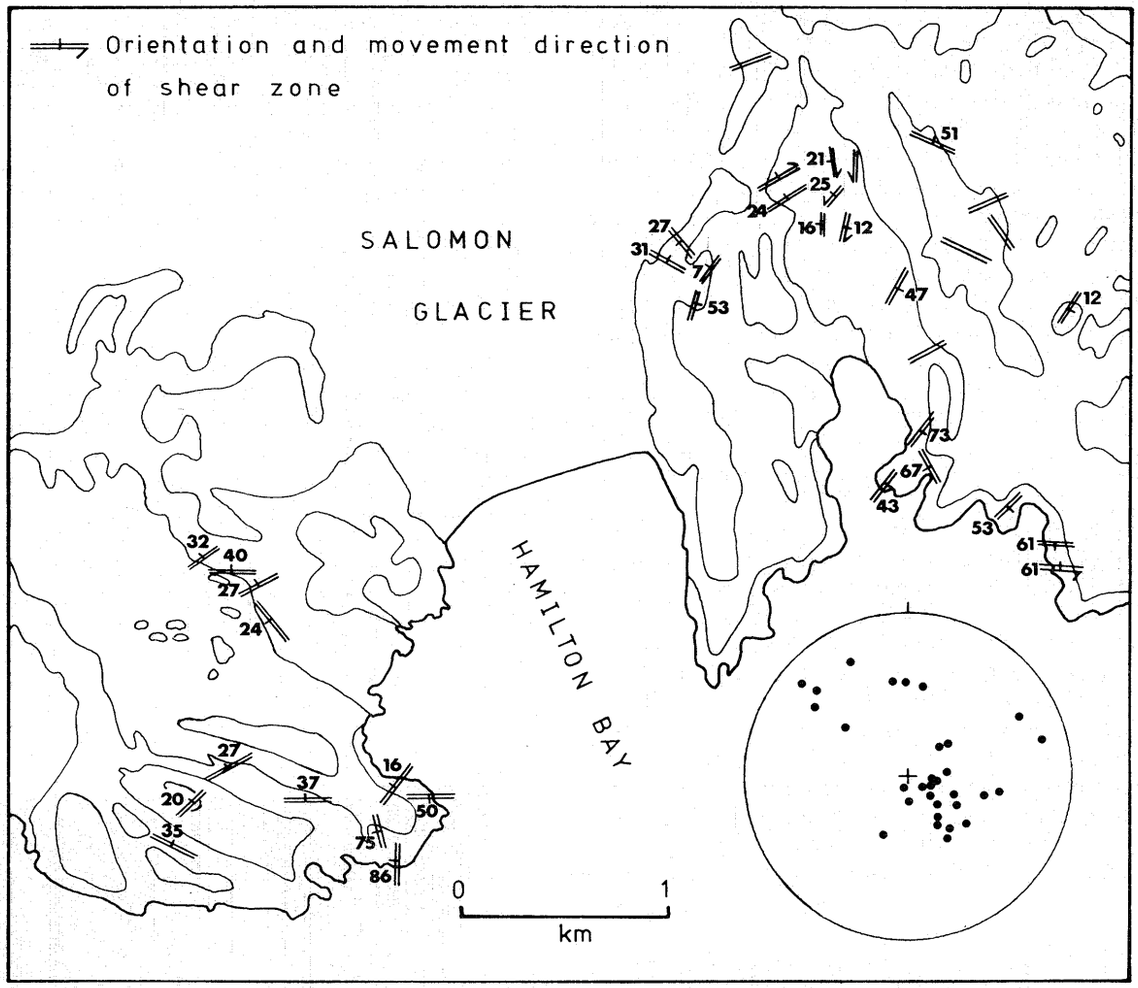

FIGURE 93
Sketch map of the minor shear zones in the Hamilton Bay area. The equal-area projection illustrates poles to shear-zone trends.

XIV. COOPER BAY FORMATION

A SEQUENCE of volcaniclastic metasediments and metabasites crops out on the eastern side of the Cooper Bay dislocation zone (Fig. 3). These rocks, originally described by Stone (1982) as the Cooper Bay metasediments, are here formally termed the Cooper Bay Formation. They form a well-defined sequence of volcaniclastic sub-quartzose sediments, derived from an acidic volcanic terrain, and interbanded dolerite sheets which have suffered intense mylonitization, polyphase deformation and regional metamorphism up to the biotite grade of the greenschist facies. Subsequent retrogression has resulted in a succession of foliated metagreywacke, phyllite, schist, slate, mylonite and metabasite.

1. *Lithology*

Although the metasediments have been intensely deformed, bedding is still preserved within some of the laminated and massive sandstone units as relict blue-grey, grey-green, brown and white colour bands. The banding is generally parallel to the local planar tectonic fabric and to thin, deformed, quartz-rich segregation lamellae or boudins. Sedimentary structures have been mostly destroyed but graded sandstone units up to 1 m thick crop out south of Twitcher Glacier (Fig. 5).

a. *Metagreywacke.* Extensive recrystallization has destroyed the original sedimentary form of many of the coarse- and medium-

grained units. Remnant quartz and plagioclase crystal fragments are surrounded by a recrystallized quartzo-feldspathic matrix with biotite, chlorite and epidote, and accessory zircon, sphene, opaque minerals and calcite. The fabric is defined by aligned aggregates of light brown to dark straw-brown biotite and retrogressed chlorite, streaks of opaque granules partially altered to sphene, epidote and zircon. Biotite also forms clusters often aligned at an angle to the fabric. The plagioclase crystal fragments are mainly of oligoclase and andesine, occasionally zoned, with some perthite and alkali-feldspar. They are variably cloudy, sericitized, saussuritized and partially replaced by albite or potash feldspar. Quartz is less abundant (rare in some thin sections) and often partially recrystallized. Epidote minerals, including zoisite and clinozoisite, are common accessories. Anhedral opaque minerals, generally altered to brown limonite are also common. A brown iron-staining is present within some thin sections, making identification of the minerals difficult.

Although the greywackes are partially recrystallized, remnant clasts are identifiable in a number of thin sections (M.630.4 and 2180). They are acidic lithic volcanic fragments (rhyolites and dacites) with quartz and feldspar crystal fragments set in a microcrystalline felsic groundmass. Partial resorption of the quartz phenocrysts supports a volcanic origin. Subsidiary intermediate volcanic clasts with aligned (pilotaxitic texture referred to as trachytic by Stone (1982)) and disorientated (felted) feldspar microlites are also present and may form up to 10% of the lithic fragments. Polycrystalline mosaic quartzose lithic clasts and epidote, sphene and zircon detrital crystal fragments are also present. The matrix of the acidic volcanic clasts is often replaced by sericite or partially recrystallized to an aggregate of mosaic quartz.

b. *Laminated siltstone, phyllite and slate.* These are similar to the above with fine- to medium-grained angular quartz and feldspar crystal fragments set in a recrystallized quartzo-feldspathic matrix. The fabric is dominated by a schistose arrangement of biotite and chlorite with thin polycrystalline quartzose segregation lamellae and epidote. Some siltstones are devoid of a penetrative foliation and have disorientated biotite, chlorite, muscovite, ragged zoisite and clinozoisite with scattered opaque minerals, zircon and sphene.

c. *Metabasites.* Metabasites, previously described by Stone (1982) as epidorites, and Trendall (1959), are found within the Cooper Bay sediments as laminated dark green schists and phyllites and boudinaged coarse-grained green sheets up to 8 m thick. The thin sheets of metabasite are very difficult to distinguish in the field from the deformed green sediments.

The metabasites vary in composition from gabbro to diorite. The gabbro shows a well-developed ophitic texture with stumpy cloudy plagioclase (An_{55}) enclosed within augite prisms (up to 6 mm wide). Common accessory opaque minerals are partially altered and rimmed by sphene and leucoxene. The diorite, which also shows an ophitic texture, is distinctive in that zoned plagioclase (An_{42}) is enclosed within pleochroic (α = pale brown; β = green; γ = green-brown) hornblende prisms. Quartz is a common accessory in some diorites. The gabbro and diorite assemblages are partially replaced by pale green actinolite–chlorite–epidote–muscovite assemblages. Sericitization and saussuritization of zoned plagioclase are common. Within zones of intense deformation, a schistose fabric, defined by aligned actinolite laths, and a granular cataclastic fabric is developed. Some feldspars are partially recrystallized to albite, whereas others have been fractured. The amount of alteration and deformation increases towards the dislocation zone.

As the texture of these rocks is unlike that of the basic dyke rocks within the Drygalski Fjord Complex, it is concluded that they were intruded as sills or small plutonic bodies within the sediments. The dykes are characterized by elongated feldspar laths surrounded by stumpy hornblende or pyroxene prisms.

d. *Mylonites.* A well-developed mylonite foliation (Fig. 94) is present within a $\frac{1}{2}$ km wide belt of pale green, white and black finely banded rocks (myloblastites of Stone (1982)) on the western margin of the Cooper Bay Formation. The foliation and colour variation is defined by alternating ferromagnesian- and quartz-rich bands. The ferromagnesian minerals are mainly zoisite and clinozoisite with aligned flakes of chlorite, muscovite and light green tremolite-actinolite. Disseminated sphene and opaque granules are common within these bands. The felsic bands are mainly elongated ribbon quartz and recrystallized aggregates of mosaic quartz. The quartz ribbons are flattened parallel to the mylonite foliation.

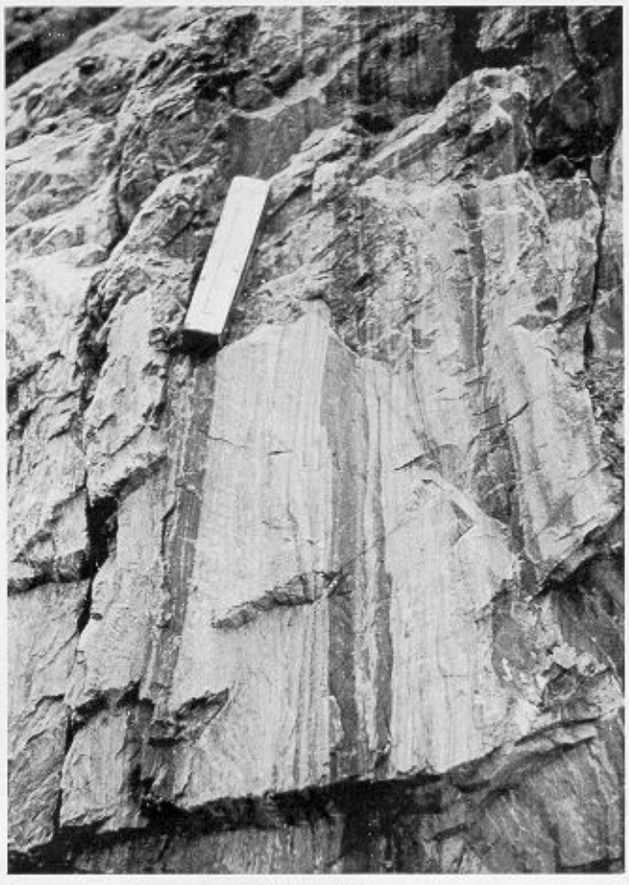

FIGURE 94
Minor folding of the mylonite fabric in the Cooper Bay Formation. The scale is 10 cm long.

2. *Structural history*

A detailed structural analysis of the Cooper Bay Formation (outlined below) has previously been established (Stone, 1982).

a. *Fold episode 1 (F1*).* Tight F1 folds were identified forming types 2 and 3 (Ramsay, 1962, 1967) interference patterns with later F2 folds. Isolated occurrences of L1 lineations were observed folded about F2 fold hinges.

b. *Fold episode 2 (F2*).* F2 folds (Fig. 95) are well developed in the Cooper Bay area as tight similar folds, plunging gently to the south-east. A strong corrugation lineation is developed on the

FIGURE 95
Zone of intense folding of the mylonites of the Cooper Bay Formation. The scale is 10 cm long.

limbs of the F2 folds parallel to the gently plunging fold hinges. A crenulation cleavage is present parallel to hinge surfaces of the F2 folds, along which the S1 fabric shows varying degrees of transposition.

c. *Fold episode 3 (F3*).* Similar close and rounded F3 folds occur as localized groups that fold the S2 fabric of the Cooper Bay–Wirik Bay–Cape Vahsel area about an axis plunging at 10° towards approximately 130°. A crenulation cleavage is parallel to the hinge surfaces of the F3 folds.

d. *Fold episode 4 (F4*).* There are isolated occurrences of minor folds of a later fold episode within the Cooper Bay Formation. They include small-scale open folds, isolated kink bands and crenulation lineations trending north-east.

Stone referred to the mylonitized rocks cropping out in the Cooper Bay area as myloblastites (due to recrystallization of the mylonite fabric) and he concluded that they were probably formed in response to local cataclasis between the F1 and F2 fold episodes. He also concluded that the basic rocks (epidiorites) pre-date the F2 fold episode and that the mylonite fabric of the dislocation zone possibly formed after the F2 episode and prior to the F3 episode.

* This is used to separate the post-mylonite folds of the Cooper Bay Formation from those of the dislocation zone.

c. *Discussion.* Although mapping was restricted to the Cooper Bay Formation cropping out along the margins of the dislocation zone, the fold episodes agree with the work of Stone. However, it is concluded that the continuous, finely laminated fabric that is folded about F1–F2 interference fold patterns is the mylonitic foliation and that mylonitization occurred prior to the F1 fold episode. Due to intense compression associated with the F2 folds, ribbon quartz is re-aligned axial planar to the F2 folds (Fig. 96) so, although the quartz-rich bands of the

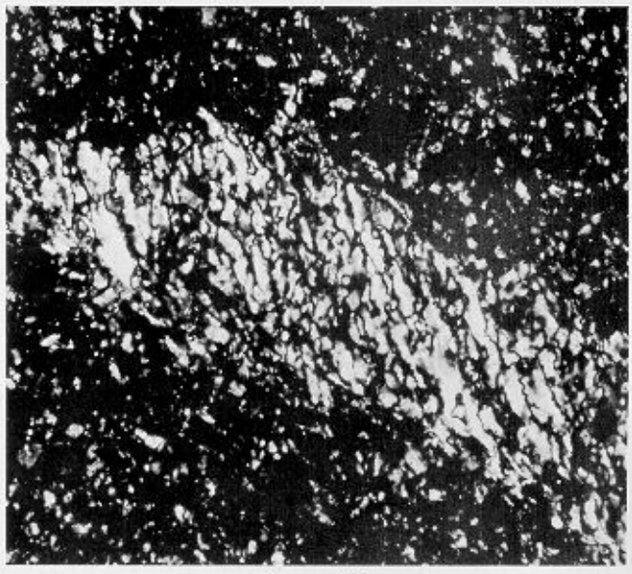

FIGURE 96
Axial planar quartz fabric of the F2 folds of the Cooper Bay Formation. (M.1271.5B; X-nicols; ×40)

mylonitic foliation are folded about F2 folds, the elongated quartz ribbons lie across the felsic bands axial planar to the F2 folds and the L2 corrugation lineations. There is also some re-alignment of the flaky minerals, chlorite and sericite, within the F2 fold hinge zone. In areas of extreme compression, the earlier mylonitic fabric has been virtually destroyed by shearing parallel to the fold limbs; tight and isoclinal fold hinges occur within this fabric. A quartz-rodding lineation parallel to the F2 fold hinges occurs on the S2 planes due to their intersection with pre-existing quartzose segregations. To the north-east of the mylonitic rocks, the main fabric is a strong biotite schistosity (S1). The metasediments have not been mylonitized and do not show the felsic laminations or flattened quartz ribbons of the mylonitized rocks. A strong S2 crenulation cleavage has been developed by varying degrees of re-alignment of biotite and chlorite along the crenulation cleavage planes.

As the metabasites are affected by the mylonite fabric, it is also concluded that these rocks intruded prior to the structural history of the rocks.

The relationship between the structural history of the metasediments within the dislocation zone and the sediments of the Cooper Bay Formation (fold episodes marked with an *) is not clear. Stone suggested that the fabric (SM) within the dislocation zone formed prior to the F3* fold episode and possibly after the F2* fold episode because the intense F2* structures

were not observed within the dislocation zone. However, as these structures have now been observed and the mylonitic fabrics are similar in thin section and have a similar orientation, it is reasonable to assume that they formed at the same time (i.e. SM = SM*). Also, the style and orientation of the F1 folds of the dislocation zone are similar to the F2* folds of the Cooper Bay Formation and they both have the quartz-ribbon texture axial planar to the folds. Although interference patterns with earlier fold phases were not recorded in the dislocation zone, the interfolial folds may be equivalent to the F1* folds of the Cooper Bay Formation and the F1 folds of the dislocation zone equivalent to the F2* folds. In contrast, the steeply plunging F2 folds of the dislocation zone are absent from the Cooper Bay Formation. The F3 folds may be equivalent to the F4* folds of the Cooper Bay Formation.

3. *Conclusions and regional correlations*

The laminated and graded volcaniclastic sandstone units of the Cooper Bay Formation indicate that these rocks are part of a turbidite sequence that was derived from a continental acidic and subsidiary intermediate volcanic terrain.

As the volcaniclastic sediments of the Novosilski Glacier Formation have been derived from a similar terrain, have in part a common structural history, and crop out alongside (within the dislocation zone) the Cooper Bay Formation, it is possible that both of these formations are part of a single sedimentary succession. However, there are a number of important differences which preclude a similar origin for these rocks: the Novosilski Glacier Formation was deformed and metamorphosed up to the biotite grade of the greenschist facies prior to intrusion of the suite of plutonic rocks and prior to mylonitization; there is extensive development of feldspar porphyroblasts which are associated with the plutonic activity within the metasediments of the Novosilski Glacier Formation. In contrast, the mylonitization of the Cooper Bay Formation occurred prior to the deformation of the sediments and the basic sills are the only signs of plutonic activity within the Cooper Bay Formation; the feldspar porphyroblasts are not seen within the Cooper Bay Formation.

It is thus concluded that the Cooper Bay Formation is unrelated to the metasediments of the Drygalski Fjord Complex and that it is equivalent to the marginal-basin infill sediments of the Sandebugten Formation (Stone, 1980) and the coastal member of the Ducloz Head Formation (Storey, in press). There are, however, some important differences, some of which were outlined by Stone (1982); quartz crystal fragments are less common than in the Sandebugten Formation where they are equal in amount to the feldspar crystal fragments and form up to 14% of the rock; perthites and potash feldspar are more abundant in the Cooper Bay Formation than in the Sandebugten Formation; microlitic feldspar fragments are more abundant in the Cooper Bay Formation where they form an estimated 10% of some thin sections. Stone counted up to 3% (trachytic and felted textures) and Winn (1978) less than 2% (pilotaxitic) microlitic fragments in the Sandebugten Formation, which is in strong contrast to the Cumberland Bay Formation which contains up to 40% microlitic fragments (Stone, 1980). Stone did not record the felsic fragments which are common in the Cooper Bay Formation.

The apparent scarcity of quartz crystal fragments in the Cooper Bay Formation, which is also a characteristic of the Cumberland Bay Formation (up to 3% recorded), may be due in part to the recrystallization of quartz fragments to polycrystalline mosaics indistinguishable from the matrix. The high proportion of perthite and potash feldspar may be a secondary effect due to mobility of potash feldspar during mylonitization, an effect observed in the dislocation zone. In thin section, the recrystallized sediments are almost identical to the Sandebugten Formation south of Royal Bay (Stone, 1980), supporting the increase in deformation and recrystallization from the least-deformed Sandebugten Formation sediments of Barff Point, which are metamorphosed to stilpnomelane-bearing greenschist facies (Tanner, 1982*b*) to the most-deformed Cooper Bay Formation.

In conclusion, the sediments of the Cooper Bay Formation are related to the Upper Mesozoic succession of South Georgia, having been derived from a volcanic terrain similar to that of the Sandebugten Formation but with a higher percentage of intermediate volcanic rocks. This conclusion is supported by the geochemical work of Clayton (1982).

XV. ORIGIN OF THE MYLONITE FABRIC

THE origin of mylonitic fabrics has been much discussed in the geological literature. There are two main possibilities in interpreting the strain associated with mylonite zones:

i. Mylonite zones are the products of large-scale shear strains (ductile shear zones) with a large-scale displacement of the rocks on either side of the zones (Ramsay and Graham, 1970; Vernon and Ransom, 1971).

ii. Mylonite zones are formed by flattening normal to foliation similar to the development of slaty cleavage with no large-scale displacement (Johnson, 1967). Johnson proposed that movement along these zones may post-date the formation of the mylonites (e.g. Moine thrust (Johnson, 1970)). Tullis and others (1973) have produced typical mylonitic microstructures commonly thought of as a product of shear strain by axial symmetrical straining.

The zone of mylonitized rocks described above has many characteristics in common with the Lethakane shear zone, a transcurrent ductile shear zone, described by Wakefield (1977) from the Limpopo orogenic belt of eastern Botswana.

A strong mylonitic foliation, mainly represented in quartz-rich rocks, is associated with conjugate minor shear zones, fracture cleavages and late faulting. Within the Lethakane zone, the shearing is defined by a change in the orientation of the regional structure towards the shear zone with a progressive steepening

of the mylonitic fabric within the shear zone sub-parallel to the margins of the shear zone. This overall sigmoidal structure of the mylonitic fabric is lacking within the Cooper Bay dislocation zone. This may in part be due to the later folding or faulting of the margins of the dislocation zone or due to extremely high shear strain. As the dislocation zone separates the Cooper Bay Formation from the intrusive and metamorphic rocks of the complex, there has been vertical movement and uplift of the complex along a reverse fault probably concentrated along the margins of the zone. The mylonitic fabric, which is not present within the country rocks on the south-western side of the dislocation zone, does occur within the Cooper Bay Formation. It does not form a sigmoidal relationship but is sub-parallel with the fabric within the dislocation zone. However, it is concluded that the mylonite fabric has formed mainly by simple shear. This may have been accompanied by an element of pure shear which was responsible for the interfolial folds within the mylonite foliation. Subsequent to mylonitization, the folding of the mylonite fabric possibly formed by pure shear. During the intense compression of the D2* event, the F2 folds became tight and isoclinal folds, and developed a flattened quartz-ribbon fabric (S2*) aligned axial planar to the folds. The fold hinges (F2*) tended to be destroyed with extensional flow parallel with the axial plane of the folds, forming a new banding within these rocks (Bell and Etheridge, 1973; Ross, 1973).

The dislocation zone is thus a composite shear zone that formed by pure and simple shear with large-scale vertical movements along reverse faults at the margins of the zone. The implications of this zone are discussed below.

XVI. SUMMARY OF THE GEOLOGICAL HISTORY OF THE DRYGALSKI FJORD COMPLEX

THE Drygalski Fjord Complex forms a wedge-shaped area of intrusive, metasedimentary and anatectic rocks, the geology of which is summarized in Table I. The area is bounded on the south-west by a topographic break separating it from the upper part of an ophiolite sequence (Larsen Harbour Formation) (Fig. 3) and on the north-east by a zone of intensely mylonitized rocks (Cooper Bay dislocation zone) separating it from volcaniclastic turbidites of the Cumberland Bay and Cooper Bay Formations.

Quartz-rich sediments and metasediments, which form the country rock of the intrusive rocks, are divided into three spatially distinct formations: the Salomon Glacier, Cooper Island and Novosilski Glacier Formations. The Salomon Glacier Formation, which crops out in the southern part of the complex, is composed of silicious *para*gneisses and layered migmatites regionally metamorphosed up to the amphibolite facies. It was migmatized and affected by polyphase-deformation prior to intrusion of a suite of gabbro, diorite, granitoid and basic dyke rocks. The Cooper Island and Novosilski Glacier Formations are deformed, low-grade, quartz-rich clastic sediments. Silicic volcaniclastic sediments and porphyritic felsites, which are in gradational contact with clastic sediments of the Novosilski Glacier Formation in the northern part of the dislocation zone, are tentatively assigned to the Novosilski Glacier Formation. They indicate that sedimentation was closely associated with, and continued during, volcanic activity.

Plutonic activity commenced during the early Jurassic with the formation of a number of layered gabbroic plutons, which are mainly exposed in the south-eastern part of the complex. The gabbroic plutons, which enclose small ultramafic bodies, dioritic segregations, pegmatites and discordant veins, are the most abundant intrusive rocks of the complex. Inclined rhythmic layering, brecciated and folded by syn-magmatic disturbances and multiple injections, indicates that crystal accumulation was followed during consolidation by *in-situ* deformation and re-intrusion of the crystal mush into its present position. Post-consolidation changes have resulted in widespread amphibolitization, recrystallization and disequilibrium mineralogical relationships.

A number of coarse-grained granitoids, the Cooper Island granophyre and the Trendall Crag granodiorite, crop out within the complex. The relationship between these bodies and the gabbro plutons is incomplete because contacts are faulted and obscured by later intrusive breccias and migmatites. However, on the north side of Storey Glacier (Fig. 5), the granodiorite intrudes and assimilates the gabbro plutons with the formation of marginal ocellar diorites, net veins, agmatites and dioritic assemblages. The widespread amphibolitization of the gabbros, recrystallization and the inclined layering may be associated with the intrusion of the granitoid plutons. Diorites, which are mostly confined to gabbro–granitoid contact zones, are primary and secondary rocks formed by differentation of the basic magma and by assimilation by the granodiorites, respectively. Small diorite dykes also intrude the metasediments.

In the northern part of the complex, and on Cooper Island, small gabbro plutons, porphyritic spherulitic felsites and porphyritic microgranites, which intrude the clastic sediments of the Novosilski Glacier and Cooper Island Formations, may represent the sub-surface and surface equivalents of the larger granitoid and basic plutons of the southern part of the complex. Contact metamorphism with growth of cordierite occurred in the Cooper Island Formation as a result of emplacement of the basic and acid rocks.

After intrusion of the granitoid rocks, there was renewed basic activity with the emplacement of numerous swarms of dilation dykes and isolated granitoid dykes. The basic dykes, the concentration of which decreases from west to east, form up to 80% of the exposure in some localities. Although chilled margins are present, trains of angular and partially assimilated basic dyke fragments in primary quartz-gabbro and diorite indicate that some basic dykes intruded semi-consolidated gabbros.

Emplacement of the basic dykes, all of which have chilled

margins, was followed by the formation of a heterogeneous migmatite complex surrounding the basic and acidic rocks. The basic, granitoid and metasedimentary rocks are broken up, injected, net veined, and form migmatitic relationships with a fine-grained granitoid neosome; angular and partially assimilated gabbroic and basic-dyke enclaves are enclosed within a granitoid matrix. The complex formed by partial melting of the metasediments, emplacement of intrusive acid–basic breccias and re-activation and mobility of the earlier granitoid phases. Plagioclase and potash feldspar porphyroblasts are common within the dislocation zone.

The migmatite complex is cut by aplites, pegmatites and occasional late basic dykes. Subsequent retrogression and percolating hydrothermal fluids (deuteric, anatectic, meteoric ground water or differentiates) have resulted in widespread development of low-amphibolite and greenschist facies retrogressed mineral assemblages (hornblende–actinolite–chlorite–epidote–sericite–quartz) and disequilibrium mineralogical conditions within many of the basic and granitoid rocks. Actinolite, chlorite, epidote and prehnite veins are also common.

A zone of mylonitized rocks (part of the Cooper Bay dislocation zone), up to 1 km wide, forms the north-eastern margin

derived sub-alkaline tholeiitic magma. Incomplete separation of the differentiated rocks resulted in quartz-gabbro and dioritic segregations, pegmatites and discontinuous veins within the layered gabbros and heterogeneous quartz-gabbro, diorite and quartz-diorite assemblages along the gabbro–granitoid contact zones. The granitoid plutons are variable in origin; the Cooper Island granophyre and some of the the porphyritic felsites and granitoid dykes formed by extreme differentiation of the basic magma contaminated by partial melting of the metasediments. Due to density differences between the acid and basic rocks, segregated pockets of acidic differentiate intruded and fragmented the basic rocks and formed the intrusive breccias. The Trendall Crag granodiorite, which shows calc-alkaline trends, was probably derived from the mantle and generated under conditions of high P_{H_2O}. The migmatitic and agmatitic granites within the metasediments formed entirely by partial melting of the metasediments.

The acid–basic relationships, and in particular the widespread re-activation, migmatization and amphibolitization of the earlier rocks within the complex, have made dating a difficult task. Dates ranging from 120 to 201 Ma however have been

XVII. DISCUSSION AND TECTONIC EVOLUTION OF THE SOUTH GEORGIA ISLAND-ARC–BACK-ARC BASIN SYSTEM

1. *Basement rocks*

The relationship between the sediments and metasediments of the Drygalski Fjord Complex is by no means conclusive. As the sediments of the Novosilski Glacier and Cooper Island Formations are petrographically similar and are both derived from a continental fragment comprising outcrops of acidic metamorphic and mainly plutonic rocks, it is proposed that they are part of the same sedimentary sequence that was deposited in an offshore basin. In contrast, the rocks of the Salomon Glacier Formation are crystallized and more intensely deformed than the above. However, as they were all deformed prior to intrusion of a similar suite of igneous rocks, the oldest of which is dated as early Jurassic, and as the hornfelsed sediments of the Cooper Island Formation are petrographically similar to the metasediments of the Salomon Glacier Formation, it is most likely that the formations can be correlated and that variable degrees of deformation and metamorphism affected them during a single orogenic event prior to intrusion of the Lower Jurassic basic rocks. As the oldest of the plutonic intrusions is dated at 200 Ma, it is concluded that the sediments originally formed part of a continental-margin assemblage that was deformed during an Upper Palaeozoic or at the latest a Lower Mesozoic (Gondwanide) orogeny, and that they now form part of the pre-Jurassic basement of South Georgia (Fig. 97).

In South America, in the Scotia Ridge and the Antarctic Peninsula there are widespread occurrences of pre-Jurassic basement rocks (Kranck, 1932; Adie, 1964; Dalziel and Elliot, 1971, 1973; Dalziel, 1982) which can be subdivided into a metamorphic complex and clastic sediments and metasediments (Dalziel, 1982). Recent workers (Stubbs, 1968; Fraser and Grimley, 1972; Skinner, 1973) have suggested that the complex is the metamorphic equivalent of the clastic sediments. This has been supported by recent dates from the metamorphic rocks (Gledhill and others, 1982), which give early Mesozoic ages for the main metamorphic event. The pre-Jurassic basement rocks of South Georgia are remarkably similar to the basement rocks of the Antarctic Peninsula and South America. In particular, the banded gneisses of the Salomon Glacier Formation are similar to the banded fine-grained quartz-biotite-*para*gneisses described by Adie (1954) from the Antarctic Peninsula. The clastic sediments of the Novosilski Glacier and Cooper Island Formations are also similar to widespread previously correlated greywacke–shale sequences; Madre de Dios sediments of South America (Cecioni, 1955; Dalziel and Elliot, 1973); the Greywacke–Shale Formation of the South Orkney Islands (Thomson, 1973), Miers Bluff Formation of the South Shetland Islands (Adie, 1964; Hobbs, 1968; Dalziel, 1969); the Trinity Peninsula Group (Hyden and Tanner, 1981), which was formerly termed the Trinity Peninsula Series (Elliot, 1965, 1966; Aitkenhead, 1975) from the Antarctic Peninsula, and the LeMay Formation of Alexander Island (Edwards, 1982). They are all poorly fossiliferous and were derived from similar granitic gneiss, metamorphic, plutonic and volcanic terrain. Structural trends of South Georgia are also similar to those recorded from Shag Rocks on the Scotia Ridge (Tanner, 1982*a*) and from South America (Dalziel, 1982).

It is therefore proposed that the South Georgia basement rocks are similar to the pre-Jurassic rocks of South America and the Antarctic Peninsula, and that they form part of a sedimentary sequence deposited on the Pacific margin of Gondwana and accreted on to the continental margin during the Gondwanian orogeny. They were probably metamorphosed in a high-temperature and low-pressure metamorphic belt. The north-east and south-east structural trends may support an original embayment in the margins of the Gondwana supercontinent (Dalziel, 1982).

It thus appears, as outlined by Dalziel (1982), that a pre-Jurassic complex of sediments, metasediments and metamorphic rocks represents part of an arc–trench gap and to a lesser extent the main volcanic arc of a pre-Jurassic subduction zone along the Pacific margin of Gondwana which was metamorphosed and deformed during a Lower Mesozoic Gondwanian orogeny. Inliers of older basement may have been deformed during the Borchgrevinck orogeny (Craddock, 1972).

2. *Upper Mesozoic rocks*

In the northern part of the Andes of Tierra del Fuego and on Mount Flora at the northern tip of the Antarctic Peninsula (Anderson, 1906; Aitkenhead, 1975), silicic volcanic rocks (Tobifera Formation) and sediments of late Jurassic age unconformably overlie deformed and metamorphosed pre-Jurassic basement rocks (Dalziel, 1972, 1982). The unconformity represents a period of uplift and erosion, which may be related to the break-up of Gondwana and which separates the Gondwanian orogeny from volcano-tectonic events of the Andean orogenic period (Dalziel, 1982). In South America, the widespread occurrences of Middle–Upper Jurassic silicic volcanic rocks (Dalziel and others, 1974) may have formed by crustal anatexis in a volcano-tectonic rift zone as a result of emplacement of subduction-related mantle diapirs along the continental margin (Bruhn and others, 1978) prior to the formation of the back-arc basin (Dalziel and others, 1974). In the Antarctic Peninsula, similar widespread occurrences of "Mesozoic Volcanic Rocks" (Weaver and others, 1982) may be related to subduction of oceanic lithosphere beneath the Antarctic Peninsula and the emplacement of the calc-alkaline plutons (Saunders and others, 1982*b*; Weaver and others, 1982).

In South Georgia, the volcaniclastic sediments and volcanic felsites tentatively assigned to the Novosilski Glacier Formation closely resemble the Tobifera Formation of southern South America. However, as the porphyritic felsites are in gradational contact with the volcaniclastic and epiclastic sediments which contain deformed biotite lamellae, these rocks were metamorphosed up to the biotite grade of the greenschist facies and were deformed prior to intrusion of Lower Jurassic plutonic rocks. They were probably deformed during the Gondwanian orogeny and are part of the pre-Jurassic basement rocks of South Georgia. If this is not the case, an unconformity must exist between the metasediments of the basement rocks and the volcaniclastic rocks of the Novosilski Glacier Formation. The deformation and mylonitization of these rocks would make

recognition of such an unconformity a difficult if not an almost impossible task in this area.

The sediments and metasediments of the Drygalski Fjord Complex are in marked contrast to the Upper Mesozoic successions on South Georgia. The Upper Mesozoic successions, which are all part of the Upper Jurassic–Lower Cretaceous marginal-basin infill, are predominantly volcaniclastic rocks that were deformed and metamorphosed in the mid-Cretaceous (80–90 Ma; Thomson and others, 1982) after intrusion of isolated basic bodies. The Drygalski Fjord Complex sediments contain only a small proportion of volcaniclastic rocks and were metamorphosed and deformed prior to intrusion of Lower Jurassic igneous rocks. However, the sub-quartzose sandstones of the Novosilski Glacier and Cooper Island Formations and the volcaniclastic felsites tentatively assigned to the Novosilski Glacier Formation are similar to the coastal member of the Ducloz Head Formation (Storey, in press). Although similar, there are a number of important differences:

i. The coastal member, similar to the Upper Mesozoic successions, was deformed and metamorphosed to the prehnite–pumpellyite facies after intrusion of the basic rocks.
ii. The sediments of the coastal member are interbanded with basic pillow lavas which are absent from the Novosilski Glacier or Cooper Island Formations.
iii. Thick intraformational breccia units form a large and significant part of the sediments of the coastal member.

It is thus probable that these sediments, although derived from similar terrains, were deposited at different times and in different tectonic environments. The Ducloz Head sediments represent initial coarse sedimentation in the Upper Mesozoic marginal basin of South Georgia which was formed by fragmentation of the continental margin, whereas the Drygalski Fjord sediments were formed along the continental margin prior to formation of the marginal basin. Some of the Ducloz Head Formation sediments may have been derived from the Novosilski Glacier Formation.

The layered gabbros, granitoids and basic dyke suites of the Drygalski Fjord Complex are similar to and were formed at the same time as the plutons of South America and the Antarctic Peninsula, and may form part of a continuous Mesozoic calc-alkaline magmatic arc. The Antarctic Peninsula plutons (Adie, 1954, 1955; Hooper, 1962; Elliot, 1964; Marsh, 1968; West, 1974; Aitkenhead, 1975; Saunders and others, 1982*b*) are part of a magmatic arc linked to subduction of Pacific Ocean crust beneath the Antarctic Peninsula during the Mesozoic and Tertiary. In South America, the batholith (Quensel, 1913; Kranck, 1932; Dalziel and others, 1975; Pitcher, 1978; Stern and Stroup, 1982) coincides in space and time with the Upper Jurassic–Lower Cretaceous island-arc volcanism, suggesting that the intrusions are the roots of the calc-alkaline volcanic chain (Dalziel and others, 1974; Suárez, 1976). It was concluded previously that the Drygalski Fjord Complex plutonic rocks correlated with a suite of plutonic rocks from the Antarctic Peninsula and that a significant part of the activity belonged to the Gondwanian cycle (Tanner and Rex, 1979). However, the proximity of the upper part of an ophiolite sequence, the Larsen Harbour Formation (floor of a back-arc basin), to the plutons of the Drygalski Fjord Complex and the presence of common basic dyke suites have led Bell and others (1977) to suggest that the gabbros, granitoids and basic dyke rocks are related to the opening of the back-arc basin and not to the calc-alkaline arc. This has been supported by geochemical analyses of these rocks which indicate that the gabbros, basic dykes and some of the granitoid rocks were formed by differentiation of mantle-derived sub-alkaline olivine-tholeiites. The Trendall Crag granodiorite, however, shows calc-alkaline trends and may have formed by partial melting of the mantle during conditions of high P_{H_2O}.

It is therefore most likely that the tholeiitic gabbros may represent the initial magmatism and be a precursor to the marginal-basin ophiolites that intruded within a volcano-tectonic rift zone (Bruhn and others, 1978) along the continental margin of a proto-South American continent. Although the marginal basin did not open until about 140 Ma, magmatic activity commenced in the early Jurassic. The magmatic activity may be associated with subduction-related tectonics or those processes that initiated the break-up of Gondwana or the opening of the South Atlantic (Bruhn and others, 1978; Dalziel, 1982). It is possible that subduction and the extensional regime may be causally related. Closely associated with emplacement of the basic rocks, partial melting of the metasedimentary country rocks formed the migmatitic aureole around the basic rocks.

Although large volumes of anatectic silicic magma were emplaced in association with extensional faulting in the broad volcano-tectonic rift zone of southern South America during the late Jurassic (Bruhn and others, 1978), *in-situ* migmatitic granites, agmatitic veins and minor granitoid dykes are the only evidence of partial melting of the metasediments within the migmatitic aureole of the Drygalski Fjord Complex plutonic rocks. There is no evidence of the large-scale melting needed to produce voluminous acidic magmas.

Continued emplacement of mantle-derived tholeiitic magma and formation of the basic dyke suite within the continental margin caused extensional rifting, extrusion of the basic magma and formation of a marginal basin floored by mafic crust (Larsen Harbour Formation) (Fig. 97). There is no evidence of the gabbros having been re-heated to melting point to produce the migmatitic structures or of a major thermal event that affected the gabbros (Tanner and Rex, 1979) to account for the late Jurassic dates of the complex. These dates represent minimum ages for the crystallization of the intermediate, acid and anatectic rocks in a zone of prolonged magmatic activity and high heat flow. Slow progressive cooling and concentration of the late-stage fluids produced the migmatitic structures, lowest dates and retrograde mineral assemblages.

3. *Evolution of the island-arc–back-arc basin system*

Subduction of oceanic crust along the western margin of the rift zone formed the calc-alkaline plutonic and volcanic suite and associated island-arc assemblages (Annenkov Island Formation (Pettigrew, 1981; Tanner and others, 1981)) on a rifted-off sliver of continental crust. Although calc-alkaline plutons of up to at least 166 Ma (de Wit, 1977) are present in South America, the oldest marginal-basin sediments on South Georgia are late Jurassic in age. Epiclastic and volcaniclastic sediments derived from the rifted continental margin and from silicic volcanic rocks (Ducloz Head Formation) were initially deposited within the back-arc basin (Fig. 97) (Storey, in press). The sediments are interbanded with basic pillow lavas of the mafic

crust. Sedimentation close to the island-arc formed pyroclastic tuffs and mudstones (tuff–mudstone facies) and a coarse-grained apron of andesitic breccias around the volcanic centres (Pettigrew, 1981; Tanner and others, 1981). The detritus from the island-arc volcanics was redeposited by turbidity currents (turbidite facies) within the basin to form the Cumberland Bay Formation (Trendall, 1959; Dalziel and others, 1975; Stone, 1980) (Fig. 97). The turbidity currents were fed from submarine canyons situated on the south-western side of South Georgia. Current indicators suggest north-west-directed sediment dispersal was commonest within an elongated basin that was parallel to the present trend of the island (Tanner, 1982*a*). Continued quartz-rich sedimentation from the continental side of the marginal basin formed the Sandebugten and Cooper Bay Formations (Dalziel and others, 1975; Stone, 1980, 1982). The occurrence of tuffs and mudstones of the Annenkov Island Formation conformable with the mafic crust of the Larsen Harbour Formation (Tanner and others, 1981) indicates that this portion of mafic crust was initially situated along the margins of the basin flanking the island-arc volcanoes. The occurrence of tuff and mudstone (inland member of the Ducloz Head Formation) on the eastern side of the initial infill of the basin (coastal member of the Ducloz Head Formation), and the presence of thin-bedded mudstone and occasional pyroclastic tuff units within the Cumberland Bay Formation, indicate some interfingering of the tuff–mudstone and turbidite facies within the basin; the regional relationships have been summarized by Tanner and others (1981). Although there are no depth indicators, the tuff–mudstone facies may represent shelf sedimentation along the margins of the basin. The shelf area was deeply dissected by the submarine canyons which fed the turbidity currents of the basin.

Although the true floor of the basin is not exposed, the fact that the tuff–mudstone facies is conformably underlain by mafic crust (Larsen Harbour Formation) and a comparison with South America (Dalziel and others, 1974) indicates that the turbidite facies may also be underlain by mafic crust. However, the scarcity of basic dykes within the dislocation zone and along the eastern margin of the Drygalski Fjord Complex compared to the western margin indicates that parts of the Cumberland Bay and Cooper Bay Formations may be floored by down-faulted blocks of continental crust (Fig. 97). The occurrence of basic sills within these formations indicates that basic magmatic activity was continuous during sedimentation and perhaps the existence of mafic crust or lenses of basic dykes within the floor of the basin.

The marginal-basin assemblage was deformed during the Andean orogeny by movement of the island-arc towards the continental landmass (Dalziel and others, 1974, 1975; Bruhn and Dalziel, 1977). Uplift of part of the floor of the basin took place initially along the dislocation zone with the formation of a 1 km wide belt of cataclastic rocks. The extent of shortening of the marginal-basin infill is indicated by large-scale chevron-type folding (Fig. 97) of the Cumberland Bay Formation (cf. Trendall, 1959). Some shortening of the floors of basins can be accounted for by tilting and disruption of the mafic crust. As this is hardly sufficient to account for the amount of shortening of the basin infill, it is possible, although there is no evidence to support this, that part of the floor of the basin was subducted by a reverse in the direction of the Benioff zone beneath the island arc (Tanner and others, 1981). Subduction would have been short-lived, however, as the (?) continental fragments within the basin floor would form a jamming mechanism for continued subduction. The intense compression within the dislocation zone and within the Cooper Bay Formation, and the ductile–brittle nature of the deformation within the Ducloz Head Formation, which is in strong contrast to the surrounding Cumberland Bay Formation sediments, indicate that the Cooper Bay dislocation zone may represent the site of this subduction. Whatever its origin, the Cooper Bay dislocation zone represents a major structural feature in South Georgia. It is parallel to the main structural trend of the island, the main dyke trends within the Larsen Harbour Formation and the Drygalski Fjord Complex, and the sediment-dispersal direction in the basin. It separates the marginal-basin infill (turbidite facies), which was deformed during the Andean orogeny, from a fragment of stable pre-Jurassic continental crust and from the marginal tuff–mudstone facies of the basin. As the initial infill of the basin (Ducloz Head Formation) lies within or immediately to the south-west of this zone, the zone may represent the site of the initial rift of the basin, or, as it separates the (?) shelf sedimentation of the tuff–mudstone facies from the turbidite facies, it may have marked the edge of the original sedimentary basin. It is possible that the dislocation is part of a deep-seated structural feature which controlled the initial opening of the basin, sedimentation and subduction. It may represent the site of a transform fault zone related to basin spreading.

Although it was suggested that the Ducloz Head Formation lies within the Cooper Bay dislocation zone (Tanner and others, 1981), this is not necessarily the case. The Cooper Bay dislocation zone (Fig. 2), which is narrower towards the north-west, may be represented by the fault zone with a vertical slaty fabric that separates the inland member of the Ducloz Head Formation from the Cumberland Bay Formation (Storey, in press). The coastal and inland members of the Ducloz Head Formation, which do not show any signs of the fabric that is present within the Cooper Bay dislocation zone, may be preserved within parallel-faulted slices.

In conclusion, the deformed sediments and metasediments of the Drygalski Fjord Complex (Fig. 98) may represent a fragment of pre-Jurassic continental crust that was split off from the continental margin during the late Jurassic by emplacement of large volumes of basic magma and the formation of a marginal basin floored by mafic crust within a volcano-tectonic rift zone (Fig. 97) in a manner similar to that described for the development of back-arc basins in the western Pacific (Karig, 1972). The plutonic rocks are wholly related to the formation of this island-arc–back-arc basin system.

A possible modern analogue of the Drygalski Fjord Complex could occur within the Gulf of California. Isla Tortuga, which may lie on the continuation line of a transform fault, is a small island within the Gulf (Batiza, 1978). It has tholeiitic mid-ocean ridge-type magmatic activity contaminated by possible underlying slivers of continental crust. The thick piles of sediment and sills of South Georgia may be similar to the central part of the Gulf where basalt cannot reach the sediment surface. The tectonic configuration of the Gulf of California (Moore, 1973) means that subduction is not now occurring beneath the adjacent inactive arc; instead, several extensive shear zones, which may be similar to the Cooper Bay dislocation zone, run along the length of the Gulf of California.

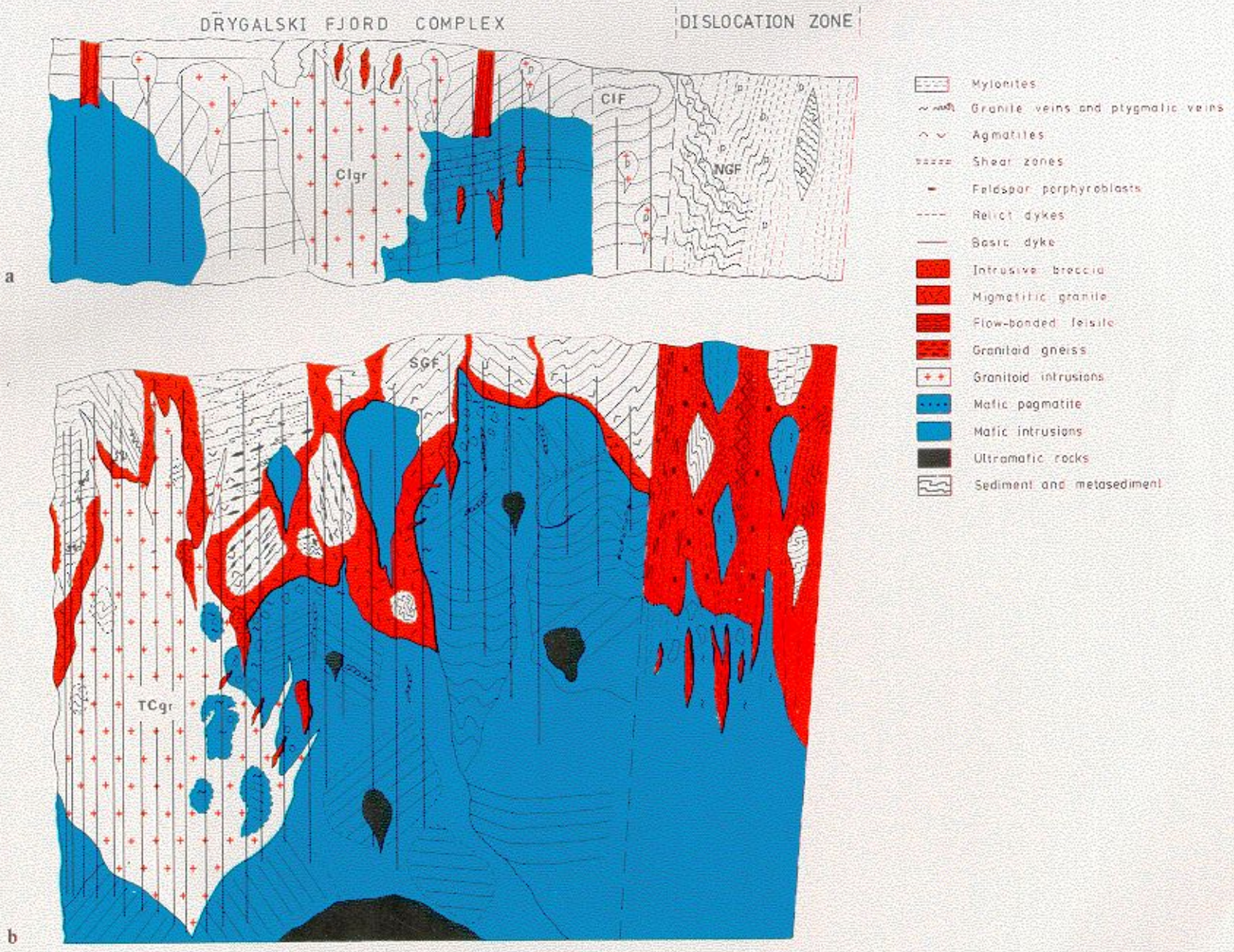

FIGURE 98
Diagrammatic section of the upper (a) and lower (b) structural levels of the Drygalski Fjord Complex. CIgr, Cooper Island granophyre; TCgr, Trendall Crag granodiorite; O, ocellar diorites; ▷, cognate xenoliths; SGF, Salomon Glacier Formation; CIF, Cooper Island Formation; NGF, Novosilski Glacier Formation; V, volcaniclastic sediment; P, porphyritic felsite.

XVIII. ACKNOWLEDGEMENTS

I AM grateful to the Officers and crews of RRS *John Biscoe,* RRS *Bransfield* and HMS *Endurance* who provided support facilities for field programmes; the South Georgia base personnel who prepared the camping units; my field companions, D. M. Burkitt, D. J. Orchard and J. H. Carter; and especially to Drs C. M. Bell, B. F. Mair and P. W. G. Tanner, who have worked on the Drygalski Fjord Complex and who have made their field collections, photographs and observations available to me.

My thanks are due to my former and present colleagues in the Earth Sciences Division of the Survey and in particular to Dr P. W. G. Tanner for much useful discussion and criticism during the work and in preparing this report. I am also grateful to Drs R. J. Adie and D. I. M. Macdonald for reading and discussing the manuscript; Dr G. Hyden for typing the tables, and Dr P. D. Clarkson, Dr P. D. Marsh and N. C. B. Donellan for assisting with computing problems. I am especially grateful to Ms G. Tew for typing the manuscript.

XIX. REFERENCES

ADIE, R. J. 1954. The petrology of Graham Land: I. The Basement Complex; early Palaeozoic plutonic and volcanic rocks. *Falkland Islands Dependencies Survey Scientific Reports,* No. 11, 22 pp.

——. 1955. The petrology of Graham Land: II. The Andean Granite–Gabbro Intrusive Suite. *Falkland Islands Dependencies Survey Scientific Reports,* No. 12, 39 pp.

——. 1964. The geochemistry of Graham Land. (*In* ADIE, R. J., *ed. Antarctic geology.* Amsterdam, North-Holland Publishing Company, 541–47.)

AHMED, A. A. *and* B. E. LEAKE. 1978. The Inishdawros metaperidotite, Callow, Ballyconnelly, Connemara, western Ireland. *Mineralogical Magazine,* **42,** 69–74.

AITKENHEAD, N. 1975. The geology of the Duse Bay–Larsen Inlet area, north-east Graham Land (with particular reference to the Trinity Peninsula Series). *British Antarctic Survey Scientific Reports,* No. 51, 62 pp.

ANDERSSON, J. G. 1906. On the geology of Graham Land. *Bulletin of the Geological Institution of the University of Upsala,* **7,** 19–71.

ANGUS, N. S. 1962. Ocellar hybrids from the Tyrone igneous series, Ireland. *Geological Magazine,* **99,** 9–26.

ARTH, J. G. *and* G. N. HANSON. 1975. Geochemistry and origin of the early Precambrian crust of north-eastern Minnesota. *Geochimica Cosmochima Acta,* **39,** 325–26.

AUMENTO, F. 1969. Diorites from the Mid-Atlantic Ridge at 45°N. *Science, New York,* **165,** 1112–13.

BAILEY, E. H. *and* M. C. BLAKE. 1974. Major chemical characteristics of Mesozoic Coast Range ophiolite in California. *Journal of Research of the U.S. Geological Survey,* **2,** 637–56.

BAKER, P. E. 1976. The South Sandwich Islands: III. Petrology of the volcanic rocks. *British Antarctic Survey Scientific Reports,* No. 93, 34 pp.

BARKER, D. S. 1970. Compositions of granophyre, myrmekite and graphic granite. *Geological Society of America. Bulletin,* **81,** 3339–50.

BARKER, P. F. *and* D. H. GRIFFITHS. 1972. The evolution of the Scotia Ridge and Scotia Sea. *Philosophical Transactions of the Royal Society,* Ser. A, **271,** 151–83.

BARTH, T. F. W. *and* P. HOLMSEN. 1939. Rocks from the Antarctandes and the Southern Antilles. Being a description of rock samples collected by Olaf Holtedahl 1927–1928, and a discussion of their mode of origin. *Scientific Results of the Norwegian Antarctic Expeditions,* No. 18, 64 pp.

BATIZA, R. 1978. Geology, petrology, and geochemistry of Isla Tortuga, a recently formed tholeiitic island in the Gulf of California. *Geological Society of America. Bulletin,* **89,** 1309–24.

BELL, C. M., MAIR, B. F. *and* B. C. STOREY. 1977. The geology of part of an island arc–marginal basin system in southern South Georgia. *British Antarctic Survey Bulletin,* No. 46, 109–27.

BELL, G. E. *and* M. A. ETHERIDGE. 1973. Microstructure of mylonites and their descriptive terminology. *Lithos,* **6,** 337–48.

BLAKE, D. H. 1966. The net-veined complex of the Austerhorn intrusion, south-eastern Iceland. *Journal of Geology,* **74,** 891–907.

BOWES, D. R. *and* A. E. WRIGHT. 1961. An explosion breccia complex at Back Settlement near Kentallen, Argyl. *Transactions of the Edinburgh Geological Society,* **18,** 293–314.

BROWN, G. C. 1963. Melting relations of Tertiary granitic rocks in Skye and Rhum. *Mineralogical Magazine,* **33,** 533–62.

——. 1973. Evolution of granite magmas at destructive plate margins. *Nature, London, Physical Sciences,* **241,** 26–28.

——. 1977. Mantle origin of Cordilleran granites. *Nature, London,* **265,** 21–24.

BRUHN, R. L. *and* I. W. D. DALZIEL. 1977. Destruction of the early Cretaceous marginal basin in the Andes of Tierra del Fuego. (*In* TALWANI, M. *and* W. C. PITMAN, *ed. Island arcs, deep sea trenches and back-arc basins.* Washington, D. C., American Geophysical Union, 393–403.) [Maurice Ewing Series, Vol. 1.]

——., STERN, C. R. *and* M. J. DE WIT. 1978. Field and geochemical data bearing on the development of a Mesozoic volcano-tectonic rift zone and back-arc basin in southernmost South America. *Earth and Planetary Science Letters,* **41,** 32–46.

CANN, J. R. 1970. Rb, Sr, Y, Zr and Nb in some ocean floor basaltic rocks. *Earth and Planetary Science Letters,* **10,** 1–11.

——. 1971. Petrology of basement rocks from Palmer Ridge, north-east Atlantic. *Philsophical Transactions of the Royal Society,* Ser. A, **268,** 605–17.

CARMICHAEL, I. S. E. 1964. The petrology of Thingmuli, a Tertiary volcano in eastern Iceland. *Journal of Petrology,* **5,** 435–60.

CECIONI, G. 1955. Noticias preliminares sobre el hallzgo del Paleozoico superior en el Archipielago Patagonico. *Boletín del Instituto de Geología. Facultad de Ciencias Fisicas y Matemáticas. Universidad de Chile,* No. 6, 241–55.

CHAYES, F. 1972. Silica saturation in Cenozoic basalt. *Philosophical Transactions of the Royal Society,* Ser. A, **271,** 285–96.

CHRISTIE, J. M. 1960. Mylonitic rocks of the Moine thrust zone in the Assynt region, northwest Scotland. *Transactions of the Edinburgh Geological Society,* **18,** 78–83.

CLAYTON, R. A. S. 1982. A preliminary investigation of the geochemistry of greywackes from South Georgia. *British Antarctic Survey Bulletin,* No. 51, 89–109.

COLEMAN, R. G. *and* Z. E. PETERMAN. 1975. Oceanic plagiogranites. *Journal of Geophysical Research,* **80,** 1099–108.

CRADDOCK, C. 1972. Antarctic tectonics. (*In* ADIE, R. J., *ed. Antarctic geology and geophysics.* Oslo, Universitetsforlaget, 137–41.)

DALZIEL, I. W. D. 1969. Structural studies in the Scotia arc: Livingston Island. *Antarctic Journal of the United States,* **4,** No. 4, 137.

——. 1972. Large-scale folding in the Scotia arc. (*In* ADIE, R. J., *ed. Antarctic geology and geophysics.* Oslo, Universitetsforlaget, 47–55.)

——. 1982. The early (pre-Middle Jurassic) history of the Scotia arc region: a review and progress report. (*In* CRADDOCK, C., *ed. Antarctic geoscience. Third Symposium on Antarctic Geology and Geophysics.* Madison, Wisconsin, The University of Wisconsin Press, 111–26.)

——. *and* D. H. ELLIOT. 1971. The evolution of the Scotia arc. *Nature, London,* **233,** 246–52.

——. *and* ——. 1973. The Scotia arc and Antarctic margin. (*In* NAIRN, A. E. M. *and* F. G. STEHLI, *ed. The ocean basins and their margins. 1. The South Atlantic.* New York, Plenum Publishing Corporation, 171–245.)

——., DE WIT, M. J. *and* K. F. PALMER. 1974. A fossil margin basin in the southern Andes. *Nature, London,* **250,** 291–94.

——., DOTT, R. H., WINN, R. D. *and* R. L. BRUHN. 1975. Tectonic relations of South Georgia island to the southernmost Andes. *Geological Society of America. Bulletin,* **86,** 1034–40.

DEWAR, G. J. 1970. The geology of Adelaide Island. *British Antarctic Survey Scientific Reports,* No. 57, 66 pp.

DE WIT, M. J. 1977. The evolution of the Scotia arc as a key to the reconstruction of southwestern Gondwanaland. *Tectonophysics,* **37,** 53–81.

DOUGLAS, G. V. 1930. Geology and topography of South Georgia. (*In Report on the Geological Collections made during the Voyage of the "Quest".* London, British Museum (Natural History), 4–24.)

DRAKE, M. J. *and* D. F. WEILL. 1975. Partition of Sr, Ba, Ca, Y, Eu^{2+}, Eu^{3+} and other REE between plagioclase feldspar and magmatic liquid: an experimental study. *Geochimica Cosmochimica Acta,* **39,** 689–712.

EALES, H. V. *and* J. VAN A. ROBEY. 1976. Differentiation of tholeiitic Karroo magma at Birds River, South Africa. *Contributions to Mineralogy and Petrology,* **56,** 101–17.

EDWARDS, C. 1982. New paleontologic evidence of Triassic sedimentation in West Antarctica. (*In* CRADDOCK, C., *ed. Antarctic geoscience. Third Symposium on Antarctic Geology and Geophysics.* Madison, Wisconsin, The University of Wisconsin Press, 325–30.)

ELLIOT, D. H. 1964. The petrology of the Argentine Islands. *British Antarctic Survey Scientific Reports,* No. 41, 31 pp.

——. 1965. Geology of north-west Trinity Peninsula, Graham Land. *British Antarctic Survey Bulletin,* No. 7, 1–24.

——. 1966. Geology of the Nordenskjöld Coast and a comparison with north-west Trinity Peninsula, Graham Land. *British Antarctic Survey Bulletin,* No. 10, 1–43.

ENGEL, A. E. J., ENGEL, C. G. *and* R. G. HAVENS. 1965. Chemical characteristics of oceanic basalts and the upper mantle. *Bulletin of the Geological Society of America,* **76,** 719–34.

ENGEL, C. G. *and* R. L. FISHER. 1975. Granitic to ultramafic rock complexes of the Indian Ocean ridge system, western Indian Ocean. *Geological Society of America. Bulletin,* **86,** 1553–78.

ERIKSON, E. H. 1977. Petrography and petrogenesis of the Mount Stewart batholith: plutonic equivalent of the high-alumina basalt association. *Contributions to Mineralogy and Petrology,* **60,** 183–207.

ERLANK, A. J. *and* E. J. D. KABLE. 1976. The significance of incompatible elements in Mid-Atlantic Ridge basalts from 45°N with particular reference to Zr/Nd. *Contributions to Mineralogy and Petrology,* **54,** 281–91.

EWART, A. *and* W. B. BRYAN. 1972. The petrology and geochemistry of the igneous rocks from Eua, Tongan Islands. *Geological Society of America. Bulletin,* **83,** 3281–98.

——., ——. *and* J. B. GILL. 1973. Mineralogy and geochemistry of the younger volcanic islands of Tonga, S. W. Pacific. *Journal of Petrology,* **14,** 429–65.

——., TAYLOR, S. R. *and* A. C. CAPP. 1968. Trace and minor element geochemistry of the rhyolitic volcanic rocks, central North Island, New Zealand. *Contributions to Mineralogy and Petrology,* **18,** 76.

FLOYD, P. A. *and* J. A. WINCHESTER. 1975. Magma type and tectonic setting discrimination using immobile elements. *Earth and Planetary Science Letters,* **27,** 211–18.

FRASER, A. G. *and* P. H. GRIMLEY. 1972. The geology of parts of the Bowman and Wilkins Coasts, Antarctic Peninsula. *British Antarctic Survey Scientific Reports,* No. 67, 59 pp.

FRENCH, W. J. 1966. Appinitic intrusions clustered around the Ardara pluton, County Donegal. *Proceedings of the Royal Irish Academy,* **64B,** 303–22.

FREY, F. A., BRYAN, W. B. *and* G. THOMPSON. 1974. Atlantic Ocean floor: geochemistry and petrology of basalts from Legs 2 and 3 of the Deep Sea Drilling Project. *Journal of Geophysical Research,* **79,** 5507–27.

GAST, P. W. 1968. Trace element fractionation and the origin of tholeiitic and alkaline magma types. *Geochimica Cosmochimica Acta,* **32,** 1057–86.

GILL, J. B. 1970. Geochemistry of Viti Levu, Fiji, and its evolution as an island arc. *Contributions to Mineralogy and Petrology,* **27,** 179–203.

GLEDHILL, A., REX, D. C. *and* P. W. G. TANNER. 1982. Rb-Sr and K-Ar geochronology of rocks from the Antarctic Peninsula between Anvers Island and Marguerite Bay. (*In* CRADDOCK, C., *ed. Antarctic geoscience. Third Symposium on Antarctic Geology and Geophysics.* Madison, Wisconsin, The University of Wisconsin Press, 315–23.)

GODFREY, J. D. 1954. The origin of ptygmatic structures. *Journal of Geology,* **62,** 375–87.

GOODE, A. D. T. 1977. Intercumulus igneous layering in the Kalka layered intrusion, central Australia. *Geological Magazine,* **114,** 215–18.

——. *and* G. W. KREIG. 1967. The geology of Edwarana intrustion, Gibs Complex, central Australia. *Journal of the Geological Society of Australia,* **14,** 185–94.

GOODSPEED, G. E. 1940. Dilation and replacement dikes. *Journal of Geology,* **48,** 175–95.

——. 1952. Replacement and rheomorphic dikes. *Journal of Geology,* **60,** 345–63.

——. 1955. Relict dikes and relict pseudodikes. *American Journal of Science,* **253,** 146–61.

GRAPES, R. H., HASHIMOTO, S. *and* S. MIYASHITA. 1977. Amphiboles of a metagabbro–amphibolite sequence, Hidaka metamorphic belt, Hokkaido. *Journal of Petrology,* **18,** 285–319.

GREEN, D. H. 1973. Contrasted melted relations in a pyrolite upper mantle under mid-ocean ridge, stable crust and island arc environments. *Tectonophysics,* **17,** 285–97.

HART, S. R., GLASSLEY, W. E. *and* D. E. KARIG. 1972. Basalt and sea floor spreading behind the Mariana island arc. *Earth and Planetary Science Letters,* **15,** 12–18.

HATCH, F. H., WELLS, A. K. *and* M. K. WELLS. 1968. *Petrology of igneous rocks.* London, Thomas Murby and Co.

HAWKINS, J. W. 1976. Petrology and geochemistry of basaltic rocks of the Lau Basin. *Earth and Planetary Science Letters,* **28,** 283–98.

——. 1977. Petrologic and geochemical characteristics of marginal basin basalts. (*In* TALWANI, M. *and* W. C. PITMAN, *ed. Island arcs, deep sea trenches and back-arc basins.* Washington, D. C., American Geophysical Union, 367–78.) [Maurice Ewing Series, Vol. 1.]

HEIM, F. 1912. Geologische Beobachtungen über Süd-Georgien. *Zeitschrift der Gesellschaft für Erdkunde zu Berlin,* 451–56.

HOBBS, B. E., MEANS, W. D. *and* P. F. WILLIAMS. 1976. *An outline of structural geology.* New York, London, Sydney, Toronto, John Wiley and Sons.

HOBBS, G. J. 1968. The geology of the South Shetland Islands: IV. The geology of Livingston Island. *British Antarctic Survey Scientific Reports,* No. 47, 34 pp.

HOLTEDAHL, O. 1929. On the geology and physiography of some Antarctic and sub-Antarctic islands. *Scientific Results of the Norwegian Antarctic Expeditions,* No. 3, 172 pp.

HOOPER, P. R. 1962. The petrology of Anvers Island and adjacent islands. *Falkland Islands Dependencies Survey Scientific Reports,* No. 34, 67 pp.

HYDEN, G. *and* P. W. G. TANNER. 1981. Late Palaeozoic—early Mesozoic fore-arc basin sedimentary rocks at the Pacific margin in western Antarctica. *Geologische Rundschau,* **70,** 529–41.

IRVINE, T. N. *and* W. R. A. BARAGER. 1971. A guide to the chemical classification of the common volcanic rocks. *Canadian Journal of Earth Sciences,* **8,** 523–48.

JAKES, P. *and* J. GILL. 1970. Rare earth elements and the island arc tholeiitic series. *Earth and Planetary Science Letters,* **9,** 17–28.

JAHNS, R. H., MARTIN, R. F. *and* O. F. TUTTLE. 1963. Origin of granophyre in dikes and sills of tholeiitic diabase. *Transactions. American Geophysical Union,* **50,** 337–50.

JAMES, R. S. *and* D. L. HAMILTON. 1969. Phase relations in the system $NaAlSi_3O_8$–$KAlSi_3O_8$–$CaAl_2Si_2O_8$–SiO_2 at 1 kilobar water vapour pressure. *Contributions to Mineralogy and Petrology,* **21,** 111–41.

JAMIESON, B. J. *and* D. B. CLARKE. 1970. Potassium and associated elements in tholeiitic basalts. *Journal of Petrology,* **11,** 183–204.

JOHNSON, M. R. W. 1967. Mylonite zones and mylonite banding. *Nature, London,* **213,** 246–47.

——. 1970. Torridonian and Moinian. (*In* CRAIG, G. Y., *ed. The geology of Scotland.* Edinburgh, Oliver and Boyd.)

JOPLIN, G. A. 1959. On the origin and occurrence of basic bodies associated with discordant batholiths. *Geological Magazine,* **96,** 361–73.

KAITARO, S. 1952. On some offset structures in dilation dykes. *Bulletin de la Commission Géologique de la Finlande,* **157,** 67–74.

KARIG, D. E. 1972. Remnant arcs. *Geological Society of America. Bulletin,* **83,** 1057–68.

KILINC, I. A. 1973. Experimental study of partial melting of crustal rocks and formation of migmatites. *24th International Geological Congress, Canada,* **2,** 109–13.

KLEEMAN, A. W. 1965. The origin of granitic magmas. *Journal of the Geological Society of Australia,* **12,** 35–51.

KRANK, E. H. 1932. Geological investigations in the Cordillera of Tierra del Fuego. *Acta Geographica, Helsingfors,* **4,** No. 2, 231 pp.

KRUPICKA, J. 1968. Sharp boundaries in crystalline rocks and their interpretation. *23rd International Geological Congress, Copenhagen,* **4,** 43–59.

KUENEN, P. H. 1938. Observations and experiments on ptygmatic folding. *Bulletin de la Commission Géologique de la Finlande,* **12,** 11–28.

LAMBERT, R. ST. J. *and* J. G. HOLLAND. 1974. Yttrium geochemistry applied to petrogenesis utilizing calcium–yttrium relationships in minerals and rocks. *Geochimica Cosmochimica Acta,* **38,** 1393–413.

LAPWORTH, 1885. The highland controversy in British geology; its causes, course and consequences. *Nature, London,* **32,** 558–59.

LEEMAN, W. P. 1976. Petrogenesis of McKinney (Snake River) olivine tholeiite in light of rare-earth element and Cr/Ni distributions. *Geological Society of America. Bulletin,* **87,** 1582–86.

LUTH, W. C., JAHNS, R. H. *and* O. F. TUTTLE. 1964. The granite system at pressures of 4 to 10 kilobars. *Journal of Geophysical Research,* **69,** 759–73.

MCBIRNEY, A. R. 1975. Differentiation of the Skaergaard intrusion. *Nature, London,* **253,** 691–94.

MAIR, B. F. 1981. Geological observations in the Moraine Fjord area, South Georgia. *British Antarctic Survey Bulletin,* No. 53, 11–19.
——. (in press *a*). The Larsen Harbour Formation and associated intrusive rocks of southern South Georgia. *British Antarctic Survey Bulletin,* No. 52.
——. (in press *b*). The geology of South Georgia: VI. Larsen Harbour Formation. *British Antarctic Survey Scientific Reports.*
MARSH, A. F. 1968. *Geology of parts of the Oscar II and Foyn Coasts, Graham Land.* Ph.D. thesis, University of Birmingham, 291 pp. [Unpublished.]
MEHNERT, K. R. 1962. Zur Systematik der Migmatite. *Krystallinikum,* **1,** 95–110.
——. 1971. *Migmatites.* 2nd edition. Amsterdam, London and New York, Elsevier Publishing Company.
MELSON, W. G. *and* G. THOMPSON. 1971. Petrology of a transform fault zone and adjacent ridge segments. *Philosophical Transactions of the Royal Society,* Ser. A, **268,** 423–41.
MIYASHIRO, A. 1972. Metamorphism and related magmatism in plate tectonics. *American Journal of Science,* **272,** 629–56.
——. 1973. The Troodos opholite complex was probably formed in an island arc. *Earth and Planetary Science Letters,* **19,** 218–24.
——. 1975. Classification, characteristics and origin of ophiolites. *Journal of Geology,* **83,** 249–81.
——., SHIDO, F. *and* M. EWING. 1969. Diversity and origin of abyssal tholeiite from the Mid-Atlantic Ridge near 24° and 30°N. *Contributions to Mineralogy and Petrology,* **23,** 38–52.
——., ——. *and* ——. 1970. Crystallization and differentiation in abyssal tholeiites and gabbros from mid-ocean ridges. *Earth and Planetary Science Letters,* **7,** 361–65.
——., ——. *and* ——. 1971. Metamorphism in the Mid-Atlantic Ridge near 24° and 30°N. *Philosophical Transactions of the Royal Society,* Ser. A, **268,** 589–603.
MOORE, D. G. 1973. Plate-edge deformation and crustal growth, Gulf of California structural province. *Geological Society of America. Bulletin,* **84,** 1883–906.
NOCKOLDS, S. R. *and* R. ALLEN. 1953. The geochemistry of some igneous rock series. *Geochimica Cosmochimica Acta,* **4,** 105–42.
O'CONNOR, J. T. 1965. A classification of quartz-rich igneous rocks based on feldspar ratios. *Professional Papers of the United States Geological Survey,* **525B,** 79–84.
O'HARA, M. J. 1977. Geochemical evolution during fractional crystallization of a periodically refilled magma chamber. *Nature, London,* **266,** 503–07.
OLDERSHAW, W. 1969. The Lochnagar granitic ring complex, Aberdeenshire. *Scottish Journal of Geology,* **10,** 297–309.
O'NIONS, R. K. *and* K. GRONVOLD. 1973. Petrogenetic relationships of acid and basic rocks in Iceland: Sr-isotopes and rare-earth elements in late and post-glacial volcanics. *Earth and Planetary Science Letters,* **19,** 397–409.
PEARCE, J. A. 1975. Basalt geochemistry used to investigate post-tectonic environments on Cyprus. *Tectonophysics,* **25,** 41–68.
——. *and* J. CANN. 1973. Tectonic setting of basic volcanic rocks determined using trace element analysis. *Earth and Planetary Science Letters,* **19,** 290–300.
PEARCE, T. H., GORMAN, P. E. *and* T. C. BIRKETT. 1975. The TiO_2–K_2O–P_2O_5 diagram: a method of discriminating between oceanic and non-oceanic basalts. *Earth and Planetary Science Letters,* **24,** 419–26.
PETTIGREW, T. H. 1981. The geology of Annenkov Island. *British Antarctic Survey Bulletin,* No. 53, 213–54.
PETTIJOHN, F. J., POTTER, P. E. *and* R. SIEVER. 1972. *Sand and sandstone.* Berlin, Heidelberg and New York, Springer-Verlag.
PITCHER, W. S. 1978. The anatomy of a batholith. *Journal of the Geological Society of London,* **135,** 157–82.
PRICE, R. C. *and* J. M. SINTON. 1978. Geochemical variations in a suite of granitoids and gabbros from Southland, New Zealand. *Contributions to Mineralogy and Petrology,* **67,** 267–78.
QUENSEL, P. D. 1913. Die Quarzporphyr- und Porphyroidformation in Südpatagonien und Feuerland. *Bulletin of the Geological Institution of the University of Upsala,* **12,** 9–40.
RAMBERG, H. 1960. Relationships between length of arc and thickness of ptygmatically folded veins. *American Journal of Science,* **258,** 36–46.
RAMSAY, J. G. 1962. Interference patterns produced by the superposition of folds of similar type. *Journal of Geology,* **70,** 466–81.
——. 1967. *Folding and fracturing of rocks.* New York, McGraw-Hill Book Co.
——. *and* R. H. GRAHAM. 1970. Strain variations in shear belts. *Canadian Journal of Earth Sciences,* **7,** 786–813.
RODDICK, J. A. *and* J. E. ARMSTRONG. 1959. Relict dikes in the coast mountains near Vancouver, B. C. *Journal of Geology,* **67,** 603–13.
ROSENBUSCH, H. 1887. *Mikroskopische Physiographie der Mineralien und Gesteine. II. Massige Gesteine.* Stuttgart.
ROSS, J. V. 1973. Mylonitic rocks and flattened garnets in the southern Octanogan of British Columbia. *Canadian Journal of Earth Sciences,* **10,** 1–17.
ROSS, M., PAPIKE, J. J. *and* P. W. WEIBLEN. 1968. Exsolution in clino-amphiboles. *Science, New York,* **159,** 1099–102.
SAUNDERS, A. D. *and* J. TARNEY. 1979. The geochemistry of basalts from a back-arc spreading centre in the east Scotia Sea. *Geochimica Cosmochimica Acta,* **43,** 555–72.
——., WEAVER, S. D. *and* J. TARNEY. 1982*b*. The pattern of Antarctic Peninsula plutonism. (*In* CRADDOCK, C., *ed. Antarctic geoscience. Third Symposium on Antarctic Geology and Geophysics.* Madison, Wisconsin, The University of Wisconsin Press, 305–14.)
——., TARNEY, J., DALZIEL, I. W. D. *and* C. R. STERN. 1979. Geochemistry of Mesozoic marginal basin floor mafic igneous rocks from southern Chile. *Geological Society of America. Bulletin,* **90,** 237–58.
——., ——., WEAVER, S. D. *and* P. F. BARKER. 1982*a*. Scotia sea floor: geochemistry of basalts from the Drake Passage and South Sandwich spreading centers. (*In* CRADDOCK, C., *ed. Antarctic geoscience. Third Symposium on Antarctic Geology and Geophysics.* Madison, Wisconsin, The University of Wisconsin Press, 213–22.)
SCHALLER, W. T. 1927. Mineral replacement in pegmatites. *American Mineralogist,* **12,** 59–63.
SCHEUMANN, K. H. 1937. Metatexis and metablastisis. *Tschermaks Mineralogische und Petrographische Mitteilungen,* **48,** 402–12.
SEDERHOLM, J. J. 1907. On granite and gneiss. *Bulletin de la Commission Géologique de la Finlande,* **23,** 1–110.
SHIDO, F., MIYASHIRO, A. *and* M. EWING. 1971. Crystallization of abyssal tholeiites. *Contributions to Mineralogy and Petrology,* **31,** 251–66.
SINGLETON, D. G. 1980. The geology of the central Black Coast, Palmer Land. *British Antarctic Survey Scientific Reports,* No. 102, 50 pp.
SKINNER, A. C. 1973. Geology of north-western Palmer Land between Eureka and Meiklejohn Glaciers. *British Antarctic Survey Bulletin,* No. 35, 1–22.
SMITH, C. G. 1977. *The geology of parts of the west coast of Palmer Land, Antarctica.* Ph.D. thesis, University of Birmingham, 185 pp. [Unpublished.]
STERN, C. R. 1979. Open and closed system igneous fractionation within two Chilean ophiolites and the tectonic implication. *Contributions to Mineralogy and Petrology,* **68,** 243–58.
——. *and* J. B. STROUP. 1982. The petrochemistry of the Patagonian Batholith, Ultima Esperanza, Chile. (*In* CRADDOCK, C., *ed. Antarctic geoscience. Third Symposium on Antarctic Geology and Geophysics.* Madison, Wisconsin, The University of Wisconsin Press, 135–42.)
——., DE WIT, M. J. *and* J. R. LAWRENCE. 1976. Igneous and metamorphic processes associated with the formation of Chilean ophiolites and their implication for ocean floor metamorphism, seismic layering and magnetism. *Journal of Geophysical Research,* **81,** 4370–80.
STONE, P. 1980. The geology of South Georgia: IV. Barff Peninsula and Royal Bay areas. *British Antarctic Survey Scientific Reports,* No. 96, 45 pp.
——. 1982. Geological observations in the Cooper Bay–Wirik Bay area, South Georgia. *British Antarctic Survey Bulletin,* No. 51, 43–53.
STOREY, B. C. In press. The geology of the Ducloz Head area, South Georgia. *British Antarctic Survey Bulletin,* No. 52.
——., MAIR, B. F. *and* C. M. BELL. 1977. The occurrence of Mesozoic oceanic floor and ancient continental crust on South Georgia. *Geological Magazine,* **114,** 203–08.
STRECKEISEN, A. L. 1973. Plutonic rocks. Classification and nomenclature recommended by the IUGS Subcommission on the Systematics of Igneous Rocks. *Geotimes,* **10,** 26–30.
STUBBS, G. M. 1968. *Geology of parts of the Foyn and Bowman Coasts, Graham Land.* Ph.D. thesis, University of Birmingham, 245 pp. [Unpublished.]
SUÁREZ, M. 1976. Plate tectonic model for southern Antarctic Peninsula and its relation to southern Andes. *Geology,* **4,** 211–14.
——. 1977*a*. Aspectos geoquimicos del complejo ofiolitico Tortuga en la Cordillera Patagonica del Sur, Chile. *Revista Geológica de Chile,* **4,** 3–14.
——. 1977*b*. Notas geoquimicas preliminares del batolito patagonico al sur de Tierra de Fuego, Chile. *Revista Geológica de Chile,* **4,** 15–33.
——. *and* T. H. PETTIGREW. 1976. An Upper Mesozoic island-arc–back-arc system in the southern Andes and South Georgia. *Geological Magazine,* **113,** 305–28.
SUK, M. 1964. Material characteristics of the metamorphism and migmatization of Moldanubian paragneiss in central Bohemia. *Krystallinikum,* **2,** 71–105.
——. 1972. Origin of the migmatites of the south Bohemian Moldanubicum by regional low-pressure metamorphism. *24th International Geological Congress, Canada,* **2,** 114–21.
TANNER, P. W. G. 1982*a*. Geology of Shag Rocks, part of a continental block on the north Scotia Ridge, and possible regional correlations. *British Antarctic Survey Bulletin,* No. 51, 125–36.
——. 1982*b*. Geologic evolution of South Georgia. (*In* CRADDOCK, C., *ed. Antarctic geoscience. Third symposium on Antarctic Geology and Geophysics.* Madison, Wisconsin, The University of Wisconsin Press, 167–76.)
——. *and* D. C. REX. 1979. Timing of events in an early Cretaceous island arc–marginal basin system on South Georgia. *Geological Magazine,* **116,** 167–79.

——., STOREY, B. C. *and* D. I. M. MACDONALD. 1981. Geology of an Upper Jurassic–Lower Cretaceous island-arc assemblage in Hauge Reef, the Pickersgill Islands and adjoining areas of South Georgia. *British Antarctic Survey Bulletin,* No. 53, 77–117.

TAYLOR, H. P. *and* R. G. COLEMAN. 1977. Oxygen isotopic evidence for meteoric-hydrothermal alteration of Jabal at Tirf igneous complex, Saudi Arabia. *Transactions. American Geophysical Union,* **58,** 516.

TAYLOR, S. R. 1965. The application of trace element data to problems in petrology. (*In* AHRENS, L. H., PRESS, F., RUNCORN, S. K. *and* H. C. UREY, *ed. Physics and chemistry of the Earth,* **6.** Oxford, London, Edinburgh, New York, Paris, Frankfurt, Pergamon Press, 133–213.)

THAYER, T. P. 1967. Chemical and structural relations of ultramafic and feldspathic rocks in Alpine intrusive complexes. (*In* WYLLIE, P. J., *ed. Ultramafic and related rocks.* New York, Wiley, 222–39.)

THOMPSON, G. 1973. Trace element distributions in fractionated oceanic rocks: 2. Gabbros and related rocks. *Chemical Geology,* **12,** 99–111.

——., SHIDO, F. *and* A. MIYASHIRO. 1972. Trace element distribution in fractionated oceanic basalts. *Chemical Geology,* **9,** 89–97.

THOMSON, J. W. 1973. The geology of Powell, Christoffersen and Michelsen Islands, South Orkney Islands. *British Antarctic Survey Bulletin,* Nos 33 and 34, 137–67.

THOMSON, M. R. A., TANNER, P. W. G. *and* D. C. REX. 1982. Fossil and radiometric evidence for ages of deposition and metamorphism of sedimentary sequences on South Georgia. (*In* CRADDOCK, C., *ed. Antarctic geoscience. Third Symposium on Antarctic Geology and Geophysics.* Madison, Wisconsin, The University of Wisconsin Press, 177–84.)

TRENDALL, A. F. 1953. The geology of South Georgia: I. *Falkland Islands Dependencies Survey Scientific Reports,* No. 7, 26 pp.

——. 1959. The geology of South Georgia: II. *Falkland Islands Dependencies Survey Scientific Reports,* No. 9, 48 pp.

TULLIS, J., CHRISTIE, J. M. *and* D. T. GRIGGS. 1973. Microstructures and preferred orientations of experimentally deformed quartzites. *Geological Society of America. Bulletin,* **84,** 297–314.

TURNER, F. J. 1968. *Metamorphic petrology.* New York, McGraw-Hill.

——. *and* L. E. WEISS. 1963. *Structural analysis of metamorphic tectonics.* New York, McGraw-Hill.

TYRRELL, G. W. 1930. The petrography and geology of South Georgia. (*In Report on the Geological Collections made during the Voyage of the "Quest".* London, British Museum (Natural History), 28–54.)

TUTTLE, D. F. *and* N. L. BOWEN. 1958. Origin of granite in the light of experimental studies in the system $NaAlSi_3O_8$–$KAlSi_3O_8$–SiO_2–H_2O. *Memoirs of the Geological Society of America,* No. 74, 153 pp.

VERNON, R. H. *and* D. M, RANSOM. 1971. Retrograde schists of the amphibolite facies at Broken Hill, New South Wales. *Journal of the Geological Society of Australia,* **18,** 267–78.

VOGT, J. H. L. 1921. Magmatic differentiation in igneous rocks. *Journal of Geology,* **29,** 318–50.

VON PLATEN, H. 1965. Experimental anatexis and genesis of migmatites. (*In* PITCHER, W. S. *and* G. W. FLINN, *ed. Controls of metamorphism. A symposium held under the auspices of the Liverpool Geological Society.* Edinburgh and London, Oliver and Boyd, 203–18.) [*Geological Journal,* Special Issue No. 1.]

WAGER, L. R. *and* G. M. BROWN. 1968. *Layered igneous rocks.* Edinburgh and London, Oliver and Boyd.

——. *and* W. A. DEER. 1939. Geological investigations in East Greenland: Pt. III. The petrology of the Skaergaard intrusion, Kangerdlugssuaq, East Greenland. *Meddelelser om Grønland,* **105,** No. 4.

——. *and* R. L. MITCHELL. 1951. The distribution of trace elements during strong fractionation of basic magma—a further study of the Skaergaard intrusion, East Greenland. *Geochimica Cosmochimica Acta,* **9,** 129–208.

WAHLSTROM, E. E. 1939. Graphic granite. *American Mineralogist,* **24,** 681–98.

WAKEFIELD, J. 1977. Mylonitization in the Lethakane shear zone, eastern Botswana. *Journal of the Geological Society of London,* **133,** 263–75.

WATTERSON, J. 1965. Plutonic development of the Ilordleq area, south Greenland, Part 1. Chronology and the occurrence and the recognition of metamorphosed dykes. *Meddelelser om Grønland,* **172,** No. 7, 147 pp.

WEAVER, S. D., SAUNDERS, A. D. *and* J. TARNEY. 1982. Mesozoic–Cenozoic volcanism in the South Shetland Islands and the Antarctic Peninsula: geochemical nature and plate tectonic significance. (*In* CRADDOCK, C., *ed. Antarctic geoscience. Third Symposium on Antarctic Geology and Geophysics.* Madison, Wisconsin, The University of Wisconsin Press, 263–73.)

——., ——., PANKHURST, R. J. *and* J. TARNEY. 1979. A geochemical study of magmatism associated with the initial stages of back-arc spreading. *Contributions to Mineralogy and Petrology,* **68,** 151–69.

WELLS, A. K. *and* A. V. BISHOP. 1955. An appinitic facies associated with certain granites in Jersey. Channel Islands. *Quarterly Journal of the Geological Society of London,* **111,** 143–66.

WEST, S. M. 1974. The geology of the Danco Coast, Graham Land. *British Antarctic Survey Scientific Reports,* No. 84, 58 pp.

WHITE, A. J. R. *and* B. W. CHAPELL. 1977. Ultrametamorphism and granitoid genesis. *Tectonophysics,* **43,** 7–22.

WINKLER, H. G. F. 1976. *Petrogenesis of metamorphic rocks.* 4th edition. Berlin, Heidelberg, New York, Springer-Verlag.

WINN, R. D. 1978. Upper Mesozoic flysch of Tierra del Fuego and South Georgia island: a sedimentological approach to lithosphere plate reconstruction. *Geological Society of America. Bulletin,* **89,** 533–47.

WYLLIE, P. J. 1967. *Ultramafic and related rocks.* New York, London, Sydney, John Wiley and Sons.

ZECK, H. P. 1974. Cataclastites, hemiclastites, holoclastites, blasto-ditto, and myloblastites—cataclastic rocks. *American Journal of Science,* **274,** 1064–73.